Scuola di Dottorato in Scienze Veterinarie
per la Salute Animale e la Sicurezza Alimentare

Università degli Studi di Milano

GRADUATE SCHOOL OF VETERINARY SCIENCES
FOR ANIMAL HEALTH AND FOOD SAFETY
Director: Prof. Valentino Bontempo

Doctoral Program in Animal Nutrition and Food Safety

Academic Year: 2014-2015

Effect of different diets in a mouse model of neurodegenerative disease

Lucia Buccarello

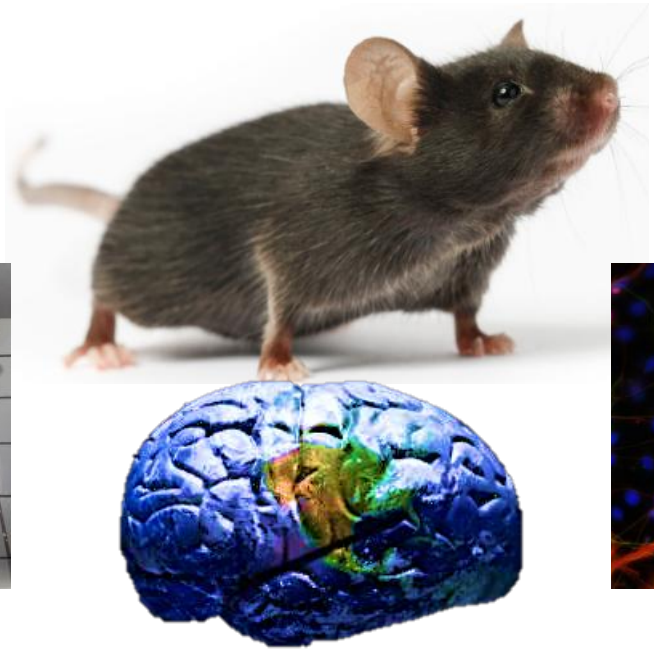

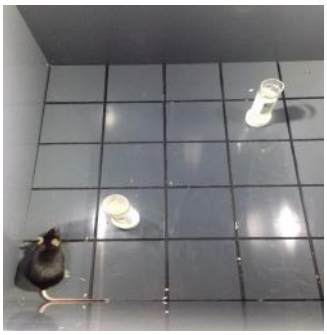

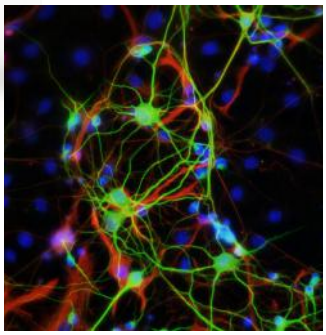

Tutor:

Prof. Cinzia Domeneghini

Coordinator:

Prof. Giovanni Savoini

Index

Chapter 1: Foreward

Chapter 2: Objectives

Chapter 3: Interaction between gender and genotype in a mouse model of tauopathy: increase of cognitive impairment and locomotor dysfunctions in young and aged females Tau P301L mice

Chapter 4: A low fat-protein diet improves lifespan and cognitive activity in young and aged Tau P301L mice model of tauopathy

Chapter 5: A low fat-protein diet improves the oxidative damage in young and aged Tau P301L mice model of tauopathy

Chapter 6: A high fat-protein diet induce nonalcoholic fatty liver disease (NAFLD) in young and aged P301L TG mice model of tauopathy

Chapter 7: General Discussion

Chapter 8: Summary

Chapter 9: References

Chapter 10: Full papers published during the PhD period

10a: Consistency of ventilation in IVCs and open cages: their normoxic atmosphere and its impact on hematological parameters of mice

10b: The effect of two different Individually Ventilated Cage systems on anxiety-related behavior and welfare in two strains of laboratory mouse

Chapter 11: Acknowledgments

CHAPTER 1

Foreword

1. TAUOPHATIES

Tauopathies are clinically, morphologically and biochemically heterogeneous neurodegenerative diseases characterized by the deposition of abnormal Tau protein in the brain. The neuropathological phenotypes are distinguished based on the involvement of different anatomical areas, cell types and presence of distinct isoforms of Tau in the pathological deposits. Neuropathological phenotypes comprise Pick's disease (PID), progressive supranuclear palsy (PSP), corticobasal degeneration (CBD), neurofibrillary tangle-only dementia (NFT-dementia) and a recently characterized entity called Globular Glial Tauophaty (GGT). Mutations in the encoding gene of the microtubule-associated protein Tau (MAPT) are associated with frontotemporal dementia (FTD) and Parkinsonism linked to chromosome 17 (FTDP-17). Several neurodegenerative conditions with diverse etiologies may be associated with Tau pathology defined as secondary tauopathies, as other proteins play a central role in their pathogenesis. Alzheimer's disease (AD) is one major neurodegenerative disorder showing neuronal Tau pathology and it defined as a primary tauophaty (table 1).

Table 1: Diseases with Tau-based neurofibrillary pathology

Alzheimer's disease (AD)
Frontotemporal dementia (FTD)
Amyotrophic lateral sclerosis/parkinsonism–dementia complex[a] (SLA)
Argyrophilic grain dementia[a] (AGD)
Corticobasal degeneration[a] (CBD)
Creutzfeldt-Jakob disease (CJD)
Diffuse neurofibrillary tangles with calcification[a]
Down's syndrome
Frontotemporal dementia with Parkinsonism linked to chromosome 17[a] (FTDP-17)
Gerstmann-Sträussler-Scheinker disease
Hallervorden-Spatz disease
Myotonic dystrophy
Niemann-Pick disease, type C
Non-Guamanian motor neuron disease with neurofibrillary tangles
Pick's disease[a] (PID)
Postencephalitic Parkinsonism
Prion protein cerebral amyloid angiopathy
Progressive subcortical gliosis[a]
Progressive supranuclear palsy[a] (PSP)
Subacute sclerosing panencephalitis
Tangle only dementia[a] (NFT-dementia)
Globular glial tauopathy (GGT)
[a]Diseases in which tau-positive neurofibrillary pathology is the most predominant neuropathological feature.

Arnold Pick provided the first clinical description of frontotemporal dementia in 1892 [1]. In 1911, Alois Alzheimer described the neuropathological lesions characteristic of Pick's disease [2]. In the 1960s, these so-called Pick bodies were shown to contain abnormal filaments [3], which are now known to be made of hyperphosphorylated microtubule-associated protein Tau [4-5].
They resemble the neurofibrillary lesions described by Alzheimer in 1907 in the disease subsequently named after him [6-7]. The Alzheimer's disease, being the major neurodegenerative disorder showing neuronal Tau pathology, is the most studied tauophaty in the literature. For this reason, it will often be used in this work as a reference. Therefore, we decide to describe briefly the major characteristics of Alzheimer's disease and, subsequently, the exact pathology that affects the animal model used in our study (Frontotemporal dementia or FTD).
Alzheimer's disease (AD) is a progressive neurodegenerative disease that leads to dementia and affects about 10% of the population over 65 years of age [8]. Memory loss is the first symptom of cognitive impairment, followed by aphasia, agnosia, apraxia and behavioral disorders.
The two main types of brain lesions seen in patients with AD are senile plaques of β amyloid and neurofibrillary tangles of hyperphosphorylated Tau (NFTs), a typical hallmark of tauopathies.
The NFTs are abnormal aggregation of hyperphosphorylated Tau [9] located in pyramidal cells of the hippocampus and in the entorinal cortex; they have been identified in many cortical and subcortical areas, such as the basal nucleus of Meynert, the amygdala, the locus coeruleus and the dorsal raphe [10]. The presence of β amyloid plaques and NTFs in specific regions of the cerebral cortex is needed to establish the definitive diagnosis of AD [11].
In fact, immunohistochemical studies of post-mortem brains showed a strong correlation between NFTs and Tau, indicating that Tau is a reliable indicator of the process of degeneration.
These analyses have shown that the detection of pathological Tau is present in all brain areas studied, with the exception of regions like the primary motor cortex and visual cortex (Brodmann areas 4 and 17 respectively). The quantification of hyperphosphorylated Tau is increased in the associative cortex than the primary sensory cortex, with highest levels in neocortical and limbic temporal areas [12].

1.1 Frontotemporal Dementia (FTD)

Most forms of tauophaty may be associated with clinical features of frontotemporal dementia (FTD) including progressive aphasia.
Frontotemporal dementia is the third cause of global neurodegeneration after AD; it has an incidence of 5-15 cases per 100000 in age group between 45 and 65 years. Affected individuals exhibit a course of slowly progressive disease that leads in most cases to death within about six years from diagnosis [13].
Clinically it is characterized by several behavioral changes, disorders of language and cognitive impairment that appear later [14]. Many cases are sporadic, but 20-30% are familiar [15-16]. The main pathologic feature of FTD is the atrophy of frontotemporal cortex with neuronal loss, gliosis and spongiosis of the superficial layers.
The involvement of medial temporal lobe structures such as the entorhinal cortex, the hippocampus and the amygdala is highly variable, while is common the degeneration of *substantia nigra* and basal ganglia. The cases of FTD are pathologically heterogeneous and can be divided into three main subgroups based on the type of protein inclusions in the brain: FTD with Tau-positive inclusions, inclusions FTD with ubiquitin-positive, Tau-negative FTD without distinctive histopathology [17].
Pick's disease is the term reserved for cases of FTD with intra-neuronal argirophilic inclusions, calls bodies Pick, composed of abnormal Tau. The Pick bodies are present in 10-30% of cases of sporadic FTD [18].
About 30% of cases of familiar FTD is caused by mutations of MAPT gene and characterized by Tau pathology [15]; until today have been identified 71 mutations of MAPT gene including 44 with pathogenetic effect clear, 1 with unclear effect and 16 non-pathogenic effect.
The pathogenic mutations can be grouped based on their position in the gene, defining their effects on mRNA and on the protein, as well as the resulting pathology.
Most of the mutations falls in the coding region and includes missense mutations, silent mutations and deletions. Most of the mutations of the coding region are located in the region of binding to microtubules (exon 9-12) or close to it (exon 13), but there are also two mutations in exon 1. Mutations that fall in exon 10 concern only the isoforms with four repeats, while the other all six isoforms (Fig.1).

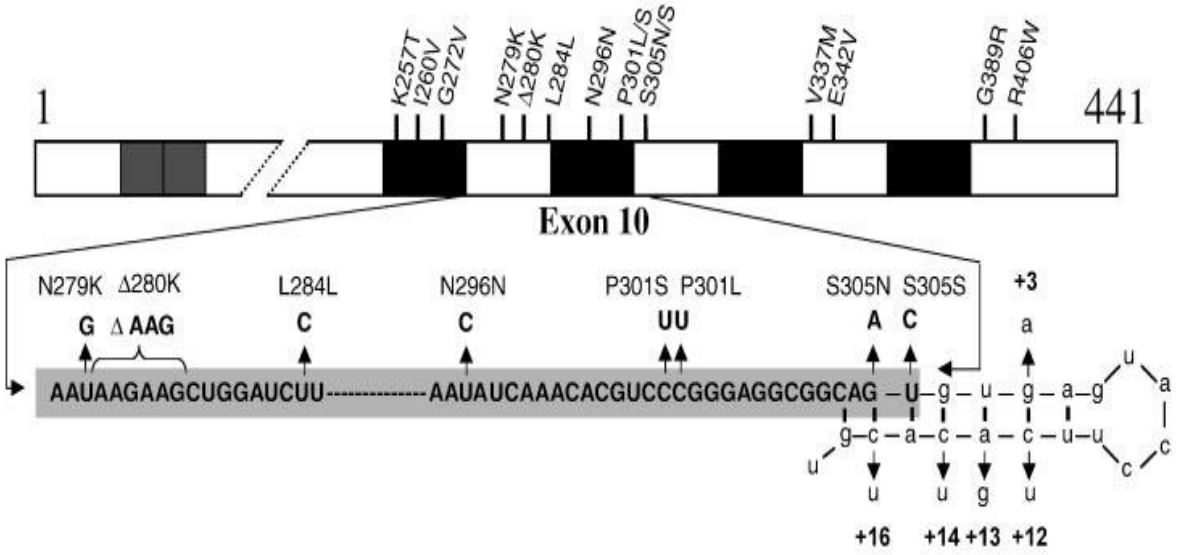

Figure 1: Schematic representation of mutations in the Tau gene identified in frontotemporal dementia and Parkinsonism linked to chromosome 17. The longest human brain Tau isoform is shown with known coding region mutations indicated above. The gray boxes near the amino terminus represent the alternatively spliced inserts encoded by exons E2 and E3, whereas the black boxes represent each of the four microtubule (MT) binding repeats (not drawn to scale). The second MT binding repeat is encoded by E10. Part of the mRNA sequence encoding E10 and the intron following E10 is shown. Mutations in E10 and the downstream intron are indicated. Intronic nucleotides that are part of intron 10 are shown in lower case.

The clinical presentation is related to the type and location of mutations in MAPT. In addition, there is a high variability inter and intra-family for some mutations. The age of onset for P301L and other mutations is between 45 and 65 years, although there are cases of later onset (65-70 years) or, for some mutations intronic, more early (about 40 years) [19].

Clinical symptoms can develop at first, between 20 and 30 years in patients with P301S mutation, L315R, G335V and G335S [20-21], or between 30 and 44 years in patients with mutations L266V and N279K [22]. In cases with R5H and I260V mutations occurred late onset after 70 years.

The average duration of the disease is between 8 and 10 years with the exception of the R406W mutation characterized by a slow rate of progression of the disease that lasts up to 25 years [23]. Patients with early age of onset often show a more aggressive progression of the disease, leading to death within 5 years [24].

1.2 Tau Protein

Tau is a microtubule-associated protein involved in microtubule assembly-stabilization and axonal transport [25-26]. It is encoded by MAPT (Microtubule-Associated Protein Tau) gene, located on the long arm of chromosome 17 (17q21) [27], it extends for approximately 100 kb and contains 16 exons. Three (4A, 6 and 8) of the 16 exons of the primary transcript are not present in mRNA brain. The exon 1 is part of the promoter; it is transcribed, but not translated, as well as exon 14. Exons 2, 3 and 10 undergo alternative splicing, giving rise to six different isoforms [28-29].
These isoforms differ for the presence or absence of 29 or 58 amino acid inserts in the amino-terminal half and the presence of three or four tandem repeats in the carboxyl-terminal region of the protein (Fig. 2).

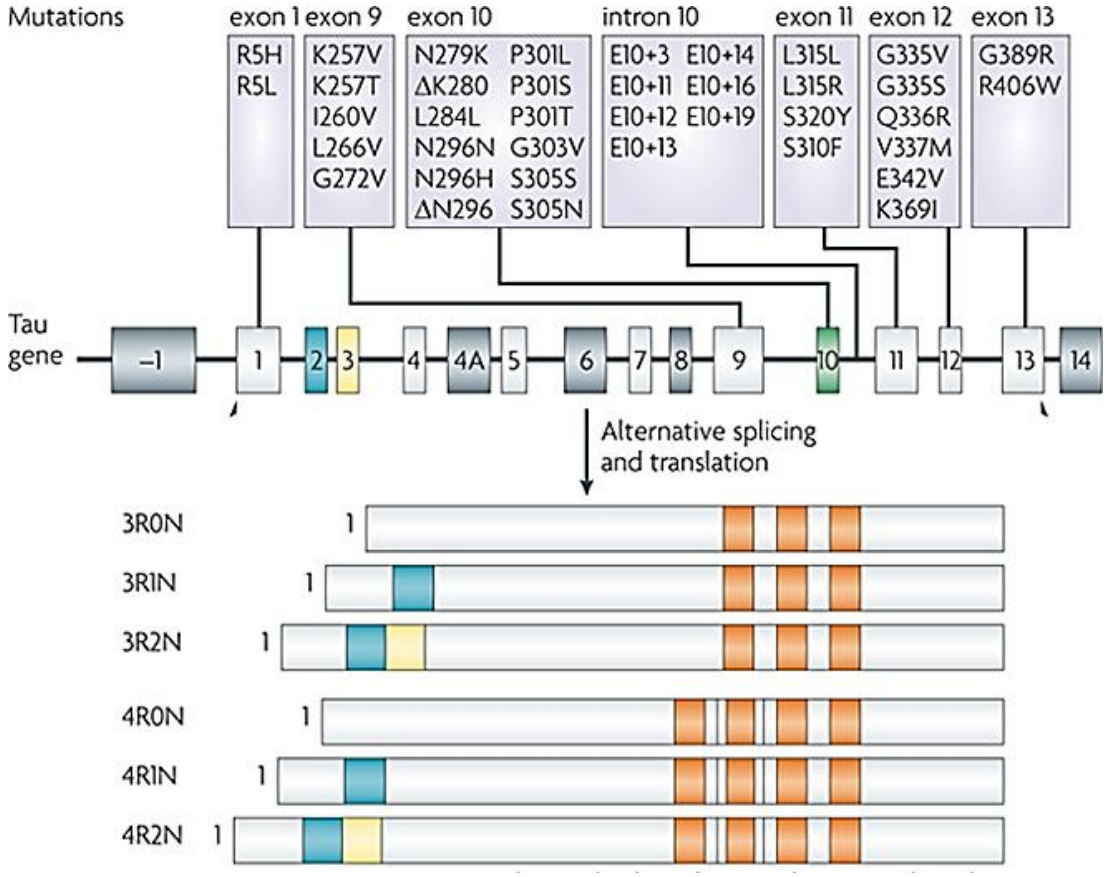

Figure 2: Human brain Tau Isoforms. The gene encoding Tau (also known as MAPT) is a multi-exon gene that undergoes alternative post-transcriptional splicing of exons 2 (shown in blue), 3 (shown in yellow) and 10 (shown in green) to yield 6 isoforms in the brain. The exons shown in dark grey are not found in translated human Tau. Exons 9–12 encode microtubule-binding repeat domains, and the exclusion or inclusion of exon 10 results in Tau with three (3R) or four (4R) microtubule -binding domains, respectively (shown as orange bars).

In adult human brain, similar levels of 3R and 4R Tau isoforms are found whereas in fetal brain, only the shortest Tau isoform with 3R is present, demonstrating developmental regulation of Tau expression. Differently from humans only 4R Tau isoforms are expressed in adult rodent brain [30]. Tau repeats constitute the microtubule-binding domain of the protein and the alternatively spliced fourth repeat is encoded by exon 10.

Tau is a phosphoprotein expressed constitutively and abundantly both in the nervous central system (CNS) and in the peripheral nervous system (PNS).

In the CNS, Tau is expressed mainly in neurons and axons in the mature state and in growth, even if it is present in lesser amounts in oligodendrocytes and astrocytes. It was, however, demonstrated the presence of the protein in non-neural cells, such as fibroblasts and lymphocytes [31-32]. The phosphorylation seems to affect its distribution in cell growth, with Tau phosphorylated mainly present in the somatodendritic compartment while dephosphorylated in the distal region of the axon [33].

The Tau protein is involved mainly in the polymerization and stabilization of microtubules, thus participating in the organization and in the integrity of the cytoskeleton, in fact, it is able to increase the rate of polymerization of microtubules and inhibit the depolarization. Stabilizing them, Tau can confer resistance to the poisons of microtubules.

Tau binds to microtubules in two ways: when these are assembled binds to their outer surface [34], whereas when it is mixed with tubulin is incorporated into microtubules growing as an integral structure [35].

A neuronal Tau is involved in the polarity of neurons in axonal transport and neuritic in stretching. It seems that Tau and other MAP can act cooperatively to adjust the axonal elongation and neuronal migration, offsetting any defective role of the protein.

In the non-neuronal cells, Tau induces the formation of long cytoplasmic extensions [36]. Tau is also able to prevent the thermal denaturation of DNA, renaturing improve, protect it from damage induced by free radicals, suggesting a function of the chaperon like protein. Tau was found to be also an inhibitor of histone deacetylase 6 (HDAC6) which regulates the acetylation of tubulin. It has been shown that Tau interacts with many other proteins, including phosphatases, the serine/threonine kinase, the tyrosine kinase Fyn and scaffold protein 14-3-3, suggesting that Tau could play a role in regulating the location and function of other proteins. For example, it was shown that the formation of oligodendrocytes involves an interaction between Tau and Fyn and the recruitment of Tau by Fyn activated in rafts in membrane appears to be an important step in myelination, suggesting an essential role of Tau for the maturation of oligodendrocytes.

1.2.1 Post-Translational Modifications

Tau is a phosphoprotein predominantly expressed in neurons, where it is mainly localized to axons. Phosphorylation is developmentally regulated such that fetal Tau is more phosphorylated than adult brain Tau [37].
The most important post-translational modification of Tau in tauopathies is hyper phosphorylation, which has serious functional effects [38]. Normal Tau is phosphorylated on two or three residues in contrast to hyperphosphorylated Tau that is phosphorylated at least on eight residues, but there are further epitopes that may theoretically be phosphorylated [39]. Phosphorylation of Tau has an impact on microtubule stability and axonal transport, dendritic positioning and synaptic health, cell signaling at plasma membranes, protection of DNA from cells stressors and release of Tau; in particular, the most studied of these residues has been serine/threonine phosphorylation.
Tau is a phosphoprotein with 80 putative serine or threonine phosphorylation sites on the longest central nervous system (CNS) Tau isoform, which contains 441 residues. These sites have been divided into two main groups: those that can be modified by proline-directed kinases like Tau protein kinase I (GSK3), Tau protein kinase II (cdk5), MAP kinase (p38), JNK and other stress kinases or cdc2; and those that can be modified by non-proline directed kinases like PKA, PKC, CaM kinase II, MARK kinases [40-41] or CKII, which modifies residues close to acidic residues mainly in exon 2 and 3.Several phosphatases, such an protein phosphatase (PP)1, PP2A, PP2B (calcineurin) and PP2C [42-43] are able to dephosphorylate Tau protein.
However, only PP1, PP2 and PP2B have been shown to dephosphorylate abnormally hyperphosphorylated Tau. It seems probable that PP2A is the phosphatase that acts on most phosphorylation sites [43-44]. PP2A binds to Tau through its tubulin-binding region [45]. Mutations in that region could decrease the capacity of PP2A to bind to Tau, and consequently produce an increase in Tau phosphorylation, a feature that has been observed in some FTDP-17 patients bearing such mutations [46].
Further post-translational modifications of Tau include N- and C-terminal truncation, acetylation, glycosylation, oxidative and nitrative injuries, transglutamination, deamination and formation of Tau oligomers [47]. Phosphorylation of Tau is tightly regulated during development; it is high in fetal neurons (which contain only 3R Tau) and decreases with age due to the presence of adult isoforms and modification of the relationship between kinase and phosphatase, for activation of the phosphatase [48].
In addition, Tau is present in all cellular compartments, but with different phosphorylation states. Phosphorylation, correlated with the type of isoform, modulates the properties of Tau.

Tau is also responsible of the physical characteristics of microtubules (stiffness, length, and stability), organization of microtubules and modulation of neurons, in particular the polarity and axonal growth (Fig.3).

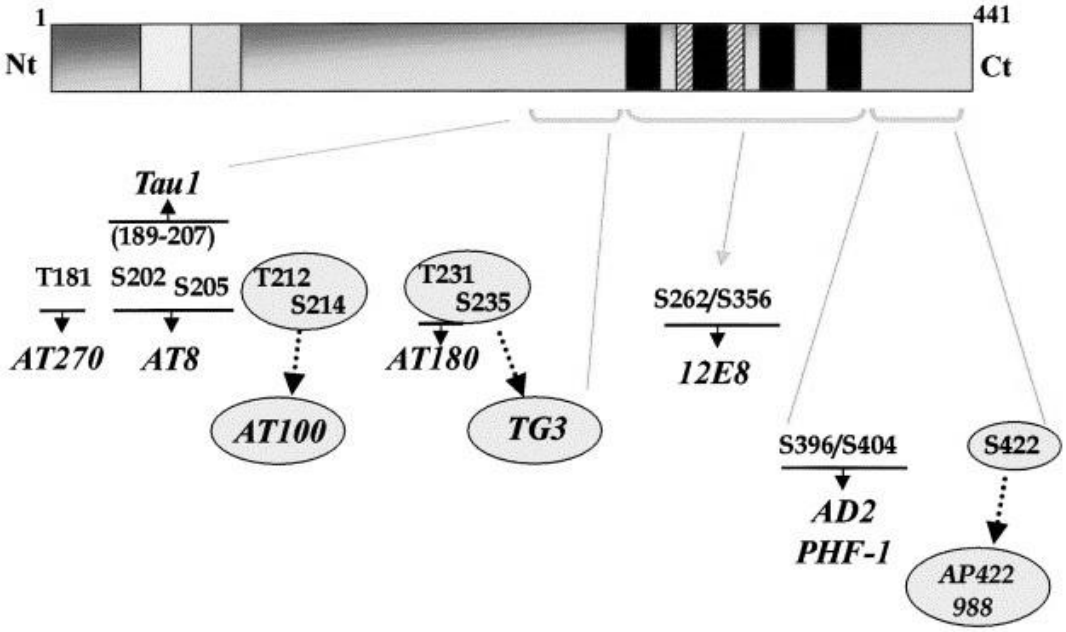

Figure 3: Schematic representation of the hyper phosphorylation sites (indicated as peptidic sequence) of the longest Tau isoform (2131101), and corresponding specific antibodies. Hyperphosphorylated sites are grouped in two clusters located on both sides of the microtubules binding domain, with the exception of Ser262/ Ser356. Phosphorylation-dependent antibodies (in italics) have been developed for each sites. AD-specific sites and corresponding antibodies are circled. Tau1 recognizes the dephosphorylated 189–207 amino acid sequence.

1.2.2 Pathogenetic Role of Tau

Although it was no clear the cause-effect relationship between errors in the MAPT gene and neuronal death and dementia, the molecular basis underlying the pathogenetic mechanisms of tauophaty are not yet known. It is known that changes in the amount or conformation of Tau can lead to the formation of hyperphosphorylated Tau and/or aggregate into insoluble tangles as was observed in Alzheimer's disease (AD), the most common tauophaty.
In the nerve cells affected are witnessing the shift of Tau from the axonal compartment that somatodendritic where it accumulates in the "pre-tangles", aggregated filamentous double helix (PHFs, Paired Helical Filaments) that eventually assembled in neurofibrillary tangles (NFT, neurofibrillary tangles) leading to neurodegeneration. There are several mechanisms that could lead to the pathogenic effect of the protein Tau (Fig.4).

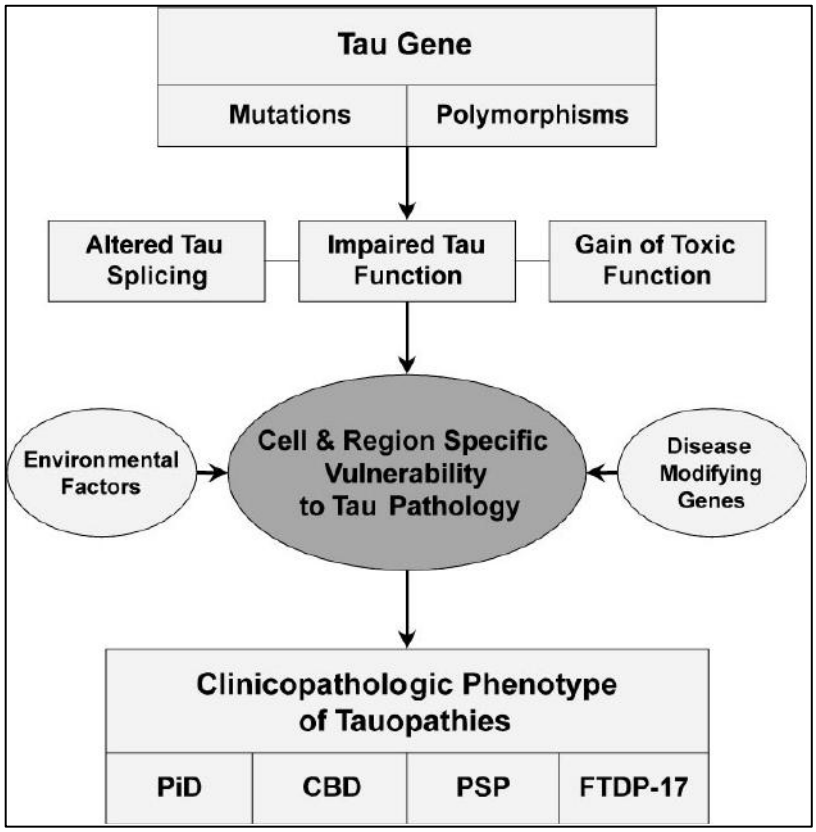

Figure 4: **Model of disease pathways in Tauopathies.** Model of disease pathways in tauopathies. Mutations and/or polymorphisms in the Tau gene in conjunction with environmental and additional genetic factors initiate pathogenic processes that cause regional and cell type–specific Tau pathology and neurodegeneration, thus leading to specific clinic pathologic phenotypes. PID, Pick's disease; CBD, corticobasal degeneration; PSP, progressive supranuclear palsy; FTDP-17, frontotemporal dementia and Parkinsonism linked to chromosome 17.

- **Aggregation of Tau**: the protein accumulates inside the cell and then associates to microtubules, making filaments enriched in β-sheet structures. Upon reaching the critical concentration, the monomers of Tau unfolded become by conformational changes oligomers, who will associate in neurofibrillary tangles, until the complete loss of cell viability and formation of "ghost tangles "fibrillar aggregates extra-cellular.
- **Increase of Tau**: the activity of the protein is in a range that must be controlled by homeostatic mechanisms, in order to ensure the neuronal survival. An increase of the protein could inhibit the transport of vesicles, neurofilaments and organelles in neurons [49] and, consequently, impair the axonal transport mediated by microtubules. Alterations in the amount or structure of Tau may also compromise its role in the stabilization of the microtubules, which in turn can affect the localization and organization other subcellular structures such as mitochondria or lysosomes.

The mechanisms for which the increased expression of 4R Tau involves neurodegeneration have not yet been identified, but it has been hypothesized that this increase in saturated sites binding to microtubules, and that the remaining Tau 4R soluble in excess is more susceptible to the phosphorylation and aggregation into insoluble filaments [50].

- **Toxicity of Tau**: the toxicity of Tau neurons was also correlated with conformational changes of protein, which could lead to the aggregation of the truncated protein, even if this hypothesis needs confirmation, from the moment that the human neurons can live for decades, while limiting the tangles neurofibrillary tangles [51]. Phospholipids, including arachidonic acid, are capable of inducing changes conformational protein that may facilitate the phosphorylation and increase the formation of filaments rights. The conformational changes may also make the filaments resistant to proteolysis, since the potential binding sites of the protease are hidden inside of the filaments becoming inaccessible, so that they can accumulate. The Tau protein isolated from the tangles, neurofibrillary tangles, is extensively modified at the post-transcriptional level by phosphorylation, glycation, racemization, and ubiquitination. Some of the modifications, such as phosphorylation, truncation and glycosylation, seem to occur at the early stage of tauophaty, while ubiquitination and glycation to be late events in the neurodegeneration. In any case, the hyperphosphorylation seems to be the modification more involved in the pathogenicity of the protein.

- **Hyperphosphorylation of Tau:** the hyperphosphorylation of Tau is not only associated with diseases, but is also used by the neuron to decrease transiently and reversibly its activity, as occurs during development. It is the state not reversible of abnormal hyper phosphorylation of Tau in tauophaty that involves an involuntary slowing of neuronal activity and the resulting chronic progressive neurodegeneration accompanied by the clinical phenotype of dementia [38]. The hyperphosphorylated Tau is prone to form aggregates, which can block the traffic intracellular neurotrophic protein and other functional proteins, giving as result in the loss or decline of transport axonal or dendritic arborisation in neurons [52]. The hyper phosphorylation of Tau induced by phosphatase inhibitors leads the aggregation and impairment of the biological activities. The pseudo phosphorylation Tau (PHP Tau), in which the residues of the serine/threonine are replaced with glutamate, which mimics the structural and functional aspects of the Tau hyperphosphorylated exhibiting, for example, a reduced interaction with the microtubules and failing in their stabilization.

1.3 Tauopathies and Mouse Models

Experimental and TG animal models of tauopathies have been developed as informative system for elucidating the role of abnormalities in Tau in the onset and progression of a variety of neurodegenerative disorders. In addition, they may be useful models for the development and testing of novel therapies.
Some models detailed below ablate the mouse Tau gene and thus the mice produce only human Tau, while others insert the human Tau gene but leave the endogenous murine gene intact. Thus, these model systems differ with respect to the presence of different ratios of mouse and human Tau isoforms, which complicates interpretation of findings in each of them. Many models also have cloned Tau transgenes that produce solely one isoform, which can further complicate comparisons between model systems. In addition to the splicing ratio difference, the N-terminal domain of the mouse Tau includes 14-amino-acid differences when compared to the human Tau.
The first transgenic mouse model for Tau expressing the isoform of the human wild-type longer (2N4R) under the control of the promoter of the human neuron-specific Thy1.
It was observed the formation of pre-tangles, the hyper phosphorylation of the Tau, but no neuropathological lesions. Another mouse model expressed the shortest human brain isoform of Tau, but it was found no NFTs in animals up to 19 months of age, attributing these findings to a pre-tangle stage of neurofibrillary pathology.
In this TG mouse model the human transgenic Tau remained abundant in cell bodies and dendrites of a subset of neurons in the adult, while the endogenous murine Tau gradually decreased during development [53]. The replacement of the human promoter with the murine (Thy1.2) has led to the appearance of axonal degeneration, but not neurofibrillary tangles or cognitive and locomotive impairment [54].
An increase of the expression of the transgene was achieved thanks to the use of the murine promoter PrP, which has allowed an increase of the expression of the Tau protein is about 10 times with the formation of inclusions similar to the NFTs in cortical neurons and in the brainstem, that are related to the degeneration and reduction of the axonal transport, gliosis, and weakness. Subsequently, a model has been created (JNPL3), which expressed the protein Tau changed P301L and that, for the first time, reproduced the formation and aggregation of the tangles neurofibrillary tangles in the brainstem, the diencephalon, but especially in the spinal cord, with a loss of about 50% of the neurons, and the resulting motor dysfunction [55-56].

The animals showed, in addition, gliosis, axonal degeneration and behavioral deficits. This is still the model the most used for the study of the mechanisms associated with Tau pathology.
In a very interesting study was used this model with a vector inducible, which gave the possibility of suppressing the expression of P301L transgene with the addition of doxycycline. The suppression of the transgene led to a recovery of functions in memory, and to a stabilization of the number of neurons, despite the continuing build-up of tangles neurofibrillary tangles.
This suggests that both the soluble Tau to be neurotoxic and not the NFTs, that alone is not sufficient to cause cognitive decline and neuronal death.
The neuronal loss is greater in mice that express the P301S mutation compared the P301L, in agreement with the early onset of the disease in patients with this mutation [57]. Filaments were also found in mice transgenic mice expressing the R406W mutations [58], and V337M [59].
A recent study has led to the emergence of a new and interesting aspect of Tau: his transmission, secretion, and diffusion. In fact, the extract brain-derived P301S mice and injected into mice ALZ17 (which express the Tau WT and that, consequently, do not develop NFT) induces the formation of NFT that do not remain confined to only the site of the injection.
Therefore, it seems that there is induction of the pathology, which would be responsible for the insoluble Tau. The theory is supported by a similar study that shows how the aggregated Tau can transmit the status fibril/not correctly folded from the outside to the inside of cells, in a manner similar to the prion.
Patients with FTD show the presence of Tau inclusions in oligodendrocytes that in astrocytes. For this reason, some studies have tried to reproduce this characteristic in vivo through the expression of human Tau P301L and WT under the control of the promoters of the 2',3'-cyclic nucleotide 3'-phosphodiesterase [60] and protein of glial fibrillary acidic (GFAP) respectively [61]. Both lines exhibit neuronal dysfunction and degeneration axonal, showing that the glial pathology also affects the neurons.
In our study, we decided to use the model discovered by Lewis (P301L TG mice) in order to investigate the cognitive impairment and behavioral deficits associated to tauophaty.

Table 2: transgenic mouse models

Gene	Promoter	Tau Pathology	Phenotype	Reference
Tau, 4R/2N	Thy1	Somatodendritic tau expression	Normal	Götz et al (1995)
Tau, 3R/0N	HMG-CoA reductase	Somatodendritic tau expression		Brion et al (1999)
Tau, 3R/0N	Prion protein	Somatodendritic tau expression; tau immunoreactive spheroids in brain and spinal cord; neurofibrillary tangles in brain at 18 months or older	Axonopathy with muscle weakness	Ishihara et al (1999, 2001)
Tau, 4R/2N	Thy1	Somatodendritic tau expression; tau immunoreactive spheroids in brain and spinal cord	Axonopathy with sensori-motor dysfunction	Spittaels et al (1999)
Tau, 4R/2N	Thy1	Somatodendritic tau expression; tau immunoreactive spheroids in brain and spinal cord	Axonopathy with muscle weakness	Probst et al (2000)
Tau, 4R/0N, P301L	Prion protein	Neurofibrillary tangles in brain and spinal cord; somatodendritic tau expression	Motor and behavioral deficits; amyotrophy	Lewis et al (2000)
Tau, 4R/2N, P301L	Thy1	Neurofibrillary tangles in brain and spinal cord; somatodendritic tau expression		Götz et al (2001)
Tau, genomic	Endogenous	Axonal expression	Normal	Duff et al (2000)
ApoE4	Multiple	Phosphorylated tau expression in neocortex, hippocampus, and amygdala	Motor dysfunction and amyotrophy	Tesseur et al (2000)
p25	Neuron specific enolase	Phosphorylated tau expression in cortex, amygdala, and thalamus	Increased loco-motor activity	Ahlijanian et al (2000)
Anti-NGF IgH/Igκ	Cytomegalovirus early region	Phosphorylated tau expression in cortex and hippocampus with associated neuron loss	Spatial memory and object recognition impairment	Capsoni et al (2000)

1.4 Tauopathies and Oxidative Stress

Oxidative stress is a pathological condition caused by the rupture of the physiological equilibrium in a living organism between the production and the elimination, on the part of the antioxidant defense systems, of oxidant chemical species. In all aerobic organisms, there is a delicate balance, said oxidation-reduction, including the production of oxidants, such as reactive oxygen species (ROS), and the antioxidant defense system, which has the duty to prevent and/or repair any damage caused.

Possible disturbances in this normal state red-ox may have toxic effects for the production of free radicals and reactive oxygen and nitrogen species, which damage all cell components, including proteins, lipids and DNA. The reactive species and free radicals play important physiological roles, such as the defense against bacteria, the transmission of biochemical signals between cells, the blood pressure control etc.

It is only their excess, generally refers to one or more classes of oxidants, to be involved in oxidative stress, today considered associated with more than a hundred human diseases (such as retrolental fibroplasia, atherosclerosis, hypertension, Parkinson's disease, Alzheimer's, diabetes mellitus, colitis, rheumatoid arthritis, etc.), and it may also be important in the aging process [62-63].

ROS and other reactive species are continuously produced by the organism through numerous biochemical processes [64]. Certain amount of oxidizing substances is in fact indispensable to maintain the proper functioning cellular mechanisms regulating its homeostasis. During the reactions of oxygen reduction, however, the reactive species generated can exceed the physiological threshold. If these molecules are not neutralized by antioxidants systems, can be established damage within the cell, capable of conducting the same apoptosis.

Therefore, if it generates an imbalance between the production of ROS and the effectiveness of the system antioxidant defense, it establishes a condition of oxidative stress, as shown in Figure 5.

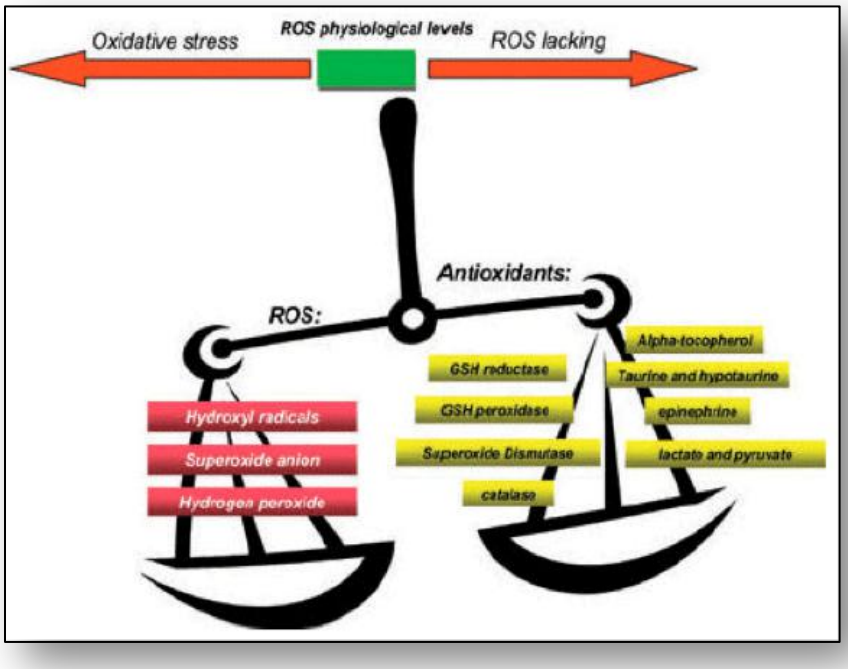

Figure 5: Modification of the normal balance between ROS and antioxidants

The central nervous system is an organ particularly vulnerable to oxidative damage: it is rich in fatty acids easily peroxidable (20: 4; 22: 6); is responsible for about 20% of the total consumption of oxygen despite its weight is equal to 2% of total body weight; possesses poor antioxidant systems (catalase activity present in the encephalon is about 10% of the liver) and otherwise has a high content of iron and ascorbate ions which form powerful pro-oxidant compounds for cell membranes.

Among the many neurological diseases in which oxidative stress may be involved, the neurodegenerative diseases play a major role because they share certain characteristics that predispose to oxidative stress and enhance it by triggering cascade mechanisms.

These characteristics are:

- neuroinflammation: activated microglia release nitric oxide, which in the presence of reactive oxygen species form peroxynitrite and other products nitrosylation;
- protein misfolding;
- the altered homeostasis of metal ions (Zn, Iron, Copper ..);
- altered mitochondrial function.

There are many studies showing that levels of oxidative stress markers in tissues increases during the progression of the disease and that there is evidence documented by immunocytochemistry autopsies of oxidative damage to bio macromolecules in brain regions affected by the disease.
The central issue is whether oxidative stress is a consequence of the degenerative process started by some other factor, such as genetic, or by itself as an early event that contributes fully to the etiology of the disease. Oxidative damage is the most common cause of cell death, and is one of the first event in patients with AD.
It has been reported that the oxidative damage decreases with the progression of the disease and the formation of tangles, neurofibrillary tangles [65], and it has been proposed that the presence of tangles neurofibrillary tangles in AD protect the cellular components crucial from the attack of reactive species oxygen (ROS).
These results indicate that the formation of tangles, neurofibrillary tangles, may represent a compensatory response to reduce the damage associated with ROS. In fact, the phosphorylation of Tau, the most regulated during oxidative stress [66], and Tau is modified by the products of oxidative stress, including the 4-hydroxy-2-nonenal (HNE) [67-68].
The aggregation of Tau is also facilitated by oxidative adducts, although other studies have shown that some of the oxidants lead to the reduction of the phosphorylation of Tau. Therefore, it appears that, depending on the specific oxidants, you may induce either an increase or a decrease in the phosphorylation of Tau.
Most of the researches about unemployment insurance are focused on the mechanism of oxidative stress and its importance in the pathogenesis of the disease. Multiple lines of evidence suggest that oxidative stress and free radical damage is implicated in the pathogenesis and etiology of AD. The first evidence to support the hypothesis of oxidative stress in AD is based on the discovery that metals are responsible for most of the production of free radicals. The chemical elements of most interest in AD are iron (Fe), aluminum (Al), mercury (Hg), copper (Cu) and zinc (Zn). The Fe is involved in the formation of the hydroxyl radical, which has deleterious effects as described by the Fenton reaction and the Haber-Weiss [69].
Several studies have shown alteration in the metabolism of Fe in brain of AD patients [69]. By techniques of histochemistry, it was found increased levels of Fe in the cerebral cortex of subjects suffering from the disease; in particular, it has been observed that the distribution of the Fe reflects the distribution of NFTs and amiloid plaques, the two key elements of the AD.
Iron, ferritin and transferrin were found in SP of AD patients and ferritin is present in microglia in association with amiloid plaques in AD.

A study by Kennard and collaborators, in 1996, showed, in AD patients, a high concentration in the cerebrospinal fluid and plasma protein p97, a protein binding of Fe, which could be a marker of the disease.
The possibility of the involvement of Cu in AD is supported by the fact that the ion can act as a catalyst in the production of ROS, and was put in evidence that APP molecules contain binding sites for the Cu.
The APP reduces Cu^{2+} to Cu^{+} and this could increase the production of OH^{-} which, in turn, lead to neuronal damage.
In fact, this metal is essential in the activity of many enzymes including cytochrome c oxidase (COX) and superoxide dismutase copper / zinc (Cu / Zn SOD). Recent studies show low concentrations of Cu in five regions of the brain of AD patients, particularly at the level of the hippocampus and amygdala [69].
The last metal cited as a possible factor of the development of AD is Zn, which induces rapid staining of amyloid plaques in humans, but not in rats.
The APP binds Zn^{2+} and this binding modulates the functional properties of the secretases (eg. β inhibits the cutting of APP by β-secretase).
Very important is the effect it has on the ROS membrane phospholipids; alterations in these structures may be specific for the pathogenesis of the disease.
It has been shown that lipid peroxidation is the major cause of the depletion of membrane lipids in AD. One of the products of lipid peroxidation, HNE has been found in high concentrations in AD patients, it is found to be toxic in cells of the hippocampus in culture.
Regarding protein oxidation, it was found that there are differences in the levels of oxidized proteins in the brain tissue of AD patients when compared with normal elderly controls [70].
In conclusion, the oxidative stress and its responses can:
1- activate pro- inflammatory networks that exacerbate organelle dysfunction and pro-apoptosis mechanisms;
2- stimulate APP gene expression and β-APP cleavage, resulting in increased formation of APP-Aβ neurotoxic fibrils;
3- activate or dis-inhibit GSK-3β, which promotes Tau phosphorylation.

1.5 Tauopathies, Oxidative Stress and Dietary interventions

Recent studies suggest that physical exercise and diets low in calories and 'bad' fats (cholesterol and saturated fats) [71-72-73] and high in "good" fats (polyunsaturated fatty acids from fish oil) may reduce the risk of AD and neurodegenerative diseases [75-75].
Because the underlying pathologies may start years before the cognitive and behavioral impairments are clinically evident, application of the knowledge on preventive nutritional strategies warrants early identification of the disease to be able to intervene and delay, or even prevent its onset.
Although epidemiological studies sometimes report conflicting results, specific associations between nutritional components and the risk for AD have been found. These include the potential protective effects of specific polyunsaturated fats, B-vitamins and antioxidants [76].
These macro- and micronutrients are dietary components that can influence brain structure and function [77-78].
Nutritional intake may provide specific nutrients that can be used as building blocks for membrane and synapse formation and neurotransmitter production but can also directly influence the availability of nutrients, energy and oxygen to the brain.
The neuronal loss and Tau protein pathology in the AD brain, as well as possible dysfunction of the cerebrovascular system and energy metabolism, may act together to accelerate the downhill cascade in cognitive and behavioral function.
The potential of nutrition for neuronal maintenance rather than as an energy substrate is illustrated by the increasing evidence that nutrients not only stimulate neural plasticity, but also ameliorate the ongoing neurodegenerative process and show the ability to reduce the pathological burden in the brain. Additional mechanisms by which high fat/energy diets impair cognitive function are beginning to be elucidated and involve adverse effects on synaptic plasticity and neurogenesis (Fig. 6). The central nervous system (CNS) is particularly vulnerable to damage from free radicals for various reasons that include a limited effectiveness of the system antioxidant and a high consumption of oxygen to produce energy. Furthermore, the brain tissue, when compared with other tissues, presents abundant lipid content, particularly polyunsaturated fatty acids (PUFAs) which are highly susceptible to lipid peroxidation process [79-80].

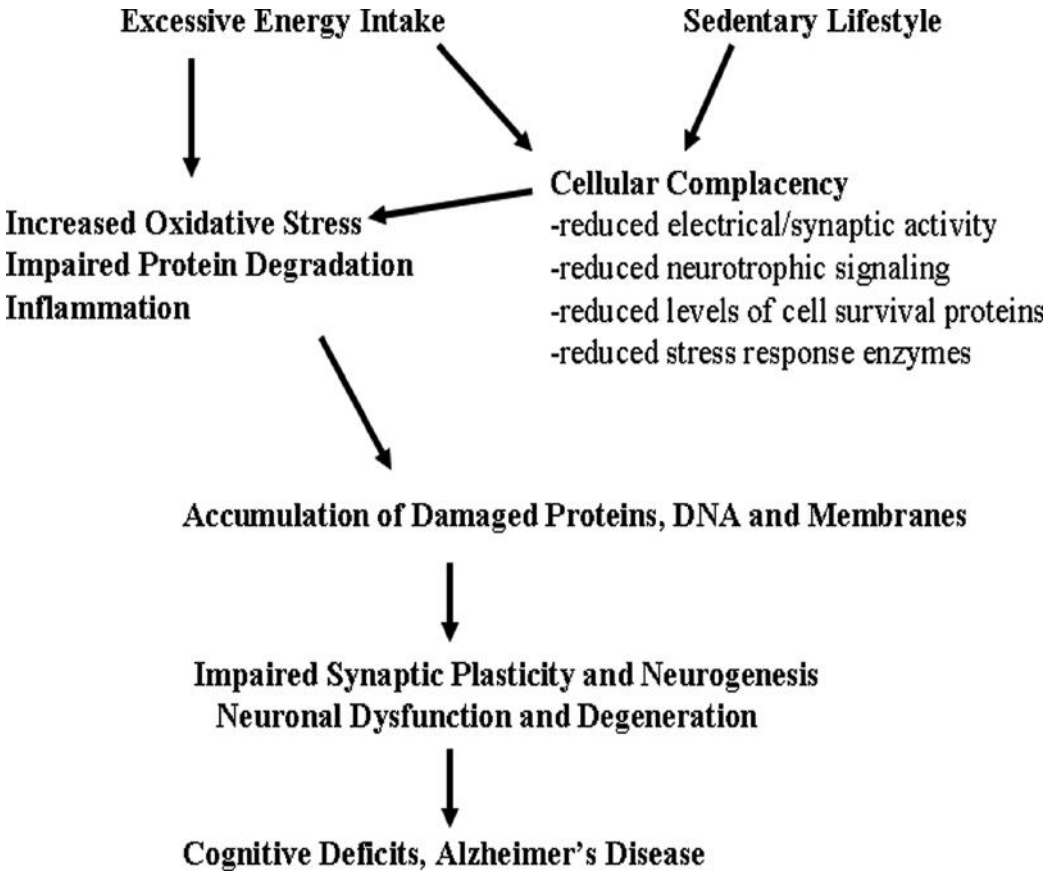

Figure 6: Mechanisms by which excessive energy intake and low levels of energy expenditure adversely affect synaptic plasticity and cognitive function.

PUFAs are involved not only as structural constituents of the membrane lipids of neuronal cells, but also for their neuro-protective, anti-oxidants and anti-inflammatory effects. The long-chain polyunsaturated fatty acids exist of two key families: omega-3 and omega-6; high total fat intake, in particular that of omega-6 saturated fatty acids are associated with poor cognitive performance and present a risk factor for AD [81-82].

The brain is extremely rich in PUFAs, particularly omega-3 fatty acids, and on average 1 out of every three fatty acids is a PUFA of dietary origin. A higher ratio of omega-6 to -3 PUFA is also associated with decreased insulin sensitivity and Diabetes Mellitus Type II. One mechanism linking the intake of high total fat and saturated fat intake to cognitive impairment and dementia may be through the development of insulin resistance [83]. Insulin resistance leads to deficiencies in energy metabolism and increased oxidative stress [83-84-85]. Very high levels of fatty acids and lipids can be found in the neuronal membrane and the myelin sheath; particularly the omega-3 fatty acids, eicosapentaenoic acid (EPA) and docosahexaenoic acid (DHA), are incorporated into neuronal phospholipids (mostly phosphatidyl ethanolamine and phosphatidyl serine) [86].

Incorporation of omega-3 fatty acids in the neuronal membrane increases fluidity of neuronal membranes and herewith improves neurotransmission and signaling via increased receptor binding and enhancement of the number and affinity of receptors and function of ion channels.
Omega-3 fatty acids increase membrane fluidity by replacing omega-6 fatty acids and cholesterol from the membrane [87] maintaining an optimal membrane fluidity as obligatory for neurotransmitter binding and signaling within the cell.
Large amounts of DHA are necessary during brain development, for neural membrane production used for synaptogenesis, axonal and dendritic outgrowth, in both brain and retina [88]. A decreased level of plasma DHA is associated with cognitive impairment with aging [89-90] and does not seem to be limited to AD patients.
There are several possible reasons for this decline: a decrease in the ability of dietary fatty acids to cross the blood brain barrier due to impaired transport function in aging, or lipid peroxidation caused by enhanced free radicals [91], decreased dietary intake or impaired liver docosahexaenoic acid shuttling to the brain. The deficiency affected mostly the cortex and hippocampus, areas that mediate learning and memory. DHA is able to shift cholesterol from the neuronal membrane increasing membrane fluidity, but an increase in membrane cholesterol due to the age or a hypercholesterolemic diet can may contribute to loss of neuronal functionality.
In addition, it has been shown that one of the types of toxicity at the level of the nervous structures rich in polyunsaturated lipids resulting from hydroxynonenal (HNE), product of lipid peroxidation that form adducts with glutathione and proteins. There is a strong correlation between nutrition and oxidative stress, being oxidative stress the result of an uncontrolled production of ROS or RNS that alters the structure of lipids, proteins and nucleic acids.
Particular attention is paid to the role of proteins as the reactive species oxygen can interact with amino acid residues, in particular histidine, arginine and lysine, forming carbonyl functions. Some researchers have found that brain levels of these compounds increase with aging without, however, note a significant difference between the tissues from elderly subjects and tissues of AD patients.
Subsequent studies, however, would indicate a greater presence of carbonyl proteins in hippocampus and in the inferior parietal lobule of the brain of AD patients [92]. Excessive glycol-oxidation of proteins could be an early event of cell neurodegeneration. The monosaccharides can induce an irreversible modification of proteins by two distinct mechanisms: the first is the formation of free radicals in the presence of transition metals, and this may give rise to reactive carbonyl groups, the second includes the involvement of a non-enzymatic glycation which results in the formation of stable compounds known as final compounds of glycation or AGE [92].

In neurodegenerative diseases a diet with a high protein content not only causes damage in the brain (as previously described), but also in peripheral organs such as the liver. Since the ROS free radicals implicated in oxidative stress, since mitochondria are a major source of ROS, an increased supply of protein can cause an increase in the production of mitochondrial ROS and can trigger oxidative stress in the liver. While ROS are able to cause cell death through a massive lipidic peroxidation which destroys the cell membranes [93-94], mostly they are implicated in the modulation of signal transduction pathways, influencing enzymes sensitive to the redox potential, organelles such as mitochondria, and transcription factors, thereby regulating or inducing cell death by apoptosis and necrosis.
Thus oxidative stress generated by ROS can activate the way of c-Jun-N-terminal kinase (JNK) and caspases to trigger apoptosis. It is therefore evident the importance of a correct nutritional intake in neurodegenerative diseases, balancing in particular the content of fatty acids and proteins to try to prevent or reduce the incidence of pathologies, both at the central level both at the peripheral level.
The importance of nutrition is also supported by animal studies in which cognition stimulating environments, exercise and caloric restricted diets inhibit neurodegeneration, enhance neurogenesis and improve cognition and furthermore, the intake of high cholesterol diets influence AD pathology and cognition in animal models [95- 96].

1.6 Diets of Laboratory Animals (mouse)

A laboratory animal's nutritional status influences its ability to reach its genetic potential for growth, reproduction, and longevity and to respond to pathogens and other environmental stresses. A nutritionally balanced diet is important both for the welfare of laboratory animals and to ensure that experimental results are not biased by unintended nutritional factors.
Laboratory animals require about 50 nutrients in appropriate dietary concentrations; feed palatability and intake, nutrient absorption and utilization, and excretion can be affected by physicochemical characteristics of feeds such as physical form, sensory properties, naturally occurring refractory or not nutritive compounds, chemical contaminants, and conditions of storage.
Laboratory animals most commonly used are: mouse, rat, hamster, guinea pig, gerbil and vole; we decide to describe the model used in this study: the mouse model. The nutrient requirements of mice (table 3) have been defined by several different criteria including growth, reproduction, longevity, nutrient storage, and enzyme activity, gross or histological appearance of tissue lesions.

Traditionally, rapid growth leading to maximum body size at maturity has been the basis for measuring dietary adequacy on the assumption that a diet promoting maximum growth would be adequate for reproduction, lactation, and maintenance.

Table 3: Estimated Nutrient Requirements of Mice

Nutrient	Unit	Amount, per kg diet	Comment/Reference
Lipid	g	50.0	
Linoleic acid	g	6.8	
Protein (N × 6.25)			
Growth	g	180.0	Equivalent to 20% casein supplemented with 0.3% DL-methionine or 24% casein
	g	200.0	Casein (see text)
Reproduction	g	180.0	Natural-ingredients
Amino acids			
Arginine	g	3.0	See text
Histidine	g	2.0	See text
Isoleucine	g	4.0	See text
Leucine	g	7.0	See text
Valine	g	5.0	See text
Threonine	g	4.0	See text
Lysine	g	4.0	See text
Methionine	g	5.0	Cystine may replace 50-66.6%
Phenylalanine	g	7.6	Tyrosine may replace 50%
Tryptophan	g	1.0	Niacin may replace 0.025% (see text)
Minerals			
Calcium	g	5.0	
Chloride	g	0.5	
Magnesium	g	0.5	0.7 g/kg for lactation (see text)
Phosphorus	g	3.0	
Potassium	g	2.0	Higher concentrations may be required for lactation (see text)
Sodium	g	0.5	
Copper	mg	6.0	8.0 mg/kg for pregnancy and lactation
Iron	mg	35.0	
Manganese	mg	10.0	
Zinc	mg	10.0	30 mg/kg for reproduction and lactation
Iodine	µg	150.0	
Molybdenum	µg	150.0	
Selenium	µg	150.0	Selenite form of Se
Vitamins			
A (retinol)[a]	mg	0.72	Santhanam et al., 1987
D (cholecalciferol)[b]	mg	0.025	Adequate; no quantitative data
E (*RRR*-α-tocopherol)[c]	mg	22.0	Yasunaga et al., 1982
K (phylloquinone)	mg	1.0	Based on the requirement for the rat; Kindberg and Suttie, 1989
Biotin (*d*-biotin)	mg	0.2	Adequate; Fenton et al., 1950
Choline (choline bitartrate)	mg	2,000.0	Adequate; insufficient data to establish requirement
Folic acid	mg	0.5	Fenton et al., 1950; Heid et al., 1992
Niacin (nicotinic acid)	mg	15.0	Based on the requirement for the rat; Hundley, 1949
Pantothenate (Ca)	mg	16.0	Morris and Lippincott, 1941, suggest 36 mg/kg for reproduction and lactation
Riboflavin	mg	7.0	Adequate; insufficient data to establish requirement
Thiamin (thiamin-HCl)	mg	5.0	
B_6 (pyridoxine-HCl)	mg	8.0	1 mg/kg for maintenance
B_{12}	µg	10.0	Adequate; insufficient data to establish requirement

NOTE: Nutrient requirements are expressed on an as-fed basis for diets containing 10% moisture and 3.8 to 4.1 kcal ME/g (16–17 kJ ME/g) and should be adjusted for diets of differing moisture and energy concentrations. Unless otherwise specified, the listed nutrient concentrations represent minimal requirements and do not include a margin of safety. Higher concentrations for many nutrients may be warranted in natural-ingredient diets.
a Equivalent to 2,400 IU/kg of diet.
b Equivalent to 1,000 IU/kg of diet.
c Equivalent to 32 IU/kg.

Diet formulation is the process of selecting the kinds and amounts of ingredients (including vitamin and mineral supplements) to be used in the production of a diet containing planned concentrations of nutrients. Choice of ingredients will be influenced by the species to be fed and the experimental or production

objectives. Various types of diets are available for use with laboratory animals. Selection of the most appropriate type will depend on the amount of control required over nutrient composition, the need to add test substances, potential effects of feed microbes, diet acceptance by the animals, and cost.
It is common to classify diets for laboratory animals according to the degree of refinement of the ingredients.

- **Natural-Ingredient Diets**: diets formulated with agricultural products and by-products such as whole grains (e.g., ground corn, ground wheat), mill by- products (e.g., wheat bran, wheat middlings, corn gluten meal), high protein meals (e.g., soybean meal, fishmeal), mined or processed mineral sources (e.g., ground limestone, bone meal), and other livestock feed ingredients (e.g., dried molasses, alfalfa meal) are often called natural-ingredient diets.
- **Purified Diets**: Diets that are formulated with a more refined and restricted set of ingredients are designated purified diets. Only relatively pure and invariant ingredients should be used in these formulations (for examples of such ingredients are casein and soybean protein isolate as sources of protein).
- **Chemically Defined Diets**: diets have been made with the most elemental ingredients available, such as individual amino acids, specific sugars, chemically defined triglycerides, essential fatty acids, inorganic salts, and vitamins.

Diets for laboratory animals can be provided in different physical forms. The most common form in use for laboratory animals is the pelleted diet, which is typically formed by adding water to the mixture of ground ingredients and then forcing it through a die. The size and shape of the holes in the die determine pellet shape and rotating blades control the length; the diet is then dried to firmness. Extruded diets are similar to pelleted diets except the meal is forced through a die under pressure and at high temperature after steam has been injected, so the product expands as it emerges from the die.
Diets in meal form are sometimes used because they permit incorporation of additives and test compounds after the diet has been manufactured. Natural-ingredient diets for mice is the most common type of diet used in scientific research; it was calculated that a mouse consumes an average of 3.5 g diet/day during 14 days post weaning and the metabolizable energy (ME) content was estimated to be 3.9 kcal/g diet (16.2 kJ/g diet).
To define the concentration of essential lipids in the diet for the needs of the mouse, Bossert et al. (1950) demonstrated that weanling (Dohme and Swiss-Webster strains) mice gained weight equally well when fed diets containing 0.5 to

40 % fat; all diets contained 0.5 % corn oil with the remainder of the fat supplied by hydrogenated cottonseed oil and 0.68 percent linoleic acid.
Typical diets fed to mice contain high concentrations of carbohydrate, although diets containing no carbohydrate (83 percent protein) have been shown to support growth rates of 0.1 g/day from 4 to 16 weeks of age in normal mice [97].
The requirement for protein to support maximal growth or reproduction depends on the content and digestibility of the amino acids in the diet and the growth and reproductive potential of the mice in question [98]. Growth rates of mouse strains used in research range from 0.6 to 1.2 g/day and litter size may vary from three to seven. The estimated requirement for a single amino acid depends on the amounts of other amino acids in the diet and the rate of growth. With the exception of D-lysine and probably D-threonine, the L-indispensable amino acid requirement may be met, in part, by D-amino acids.
The concentration of amino acids in these diets exceeds the estimated requirement (National Research Council, 1978) by 25 to 200 %. Reports regarding the quantitative calcium and phosphorus requirements of mice have not been published; therefore, the estimated requirements for these minerals are based on the dietary concentrations that have resulted in acceptable performance in mice. Natural-ingredient diets containing 12 g Ca/kg and 8.6 g P/kg [99] also have been reported to support growth and reproduction in different strains of mice. Magnesium has been shown to be a dietary essential for mice, but the optimal intake for this species has not been well established.
Sodium and chloride requirements of mice have not been studied.
Two natural-ingredient diets containing 3.6 and 4.9 g Na/kg diet [99] and a purified diet containing 3.9 g Na/kg diet are known to support good growth and reproduction. However, the estimated requirement for sodium and chloride is 0.5 g Na/kg diet and 0.5 g Cl/kg diet. Sorbie and Valberg (1974) reported that iron concentrations of 25 to 100 mg Fe/kg diet supported normal growth and hematopoiesis in male C57BL/6J mice, although, liver iron storage in these animals was low compared to mice fed natural-ingredient diets containing between 220 to 240 mg Fe/kg diet. The vitamin A (retinol) requirement of the mouse seems to be similar to the requirement of the rat; a dietary concentration of 2,400 IU/kg diet (2.5 µmol/kg diet; 0.72 mg/kg diet) is adequate to meet the requirements of the mouse. For the vitamin D, a dietary concentration of 0.025 mg cholecalciferol/kg (0.65 µmol or 1,000 IU/kg) (American Institute of Nutrition, 1977) is adequate to meet the requirements of the mouse.
The vitamin E requirement for mice is estimated to be 22 mg/kg or 32 IU/kg RRR - α-tocopherol/kg diet (50 µmol/kg diet) when lipids comprise less than 10 percent of the diet; the estimated requirement of vitamin K for mice is 1 mg phylloquinone/kg diet (2.22 µmol/kg diet).

CHAPTER 2

Objectives

2. OBJECTIVES

The aim of this study was to investigate the effects of two different diets, whose most important variables are constituted by the different protein and fat content (diet 1: 18% protein and 5% fat, diet 2: 14% protein and 3.5% fat) on survival, locomotor and exploratory activity and cognitive and mnemonic abilities in transgenic mice affected by tauophaty (P301L) and relative control mice, with the purpose to analyze the interaction nutrition-neurodegeneration, checking whether different diets can:
- change of development of pathology;
- change the incidence of diseases related to sex, age and overweight;
- improve the well being of the animals.

For this purpose, we decided to divide our work in four items, starting from the characterization of our transgenic mouse model, assessing then in our mouse model the effect of different diets, the interaction between oxidative stress, diets and tauophaty and finally investigating the interaction between disturbance of the metabolism and tauophaty.

2.1 CHARACTERIZATION OF P301L TG MICE

The aim of this study was investigated the interaction between gender, genotype and progression of neurodegenerative disease in males and females P301L TG mice and B6D2F1 control mice at 7 and 15 months of age, evaluating the growth curve of the body weight, survival rate, cognitive and locomotor impairment, immunohistochemical localization and deposition of hyperphosphorylated Tau, neuronal loss and astrogliosis in the brain.

2.2 EFFECT OF DIFFERENT DIETS IN P301L TG MICE

After the characterization of our mouse model, it was decided to investigate the effect of two different diets (high and low fat-protein diet) on the onset and development of neurodegenerative disease in males and females P301L TG mice and B6D2F1 control mice at 7 and 15 months of age, evaluating the growth curve of the body weight, survival rate, cognitive and locomotor impairment, immunohistochemical localization and deposition of hyperphosphorylated Tau, neuronal loss and astrogliosis in the brain.

2.3 INTERACTION BETWEEN OXIDATIVE STRESS, DIETS AND TAUOPATHY IN P301L TG MICE

Since it is known in the scientific community as oxidative stress is a pathological condition associated with neurodegenerative diseases, it was decided to investigate a possible link between oxidative stress and tauophaty, considering how different diets administered to males and females P301L TG mice and B6D2F1 control mice at 7 and 15 months of age can change the oxidative damage. We investigated these interactions evaluating immunohistochemical localization and deposition of nitrotyrosine, acrolein and nitric oxide (NOS2 and NOS3).

2.4 CORRELATION BETWEEN OXIDATIVE STRESS, DIETS AND TAUOPATHY IN P301L TG MICE: A CASE OF METABOLIC SYNDROME

During necropsy analysis was detected a condition of hepatomegaly associated with hepatic steatosis in transgenic mice fed with a high fat-protein diet (diet 1) both male and female at 7 and 15 months of age. So we decided to investigate a possible interaction between diet, sex and disease, evaluating: macroscopy and histology of various tissues such as liver and spleen, the concentration of cholesterol, triglycerides, alanine aminotransferase and aspartate aminotransferase in plasma of males and females P301L TG mice and B6D2F1 control mice at 7 and 15 months of age.

CHAPTER 3

Interaction between gender and genotype in a mouse model of tauophaty: increase of cognitive impairment and locomotor dysfunctions in young and aged females Tau P301L mice

Submitted for publication to Plos One (December 2015)

3. Interaction between gender and genotype in a mouse model of tauophaty: increase of cognitive impairment and locomotor dysfunctions in young and aged females Tau P301L mice

AUTHORS*:* L. Buccarello[1], G. Grignaschi[2], A. Di Giancamillo[1], C. Domeneghini[1]
[1]Department of Health, Animal Science and Food Safety, Università degli Studi di Milano, Milan, Italy
[2]Department of Animal welfare, IRCCS-Mario Negri Institute for Pharmacological Research, Milan, Italy

3.1 ABSTRACT

Mice expressing P301L mutant Tau mimics features of human tauopathies and provides a model for investigating the neuropathogenesis of diseases. We had investigated the interaction between gender, genotype and progression of neurodegenerative disease in males and females P301L TG mice and B6D2F1 control mice at 7 and 15 months of age, evaluating the growth curve of the body weight, survival rate, cognitive and locomotor impairment, immunohistochemical localization and deposition of hyperphosphorylated Tau, neuronal loss and astrogliosis in the brain.
Compared to control mice, P301L TG mice had a decreased body weight and a reduced survival rate, with an interaction between gender and genotype more pronounced in females than males in either time points. The behavioral analysis had revealed that in novel object recognition test P301L TG mice shown a cognitive impairment across the ages tested, with a further reduction of discriminatory activity at 15 months of age most marked in males than in females. In the open field test, compared to control mice, P301L TG mice had a reduced locomotor activity across the ages tested and a further reduction of exploration activity at 15 months of age. Females P301L TG mice showed a greater reduction in locomotor and exploratory performance than males age-related. Immunohistochemical analysis revealed in the cortex and hippocampus of P301L TG mice the presence of aggregates of hyperphosphorylated Tau, reactive gliosis and neuronal loss age dependent. These results indicated that the P301L TG mice replicates the impairments found in patients affected by Tauophaty in a way age-gender-dependent. The finding that females were more affected than males suggests that more attention should be paid to sex differences in transgenic P301L mice for future potential treatments for tauopathies.

Keywords:
AD: Alzheimer disease, CTR: control, FTDP-17: familiar frontotemporal dementia, MAPT: microtubule-associated protein Tau, NFTs: neurofilaments, PP1: protein phosphatase 1, PP2A: protein phosphatase 2A, TG: transgenic

3.2 INTRODUCTION

Tau aggregation is a common feature in Alzheimer's disease (AD), frontotemporal dementia, and other tauopathies. The identification of Tau mutations has helped establish that Tau dysfunction is important to the neurodegenerative processes leading to dementia [1]. The most frequent human Tau mutation, *P301L* [2], results in the production of an aggregation-prone form of the protein. Expression of pathogenic P301L-Tau in mice results in the formation of Tau aggregates and neurofibrillary tangles, similar to those observed in AD brains; P301L-Tau was previously demonstrated to promote the assembly and accumulation of abnormal and insoluble Tau that triggers neuronal degeneration and loss [3].

Tauopathies are neurodegenerative disorders characterized by the accumulation of abnormal Tau protein leading to cognitive and/or motor dysfunction [4]. The progressive accumulation of Tau protein in tauopathies such as Alzheimer's disease (AD), progressive supranuclear palsy, corticobasal degeneration, and familiar frontotemporal dementia (FTDP-17) implicates Tau as one of factors in neurodegeneration. The discovery of mutations in the Tau gene in FTDP-17 established that dysfunction of Tau alone causes neurodegeneration and leads to dementia [5-6-7].

Tau is a phosphoprotein and its biological activity is regulated by the degree of its phosphorylation, and in turn the phosphorylation rate regulates the interaction with tubulin and the promotion of microtubule assembly [8-9]. The control of Tau phosphorylation is a complex mechanism that includes the activity of several Ser/Thr kinases [10] and phosphatases, whose inhibition has been suggested as one mechanism by which Tau acquires its hyperphosphorylated state during the neurodegenerative process [11]. Both protein phosphatase 1(PP1) and protein phosphatase 2A (PP2A) associate with and dephosphorylate Tau with PP2A, accounting for 70% of the Tau phosphatase activity in the brain [12-13-14]. FTDP-17 mutations reduced the interaction between PP2A and Tau, suggesting another route by which these mutations would result in hyperphosphorylation and disease [15]. Really, abnormally hyperphosphorylated Tau polymerizes into straight filaments and paired helical filaments, which aggregate to form neurofibrillary tangles (NFTs), a neuropathological hallmark of many neurodegenerative diseases.

Many models (both knock out and transgenic murine animal models) of tauophaty have been developed: some models ablate the mouse Tau gene and display only human Tau, while others insert the human Tau gene as well as the endogenous murine gene.

There are also Tau transgenes that produce solely one isoform, which can further complicate comparisons among different animal models (table 1).

Table 1: transgenic mouse model

Authors	year	Promotor	Mutation	Isoform	Begin of Tau pathology	Characteristics
Brion et al.	1999	Thy-1	P301L	3R murine	6 months	At 19 months detected NFT; Tau was also detected on microtubules in axons and in dendrites but not in cell bodies in astrocytes
Ishiara et al.	1999	Thy-1	P301L	Thy-1	3 months	At 3 and 12 months of age detected NFT in cortical and brainstem neurons motor weakness
Ishiara et al.	1999	Thy-1	P301L	Thy-1	12 months	At 12 and 24 months of age detected pretangles-tangles -NFT in cortical and brainstem neurons
Duff et al.	2000	8cmice	KI for human Tau	Human Tau 6 isoforms	7 months	No NFT
Lewis et al.	2000	PrP	P301L	4R	5 months	Locomotor deficit at 6.5 months (hemizygous)
Gotz et al.	2001	Thy 1.2	P301L	4R	3 months	Muscle atrophy and weakness, NFTs in cortical and brainstem neurons
Lim et al.	2001	Thy-1	G272V P301L R406W	-	1.5 months	No abnormality up to 12 months
Tatebayashi et al.	2002	CamK-II	R406W	-	5 months	No abnormality up to 23 months
Allen et al.	2002	Thy 1.2	P301S	4R	5 months	Locomotor deficit at 6.5 months (homozygous)
Andorfer et al.	2003	KO mice for Tau murine	KO mice for Tau murine	4R	13 months	At 13 months of age detected Tau in cortical and brainstem neurons
Santacruz et al.	2005	CamK-II (inducibile tet-off)	P301L	-	2.5 months	Locomotor deficit at 9.5 months (hemizygous)

The most common MAPT mutation is referred to as P301L, a human missense mutation of Pro_{301} Leu [16], this mutation appears to promote the self-assembly of mutant Tau protein in form of filaments and tangles. The P301L mutant Tau mice mimic features of human Tauopathies and provide a good model for investigating the pathogenesis of diseases with NFTs [17].
Really these mutant mice have been shown to exhibit a phenotype characterized by altered behavioral aspects and pathological lesions early as 6.5 months of age in hemizygous animals and at 4.5 months in homozygotes.

NFT formation in the P301L mice was age and gene-dependent, with aggregates of hyperphosphorylated Tau in the cerebral cortex and hippocampus. Other authors indicate that age of phenotypic onset is later than previously described, starting around 10 months [18] and describe that abundant hyperphosphorylated Tau has been observed in the brains of mice at 10-18 months of age.
Many studies described transgenic mouse models of tauophaty, focusing on the neuropathogenic mechanisms underlying the disease, without evaluating a possible impact that gender may have on the onset and progression of the disease. Infact, the aggregation of hyperphosphorylated Tau is one of the typical hallmarks of AD and age, sex, and stressful life events are known as etiopathogenic factors in AD: more in detail, women are more prone to develop AD [19] and elevated levels of glucocorticoid secretion are associated with hippocampal degeneration and cognitive deficits in AD patients [20-21-22].
In this study young and old male and female transgenic P301L-Tau mice were studied in comparison with wild type mice to explore the possible mechanisms through which gender, age and genotype contributes to the onset and progress of tauophaty.
Taken together, these results will possibly add new perspectives to our capability of understanding how genotype and gender contribute to the precipitation of AD and other Tau-related pathologies, with the aim to add new tool to potential treatments for Tauopathies.

3.3 MATERIALS AND METHODS

3.3.1 Animals

Two hundred mice were used in this study. One hundred were hemizygous Tau transgenic mice of mixed gender with a mutant form (P301L) of human Tau protein including four-repeats without amino terminal inserts, and driven by the mouse prion promoter 6 (MoPrP) [23]. One hundred age-compatible wild type mice (B6D2F1) of mixed gender served as controls. Mice originated from Taconic Laboratories, USA, were bred at IRCCS Mario Negri Institute of Pharmacological Research in a Specific Pathogen free (SPF) facility with a regular 12:12 h light/dark cycle (lights on 07:00 a.m.), at a constant room temperature of 22 ± 2 °C, and relative humidity approximately 55 ± 10%. Animals were housed (n= 4 per group) in standard mouse cages; all mice were provisioned with bedding material (hard wood shavings) ad libitum food (Global Diet 2018S, Harlan Italy) and water. No environmental enrichment was used because it notably improves AD pathology in mouse models of AD [24-25].

3.3.2 Ethics statement

Procedures involving animals and their care were in accordance with the national and international laws and policies (EEC Council Directive 86/609, OJ L 358, 1 Dec.12, 1987; NIH Guide for the Care and use of Laboratory Animals, U.S. National Research Council, 2011). The Mario Negri Institute for Pharmacological Research (IRCCS, Milan, Italy) Animal Care and Use Committee (IACUC) approved the trials, which was conducted according to the institutional guidelines. These latter were in accordance with Italian laws (D.L. no. 116, G.U. suppl. 40, Feb. 18, 1992, Circular No.8, G.U., Juli14, 1994). The scientific project was approved by Italian Ministry of Health (Permit Number: 71/2014 B).

3.3.3 Study design

The aim of this study was to investigate the interaction between gender and genotype (P301L mice TG and B6D2F1 mice CTR) on the onset and progression of neurodegenerative disease in the used mouse model of tauophaty. Animals (total number = 200) were divided into two separate groups for studying either behavior or survival profiles. The experimental group aimed at analyzing survival rate (accompanied by body weight records) was composed by 120 animals, half TG half CTR mice, both of them equally composed by male and female mice. The experimental group aimed at performing behavioral tests (cognitive and locomotor aspects) was composed by 80 animals, half TG half CTR mice, both of them equally composed by male and female mice.
In the second group, on the basis of the data from other authors [17-18], two time points of analysis were defined at 7 and 15 months of age (the first time point the symptoms of the disease were evidently expressed, the second time point was evidenced as the maximum survival for mice affected by tauophaty). The animals were sacrificed after the behavioral tests and the brains were analyzed for immunohistochemical (IHC) studies, aimed to labeling the neuropathological hallmarks of tauophaty such as aggregates of Tau and NFTs, neuronal death, inflammation aspects and gliosis (Fig. 1).

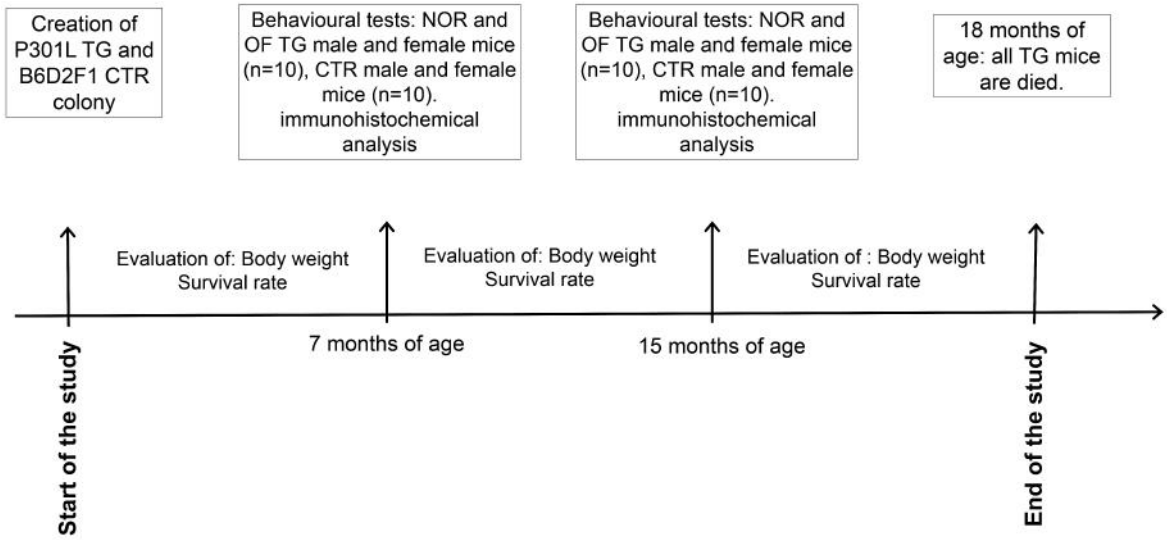

Figure 1. Time frame of experimental design. In the study were set the onset of neurodisease symptoms (7 months) and (15 months) two time points: the first as the manifestation of the neurodisease and the second as maximum survival of TG animals (time points for behavioral tests). During all experiment were valuated bodyweight and survival of all animals.

3.3.4 First experimental group: body weight and survival rate

Animals were monitored daily for wellbeing and welfare-related disease symptoms and their body weights were recorded weekly. A decrease in body weight greater than 15% in two consecutive weeks (15% +15%) was considered as humanitary end-point of the study and the respective animals were sacrificed. During the entire experiment, a large number of data was recorded, so we decided to group the values showing the average values for each experimental group every 4 weeks. This point of the trial was stopped after 18 months from the starting of the study on the basis of the higher and higher mortality rates recorded in TG groups.

3.4 SECOND EXPERIMENTAL GROUP: BEHAVIORAL TESTS

3.4.1 Novel-object recognition test (NORT)

The novel-object recognition test (NORT) is a memory test relied on spontaneous without the need of stressful elements animal behavior [26-27]. In the present study, the object recognition task was conducted in an open-field arena (40 × 40 × 40 cm) with floor divided into 25 squares by black lines; three stimulus objects of similar size were used: a black plastic cylinder (4 × 5 cm), a glass vial with a white cup (3 × 6 cm), and a metal cube (3 × 5 cm). The task started with a habituation trial during which the animals were placed in the empty arena for 5 min, and their movements were recorded as the number of

line crossings, which provided an indication of both CTR and TG mice locomotor activities. In the next day, mice were re-placed in the same arena containing two identical objects (familiarization phase). The objects were randomly selected to avoid bias among animals and between groups. Exploration was recorded in a 10 min trial by an investigator blinded to the genotype and treatment. Sniffing, touching, and stretching the head toward the object at a distance of no more than 2 cm were scored as object investigation. Twenty-four hours later (test phase), mice were placed again in the arena containing two objects: one already presented during the familiarization phase (familiar object) and a new different one (novel object). The time spent exploring the two objects was recorded for 10 min. Following each session of NORT, the arena and objects were cleaned with 70% ethanol to ensure that the animal's behavior was not guided by odor cues. Results were expressed as percentage time of investigation on objects per 10 min or as discrimination index (DI), i.e., (seconds spent on novel - seconds spent on familiar)/ (total time spent on objects). Animals with no memory impairment spent a longer time investigating the novel object, giving a higher DI.

3.4.2 Open field (OF) and spontaneous locomotor activity

The OF test is used to examine the general locomotion, as well as exploration activities, and consequent level of anxiety by exposing mice to a novel and open space [28-29]. We used a grey Perspex OF box (40 × 40 × 40 cm) with the floor divided into 25 (8 × 8 cm) squares. Mice were placed into the center of the floor defined as a 'starting point' and their behavior video-recorded for 5 min. The parameters analyzed as measure of spontaneous locomotor activity, exploratory activity and state of anxiety were: the duration of locomotion divided into the number of internal (the nine central squares) and external (the sixteen peripheral squares) squares crossed, the time spent in the central and external area of the open field, the number and duration of rearing (standing on the hind paws), the number and duration of self-grooming (rubbing the body with paws or mouth and rubbing the head with paws)[30].

3.4.3 Immunohistochemistry

At the end of behavioral tests animals were euthanized by cervical dislocation [31-32]; brains were removed and fixed in 10% formalin for 24–48 h with the usual procedure and embedded in paraffin. After deparaffinization brain coronal sections (3 μm thick; three slices per mouse) were stained for immunohistochemistry utilizing different primary antibodies (see table 2).
The sections were incubated for 1 h at room temperature with blocking solutions [AT8 and AT100: 0.3% Triton X-100 plus 10% NGS; NFTS: 0.4% Triton X-100 plus 3% NGS; GFAP: 0.4% Triton X-100 plus 3% NGS; NeuN: 0.1% Triton X-100 plus 10% NGS] and then overnight at 4°C with the primary antibodies. After incubation with the biotinylated secondary antibody (1:200; 1 h at room temperature; Vector Laboratories, Burlingame, CA), the sections were then incubated for 30 minutes at room temperature with the avidin-biotin-peroxidase complex (Vector Laboratories, Burlingame, CA) and diaminobenzidine (Sigma). The sections were then slightly counterstained with hematoxylin. The specificity of the immunostaining was verified by incubating in parallel other sections with PBS instead of the specific primary antibodies.
To determine the level of apoptosis in the brain, TUNEL assay were performed using Dead-end™ Colorimetric TUNEL System (Promega, nr G3250). Briefly, after the deparaffinization, sections were immersed at room temperature in a 0.85% NaCl solution for 5 minutes, washed twice in PBS (5 min), placed in the Proteinase-K solution from the TUNEL assay kit for 10 min at room temperature and fixed in 10% buffered formalin solution (5 min).
After washing in PBS three times (5 min each), sections were immersed in Equilibration buffer from the TUNEL assay kit (10 min), and incubated with a rTdT reaction mix (from the TUNEL assay kit) in a humidified chamber at 37°C for 1 h. To stop the reaction, sections were immersed in stop buffer for 15 min at RT and washed twice with PBS (5 min each); for blocking endogenous peroxidases, the sections were immersed in 0.3% hydrogen peroxide solution for 5 min, washed twice in PBS (5 min each) and covered with Strep-HRP solution for 30 min at RT.
After washing twice in PBS (5 min/wash) to remove the Strep- HRP, sections were immersed in DAB solution for 3 min at room temperature. The brain sections were then counterstained with hematoxylin for 2 min at room temperature.

Table 2: antibodies used in this study

Antibody	Species	Specificity	Use	Dilution	Source, type
AT 8	Mouse	Tau; Ser(P)^{202}/Thr (P)^{205}	Pre-tangles; Tau marker	1:1000	Euroclone, mAb IgG1
AT 100	Mouse	Tau; Thr(P)^{212}/Ser(P)^{214}	Tau marker	1:1000	Euroclone, mAb IgG1
NFTs	Mouse	Neurofilaments	Axonal marker	1:50	Dako, mAb IgG1
GFAP	Rabbit	Astrocytes	Astrocytic marker	1:2500	Dako, mAb IgG
NeuN	Mouse	Neurons	Neuronal marker	1:1000	Chemicon, mAb IgG1

3.4.4 Neuronal counts

In the Tauophaty mouse model used in this study, the accumulation of pathological Tau species (AT8, AT100), the neuronal loss (NeuN) and the level of apoptosis (TUNEL) were quantified in the cerebral cortex and in the hippocampus (upon frontal sections). Immunoreactive cells were counted by image analysis software in 3 fields using an Olympus Bx51 light microscope (Olympus, Italy) equipped with a digital camera (at x400 each field represented a tissue section area of about 0.036 mm^2). Following manual tracing of the cortex and hippocampus at the same stereotactic level in all mice, the number of positive cells were manually tagged and counted. Every section was individually examined for the presence or absence of visible Tau filaments (AT8 and AT100) and for the presence of positive signaling in the neuronal nucleus (NeuN and TUNEL reactivities). The observer was not aware of the origin of the sections.

3.4.5 Statistical analysis

Statistical analyses were performed using Graph Pad Prism 6 program. Body weight data, NOR data, OF data and neuronal counts data were analyzed using two-way ANOVA, followed by Tukey's *post hoc* test. Survival ratio was analyzed by Log-rank (Mantel-Cox) test. All data were expressed as mean ± SEM with a statistical significance given at $P< 0.05$.

3.5 RESULTS

3.5.1 First experimental group: body weight and survival rate

The increase in body weight was significantly reduced in both male and female TG mice in comparison with CTR ones at 7 months (data not shown) and 15 months (ANOVA, $F_{genotype}$ $(_{3,1856})$ = 163.9, P<0.0001, F_{gender} $(_{15,1856})$ = 59.79, P<0.0001, $F_{interaction}$ $(_{45,1856})$ = 2.750, P<0.0001; Fig. 2A). The effect was more pronounced in female animals, as shown by the reduction of 34% of body weight in TG female compared to CTR female mice. A reduction of body weight in TG male compared to CTR male mice (Fig. 2A) was also evident, but it was lesser. The analysis of survival rate showed that both male and female TG mice had a significantly reduced survival rate compared to CTR mice (Chi square= 17.30, P<0.0001, Fig. 2 B and Chi square= 26.24, P<0.0001 Fig. 2C). In order to analyze the possible interaction between gender and genotype, the survival rates of TG male and female mice were compared, showing a significant reduction of percentage of survival in TG female mice (Chi square= 6.150, P<0.05, Fig. 2D).

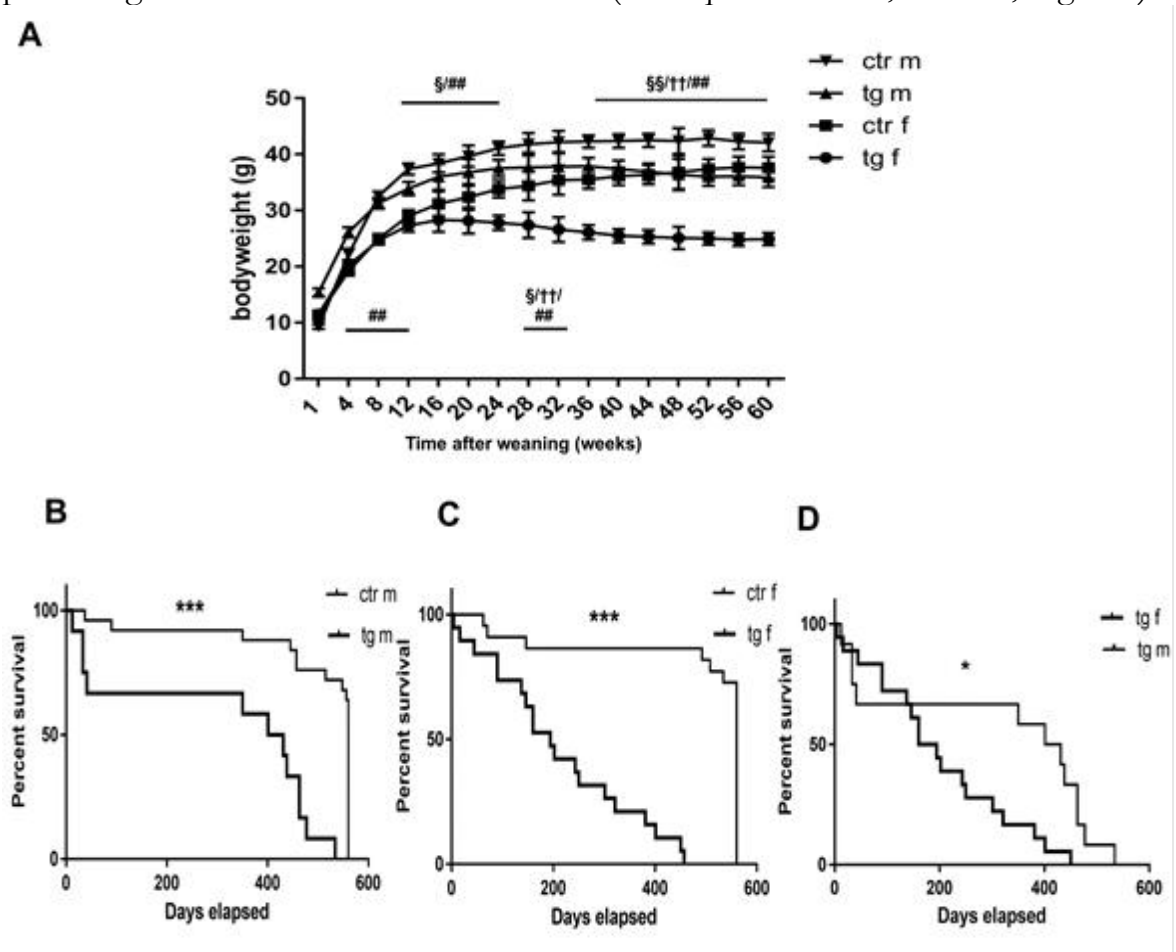

Figure 2. Body weight and survival rates. A) Significant reduction of body weight gain in male and female TG compared to CTR mice all along the experiment (n=30 for each group). TG male vs CTR

male mice § P< 0.05, §§ P< 0.01, TG female vs CTR female mice † P< 0.05, †† P< 0.01, TG female vs TG male mice # P< 0.05, ## P< 0.01. **B, C**). Significant decrease of survival rate in TG males and females compared to CTR all along the experiment (n=30 for each group), TG male vs CTR male mice *** P>0.0001 and TG female vs CTR female mice *** P<0.0001). **D**) Significant decrease of survival rate in female vs male TG mice (* P<0.01). Data were shown as mean ± SEM.

3.5.2 Second experimental group: behavioral tests

To investigate the cognitive impairment in the mouse model of tauophaty used in this study, both male and female TG and CTR mice at 7 and 15 months of age were tested in novel object recognition test. In either time points TG mice spent less time investigating the novel object compared to CTR mice (Fig. 3A, 3C); a significant genotype effect was found for measures of cognitive impairment such as discrimination index (7 months $F_{(3,27)} = 13.87$, $P<0.0001$) (Fig. 3B), (15 months ($F_{(3,27)} = 13.07$, $P<0.0001$) (Fig. 3D). In order to analyze the interaction between gender and genotype, discrimination indexes of TG male and female mice were compared. A statistically significant difference between two groups in each time point was not identified, but a trend towards a difference at 7 months of age ($F_{(3,27)} = 2.40$, $P= 0.06$) was observed.
In order to understand if the disease would increase with the age, the possible interaction between time and genotype was analyzed: discrimination indexes of TG female mice at 7 and 15 months of age were compared, but a significant difference between two groups ($P= 0.27$) was not evident. The same analysis was conducted for TG male mice at 7 and 15 months of age and a significantly decreased discriminatory activity was observed in 15 month-old TG mice compared to 7-month-old TG mice ($P<0.05$, data not shown).

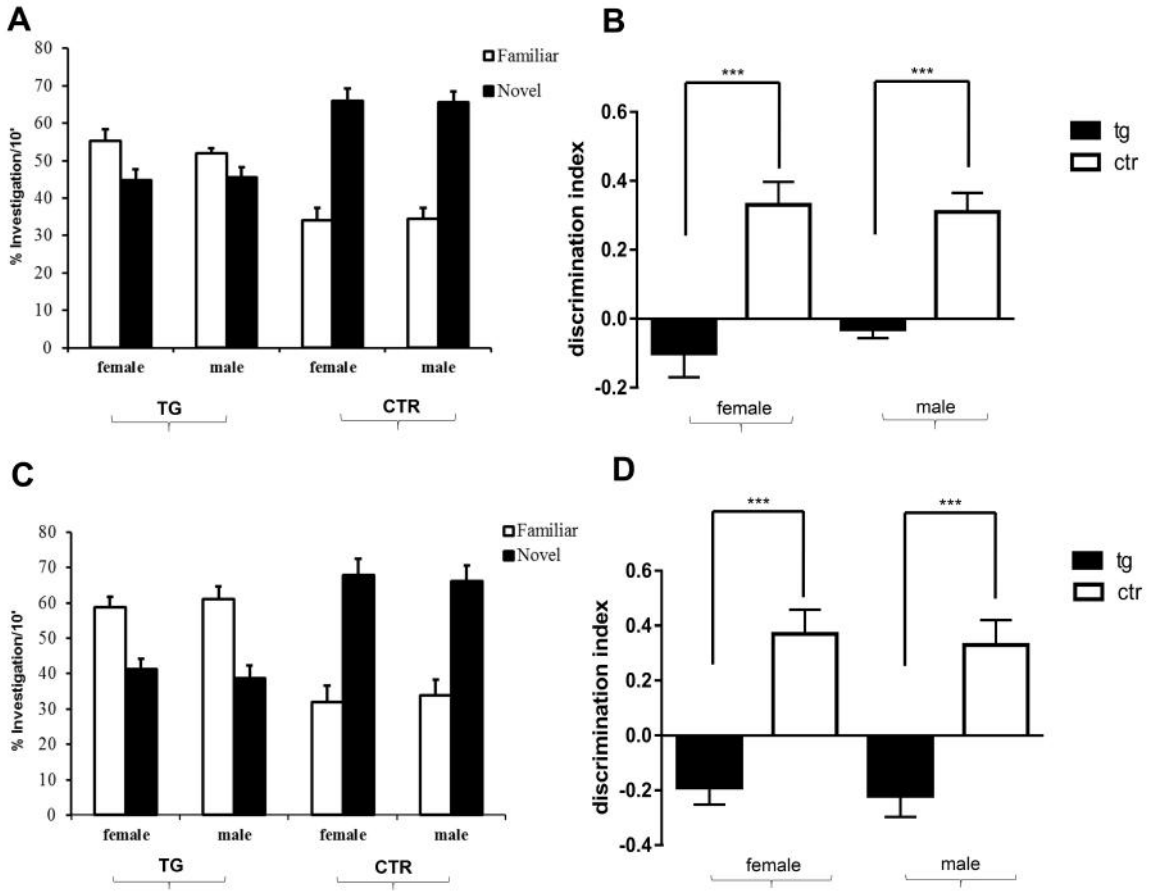

Figure 3. Discriminatory activity at 7 and 15 months of age in novel object recognition test. A-C) Histograms indicate percentage of exploration of the familiar and novel objects at 7 (a) and 15 (c) months of age. At 7 and 15 months of age tauophaty significantly impaired memory, as shown by the inability of the P301L mice both male and female to recognize the familiar object (each experimental group n=10). **B-D**) Histograms show the corresponding discrimination index for the data shown in the figure A and in the figure C. Significant relative to control *** P< 0.0001. Data were shown as mean ± SEM.

In order to investigate spontaneous locomotor and exploratory activities in the mouse model of tauophaty used in this study, both male and female TG and CTR mice at 7 months of age were tested in the open field test. A significant male gender-genotype effect was found for a locomotor activity measurement such as total number of crossing ($F_{(3,27)} = 0.0273$, $P<0.05$) (Fig. 4A), but the measured value was not significant for the number of internal crossing ($F_{(3,27)} = 1.233$, $P= 0.3170$) (Fig. 4B) and external crossing ($F_{(3,27)} = 1.940$, $P= 0.1470$) (Fig. 4C). In contrast, no genotype/gender effect was detected for measures of exploratory activity such as the time spent in the inner zone ($F_{(3,27)} = 1.521$, $P= 0.2316$) (Suppl. Fig. 2A) and the time spent in the external zone ($F_{(3,27)} = 1.589$, $P= 0.2151$, Suppl. Fig. 2B).

At 15 months of age, a significant female gender-genotype effect was found for measures of locomotor activity such as total number of crossing ($F_{(3,27)}$ = 0.0116, P< 0.05) (Fig. 4D), but the value was not significant for the number of internal crossing ($F_{(3,27)}$ = 0.8744, P= 0.4665) (Fig. 4E) and the number of external crossing ($F_{(3,27)}$ = 0.8896, P= 0.4591) (Fig. 4F). At 15 months of age again, no genotype/gender effect was detected for measures of exploratory activity such as the time spent in the inner zone ($F_{(3,27)}$ = 0.1266, P= 0.9460, Suppl. Fig. 2C) and the time spent in the external zone ($F_{(3,27)}$ = 0.1490, P= 0.9294, Suppl. Fig. 2D). With the aim to investigate if the disease signs would increase with the age, the interaction between time and genotype was analyzed; parameters for measuring locomotor activity of TG female mice at 7 and 15 months of age were compared, but there was no significant difference between two groups (nr total crossing $F_{(3,27)}$ = 0.2554, P= 0.8568, Suppl. Fig. 2E; nr internal crossing ($F_{(3,27)}$ = 0.3209, P= 0.8101, Suppl. Fig. 2F; nr external crossing ($F_{(3,27)}$ = 0.4815, P= 0.6979, Suppl. Fig. 2G). The same analysis was conducted for measures concerning exploratory activity, but no time/genotype effect was observed for the time spent in the inner zone ($F_{(3,27)}$ = 1.488, P= 0.2402, Suppl. Fig. 2H) and the time spent in the external zone ($F_{(3,27)}$ = 1.641, P= 0.2032, Suppl. Fig. 2I).

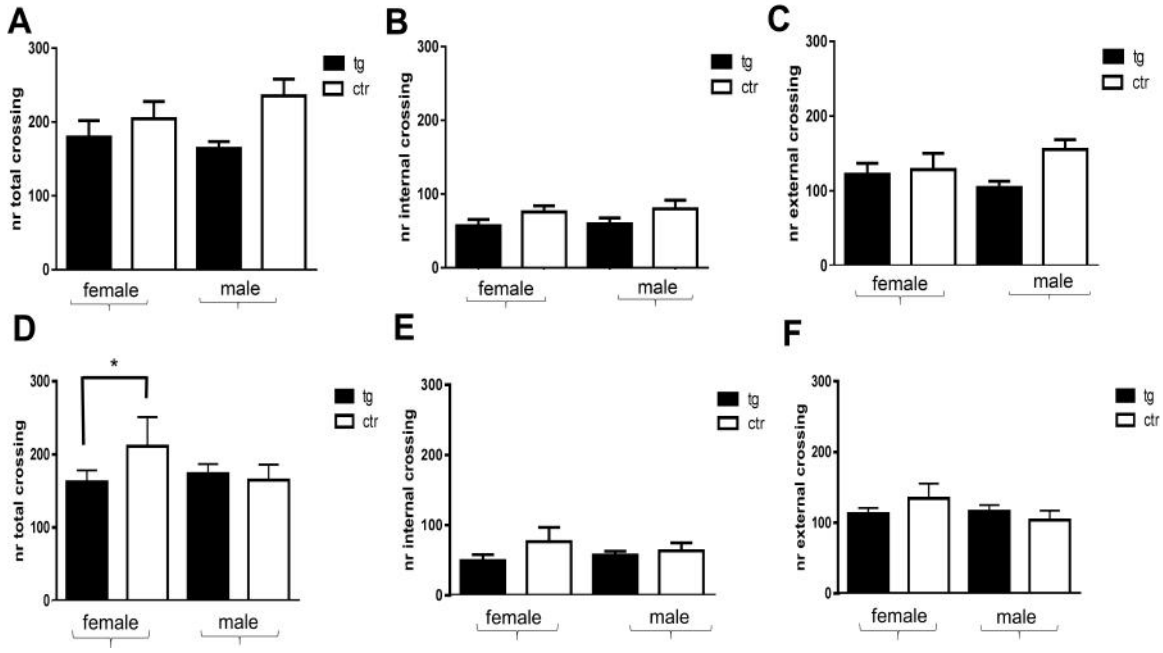

Figure 4. Locomotor activity at 7 and 15 months of age. A-F) Locomotor activity. Tauophaty significantly affected locomotor activity in 7-month TG male mice, as shown by the decrease of the number of total crossing performed by TG male mice compared to CTR male mice. Tauophaty significantly affected locomotor activity in 15-month TG female mice, as shown by the decrease of the number of total crossing performed by TG female mice compared to CTR female mice (each experimental group n=10). Significant relative to control * P< 0.05. Data were shown as mean ± SEM.

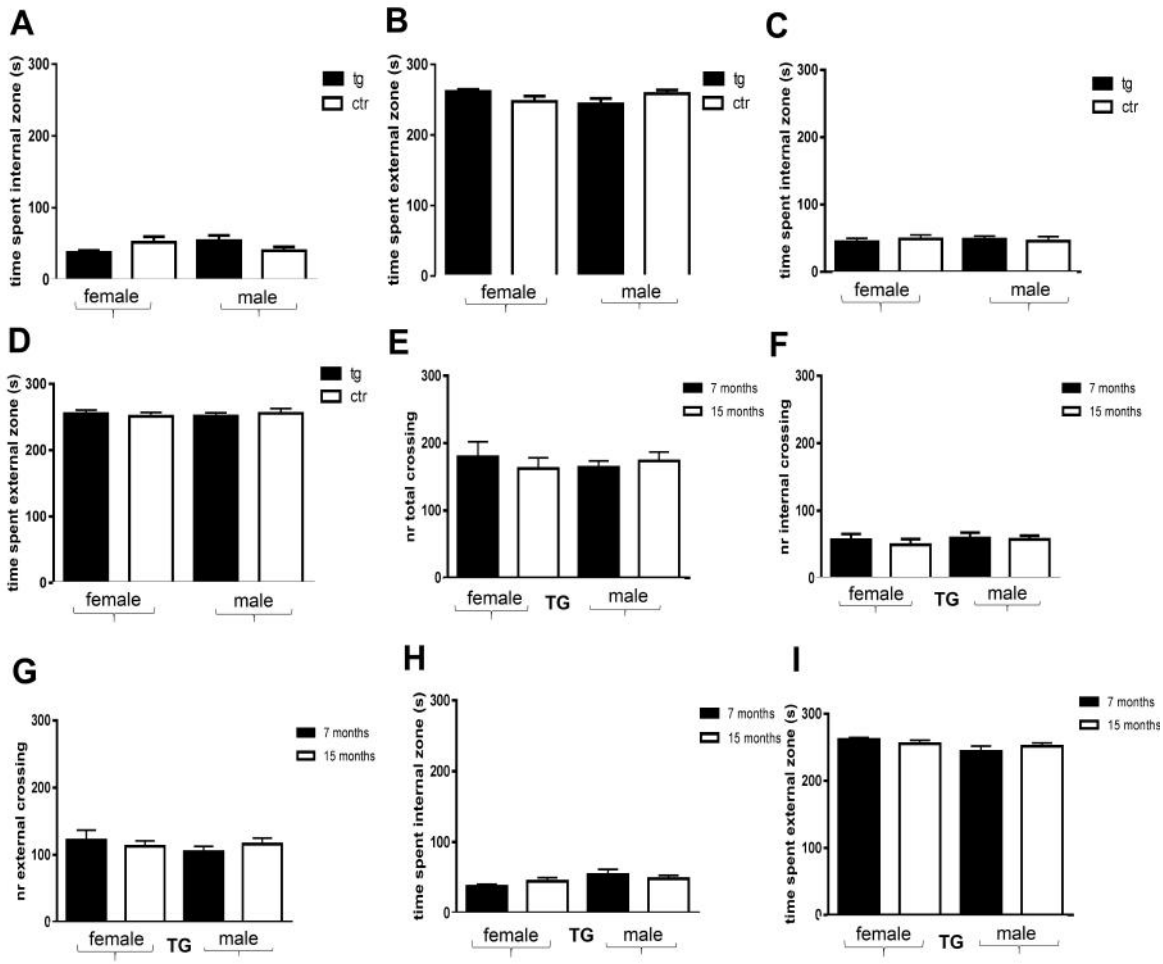

Supplementary Fig. 2. Tauophaty does not affect exploratory activity in P301L TG mice at 7 and 15 months of age. A-F) Tauophaty didn't affect significantly the exploratory activity in 7 and 15 month-old TG male and female mice compared to relative CTR mice (each experimental group n= 10), as shown by histograms related to time spent in internal and external zone performed by animals.

3.5.3 Immunohistochemistry

Sections of both P301L TG and CTR mice brains were tested with phospho-specific antibodies for AT8 and AT100 (Fig.5 and Fig.6 respectively). Immunostaining applied to cerebral cortex and hippocampus with AT8 and AT100 antibodies revealed that in P301L TG mice the phosphorylation of Tau was present at both 7 months (data not shown) and 15 months of age (Fig. 5B, 5D, 5F, 5H and 6B, 6D, 6F, 6H). Abnormal Tau species were also detected in the striatum, in the ventral thalamic nuclei, and in the entorhinal cortex (data not shown). These brain areas were subsequently quantified by AT8-immunoreactive cell counts (Fig. 5I and 5J), and in both the time points a significant genotype-gender effect in the cortex was detected (ANOVA, $F_{interaction\ (3,\ 40)} = 2.857$, $P<0.05$; $F_{genotype\ (1,40)} = 88.29$, $P<0.0001$; $F_{gender\ (3,40)} = 6.716$, $P<0.0001$) (Fig. 5I) and in the hippocampus ($F_{interaction\ (3,\ 40)} = 15.77$, $P<0.0001$; $F_{genotype\ (1,40)} = 15.77$, $P<0.0001$; $F_{gender\ (3,40)} = 49.89$, $P<0.0001$) (Fig. 5I-5J). In order to understand if the accumulation of pathological Tau species would increase with the age, the interaction between time and genotype was investigated too: a significant interaction genotype-time was found, as shown by the increase of AT8-immunopositive cell numbers in 15-month-old female TG mice compared to 7-month-old female TG mice in the cortex and in the hippocampus ($P<0.0001$) (Fig. 5J).
The quantification of AT100-immunopositive cells (Fig. 6I and Fig. 6J), in either time points revealed a significant genotype-gender effect in the cortex ($F_{interaction\ (3,40)} = 16.63$, $P<0.05$; $F_{genotype\ (1,40)} = 101.8$, $P<0.0001$ and $F_{gender\ (3,40)} = 14.05$, $P<0.0001$) (Fig. 5I) and in the hippocampus ($F_{interaction\ (3,40)} = 6.51$, $P<0.0001$; $F_{genotype\ (1,40)} = 64.18$, $P<0.0001$ and $F_{gender\ (3,40)} = 10.18$, $P<0.0001$) (Fig. 6J) (but the comparison between TG and CTR male mice at 7 months of age was not significant). A significant time-genotype interaction was also observed, as shown by an increase of AT100-immunopositive cell numbers in 15-month-old TG female mice compared to 7-month-old TG female mice both in the cortex and hippocampus ($P<0.0001$) (Fig. 6I-6J).

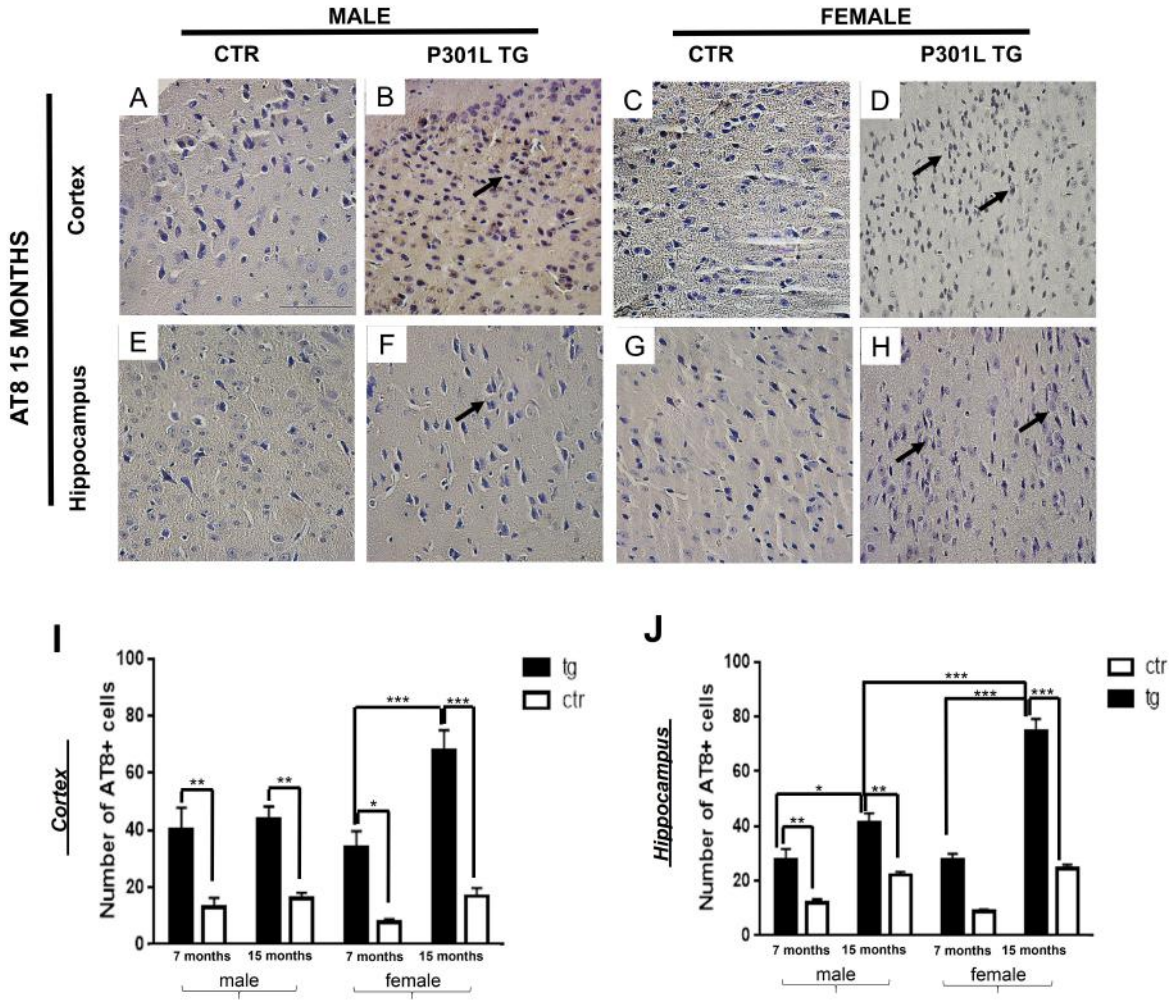

Figure 5. AT8 immunoreactivity and neuronal counts. PSer202–Thr205 (AT8)-stained sections revealed the accumulation of abnormal Tau conformation and phosphorylation in 15-month-old males and females (P301L TG mice and CTR mice) in cortex **(A-D**) and in hippocampus (**E-H**, note the arrows pointing to the most representative aspects in TG mice). Representative sections are shown of 4 animals used per each group. Scale bar: 40 μm. **I**) Quantification of AT8 immunoreactive cells in the cortex showed a significantly increased number of AT8+ cells in TG mice compared to CTR mice both at 7 and at 15 months of age. At 15 months of age there was a significant gender effect, as shown by a significantly increase of AT8+ cells of female TG mice compared to male TG mice and a significant interaction gender-time, as shown by the increase of AT8+ cells of 15-month-old females TG mice compared to 7-month-old female TG mice. The same results were obtained in the hippocampus (**J**). Significant relative to control *** P< 0.0001,7 months *vs* 15 months TG mice *** P< 0.0001, TG male *vs* TG female * P< 0.05. Data were shown as mean ± SEM.

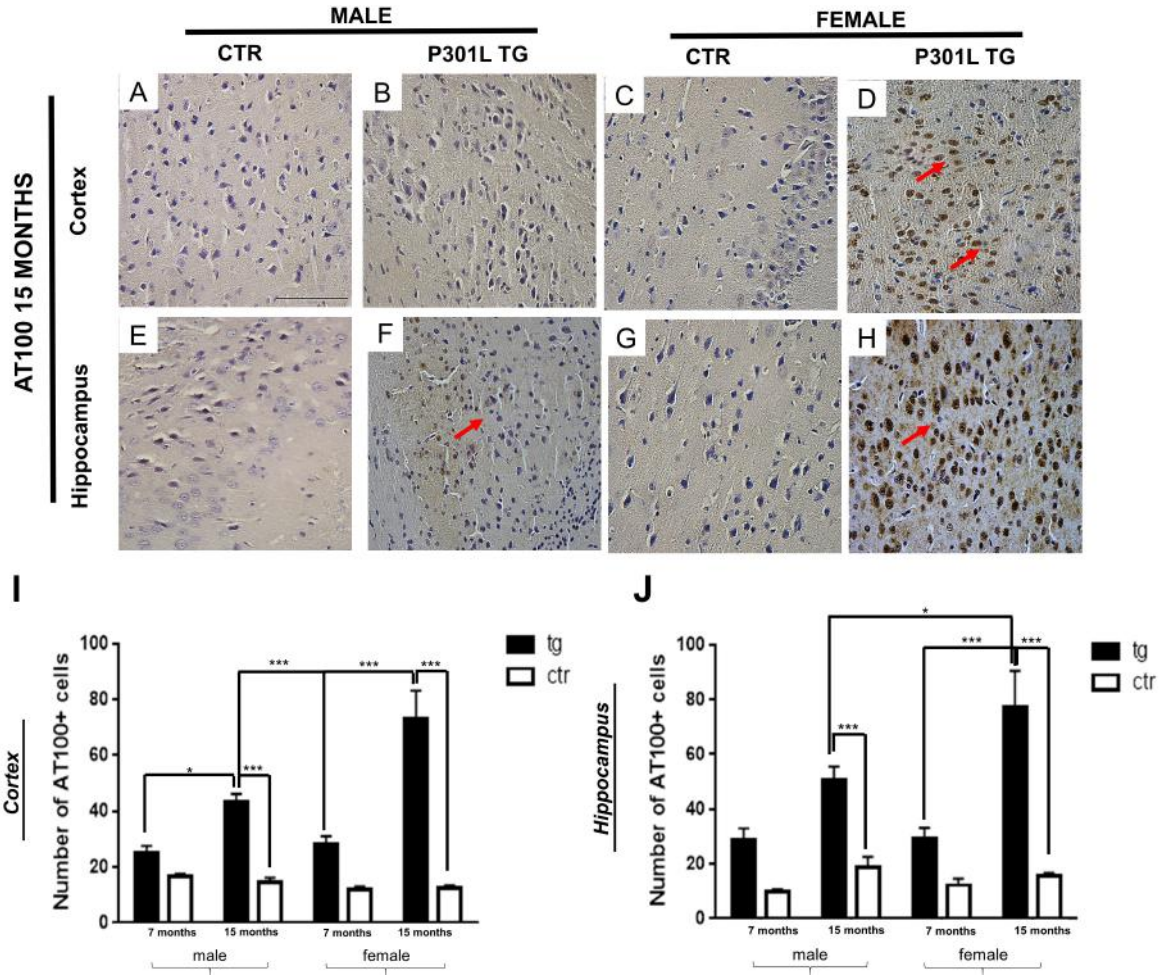

Figure 6. AT100 immunoreactivity and neuronal counts. PThr212/pSer214 (AT100)-stained sections revealed the accumulation of abnormal Tau conformation and phosphorylation in 15-month-old males and females (P301L TG mice and CTR mice) in cortex **(A-D)** and in hippocampus (**E-H**, note the arrows pointing to the most representative aspects in TG mice). Representative sections are shown of 4 animals used per each group. Scale bar: 40 μm. **I-J)** Quantification of AT100 immunoreactive cells in the cortex **(I)** and in hippocampus **(J)** showed a significantly increased of the number of AT100+ cells in TG mice compared to CTR mice both at 7 and at 15 months of age. At 15 months of age there was a significant gender effect, as shown by a significantly increase of AT100+ cells of female TG mice compared to male TG mice and a significant interaction gender-time, as shown by the increase of AT100+ cells of 15-month-old females TG mice compared to 7-month-old female TG mice. Significant relative to control *** P< 0.0001,7 months vs 15 months TG mice *** P< 0.0001, TG male *vs* TG female * P< 0.05. Data were shown as mean ± SEM.

In order to describe the neurodegeneration aspects, sections of both P301L TG and CTR mice brains were treated with neuronal nuclei (NeuN) antibody to value the survival of neuronal populations and with TUNEL to value apoptotic neurons. Immunostaining of cortex and hippocampus with NeuN revealed a loss of neurons in TG mice compared to CTR mice at 7 months of age (data not shown), with an abnormal neuronal morphology (Fig. 7A-H).

NeuN-immunopositive cells in the cortex and in the hippocampus were quantified; at 7 months of age no significant genotype effect was found between TG and CTR mice of both sexes in the cortex ($F_{genotype}(_{1,40}) = 2.493$, P= 0.1223; Fig. 7I) and in the hippocampus ($F_{genotype}(_{1,40}) = 3.366$, P= 0.0740; Fig. 7J). At 15 months of age a significant genotype-gender effect was detected in the cortex of TG female mice compared to CTR mice ($F_{interaction}(_{3,40}) = 7.774$, P<0.001, $F_{gender}(_{3,40}) = 46,58$, P< 0.05) (Fig. 7I). A significant genotype-time effect in either time points was in addition observed, with an increase of NeuN immunopositive cell numbers in 7-month-old TG mice compared to 15-month-old TG mice in the cortex and in the hippocampus ($F_{interaction}(_{3,40}) =3.041$, P<0.05, $F_{gender}(_{3,40}) =32.88$, P<0.0001) (Fig. 7J). Immunostaining with TUNEL revealed that at 7 months of age some neurons were apoptotic in a larger quantity in TG mice than respective CTR mice, with a major density of them in the cortical region compared to the hippocampal region (data not shown). Similar data have been shown at 15 months of age too, with a small increase of apoptotic neurons (Fig. 8A-H). Immunoreactivity of TUNEL+ neurons in the cortex and in the hippocampus was quantified; in either time points a significant genotype effect was found in the cortex ($F_{genotype}(_{1,40})= 72,26$, P<0.0001; $F_{gender}(_{3,40})= 7.337$, P<0.0001) (Fig. 8I) and in the hippocampus ($F_{genotype}(_{1,40})= 72,26$, P<0.0001; $F_{gender}(_{3,40})= 105.4$, P<0.0001) (Fig. 8J); no significant genotype-gender-time interaction was observed in the cortex ($F(_{3,40})= 2.095$, P=0.1162) (Fig. 8I) and in the hippocampus ($F(_{3,40})= 0.4845$, P=0.6149) (Fig. 8J).

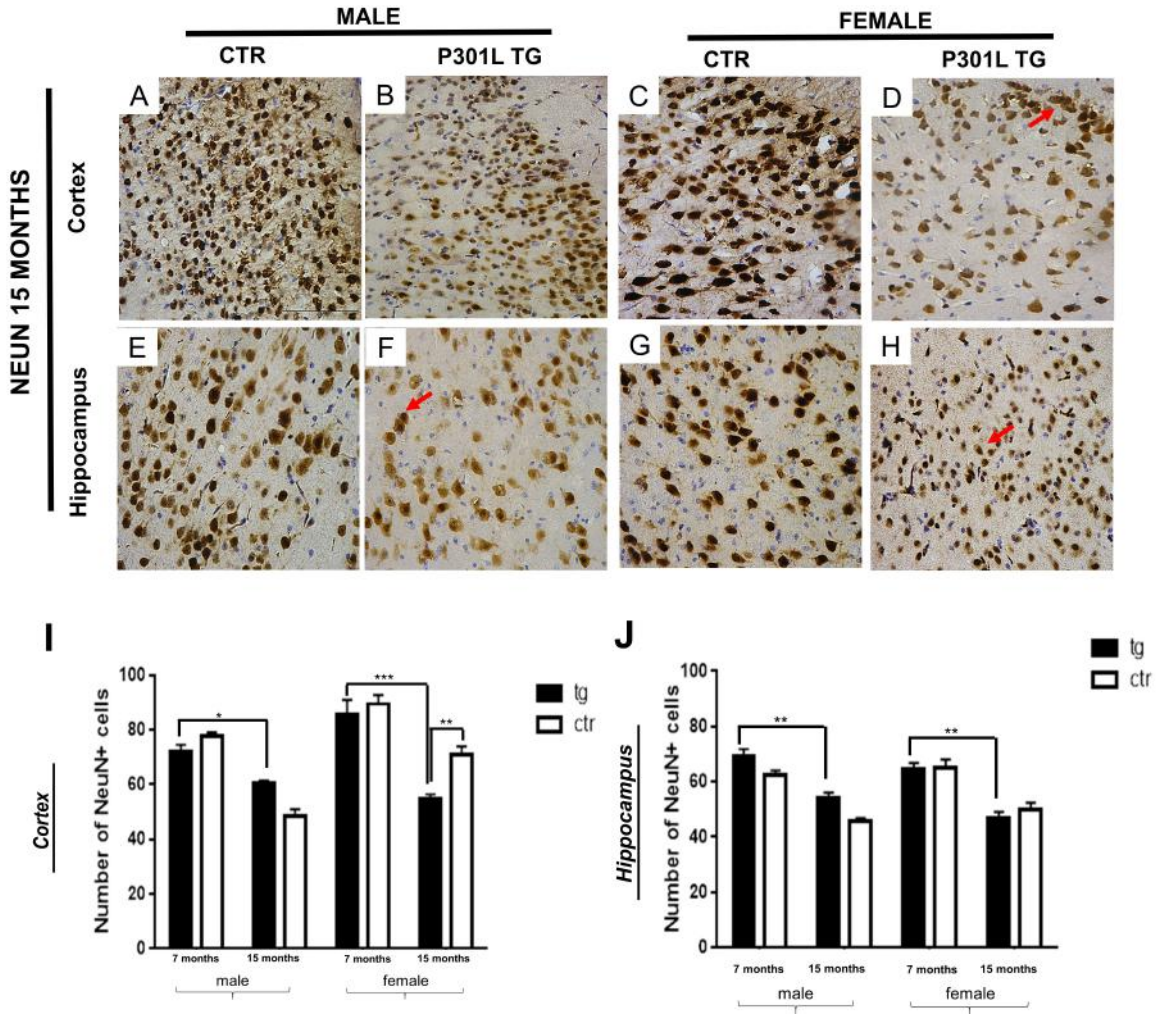

Figure 7. NeuN immunoreactivity and neuronal counts. Neuronal nuclei (NeuN) antibody stained sections of the cortex (**A-D**) and hippocampus (**E-H)** of CTR and P301L TG mice at 15 months of age (note the arrows pointing to the most representative dots in TG). Representative sections are shown of 4 animals used per each group. Scale bar: 40 μm. **I-J).** Quantification of NeuN+ cells in the cortex (**I**) and in hippocampus (**J**) showed a significant decrease of the number of NeuN+ cells in 15-month-old TG mice compared to 7-month-old TG mice (both males and females). In the cortex at 15 months of age there was also a significant decrease of the number of NeuN+ cells in TG female mice compared to relative CTR. Significant relative to control *** P< 0.0001,7 months *vs* 15 months TG mice * P< 0.05 and ** P< 0. 001. Data were shown as mean ± SEM.

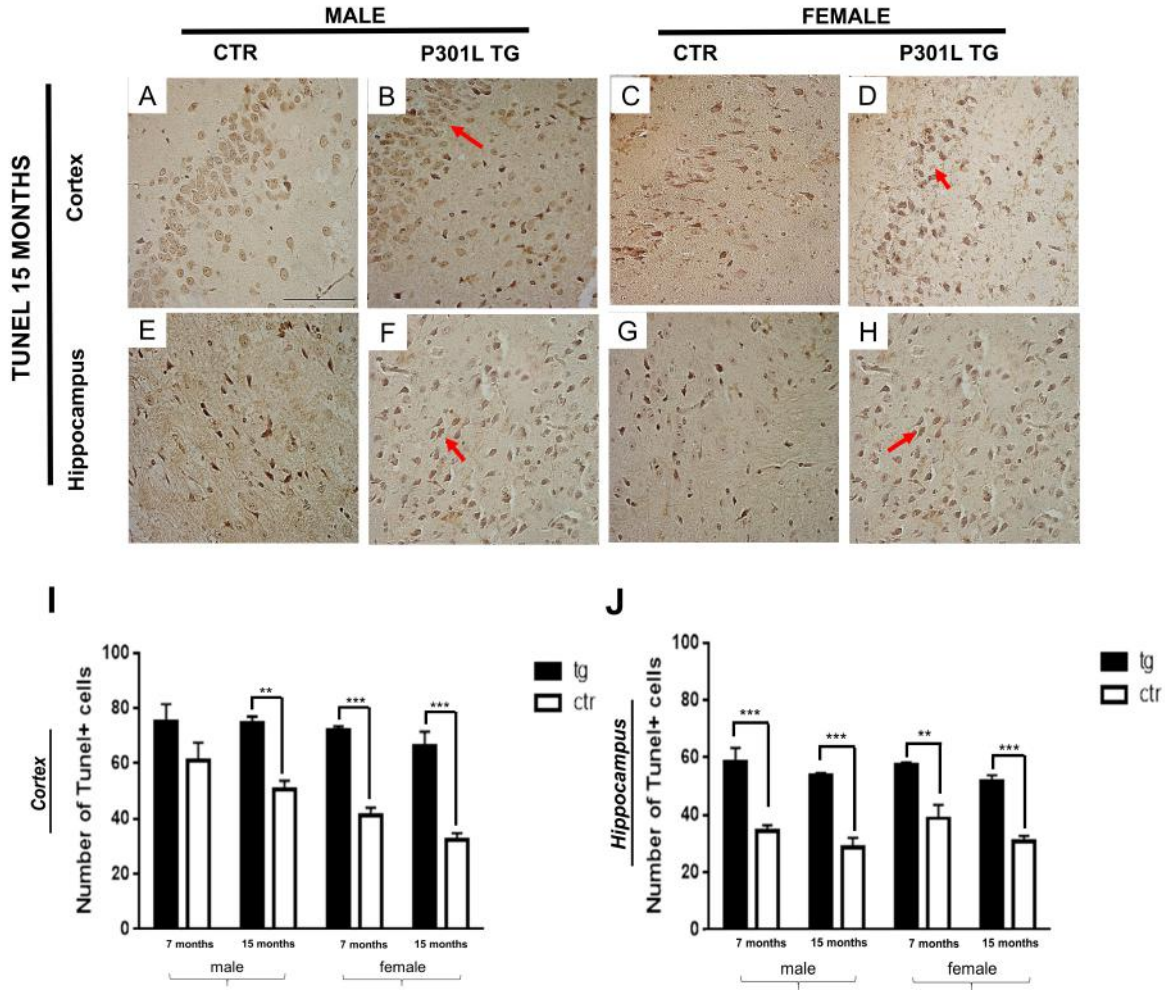

Figure 8. Level of apoptosis and quantification of TUNEL+ cells in P301L TG mice. TUNEL stained sections of the cortex (**A-D**) and hippocampus (**E-H**) of males and females P301L TG mice and CTR mice at 15 months of age (note the arrows pointing to the most representative dots in TG). Representative sections are shown of 4 animals used per each group. Scale bar: 40 μm. **I-J**) Quantification of TUNEL+ cells in the cortex (**I**) and in hippocampus (**J**) showed a significant increase of the number of TUNEL+ cells in P301L TG mice compared to relative CTR mice in each time point (excluding comparison between TG and CTR male mice at 7 months of age for the cortex analysis). Significant relative to control *** P< 0.0001,7 months *vs* 15 months TG mice * P< 0.05 and ** P< 0.001. Data were shown as mean ± SEM.

To analyze gliosis coronal sections of both TG and CTR mouse brain were immunostained with glial fibrillary acid protein (GFAP) (Suppl. Fig. 2I-2P). Immunostaining of cortex and hippocampus with GFAP revealed a state of gliosis in TG mice compared to CTR mice at 7 months of age (data not shown), with an increase of the number of GFAP+ cells confirmed also at 15 months of age (GFAP) (Suppl. Fig. 2I-2P).

An increase in the number of astroglial GFAP-positive cells was observed in the hippocampal area and in the cortex of 15-month-old P301L TG mice compared to 7-month-old P301L TG mice (Suppl. Fig. 2I-2P). The number of GFAP-positive cells increases with age in both CTR and TG mice.

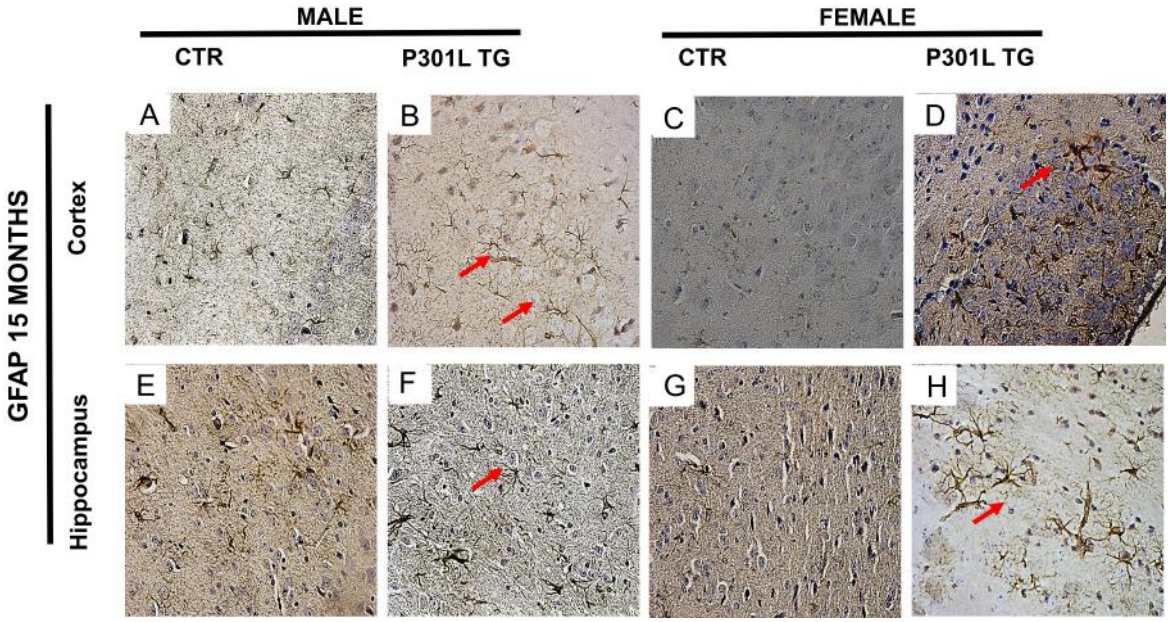

Supplementary Fig. 1. Accumulation of neurofibrillary inclusions and gliosis in P301L TG mice. A-H) Glial fibrillary acidic protein (GFAP) stained sections of the cortex (**A-D**) and hippocampus (**E-H**) of males and females P301L TG mice and CTR mice at 15 months of age (note the arrows pointing to the most representative dots in TG). Representative sections are shown of 4 animals used per each group. Scale bar: 40 μm.

3.4 DISCUSSION AND CONCLUSION

Alzheimer disease is a complex multifactorial disease with many risk factors such as age, sex and stress and many others, the relevance of these risks occur largely through unknown mechanisms.

The pathological mechanisms need to be clarified in order to develop therapeutically strategy to slow or spot the Tauopathies.

In the present study, we consider gender, genotype and age as a relevant risk factor for the progression of Tau pathology.

We characterized a Tau transgenic mutant form (P301L) of human Tau protein including four-repeats without amino terminal inserts, and driven by the mouse prion promoter 6 (MoPrP). Lewis et al. [17-18] had shown that in the same model that motor dysfunction started at as 6.5 months of age in hemizygous animals and at 4.5 months in homozygotes with a short lifespan (10 months of age). In the brain, NFTs formation was age and gene-dependent and increasing insolubility and hyperphosphorylation of Tau paralleled the increasing observed NFTs. NFTs and Pick-body-like neuronal lesions were widespread in the brain and spinal cord; areas of the brain with the most NFTs also had reactive gliosis.

The brain areas most affected by the toxic role of Tau, characterized by the presence of aggregates of hyperphosphorylated Tau, deposition of neurofibrillary tangles, axonal dilatations, neuronal and synaptic loss, are hippocampus, entorhinal cortex, CA1 pyramidal layer and the basal forebrain [33-34-35-36-37].
In our experiments P301L model has an onset of Tau pathology starting at 7 months of age, and all the described features were similar to those ones described by Lewis et al.
Differently for Lewis et al. lifespan of our animals was slightly higher, that is 16-18 months (instead of 10), with a reduction in weight, grooming and vocalization as described by Lewis, and an increase in docility age-dependent. One possible explanation for these two different observations is the sub-strain background of this transgenic line [39-40].
Previous work with JNPL3 mice showed that backcrossing onto C57BL/6 strain background significantly delayed the onset of disease and altered the pathological presentation of the original model [41-42]. Although JNPL3 mice express the same P301L 0N4R Tau as other Tau mouse models, there are several important differences between the two models that may explain the disparate effects of the C57BL/6 strain on tauophaty in each model. The Tau transgenic integration sites in JNPL3 have not been published, but it is likely that the incorporation of the human Tau cDNA into the murine genome occurred at different locations for each model. Based on the integration site of the transgenes and the endogenous activity of that chromosomal region, strain background could differentially affect promoter activity in each model [43]. Additionally, the C57BL/6 sub-strain utilized in each study could also contribute to the difference.
In this study, we have chosen for our Tau TG model the C57BL/6J sub-strain while Lewis et al. crossed Tau-expressing mice to a C57BL/6NTac sub-strain (crossed with DBA2 x SW to obtain B6D2F1). The B6/N Tac sub-strain from Taconic was originally derived from the B6/J strain from Jackson laboratory, but over time genetic and phenotypic differences have developed between the two sub-strains [44].
Concerning age as a risk factor, we found that tauophaty progresses with age, because exploratory locomotor performance was shown to decrease at 15 months compared to 7 months of age. Accordingly, important motor impairment well correlated with the accumulation of hyperphosphorylated Tau in the cortex and in the hippocampus and this progress with age from 7 to 15 months. The neuronal loss is age- dependent too and located mainly in hippocampus in this model.
Analyzing more in details the interaction between cognitive performance and brain histology, there is a significant correlation between behavioral performance and Tau pathology in our model.

A very recent study [45] revealed that environmental stress triggered memory impairments in female, but not male, P301L-Tau transgenic mice, and links memory deficit with Tau hyperphosphorylation and accumulation.
Interestingly, in our study poorer "cognitive" performance in the novel object recognition test was associated with higher numbers of p-Tau+ (both AT8 and AT100) neurons in both cerebral cortex and hippocampus at both 7 and 15 months of age. Moreover, a greater reduction of discriminatory activity is correlated to gender: in female TG mice was associated with higher numbers of p-Tau+ neurons in both cerebral cortex and hippocampus compared to male TG mice. The P301L mouse develops p-Tau+ stained neuronal cell bodies in brainstem and forebrain by 7 months of age, with "pre-tangle" p-Tau+ deposits occurring in neocortical and hippocampal cell bodies by that time as well. In these areas, we also detected GFAP-positive cells at 7 months of age, with an increase of the number of GFAP+ cells age-gender-dependent, revealing a state of astrogliosis age-dependent more pronounced in female than in male. Several evidences showed that the astrogliosis is a common feature in Tau TG models, this is, however, mild compared AD transgenic models [46] or AD brain [47]. A key finding of this work is that the interaction between genotype and gender triggers a number of mechanisms, Tau aggregation in the cortex and hippocampus is mediated by hyperactivation of PP1 and PP2A and the hyperphosphorylation of Tau in female is greater than in male P301L-Tau mice. Tau aggregation in female mice was also accompanied by altered expression of molecular chaperones known to regulate the process of neuronal degeneration and loss, inflammation and gliosis, and an important cognitive and locomotor impairment compared to male P301L- Tau mice.
In conclusion, we found an important interaction between gender and pathology until now never reported in tauophaty models, in fact we found that female have strong cognitive impairment and this is strongly correlated with an increase in P-Tau, in both cerebral cortex and hippocampus, as well as astrogliosis.
Although we found a higher attitude in female then in male to develop tauophaty we do not correlated this with an increase of neuronal death or neurodegeneration in female compare to male (TUNEL labeling).
Since Tau is a typical hallmark of AD and sex is a well-known etiopathogenic factors in AD, this P301L-Tau model could represent a valuable tool to study the role and the mechanisms through which gender interacts with hyperphosphorylation and Tau aggregation, leading to cognitive and memory impairment.
Moreover, preventing or reducing the accumulation of hyperphosphorylated Tau in this model may represent a system to study molecular mechanism of AD like-disease and could finally lead to the development of potential treatments for tauopathies, like AD.

3.5 ACKNOWLEDGMENTS

We thank D. Corna, I. Bertani for technical help.

3.6 REFERENCES

1. Iqbal K, Alonso Adel C, Chen S, Chohan MO, El-Akkad E, Gong CX et al. Tau pathology in Alzheimer disease and other Tauopathies. Biochim BiophysActa. 2005 Jan 3; 1739(2-3):198-210.
2. Nasreddine ZS, Loginov M, Clark LN, Lamarche J, Miller BL, Lamontagne A et al. From genotype to phenotype: a clinical pathological, and biochemical investigation of frontotemporal dementia and Parkinsonism (FTDP-17) caused by the P301L Tau mutation. Ann Neurol. 1999 Jun; 45(6):704-15.
3. Kimura T, Fukuda T, Sahara N, Yamashita S, Murayama M, Mizoroki T et al. Aggregation of detergent-insoluble Tau is involved in neuronal loss but not in synaptic loss. J Biol Chem. 2010 Dec 3; 285(49):38692-9.
4. Yancopoulou D, Spillantini MG. Tau protein in familial and sporadic diseases. Neuromolecular Med. 2003;4(1-2):37-48.
5. Hutton, M., Lendon, C.L., Rizzu, P. et al. (1998) Association of missense and 50-splice-site mutations in Tau with the inherited dementia FTDP-17. Nature 393, 702–705.
6. Poorkaj P., Bird T.D., Wijsman, E., Nemens, E., Garruto, R.M., Anderson, L. et al. (1998) Tau is a candidate gene for chromosome 17 frontotemporal dementia. Ann Neurol 43, 815–825
7. Spillantini, M.G., Murrell, J.R., Goedert, M., Farlow, M.R., Klug, A. &Ghetti, B. (1998) Mutation in the Tau gene in familial multiple system Tauopathy with presenile dementia. Proc Natl AcadSci USA 95, 7737–7741.
8. Weingarten MD, Lockwood AH, Hwo SY, Kirschner MW. A protein factor essential formicrotubule assembly. Proc Natl AcadSci USA. 1975; 72:1858–1862.
9. Kopke E, Tung YC, Shaikh S, Alonso AC, Iqbal K, Grundke-Iqbal I. Microtubule-associated protein Tau. Abnormal phosphorylation of a non-paired helical filament pool in Alzheimer disease. JBiol Chem. 1993; 268:24374–24384.
10. Chun W, Johnson GV. The role of Tau phosphorylation and cleavage in neuronal cell death. FrontBiosci. 2007; 12:733–56.
11. Matsuo ES, Shin RW, Billingsley ML, Van deVoorde A, O'Connor M, Trojanowski JQ et al. Biopsy-derived adult human brain Tau is phosphorylated at many of the same sites as Alzheimer'sdisease paired helical filament Tau. Neuron. 1994; 13:989–1002.

12. Sontag E, Nunbhakdi-Craig V, Lee G, Bloom GS, Mumby MC. Regulation of the phosphorylation state and microtubule-binding activity of Tau by protein phosphatase 2A. Neuron. 1996; 17:1201–7.
13. Sontag E, Nunbhakdi-Craig V, Lee G, Brandt R, Kamibayashi C, Kuret J et al. Molecular interactions among protein phosphatase 2A, Tau, and microtubules. Implications for the regulation of Tau phosphorylation and the development of Tauopathies. J Biol Chem. 1999; 274:25490–8.
14. Rahman A, Grundke-Iqbal I, Iqbal K. Phosphothreonine-212 of Alzheimer abnormally hyperphosphorylated Tau is a preferred substrate of protein phosphatase-1. Neurochem Res. 2005;30: 277–87.
15. Goedert M, Satumtira S, Jakes R, Smith MJ, Kamibayashi C, White CL 3rd et al. Reduced binding of protein phosphatase 2A to Tau protein with frontotemporal dementia and parkinsonism linked to chromosome 17 mutations. J Neurochem. 2000; 75:2155–62.
16. M.G. Spillantini, R.A. Crowther, W. Kamphorst, P. Heutink, J.C. vanSwieten, Tau pathology in two Dutch families with mutations in the microtubule-binding region of Tau, Am. J. Pathol. 153 (1998)1359– 1363.
17. Lewis, J., McGowan, E., Rockwood, J., Melrose, H., Nacaraju, P., Van Slegtenhorst, M. et al. (2000) Neurofibrillary tangles, amyotrophy and progressive motor disturbance in mice expressing mutant (P301L) Tau protein. Nature Genetics 25:402-406.
18. Lewis, J., Dickson, D.W., Lin, W-L., Chisholm, L., Corral, A., Jones, G. et al. (2001) Enhanced neurofibrillary degeneration in transgenic mice expressing mutant Tau and APP. *Science*. 93:1487-1491.
19. Barnes LL, Wilson RS, Bienias JL, Schneider JA, Evans DA, Bennett DA (2005) Sex differences in the clinical manifestations of Alzheimer disease pathology. Arch Gen Psychiatry 62, 685-691.
20. Elgh E, LindqvistAstot A, Fagerlund M, Eriksson S, Olsson T, Nasman B (2006) Cognitive dysfunction, hippocampal atrophy and glucocorticoid feedback in Alzheimer's disease. Biol Psychiatry 59, 155-161.
21. Wilson RS, Scherr PA, Schneider JA, Tang Y, Bennett DA(2007) Relation of cognitive activity to risk of developing Alzheimer disease. Neurology 69, 1911-1920.
22. Weiner MF, Vobach S, Olsson K, Svetlik D, Risser RC (1997) Cortisol secretion and Alzheimer's disease progression. Biol Psychiatry 42, 1030-1038.
23. Borchelt DR, Davis J, Fischer M, Lee MK, Slunt HH, Ratovitsky T. et al. A vector for expressing foreign genes in the brains and hearts of transgenic mice. Genet Anal. 1996 Dec; 13(6):159-63.

24. Lazarov O, Robinson J, Tang YP, Hairston IS, Korade-Mirnics Z, Lee VM et al. Environmental enrichment reduces Abeta levels and amyloid deposition in transgenic mice. Cell. 2005 Mar 11; 120(5):701-13.
25. Valero J1, España J, Parra-Damas A, Martín E, Rodríguez-Álvarez J, SauraCA. Short-term environmental enrichment rescues adult neurogenesis and memory deficits in APP(Sw, Ind) transgenic mice. PLoSOne. 2011 Feb 9; 6(2): e16832.
26. Clarke JR, Cammarota M, Gruart A, Izquierdo I and Delgado-García JM (2010) Plastic modifications induced by object recognition memory processing. Proc Natl AcadSci USA 107, 2652–2657.
27. Ennaceur A and Delacour J (1988) A new one-trial test for neurobiological studies of memory in rats. 1: Behavioral data. Behav Brain Res 31, 47–59.
28. Seibenhener ML, Wooten MC. Use of the Open Field Maze to Measure Locomotor and Anxiety-like Behavior in Mice. J Vis Exp. 2015 Feb 6 ;(96).
29. Crawley JN (2007) What's wrong with my mouse? behavioral phenotyping of transgenic and knockout mice. Hoboken, N.J.: Wiley-Interscience. xvi, 523 p.
30. Li SJ, Huang ZY, Ye YL, Yu YP, Zhang WP, Wei EQ et al. Influence of object material and inter-trial interval on novel object recognition test in mice Ban. 2014 May; 43(3):346-52.
31. Carbone L1, Carbone ET, Yi EM, Bauer DB, Lindstrom KA, Parker JM, Austin JA, Seo Y, Gandhi AD, Wilkerson JD. Assessing cervical dislocation as a humane euthanasia method in mice. J Am Assoc Lab Anim Sci. 2012 May; 51(3):352-6.
32. Angus DW1, Baker JA, Mason R, Martin IJ. The potential influence of CO2, as an agent for euthanasia, on the pharmacokinetics of basic compounds in rodents. Drug MetabDispos. 2008 Feb; 36(2):375-9. Epub 2007 Nov 15.
33. Cras, P., Smith, M. A., Richey, P. L., Siedlak, S. L., Mulvihill, P. and Perry, G. (1995) Extracellular neurofibrillary tangles reflect neuronal loss and provide further evidence of extensive protein cross-linking in Alzheimer disease. ActaNeuropathologica 89, 291 – 295.
34. Fukutani, Y., Kobayashi, K., Nakamura, I., Watanabe, K., Isaki, K. and Cairns, N. J. (1995) Neurons, intracellular and extracellular neurofibrillary tangles in subdivisions of the hippocampal cortex in normal ageing and Alzheimer_s disease. Neurosci. Lett. 200, 57 –60.
35. Goedert, M. (1999) Filamentous nerve cell inclusions in neurodegenerative diseases: Tauopathies and alpha-synucleinopathies. Philos. Trans. R. Soc. Lond. B Biol. Sci. 354, 1101 – 1118.

36. Bondareff, W., Mountjoy, C. Q., Roth, M. and Hauser, D. L. (1989) Neurofibrillary degeneration and neuronal loss in Alzheimer's disease. Neurobiol. Aging 10, 709 – 715.
37. Ludvigson AE1, Luebke JI, Lewis J., Peters A. Structural abnormalities in the cortex of the rTg4510 mouse model of Tauopathy: a light and electron microscopy study. Brain StructFunct. 2011 Mar; 216(1):31-42.
38. Allen B, Ingram E, Takao M, Smith MJ, Jakes R, Virdee K. et al. Abundant Tau filaments and non-apoptotic neurodegeneration in transgenic mice expressing human P301S Tau protein.J Neurosci. 2002 Nov 1; 22(21):9340-51.
39. Rachel M Bailey, John Howard, Joshua Knight, Naruhiko Sahara, Dennis W Dickson, Jada Lewis Effects of the C57BL/6 strain background on Tauopathy progression in the rTg4510 mouse modelMolNeurodegener. 2014; 9: 8. Published online 2014 January 15.
40. Bolmont T, Clavaguera F, Meyer-Luehmann M, Herzig MC, Radde R,S Taufenbiel M, et al. Induction of Taupathology by intracerebral infusion of amyloid-beta-containing brain extract and by amyloid-beta deposition in APP x Tau transgenic mice. Am J Pathol 2007, 171:2012–2020
41. Krezowski J, Knudson D, Ebeling C, Pitstick R, Giri RK, Schenk D, et al. Identification of loci determining susceptibility to the lethal effects of amyloid precursor protein transgene overexpression. Hum Mol Genet 2004, 13:1989–1997.
42. Bryant CD, Zhang NN, Sokoloff G, Fanselow MS, Ennes HS, Palmer AA et al. Behavioral differences among C57BL/6 substrains: implications for transgenic and knockout studies. J Neurogenet 2008,22:315–331.
43. Morgan, D Diamond, P Gottschall, K Ugen, C Dickey, J Hardy et al. A□-peptide vaccination prevents memory loss in an animal model of Alzheimer's disease. Nature, 408 (2000), pp. 982–985 g4510 mouse model. Molecular Neurodegeneration 2014, 9:8.
44. Bellucci A, Westwood AJ, Ingram E, Casamenti F, Goedert M, Spillantini MG: Induction of inflammatory mediators and microglial activation in mice transgenic for mutant human P301S Tau protein. Am JPathol 2004, 165:1643–1652.
45. Sotiropoulos I, Silva J, Kimura T, Rodrigues AJ, Costa P, Almeida OF et al. Female hippocampus vulnerability to environmental stress, a precipitating factor in Tau aggregation pathology J Alzheimers Dis. 2015;43(3):763-74.
46. Gotz J, Chen F, Barmettler R, Nitsch RM: Tau filament formation in transgenic mice expressing P301L Tau. J BiolChem 2001, 276:529–534.
47. Blanchard V, Moussaoui S, Czech C, Touchet N, Bonici B, Planche M. et al. Time sequence of maturation of dystrophicneurites associated with

Abeta deposits in APP/PS1 transgenic mice. ExpNeurol 2003, 184:247–263.
48. Coleman P, Federoff H, Kurlan R: A focus on the synapse for neuroprotection in Alzheimer disease and other dementias. Neurology 2004, 63:1155–111.

CHAPTER 4

A low fat-protein diet improves lifespan and cognitive activity in young and aged Tau P301L mice model of tauophaty

Submitted for publication to Laboratory Animal (December 2015)

4. A low fat-protein diet improves lifespan and cognitive activity in young and aged Tau P301L mice model of tauophaty

AUTHORS: L. Buccarello[1], G. Grignaschi[2], A. Di Giancamillo[1], C. Domeneghini[1]
[1]Department of Health, Animal Science and Food Safety, Università degli Studi di Milano, Italy
[2]Department of Animal welfare, IRCCS-Mario Negri Institute for Pharmacological Research, Milan, Italy

4.1 ABSTRACT

Dietary manipulations are increasingly viewed as possible approaches to treating neurodegenerative diseases. Previous studies suggest that an excessive caloric intake is associated with an increase of the risk of neurodegenerative disorders, while low caloric intake could delay aging and protect the central nervous system from neurodegenerative disorders. Low fat-protein diets, widely investigated in the treatment and prevention of neurodegenerative diseases, have been suggested to reduce the typical hallmarks of tauophaty as hyperphosphorylated tau, neurofibrillary tangles and improve cognitive impairment and lifespan. We investigate the effects of a low fat-protein diet (diet 14) and a high protein diet (diet 18) in a transgenic mouse model of tauophaty (P301L TG). At 3 months of age males and females P301L TG mice and B6D2F1 control mice were fed with different diets; body weight, food and water intake and survival rate were monitored throughout the experiment. Both male and female TG mice weighed less than CTR mice, regardless of diets administrated, but male TG and CTR mice fed with diet 18 ate and drank more of mice fed with diet 14. Lifespan of TG mice were significantly reduced than CTR mice, but lifespan of female mice fed with diet 14 was significantly higher than female mice fed with diet 18. At 7 and 15 months of age behavioral, exploratory and locomotor testing did not show any diet effects. Tissue measures of hyperphosphorylated tau, neuronal loss, astroglial and microglial markers in TG and CTR mice showed a strong genotype effect, but also an improve of cognitive activity corresponding to a decrease of aggregates of hyperphosphorylated tau, an increase of number of live neurons (NeuN) and a decrease of death neurons (TUNEL) in the cortex and in the hippocampus in TG mice fed with diet 14 compared with TG mice fed with diet 18. This effect was more pronounced in female than male TG mice at 7 months of age, because at 15 months of age pathological conditions of TG animals were too severe. These data suggest that a low fat-protein diet may play an important role to improve the lifespan and cognitive activity in a mouse model of tauophaty, but this type of nutritional formulation have minimal impact on the phenotype of this murine model of Tau deposition.

Furthermore, these data show the importance of a correct dietary intake that can be a useful tool for intervene in early identification of the neurodegenerative disease before the cognitive and behavioral impairments are clinically evident, in order to delay or even prevent the onset of tauophaty and neurodegenerative diseases.

Keywords:
AD: Alzheimer disease, CTR: control, NFTs: neurofilaments, PUFAs: polyunsaturated fatty acids TG: transgenic.

4.2 INTRODUCTION

Abnormal deposition of the tau protein is the hallmark feature of tauopathies, which encompasses a growing list of neurodegenerative diseases, including Alzheimer's disease (AD), frontotemporal dementia (FTD), progressive supranuclear palsy (PSP), corticobasal degeneration (CBD) and chronic traumatic encephalopathy (CTE). Additionally, pathogenic mutations in the MAPT gene encoding the tau protein are associated with FTD and Parkinsonism linked to chromosome 17 (FTDP-17), indicating that tau dysfunction alone is sufficient to cause disease [1-2].
Tauophaty is defined by fibrillary and tangled aggregates of phosphorylated protein tau, which is normally a very soluble protein that binds to microtubules to secure their assembly, stability and spacing [3-4]. Because the underlying pathologies may start years before the cognitive and behavioral impairments are clinically evident, application of the knowledge on preventive nutritional strategies warrants early identification of the disease to be able to intervene and delay, or even prevent its onset.
Recent epidemiological studies had shown specific associations between nutritional components and the risk for neurodegenerative diseases. These include the potential protective effects of specific polyunsaturated fats, B-vitamins and antioxidants [5-6-7]. These macro- and micronutrients are dietary components that can influence brain structure and function [8-9].
Nutritional intake may provide specific nutrients that can be used as building blocks for membrane and synapse formation and neurotransmitter production, but can also directly influence the availability of nutrients, energy and oxygen to the brain. It is well known the importance of nutrition in the onset and progression of neurodegenerative diseases, in particular the role of polyunsaturated fatty acids (PUFAs) and protein on cognitive and behavioral functions. PUFAs are involved not only as structural constituents of the membrane lipids of neuronal cells, but also for their neuro-protective, anti-oxidants and anti-inflammatory effects.

The proteins, as the reactive species oxygen, can interact with amino acid residues, in particular histidine, arginine and lysine, forming carbonyl functions. Some researchers have found that brain levels of these compounds increase with aging. Recent studies indicated that different caloric intake might influence neuronal function. Excessive caloric intake associated with accelerated aging of the brain and increased the risk of neurodegenerative disorders and low caloric intake could delay aging, and protect the central nervous system from neurodegenerative disorders.
Excessive caloric intake will easily lead to obesity, so long-term consumption of a high-caloric diet is a risk factor that can significantly contribute to the development of neurological disease [10].
An epidemiological study suggested that individuals following diets with high caloric intake have a 1.5 times greater risk of AD than those with low caloric intake [11]. The availability of transgenic animal models of tauophaty has permitted investigations into the impact of nutrients and other compounds isolated from foods on disease-related neuropathology, particularly amyloid-beta peptide in AD (the major for of tauophaty), and behavioral deficits.
In our previous study, we demonstrated that the P301L TG mice replicates the impairments found in patients affected by tauophaty in a way age-gender-dependent, with cognitive and behavioral impairment more pronounced in female than male P301L TG mice.
In this study, young and old male and female transgenic P301L-Tau mice were studied in comparison with wild type mice fed with different diets (low fat-protein diet and high fat-protein diet) to explore the possible mechanisms through which diets can contribute to the onset and progress of tauophaty. Together, these results add new perspectives to our understanding how dietary intake can contribute to the precipitation of AD and other Tau-related pathologies, and with the aim to prevent the incidence of neurodegenerative diseases with a correct nutrition.

4.3 MATERIALS AND METHODS

4.3.1 Animals and Diets

Four hundred mice were used in this study. Two hundred were hemizygous tau transgenic mice of mixed gender with a mutant form (P301L) of human tau protein including four-repeats without amino terminal inserts, and driven by the mouse prion promoter 6 (MoPrP) [12]. Two hundred age-compatible wild type mice (B6D2F1) of mixed gender served as controls.

Mice originated from Taconic Laboratories, USA, were bred at IRCCS Mario Negri Institute of Pharmacological Research in a Specific Pathogen free (SPF) facility with a regular 12:12 h light/dark cycle (lights on 07:00 a.m.), at a constant room temperature of 22 ± 2 °C, and relative humidity approximately 55 ± 10%. Animals were housed (n= 4 per group) in standard mouse cages, until three months of ages all animals were fed with standard rodent chow (**diet 1**: 18% protein and 5% fat, Harlan Lab. Tekland global diet), then animals were divided into two experimental groups, balanced for body weight and sex.

The first group was fed with a standard rodent chow (**diet 1**: 18% protein and 5% fat, Harlan Lab. Tekland global diet), and the second group was fed with a low protein diet (**diet 2**: 14% protein and 3.5% fat Harlan Lab. Tekland global diet).

Since the animals were bred in a SPF facility, where all materials introduced are sterilized, we had to use an autoclavable diet manufactured with high quality ingredients and supplemented with additional vitamins to ensure nutritional adequacy after autoclaving.

The diet 1 is a fixed formula, autoclavable diet designed to support gestation, lactation, and growth of rodents. This diet does not contain alfalfa, thus lowering the occurrence of natural phytoestrogens. Typical isoflavone concentrations (daidzein + genistein aglycone equivalents) range from 150 to 250 mg/kg. Exclusion of alfalfa reduces chlorophyll, improving optical imaging clarity. Absence of animal protein and fishmeal minimizes the presence of nitrosamines (Fig. 1).

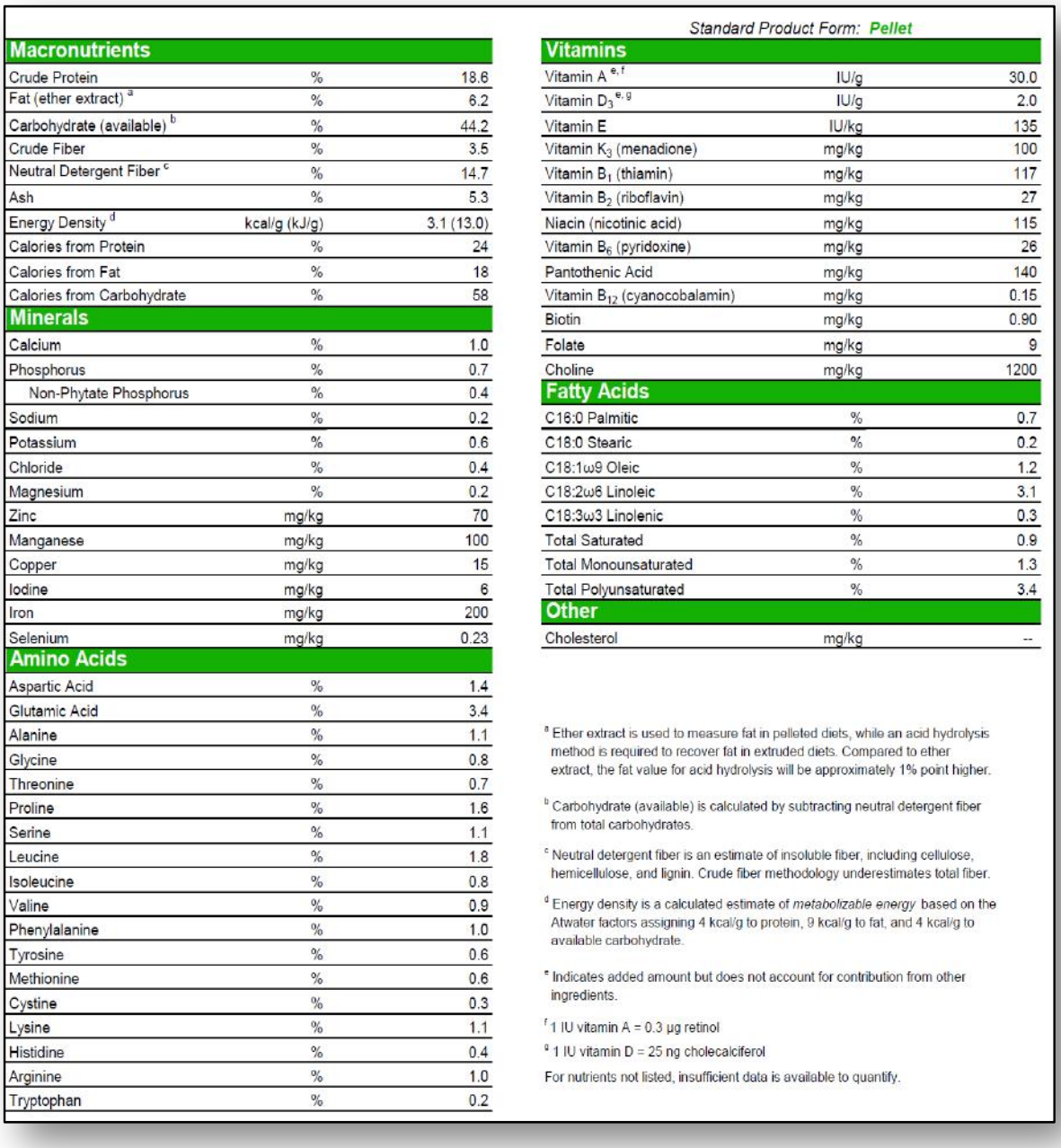

Standard Product Form: **Pellet**

Macronutrients		
Crude Protein	%	18.6
Fat (ether extract) [a]	%	6.2
Carbohydrate (available) [b]	%	44.2
Crude Fiber	%	3.5
Neutral Detergent Fiber [c]	%	14.7
Ash	%	5.3
Energy Density [d]	kcal/g (kJ/g)	3.1 (13.0)
Calories from Protein	%	24
Calories from Fat	%	18
Calories from Carbohydrate	%	58
Minerals		
Calcium	%	1.0
Phosphorus	%	0.7
Non-Phytate Phosphorus	%	0.4
Sodium	%	0.2
Potassium	%	0.6
Chloride	%	0.4
Magnesium	%	0.2
Zinc	mg/kg	70
Manganese	mg/kg	100
Copper	mg/kg	15
Iodine	mg/kg	6
Iron	mg/kg	200
Selenium	mg/kg	0.23
Amino Acids		
Aspartic Acid	%	1.4
Glutamic Acid	%	3.4
Alanine	%	1.1
Glycine	%	0.8
Threonine	%	0.7
Proline	%	1.6
Serine	%	1.1
Leucine	%	1.8
Isoleucine	%	0.8
Valine	%	0.9
Phenylalanine	%	1.0
Tyrosine	%	0.6
Methionine	%	0.6
Cystine	%	0.3
Lysine	%	1.1
Histidine	%	0.4
Arginine	%	1.0
Tryptophan	%	0.2

Vitamins		
Vitamin A [e, f]	IU/g	30.0
Vitamin D_3 [e, g]	IU/g	2.0
Vitamin E	IU/kg	135
Vitamin K_3 (menadione)	mg/kg	100
Vitamin B_1 (thiamin)	mg/kg	117
Vitamin B_2 (riboflavin)	mg/kg	27
Niacin (nicotinic acid)	mg/kg	115
Vitamin B_6 (pyridoxine)	mg/kg	26
Pantothenic Acid	mg/kg	140
Vitamin B_{12} (cyanocobalamin)	mg/kg	0.15
Biotin	mg/kg	0.90
Folate	mg/kg	9
Choline	mg/kg	1200
Fatty Acids		
C16:0 Palmitic	%	0.7
C18:0 Stearic	%	0.2
C18:1ω9 Oleic	%	1.2
C18:2ω6 Linoleic	%	3.1
C18:3ω3 Linolenic	%	0.3
Total Saturated	%	0.9
Total Monounsaturated	%	1.3
Total Polyunsaturated	%	3.4
Other		
Cholesterol	mg/kg	--

[a] Ether extract is used to measure fat in pelleted diets, while an acid hydrolysis method is required to recover fat in extruded diets. Compared to ether extract, the fat value for acid hydrolysis will be approximately 1% point higher.

[b] Carbohydrate (available) is calculated by subtracting neutral detergent fiber from total carbohydrates.

[c] Neutral detergent fiber is an estimate of insoluble fiber, including cellulose, hemicellulose, and lignin. Crude fiber methodology underestimates total fiber.

[d] Energy density is a calculated estimate of *metabolizable energy* based on the Atwater factors assigning 4 kcal/g to protein, 9 kcal/g to fat, and 4 kcal/g to available carbohydrate.

[e] Indicates added amount but does not account for contribution from other ingredients.

[f] 1 IU vitamin A = 0.3 µg retinol

[g] 1 IU vitamin D = 25 ng cholecalciferol

For nutrients not listed, insufficient data is available to quantify.

Figure 1: Composition of diet 1: 18% protein and 5% fat (Harlan Tekland global diet)

The **diet 2** is a fixed formula, autoclavable diet designed to promote longevity and normal body weight in rodents. Diet 2 does not contain alfalfa or soybean meal, thus minimizing the occurrence of natural phytoestrogens.
Typical isoflavone concentrations (daidzein + genistein aglycone equivalents) range from non-detectable to 20 mg/kg. Exclusion of alfalfa reduces chlorophyll, improving optical imaging clarity. Absence of animal protein and fishmeal minimizes the presence of nitrosamines (Fig. 2).

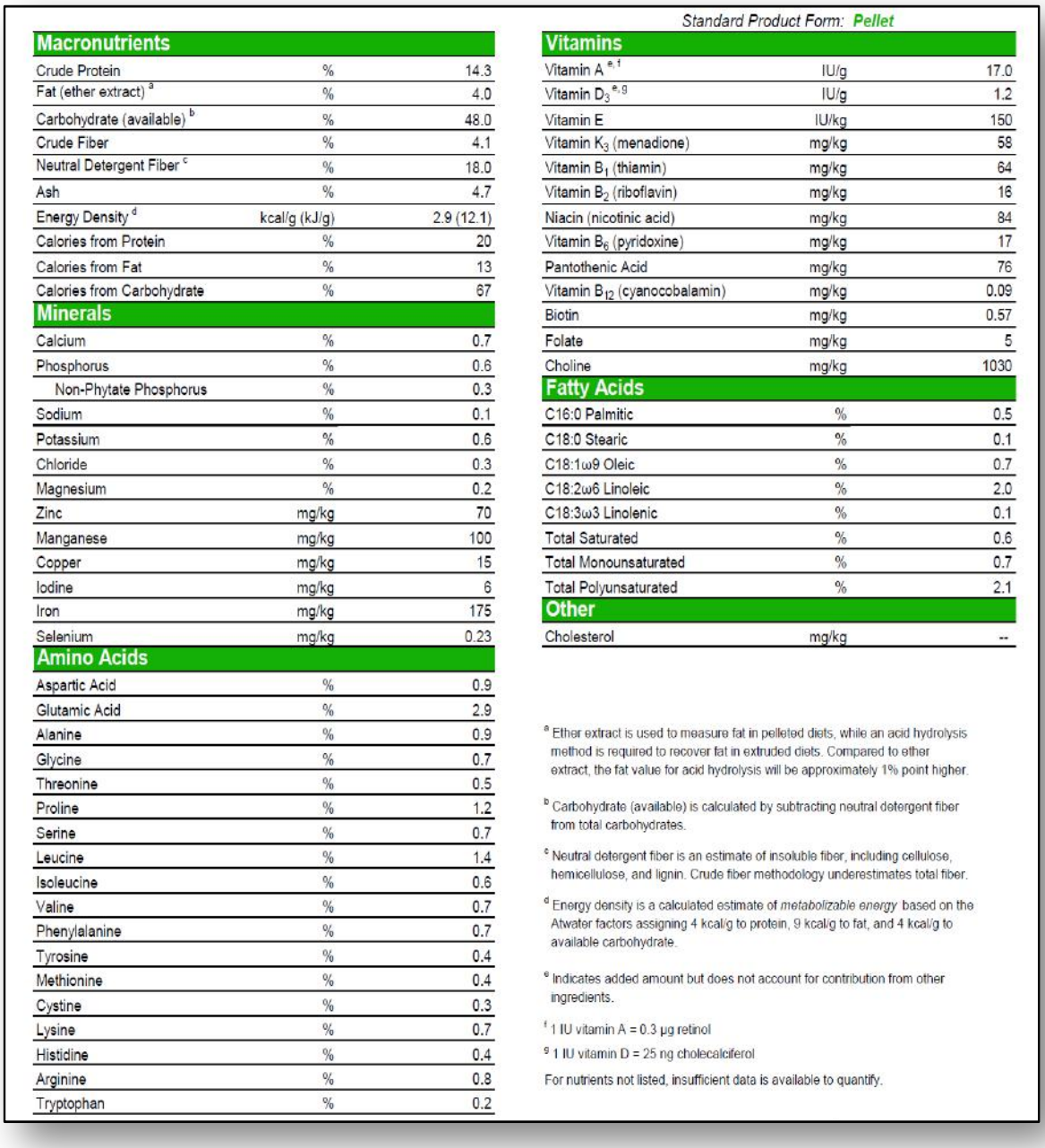

Standard Product Form: **Pellet**

Macronutrients		
Crude Protein	%	14.3
Fat (ether extract) [a]	%	4.0
Carbohydrate (available) [b]	%	48.0
Crude Fiber	%	4.1
Neutral Detergent Fiber [c]	%	18.0
Ash	%	4.7
Energy Density [d]	kcal/g (kJ/g)	2.9 (12.1)
Calories from Protein	%	20
Calories from Fat	%	13
Calories from Carbohydrate	%	67
Minerals		
Calcium	%	0.7
Phosphorus	%	0.6
Non-Phytate Phosphorus	%	0.3
Sodium	%	0.1
Potassium	%	0.6
Chloride	%	0.3
Magnesium	%	0.2
Zinc	mg/kg	70
Manganese	mg/kg	100
Copper	mg/kg	15
Iodine	mg/kg	6
Iron	mg/kg	175
Selenium	mg/kg	0.23
Amino Acids		
Aspartic Acid	%	0.9
Glutamic Acid	%	2.9
Alanine	%	0.9
Glycine	%	0.7
Threonine	%	0.5
Proline	%	1.2
Serine	%	0.7
Leucine	%	1.4
Isoleucine	%	0.6
Valine	%	0.7
Phenylalanine	%	0.7
Tyrosine	%	0.4
Methionine	%	0.4
Cystine	%	0.3
Lysine	%	0.7
Histidine	%	0.4
Arginine	%	0.8
Tryptophan	%	0.2

Vitamins		
Vitamin A [e, f]	IU/g	17.0
Vitamin D_3 [e, g]	IU/g	1.2
Vitamin E	IU/kg	150
Vitamin K_3 (menadione)	mg/kg	58
Vitamin B_1 (thiamin)	mg/kg	64
Vitamin B_2 (riboflavin)	mg/kg	16
Niacin (nicotinic acid)	mg/kg	84
Vitamin B_6 (pyridoxine)	mg/kg	17
Pantothenic Acid	mg/kg	76
Vitamin B_{12} (cyanocobalamin)	mg/kg	0.09
Biotin	mg/kg	0.57
Folate	mg/kg	5
Choline	mg/kg	1030
Fatty Acids		
C16:0 Palmitic	%	0.5
C18:0 Stearic	%	0.1
C18:1ω9 Oleic	%	0.7
C18:2ω6 Linoleic	%	2.0
C18:3ω3 Linolenic	%	0.1
Total Saturated	%	0.6
Total Monounsaturated	%	0.7
Total Polyunsaturated	%	2.1
Other		
Cholesterol	mg/kg	--

[a] Ether extract is used to measure fat in pelleted diets, while an acid hydrolysis method is required to recover fat in extruded diets. Compared to ether extract, the fat value for acid hydrolysis will be approximately 1% point higher.

[b] Carbohydrate (available) is calculated by subtracting neutral detergent fiber from total carbohydrates.

[c] Neutral detergent fiber is an estimate of insoluble fiber, including cellulose, hemicellulose, and lignin. Crude fiber methodology underestimates total fiber.

[d] Energy density is a calculated estimate of *metabolizable energy* based on the Atwater factors assigning 4 kcal/g to protein, 9 kcal/g to fat, and 4 kcal/g to available carbohydrate.

[e] Indicates added amount but does not account for contribution from other ingredients.

[f] 1 IU vitamin A = 0.3 µg retinol

[g] 1 IU vitamin D = 25 ng cholecalciferol

For nutrients not listed, insufficient data is available to quantify.

Figure 2: Composition of diet 2: 14% protein and 3.5% fat (Harlan Tekland global diet)

4.3.2 Ethics Statement

Procedures involving animals and their care were in accordance to the national and international laws and policies (EEC Council Directive 86/609, OJ L 358, 1 Dec.12, 1987; NIH Guide for the Care and use of Laboratory Animals, U.S. National Research Council, 2011). The Mario Negri Institute for Pharmacological Research (IRCCS, Milan, Italy) Animal Care and Use Committee (IACUC) approved the experiments, which were conducted according to the institutional guidelines, which are in compliance with Italian laws (D.L. no. 116, G.U. suppl. 40, Feb. 18, 1992, Circular No.8, G.U., Juli14, 1994). The scientific project was approved by Italian Ministry of Health (Permit Number: 71/2014 B).

4.3.3 Study Design

After the characterization of our mouse model of tauophaty, that replicates the impairments found in patients affected by tauophaty in a way age-gender-dependent showing that females were more affected than males, the aim of this study was to investigate the interaction between diets and genotype (P301L TG and B6D2F1 CTR mice) on the onset and progression of neurodegenerative disease in the used TG mouse model. After the weaning, all animals were fed with the same diet (diet 1 required for the growth of the mice); at 3 months of age the animals were divided into two experimental groups: the first group fed with diet 1 and the second group fed with diet 2. Mice were further divided into two separate groups for studying either behavior or metabolic profile linked to different diets administered; in the first group (n=240) body weight, food and water consumption and survival rates were analyzed.

In the second group (n=160), on the basis of the data from other authors [17-18], two time points of analysis were defined at 7 and 15 months of age (the first time point the symptoms of the disease were evidently expressed, the second time point was evidenced as the maximum survival for mice affected by tauophaty).

To investigate the onset and progression of neurodegenerative disease, animals were sacrificed after the behavioral tests and the brain were analyzed for immunohistochemical (IHC) studies, labeling the neuropathological hallmarks of tauophaty such as aggregates of tau and NFTs, neuronal death, inflammation aspects and gliosis (Fig. 3).

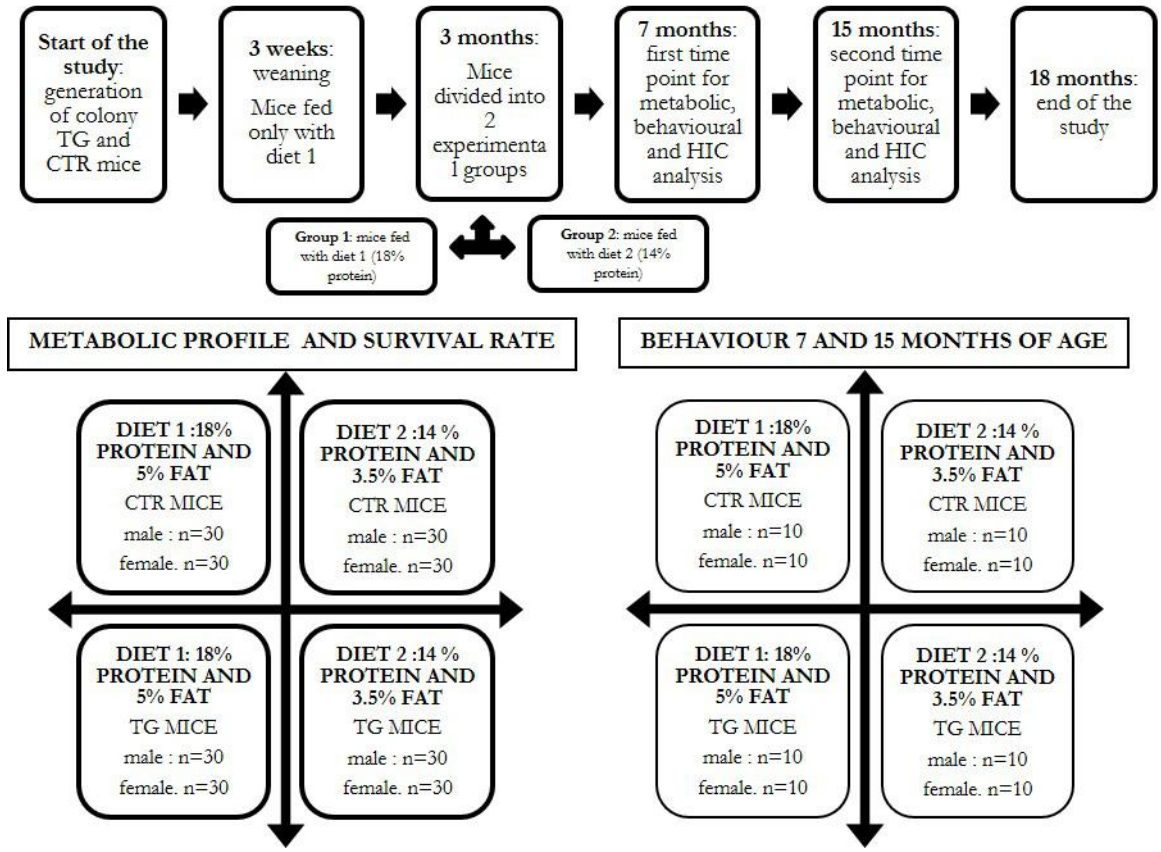

Figure 3: Experimental design of the study. In the study were set three time points: 3 months of age related to the administration of two different diets (diet1 anddiet2), 7 and 15 months of age related to manifestation of the neurodisease and maximum survival of TG animals (time points for behavioral tests). During all experiment were valuated metabolic profile and survival of all animals randomized in 4 experimental groups related to the strain and type of diet administrated.

4.3.4 Metabolic profile and survival rate

Animals were monitored daily for wellbeing welfare-related disease symptoms and their body weights, food and water consumption were recorded weekly. Based on the daily consumption of food of a mouse (5gr/daily for each mouse), it was decided to administer 200 grams of food per cage containing 4 mice (both diet 1 both diet 2). A decrease in body weight greater than 15% in two consecutive weeks (15% +15%) was considered as humanitary end-point of the study and the animal sacrificed.

During the entire experiment, a large number of data was recorded, so we decided to group the values showing the average values for each experimental group every 4 weeks, except for the metabolic data collected in the first 12 weeks.

4.4 BEHAVIORAL TESTS

4.4.1 Novel-Object Recognition Test (NORT)

The novel-object recognition test (NORT) is a memory test relied on spontaneous without the need of stressful elements animal behavior [13-14]. In the present study, the object recognition task was conducted in an open-field arena (40 × 40 × 40 cm) with floor divided into 25 squares by black lines; three stimulus objects of similar size were used: a black plastic cylinder (4 × 5 cm), a glass vial with a white cup (3 × 6 cm), and a metal cube (3 × 5 cm).
The task started with a habituation trial during which the animals were placed in the empty arena for 5 min, and their movements were recorded as the number of line crossings, which provided an indication of both CTR and TG mice locomotion motor activities. In the next day, mice were re-placed in the same arena containing two identical objects (familiarization phase).
The objects were randomly selected to avoid bias among animals and between groups. Exploration was recorded in a 10 min trial by an investigator blinded to the genotype and treatment. Sniffing, touching, and stretching the head toward the object at a distance of no more than 2 cm were scored as object investigation. Twenty-four hours later (test phase), mice were placed again in the arena containing two objects: one already presented during the familiarization phase (familiar object) and a new different one (novel object). The time spent exploring the two objects was recorded for 10 min. Following each session of NORT, the arena and objects were cleaned with 70% ethanol to ensure that the animal's behavior was not guided by odor cues. Results were expressed as percentage time of investigation on objects per 10 min or as discrimination index (DI), i.e., (seconds spent on novel - seconds spent on familiar)/ (total time spent on objects). Animals with no memory impairment spent a longer time investigating the novel object, giving a higher DI.

4.4.2 Open Field (OF) and spontaneous locomotor activity

The OF test is used to examine the general locomotion, as well as exploration activities, and consequent level of anxiety by exposing mice to a novel and open space [15-16]. We used a grey Perspex OF box (40 × 40 × 40 cm) with the floor divided into 25 (8 × 8 cm) squares. Mice were placed into the center of the floor defined as a 'starting point' and their behavior video-recorded for 5 min.
The parameters analyzed as measure of spontaneous locomotor activity, exploratory activity and state of anxiety were: the duration of locomotion divided into the number of internal (the nine central squares) and external (the sixteen peripheral squares) squares crossed, the time spent in the central and external area of the open field, the number and duration of rearing (standing on the hind

paws), the number and duration of self-grooming (rubbing the body with paws or mouth and rubbing the head with paws)[30].

4.4.3 Immunohistochemistry

At the end of behavioral tests animals were euthanized by cervical dislocation [17-18]; brains were removed and fixed in 10% formalin for 24–48 h with the usual procedure and embedded in paraffin. After deparaffinization brain coronal sections (3 μm thick; three slices per mouse) were stained for immunohistochemistry utilizing different antibodies (see table 1). The sections were incubated for 1 h at room temperature with blocking solutions [AT8 and AT100: 0.3% Triton X-100 plus 10% NGS; NFTS: 0.4% Triton X-100 plus 3% NGS; GFAP: 0.4% Triton X-100 plus 3% NGS; NeuN: 0.1% Triton X-100 plus 10% NGS] and then overnight at 4°C with the primary antibodies. After incubation with the biotinylated secondary antibody (1:200; 1 h at room temperature; Vector Laboratories), the sections were then incubated for 30 minutes at room temperature with the avidin-biotin-peroxidase complex (Vector Laboratories, Burlingame, CA) and diaminobenzidine (Sigma).
The sections were then lightly counterstained with hematoxylin. The specificity of the immunostaining was verified by incubating sections with PBS instead of the specific primary antibodies. To determine the level of apoptosis in the brain, TUNEL assay were performed using Dead-end™ Colorimetric TUNEL System (Promega, nr G3250).
Briefly, after the deparaffinization, sections were immersed at room temperature in a 0.85% NaCl solution for 5 minutes, washed twice in PBS (5 min), placed in the Proteinase-K solution from the TUNEL assay kit for 10 min at room temperature and fixed in 10% buffered formalin solution (5 min). After washing in PBS three times (5 min each), sections were immersed in Equilibration buffer from the TUNEL assay kit (10 min), and incubated with a rTdT reaction mix (from the TUNEL assay kit) in a humidified chamber at 37°C for 1 h.
To stop the reaction, sections were immersed in stop buffer for 15 min at RT and washed twice with PBS (5 min each); for blocking endogenous peroxidases, the sections were immersed in 0.3% hydrogen peroxide solution for 5 min, washed twice in PBS (5 min each) and covered with Strep-HRP solution for 30 min at RT. After washing twice in PBS (5 min/wash) to remove the Strep- HRP, sections were immersed in DAB solution for 3 min at room temperature. The brain sections were then counterstained with hematoxylin for 2 min at room temperature.

Table 1: primary antibodies

Antibody	Species	Specificity	Use	Dilution	Source, type
AT 8	Mouse	Tau; Ser(P)^{202}/Thr(P)^{205}	Pre-tangles; Tau marker	1:1000	Euroclone, mAb IgG1
AT 100	Mouse	Tau; Thr(P)^{212}/Ser(P)^{214}	Tau marker	1:1000	Euroclone, mAb IgG1
NFTs	Mouse	Neurofilaments	Axonal marker	1:50	Dako, mAb IgG1
GFAP	Rabbit	Astrocytes	Astrocytic marker	1:2500	Dako, mAb IgG
NeuN	Mouse	Neurons	Neuronal marker	1:1000	Chemicon, mAb IgG1

4.4.4 Neuronal Counts

The brain areas most affected by the toxic role of Tau, characterized by the presence of aggregates of hyperphosphorylated tau, deposition of neurofibrillary tangles, axonal dilatations, neuronal and synaptic loss, are hippocampus, entorhinal cortex, CA1 pyramidal layer and the basal forebrain [19-20-21-22-23]. In our tauophaty mouse model the accumulation of pathological Tau species (AT8, AT100), the neuronal loss (NeuN) and the level of apoptosis (TUNEL) were quantified in the cortex and in the hippocampus (brain coronal sections). Immunoreactive cells were counted by image analysis software in 3 fields using an Olympus Bx51light microscope (Olympus, Italy) equipped with a digital camera (at x400 each field represented a tissue section area of about 0.036 mm^2). Following manual tracing of the cortex and hippocampus at the same stereotactic level in all mice, the number of positive cells were manually tagged and counted. Every section was individually examined for the presence or absence of visible Tau filaments (AT8 and AT100) and for the presence of positive signaling in the nucleus neuronal (NeuN and TUNEL). The observer was not aware of the origin of the sections.

4.4.5 Statistical Analysis

Statistical analyses were performed using Graph Pad Prism 6 program. Body weight data, food and water consumption data, NOR data, OF data and neuronal counts data were analyzed using two-way ANOVA, followed by Tukey's *post hoc* test. Survival ratio was analyzed by Log-rank (Mantel-Cox) test. All data were expressed as mean ± SEM with a statistical significance given at $P< 0.05$.

4.5 RESULTS

4.5.1 Metabolic profile: weight gain, food and water consumption

During the first 12 weeks of experiment, all animals were fed with diet 1 (18% protein and 5% fat). The increase in body weight was significantly reduced in female mice compared to male mice both in TG and CTR mice (ANOVA, $F_{genotype\ (3,\ 1392)} = 306.8$, $P<0.0001$, $F_{time\ (11,\ 1392)} = 308.9$, $P<0.0001$, $F_{interaction\ (33,\ 1392)} = 2.623$, $P<0.0001$; Fig. 4A). In correspondence of 10, 11 and 12 weeks of the experiment, an increase in body weight was significantly reduced in CTR male mice compared to TG male mice ($P<0.0001$; Fig. 4A). No statistically significant difference between experimental groups was identified for food intake ($F_{interaction\ (11,696)} = 1.169$, $P= 0.4510$ Fig. 4B; $F_{interaction\ (11,696)} = 1.044$, $P= 0.4053$ Fig. 4D). From 9 to 12 weeks of the experiment, an increase in water consumption was significantly reduced in CTR male mice compared to TG male mice (ANOVA, $F_{genotype\ (1,696)} =43.87$, $P<0.0001$, $F_{time\ (11,696)} = 44.77$, $P<0.0001$, $F_{interaction\ (11,696)} = 5.941$, $P<0.0001$; Fig. 4C).

In correspondence of 3 and 4 weeks of the experiment, an increase in water consumption was significantly reduced in CTR female mice compared to TG female mice (ANOVA, $F_{genotype\ (1,696)} = 19.26$, $P<0.001$, $F_{time\ (11,696)} = 89.01$, $P<0.0001$, $F_{interaction\ (11,696)} = 2.844$, $P<0.0001$; Fig. 4E).

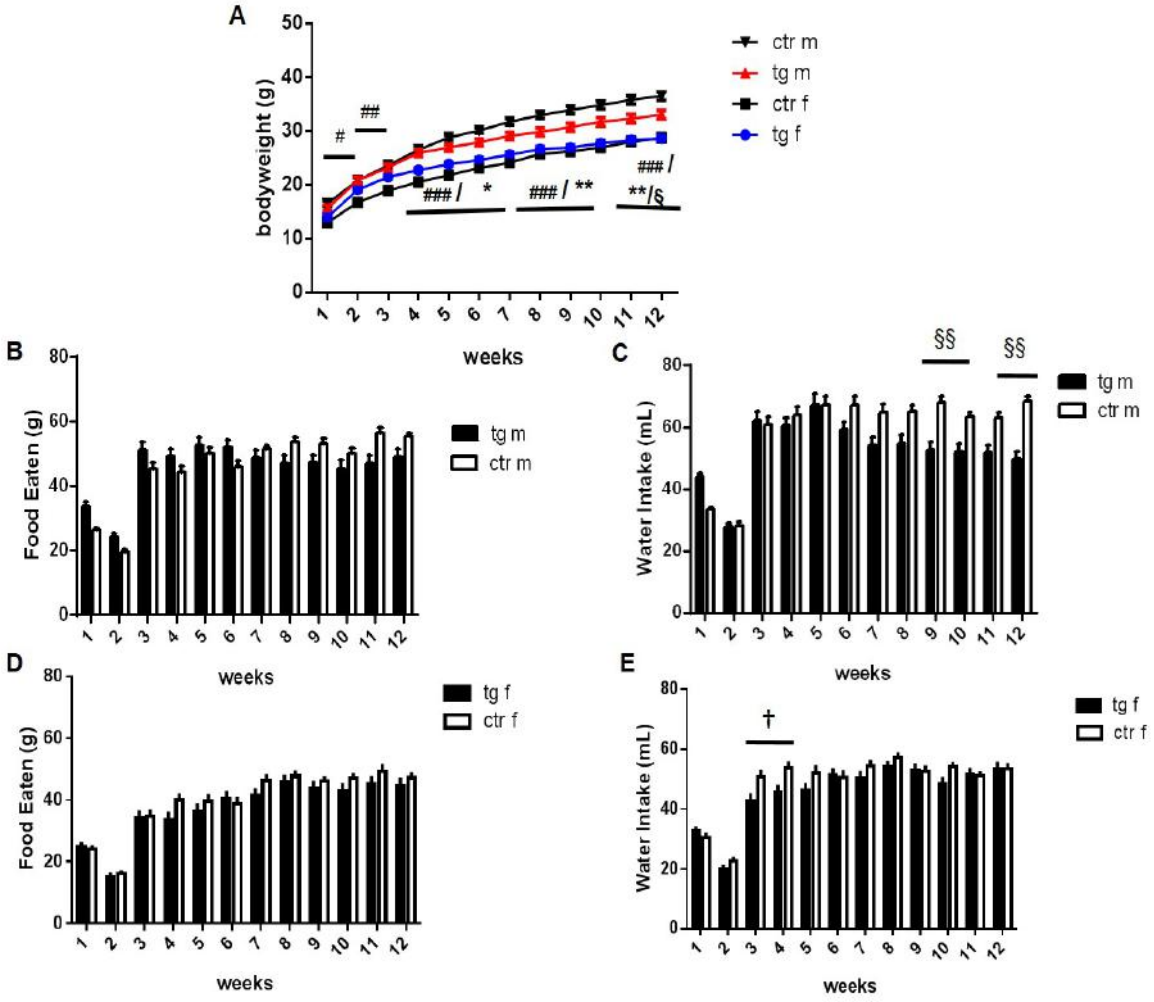

Figure 4. Metabolic profile during 12 weeks of experiment. A) Assessments of body weight and **B, E**) food and water consumption in TG and CTR mice (n=30 for each group). **A)** Both female TG and CTR mice weighed significantly less than male TG and CTR mice. **B-D**) No significant difference in food intake between CTR and TG mice. **C-D**) Significant reduction of water consumption of TG male mice compared to CTR male mice and TG female mice compared to CTR female mice. Data were shown as mean ± SEM.CTR female vs CTR male mice # P< 0.05, ## P< 0.001, ### P< 0.0001, TG male vs CTR male mice § P< 0.05, TG female vs TG male mice * P< 0.05, ** P< 0.001, TG female vs CTR female mice † P< 0.05.

At 3 months of age (corresponding to 12 weeks of experiment), mice were randomized and divided into 2 experimental groups: one fed with diet 1(18% protein and 5% fat) and the second fed with diet 2 (14% protein and 3.5% fat). In order to analyze a possible interaction between diets and genotype, body weight of TG and CTR mice fed with different diets were compared. No diet effects were observed in any genotype (both CTR and TG mice) at 7 months (CTR mice P=0.99 and TG mice P= 0.87; Fig. 5A-5C) and 15 months of age (CTR mice P=0.99 and TG mice P= 0.8829; Fig. 5B-5D).

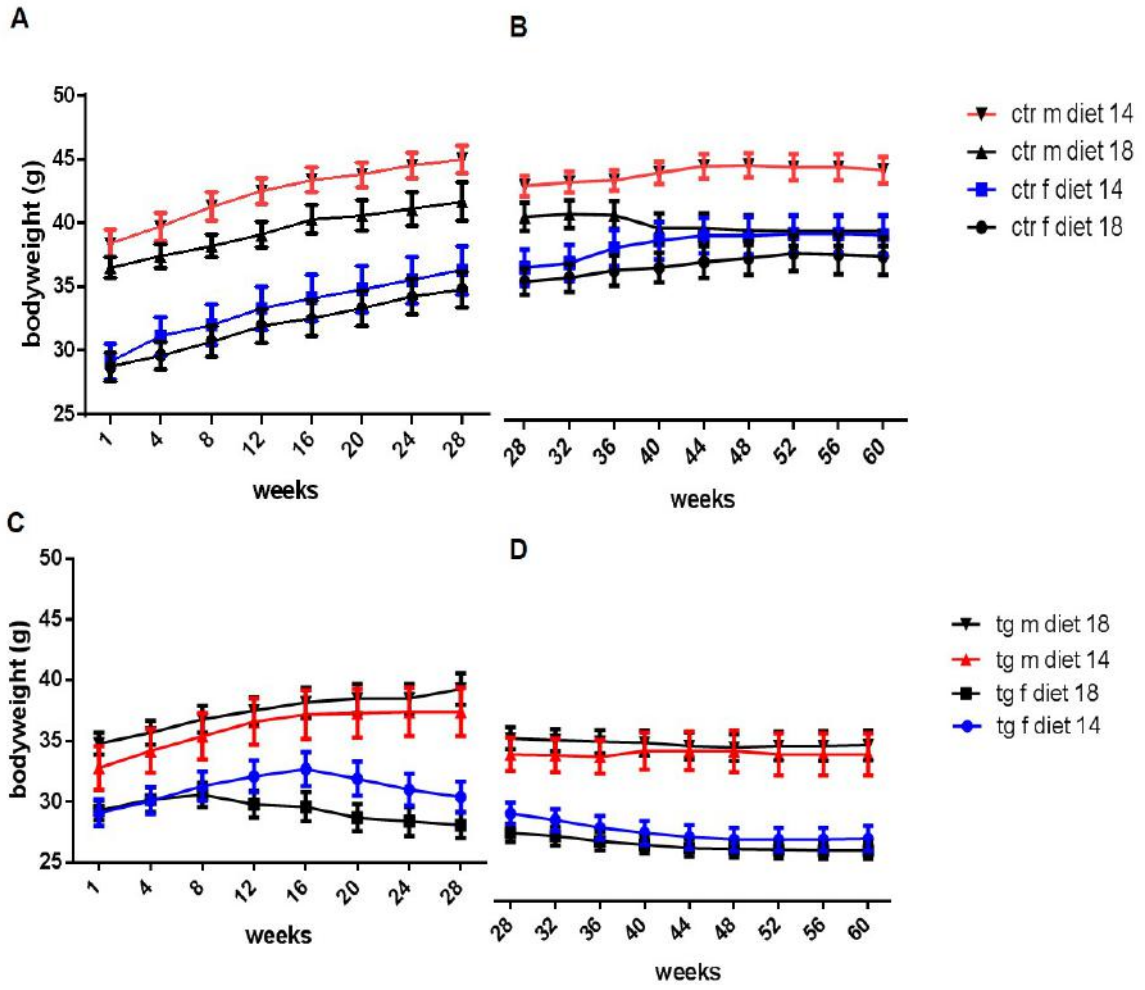

Figure 5. Body weight gain during 60 weeks of experiment. A,B) Assessments of body weight of male and female CTR mice fed with diet 18 and diet 14 at 7 (**A**) and 15 months of age (**B**) (n=30 for each group). **C,D)** Assessments of body weight of male and female TG mice fed with diet 18 and diet 14 at 7 (**C**) and 15 months of age (**D**).

An overall main effect of genotype on body weight was observed throughout the course of the study; from 36 to 60 weeks, female TG mice had smaller body weights, not affected by diet, relative to CTR female mice (ANOVA, $P< 0.001$ and $P< 0.0001$; Fig.6A). From 36 to 60 weeks of experiment, an increase in body weight was significantly reduced in male TG mice fed with diet 14compared to relative CTR male mice fed with the same diet (ANOVA, $P< 0.05$, Fig. 6D).

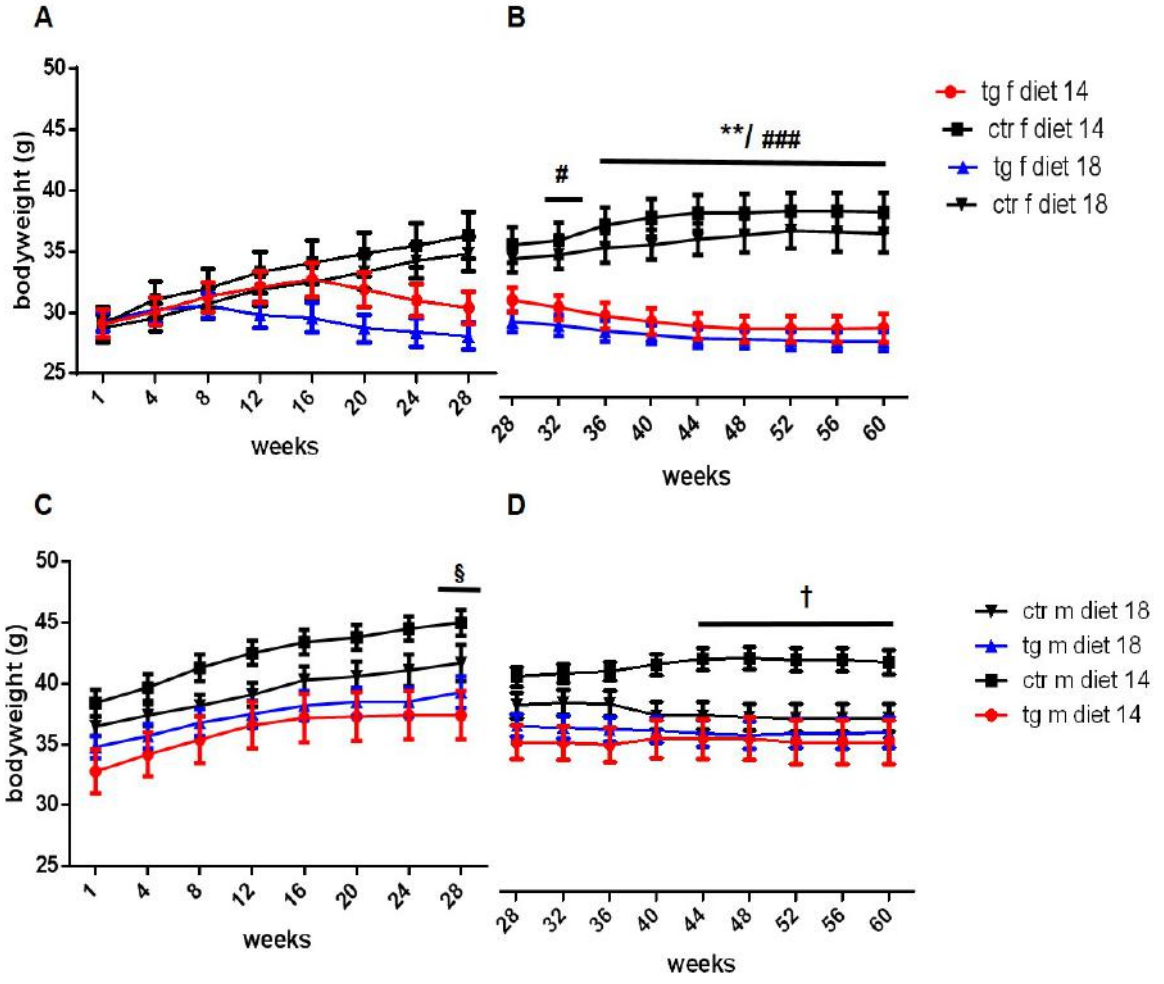

Figure 6. Body weight gain during 60 weeks of experiment. A, B) Assessments of body weight of female TG and CTR mice fed with diet 18 and diet 14 at 7 (**A**) and 15 months of age (**B**) (n=30 for each group). Significant reduction of body weight gain in female TG mice compared to CTR mice fed with diet 18 and 14 at 32 weeks and from 36 to 60 weeks. **C, D**) Assessments of body weight gain in male TG and CTR mice fed with diet 18 and diet 14 at 7 (**C**) and 15 months of age (**D**). Significant reduction of body weight gain in male TG mice compared to CTR mice fed with diet 14 from 44 to 60 weeks, and at 28 weeks in mice fed with diet 18. Data were shown as mean ± SEM. DIET 14: TG female vs CTR female mice ** P< 0.001; TG male vs CTR male mice † P< 0.05. DIET 18: TG female vs CTR female mice # P< 0.05, ### P< 0.0001; TG male vs CTR male mice. § P< 0.05.

In order to analyze the possible interaction between diets and genotype, food and water intake of TG and CTR mice fed with different diets were compared. All CTR mice fed with diet 18 presented significantly greater food intake and water consumption than TG mice throughout the experiment (ANOVA, P< 0.0001, Fig. 7A-B); CTR female mice fed with diet 14 presented significantly greater food intake than TG female mice (P< 0.0001), but not a significant difference in water consumption.

The opposite effect was detected in CTR male mice fed with diet 14: it was any significant difference in food intake compared to TG male mice fed with the same diet, but a significant increase of water consumption of CTR male mice respect to TG male mice (Fig. 7A-B).

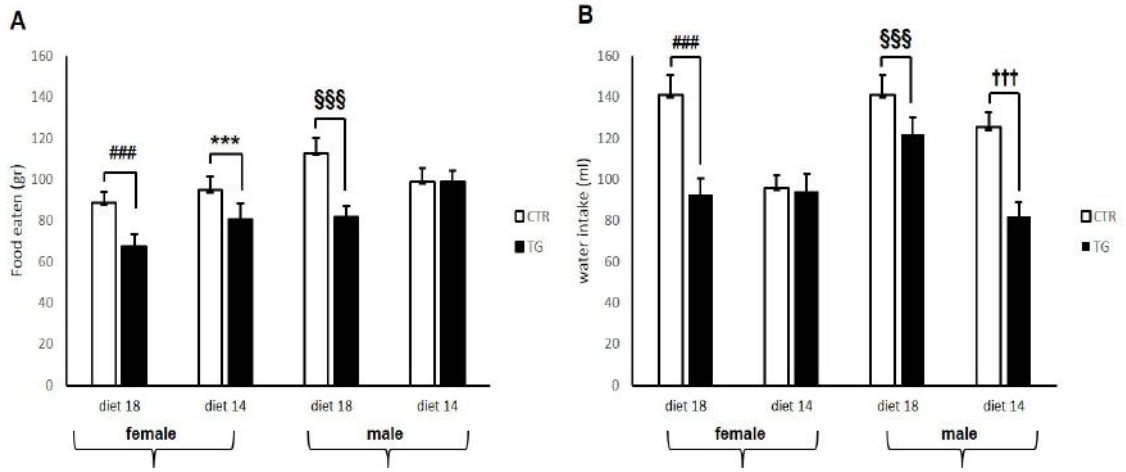

Figure 7. Food and water consumption during 60 weeks of experiment. A, B) Assessments of food intake (**A**) and water consumption (**B**) of TG and CTR mice fed with diet 18 and diet 14 (n=30 for each group). Significant increase of food and water consumption in CTR mice compared to TG mice fed with diet 18. Significant increase of food intake in female CTR mice compared TG mice fed with diet 14 and significant increase of water intake in male CTR mice compared TG mice fed with diet 14. Data were shown as mean ± SEM. DIET 14: TG female vs CTR female mice *** P< 0.001; TG male vs CTR male mice ††† P< 0.0001. DIET 18: TG female vs CTR female mice ### P< 0.0001; TG male vs CTR male mice §§§ P< 0.0001.

After detected a genotype effect, in order to analyze a possible effect of a specific diet within a strain, at 7 and 15 months of age food and water consumption of CTR mice fed with diet 18 and diet 14 were compared. At 12, 20, 28, 32-36 weeks a significant increase of food intake was found in CTR male mice fed with diet 18 compared to CTR male mice fed with diet 14 (ANOVA, P< 0.0001, Fig. 8A-B).

At 12, 32 and 48 weeks a significant increase of water intake was found in CTR male mice fed with diet 18 compared to CTR male mice fed with diet 14 (ANOVA, P< 0.0001, Fig. 8C-D).

A statistically difference in food intake between CTR female mice fed with diet 18 and 14 in each time point was not identified (except at 60 weeks, P< 0.05, Fig. 9A-B). At 12, 24, 48-60 weeks a significant increase of water intake was found in CTR female mice fed with diet 18 compared to mice fed with diet 14 (ANOVA, P< 0.0001, Fig. 9C-D).

At 7 and 15 months of age food and water consumption of TG mice fed with diet 18 and diet 14 were compared.

P< 0.001.

At 12, 40, 48-60 weeks a significant increase of food intake was found in TG male mice fed with diet 18 compared to TG male mice fed with diet 14 (ANOVA, P< 0.0001, Fig. 10A-B); at 12, 24-32, 40 and 48-56 weeks a significant increase of water intake was found in TG male mice fed with diet 18 compared to TG male mice fed with diet 14 (ANOVA, P< 0.0001, Fig. 10C-D).

At 20-32 and 40-48 weeks a significant increase of food intake was found in TG female mice fed with diet 18 compared to mice fed with diet 14 (ANOVA, P< 0.0001, Fig. 11A-B).
A statistically difference in water intake between TG female mice fed with diet 18 and 14 in each time point was not identified (P> 0.05, Fig. 11C-D).

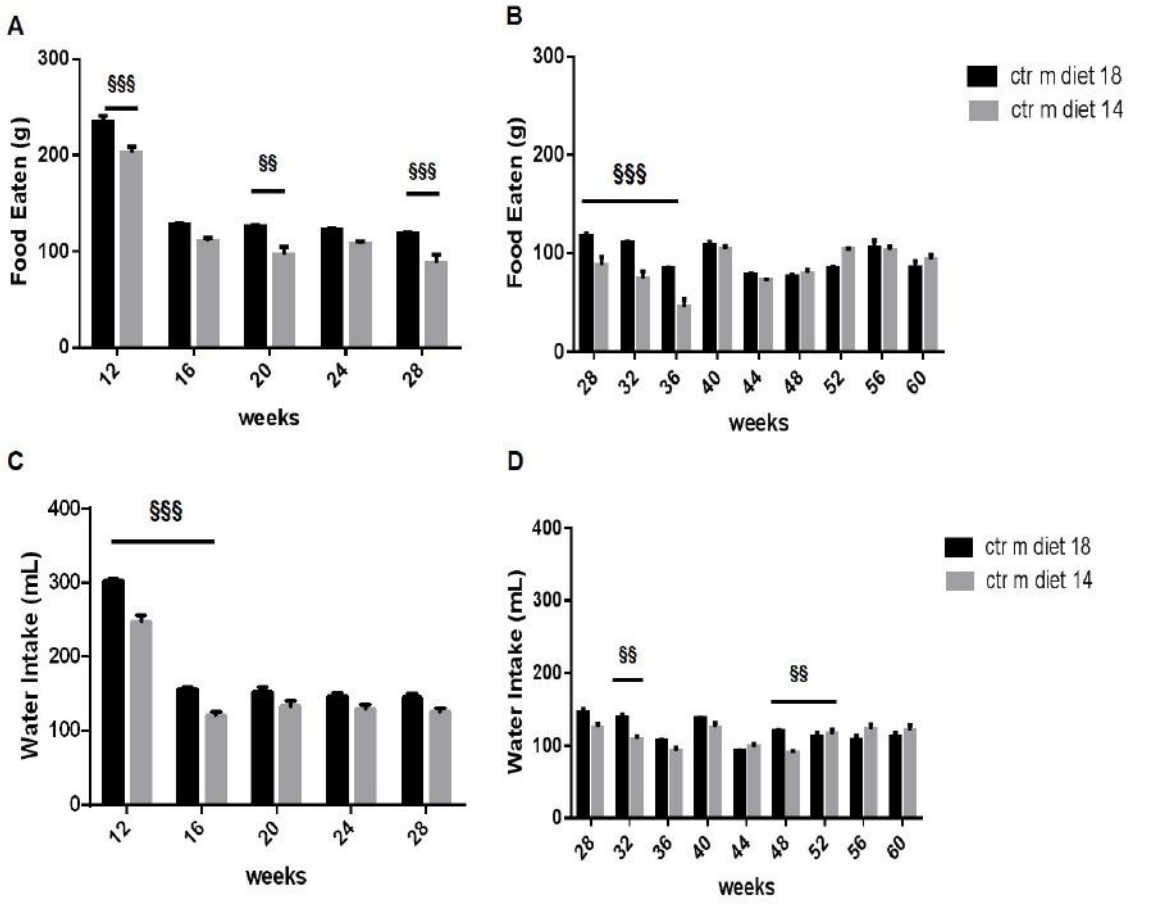

Figure 8. Food and water consumption of CTR male mice at 7 and 15 month of age. A, B) Assessments of food intake and **C, D)** water intake at 7 (**A**) and 15 (**B**) month of age of CTR male mice fed with diet 18 and diet 14(n=30 for each group). Significant increase of food consumption in CTR mice fed with diet 18 compared to CTR mice fed with diet 14. **C, D**) Significant increase of water intake in CTR mice fed with diet 18 compared to CTR mice fed with diet 14. Data were shown as mean ± SEM. CTR male diet 18 vs CTR male diet 14 mice §§ P< 0.001; §§§ P< 0.0001.

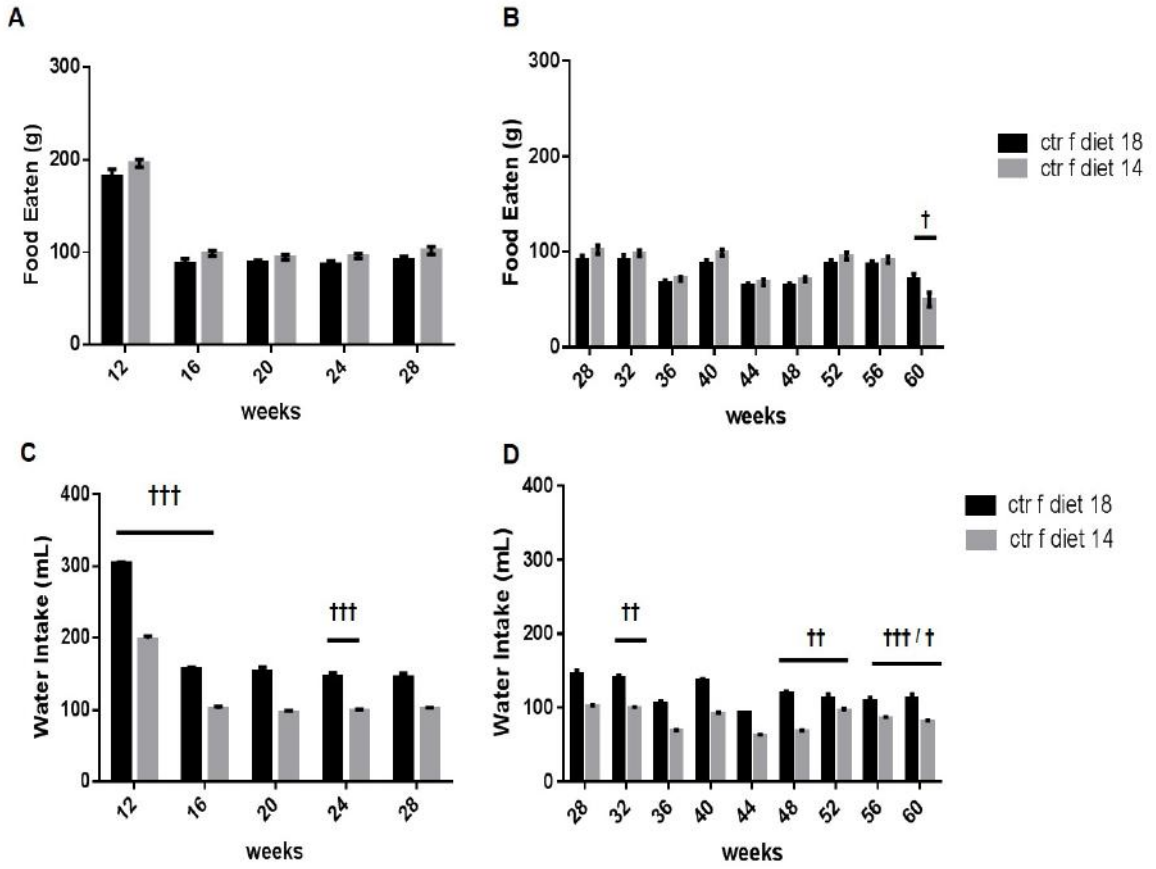

Figure 9. Food and water consumption of CTR female mice at 7 and 15 month of age. A, B) Assessments of food intake and **C, D)** water intake at 7 (**A**) and 15 (**B**) month of age of CTR female mice fed with diet 18 and diet 14 (n=30 for each group). No significant difference of food consumption between two groups was found (except at 60 weeks). **C, D)** Significant increase of water intake in CTR mice fed with diet 18 compared to CTR mice fed with diet 14. Data were shown as mean ± SEM. CTR female diet 18 vs CTR female diet 14 mice † P< 0.05; †† P< 0.001; ††† P< 0.0001.

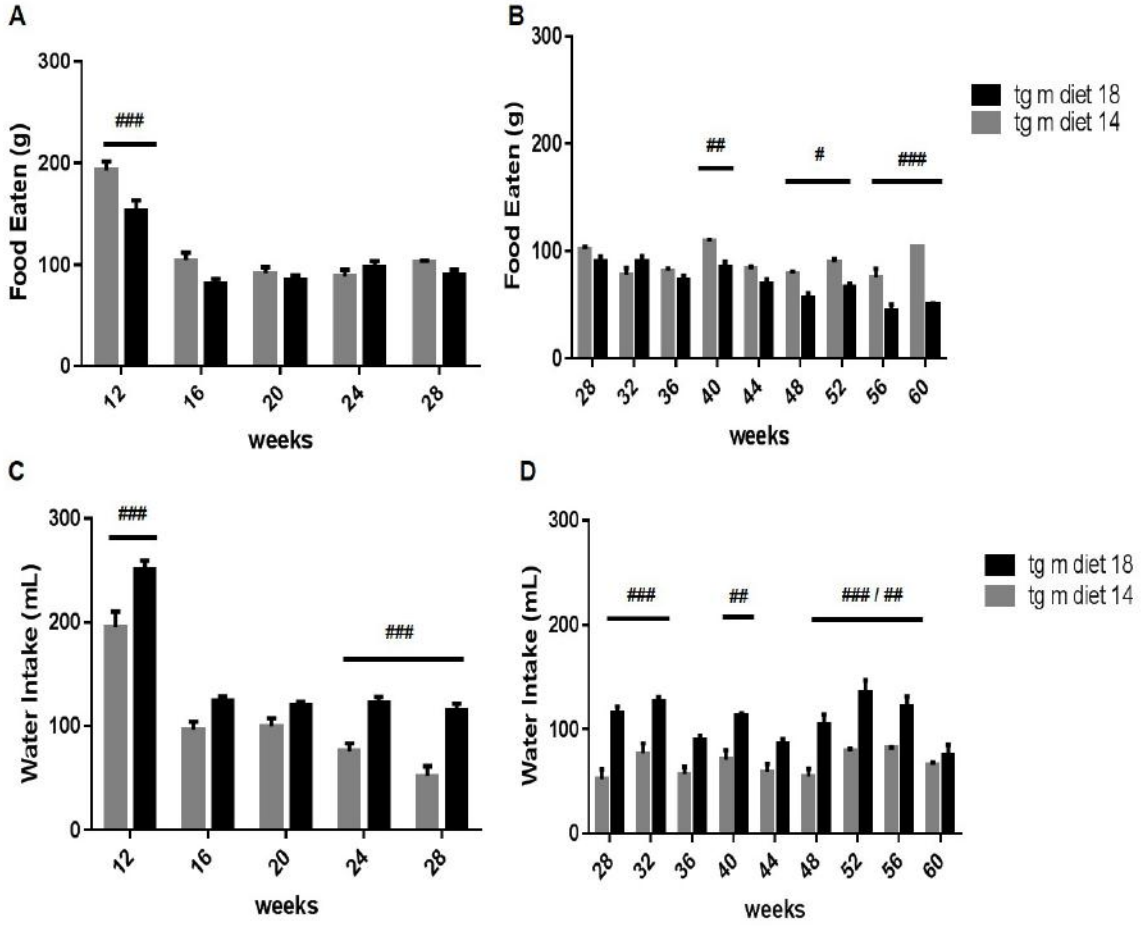

Figure 10. Food and water consumption of TG male mice at 7 and 15 month of age. **A, B)** Assessments of food intake and **C, D)** water intake at 7 (**A**) and 15 (**B**) month of age of TG male mice fed with diet 18 and diet 14 (n=30 for each group). Significant increase of food consumption in TG mice fed with diet 18 compared to TG mice fed with diet 14. **C, D)** Significant increase of water intake in TG mice fed with diet 18 compared to TG mice fed with diet 14. Data were shown as mean ± SEM. TG male diet 18 vs TG male diet 14 mice #p< 0.05; ## P< 0.001; ### P< 0.0001.

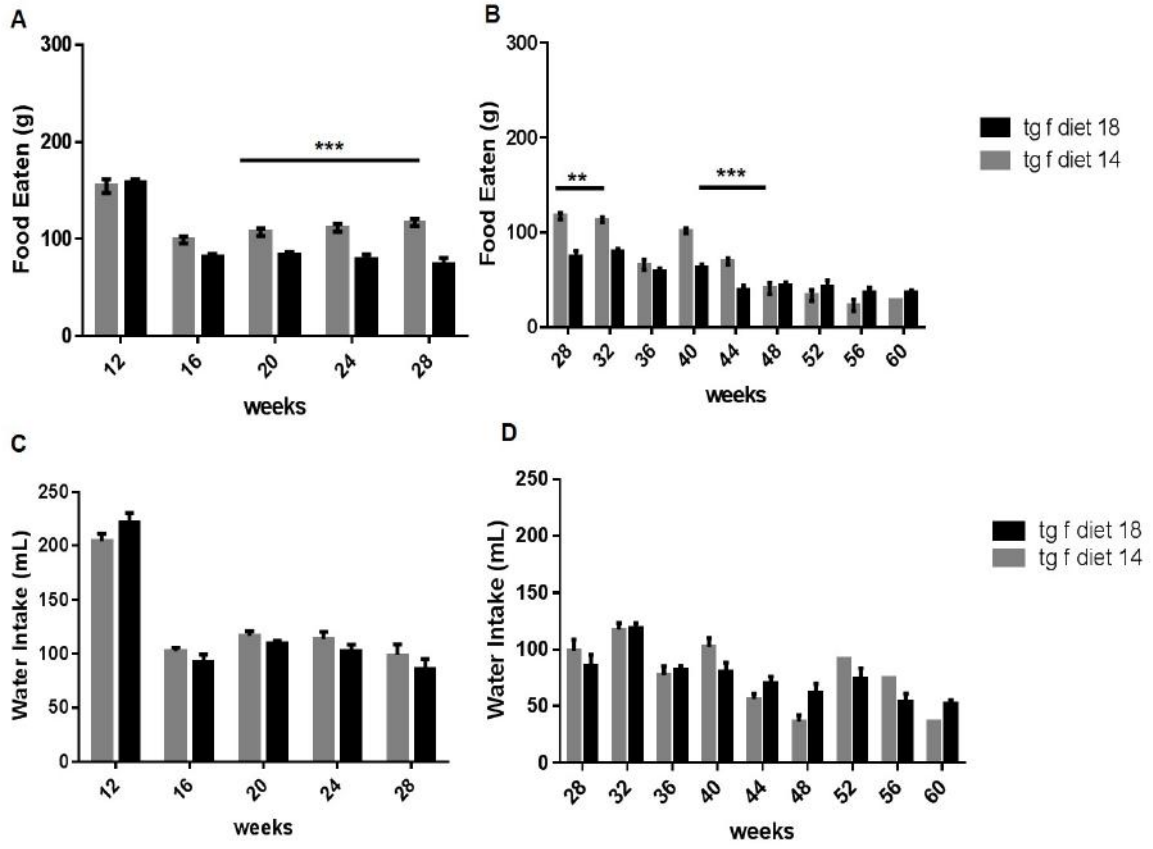

Figure 11. Food and water consumption of TG female mice at 7 and 15 month of age. A, B) Assessments of food intake and water intake **C, D)** at 7 (**A**) and 15 (**B**) month of age of TG female mice fed with diet 18 and diet 14 (n=30 for each group). Significant increase of food intake in TG mice fed with diet 18 compared to TG mice fed with diet 14. **C, D**) No significant difference of water intake between two groups was found. Data were shown as mean ± SEM. CTR female diet 18 vs CTR female diet 14 mice ** P< 0.001; *** P< 0.0001.

4.5.2 Survival Rate

The analysis of survival rate showed that both male and female TG mice had a significantly reduced survival rate compared to CTR mice, regardless of diet administered (Chi square= 37.39, P<0.0001, Fig. 12A, Chi square= 33.50, P<0.0001 Fig. 12B, Chi square= 47.44, P<0.0001, Fig. 12C, Chi square= 41.95, P<0.0001 Fig. 12D).

After detected a genotype effect, in order to analyze the possible interaction between diets and genotype, the survival rates of CTR male mice fed with different diets and females mice fed with different diets were compared, but was not significant difference between two groups (P> 0.05, Fig. 13A-B).

The same analysis was conducted for TG male and female mice fed with different diets, showing a significantly reduction of percentage of survival in TG female mice fed with diet 18 compared to mice fed with diet 14 (Chi square= 11.06, P<0.0001, Fig. 13D). A significant effect of diets was not found for the comparison of TG male mice fed with different diets (P> 0.05, Fig. 13C).

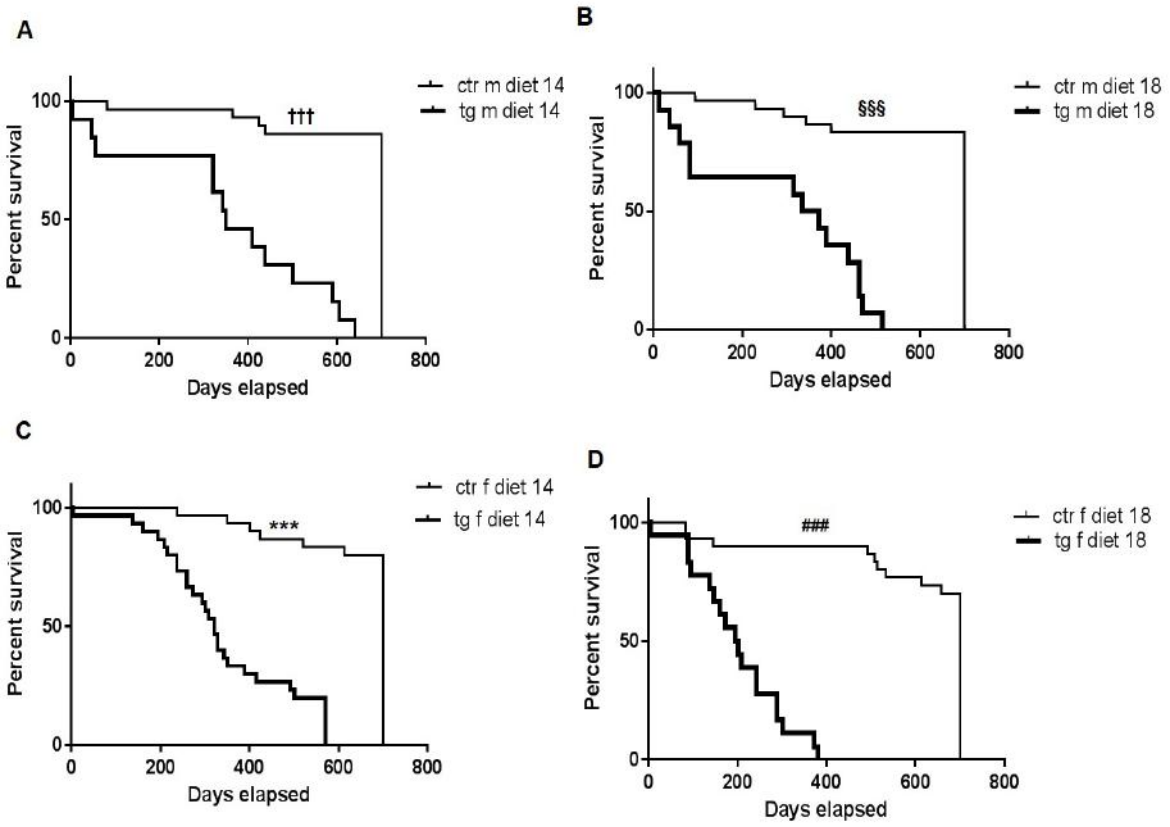

Figure 12. Survival rate of TG and CTR mice fed with different diets. A-D) Significant decrease of survival rate in TG males and females compared to CTR all along the experiment (n=30 for each group). Data were shown as mean ± SEM. DIET 14: TG male vs CTR male mice ††† P< 0.0001, TG female vs CTR female mice *** P< 0.0001. DIET 18: TG male vs CTR male mice §§§ P< 0.0001, TG female vs CTR female mice ### P< 0.0001.

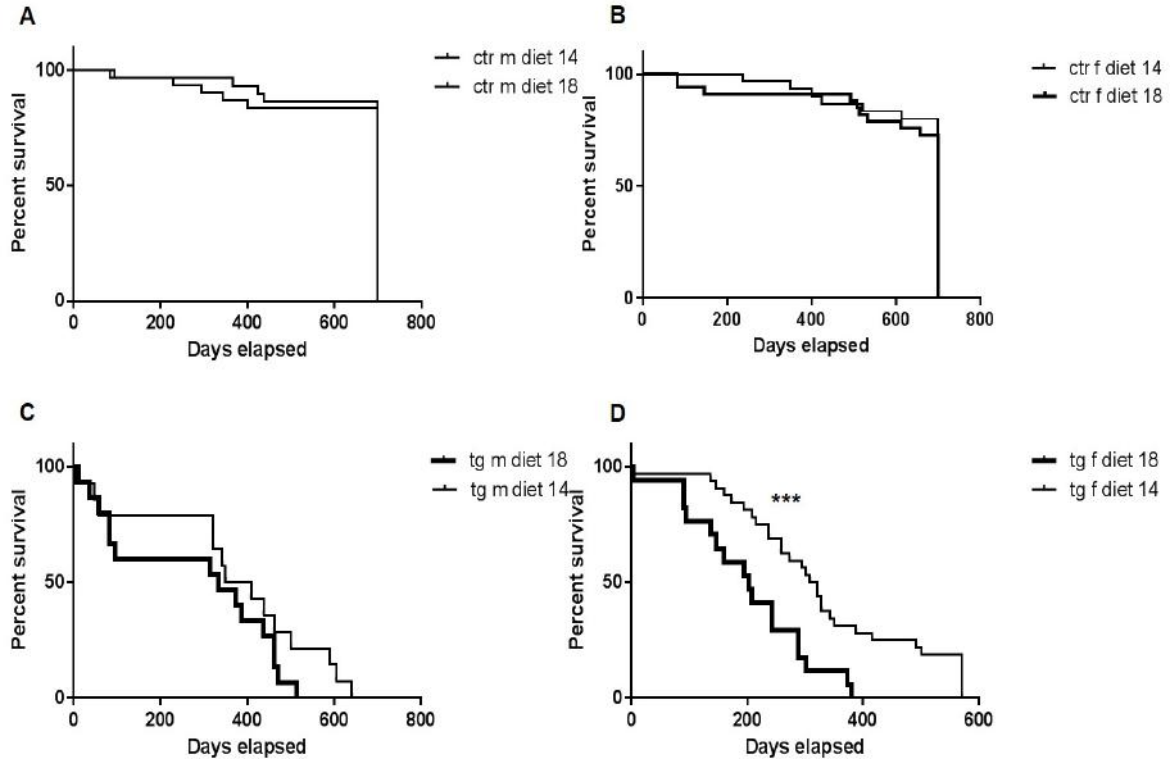

Figure 13. Survival rate of TG and CTR mice fed with different diets. A, B) No significant difference of survival rate between CTR mice fed with diet 18 and 14 (both male and female) was found. **C, D)** Significant decrease of survival rate in TG female mice fed with diet 18 compared to TG female mice fed with diet 14 all along the experiment (n=30 for each group). No significant difference of survival rate between TG male mice fed with diet 18 and 14 was found. Data were shown as mean ± SEM. TG female diet 18 vs TG female diet 14 mice *** P< 0.0001.

4.5.3 Behavioral Tests

After detected a gender-genotype interaction in the mouse model of tauophaty used in this study, it was decided to investigate a possible effect of the diets on the cognitive impairment and progression of tauophaty in this mouse model. For this purpose, both male and female TG and CTR mice fed with different diets at 7 and 15 months of age were tested in novel object recognition test.

In either time points, regardless of diets both male and female TG mice spent less time investigating the novel object compared to CTR mice (for male Fig. 14A, 15A, for female Fig. 14C, 15C).

A significant genotype effect was found for measures of cognitive impairment such as discrimination index (7 months: male $F_{(1, 36)} = 10.02$, $P<0.05$; female $F_{(1,36)} = 33.32$, $P<0.0001$) (Fig. 14B-14D), (15 months: male $F_{(1,36)} = 91.19$, $P<0.0001$; female $F_{(1, 36)} = 91.19$, $P<0.0001$) (Fig. 15B-15D).

In either time points any statistically significant effect of diets was found (P>0.05).

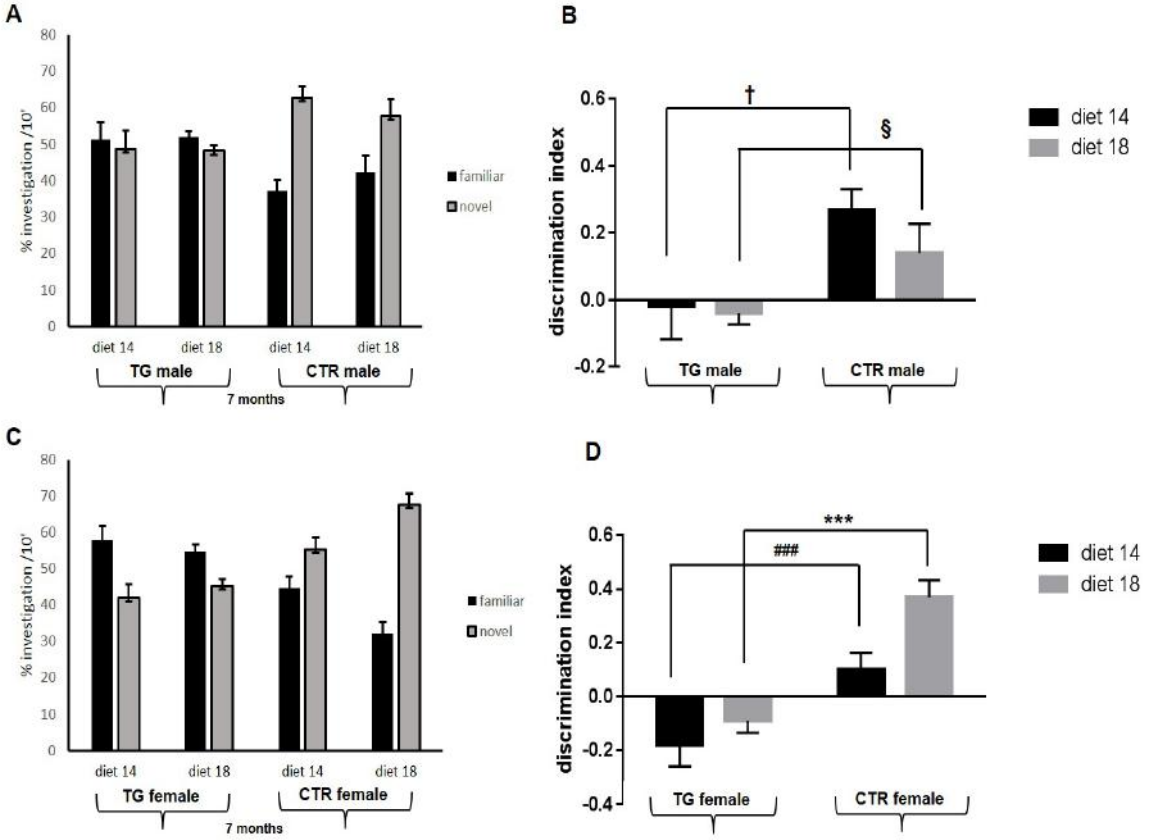

Figure 14. Discriminatory activity at 7 months of age in novel object recognition test. A-C) Histograms indicate percentage of exploration of the familiar and novel objects at 7 months of age. Regardless of diets administrated, at 7 months of age tauophaty significantly impaired memory (each experimental group n=10). **B-D)** Histograms show the corresponding discrimination index for the data shown in the figure A and in the figure C. Data were shown as mean ± SEM. DIET 14: TG male vs CTR male mice † P< 0.05, TG female vs CTR female mice *** P< 0.0001. DIET 18: TG male vs CTR male mice § P< 0.05, TG female vs CTR female mice ### P< 0.0001.

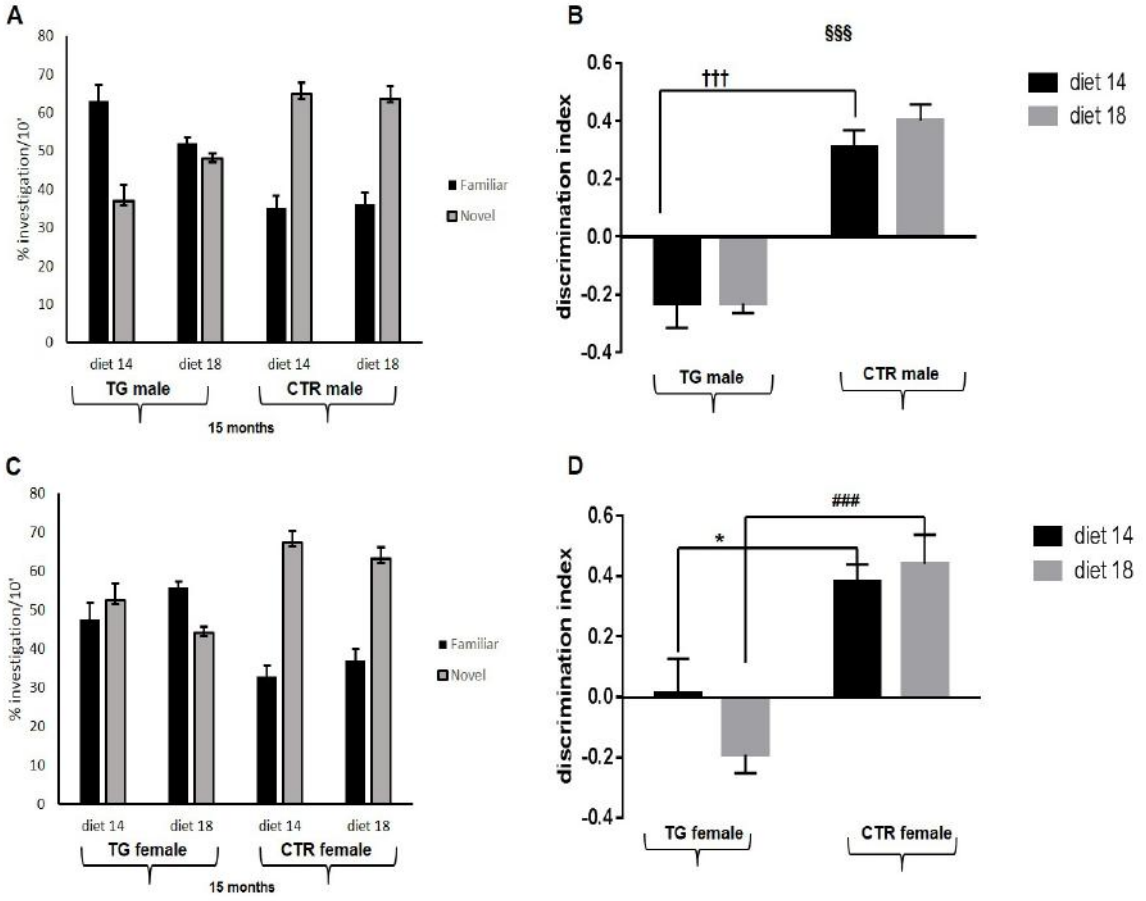

Figure 15. Discriminatory activity at 15 months of age in novel object recognition test. A-C) Histograms indicate percentage of exploration of the familiar and novel objects at 15 months of age. Regardless of diets administrated, at 15 months of age tauophaty significantly impaired memory (each experimental group n=10). **B-D)** Histograms show the corresponding discrimination index for the data shown in the figure A and in the figure C. Data were shown as mean ± SEM. DIET 14: TG male vs CTR male mice ††† P< 0.0001, TG female vs CTR female mice * P< 0.05. DIET 18: TG male vs CTR male mice §§§ P< 0.0001, TG female vs CTR female mice ### P< 0.0001.

After detected in the first work a correlation between time and genotype, a possible interaction between time and diets was analyzed; discrimination indexes of TG female mice fed with diet 14 and 18 at 7 and 15 months of age were compared, but a significant difference between two groups (P= 0.07) was not evident (Fig. 16A).

The same analysis was conducted for TG male mice fed with diet 14 and 18at 7 and 15 months of age, but only a significant time effect (P< 0.001) and not an interaction between time and diets was found (Fig 16B).

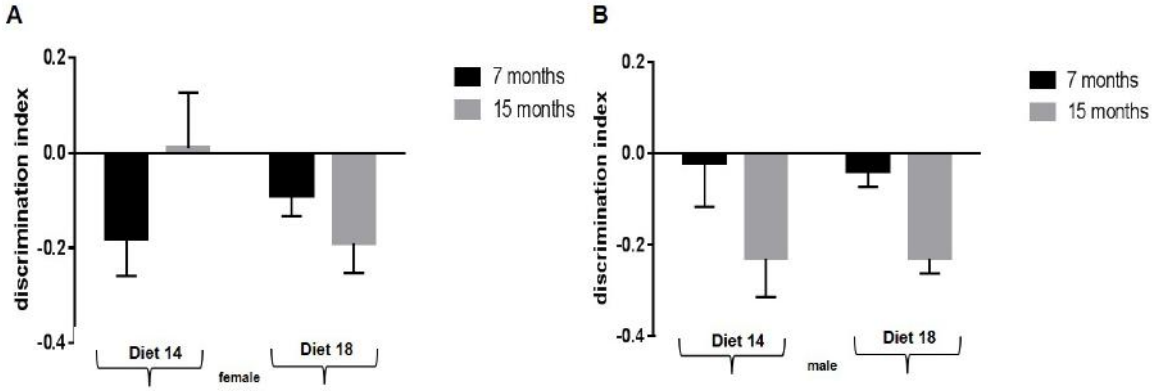

Figure 16. Discriminatory activity at 7 and 15 months of age in novel object recognition test. A-B) Histograms show the corresponding discrimination indexes of male and female TG mice fed with diet 14 and 18 at 7 and 15 months of age (each experimental group n=10). Any statistically significant interaction time-diets was found.

In order to investigate a possible effect of diets correlated to spontaneous locomotor and exploratory activities in the mouse model of tauophaty used in this study, both male and female TG and CTR mice fed with different diets at 7 months of age were tested in the open field test. At 7 months of age, any significant effect of diets was found for parameters analyzed as total number of crossing, number of internal and external crossing (for measures of locomotor activity, P> 0.05, Fig. 17A-C), time spent in the inner and external zone (for measures of exploratory activity, P> 0.05, Fig. 17D-E) and number of rearing, number of grooming, time spent for rearings and time spent for grooming (for measures of exploratory activity, P> 0.05, Fig. 17F-I).
At 15 months of age, any significant effect of diets was detected for parameters related to locomotor and exploratory activity (P> 0.05, Fig. 18A-G); a significant diet effect was found for measures of number of grooming in male TG mice fed with different diets and a significant genotype effect in TG male mice compared to CTR male mice fed with diet 14 was found (P< 0.001, Fig. 18H).
A significant diet effect was found also for the other parameter as time spent for grooming in male TG mice fed with different diets and a significant genotype effect in TG mice (both male and female) compared to CTR male mice fed with diet 14 was found (P< 0.001, Fig. 18I).

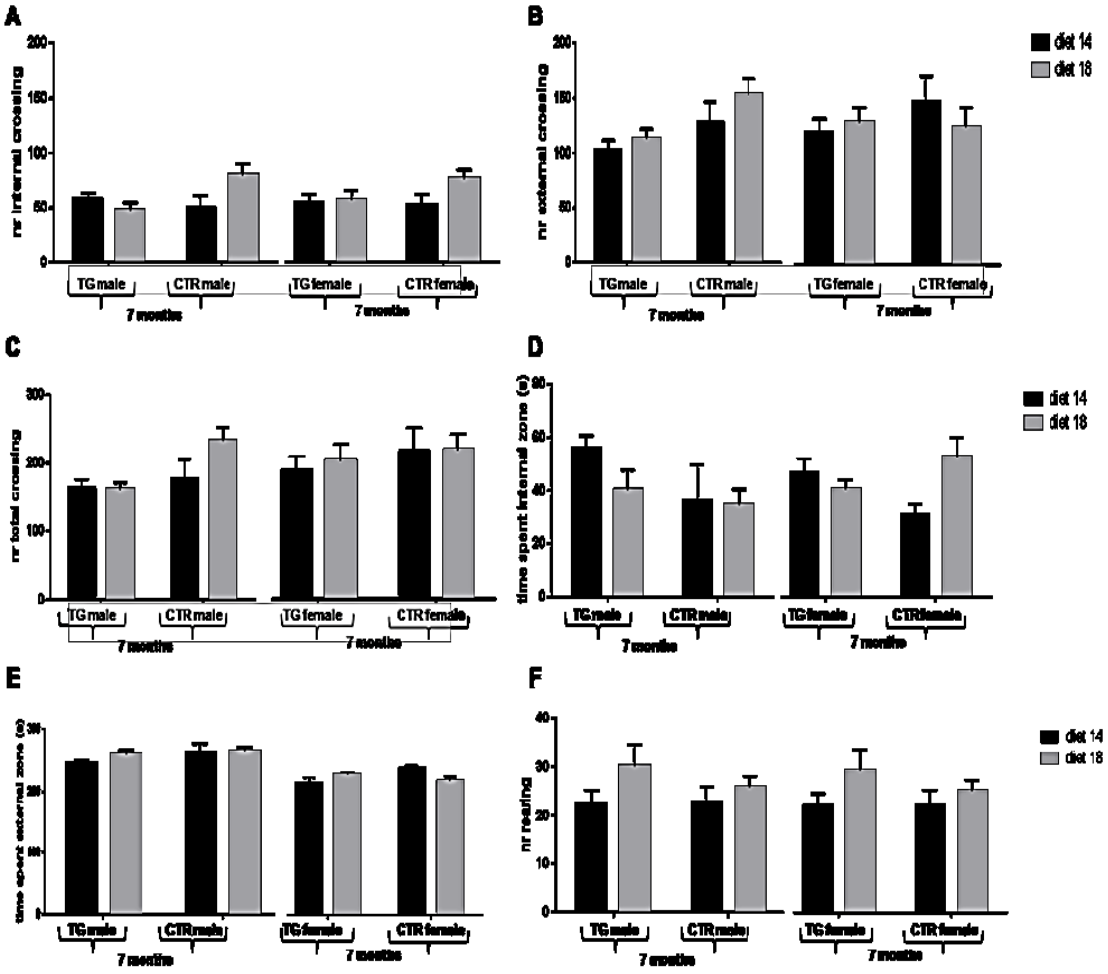
A
B
C
D
E
F
nr internal crossing
nr external crossing
nr total crossing
time spent internal zone (s)
time spent external zone (s)
nr rearing
diet 14
diet 18
TGmale
CTRmale
TGfemale
CTRfemale
7 months

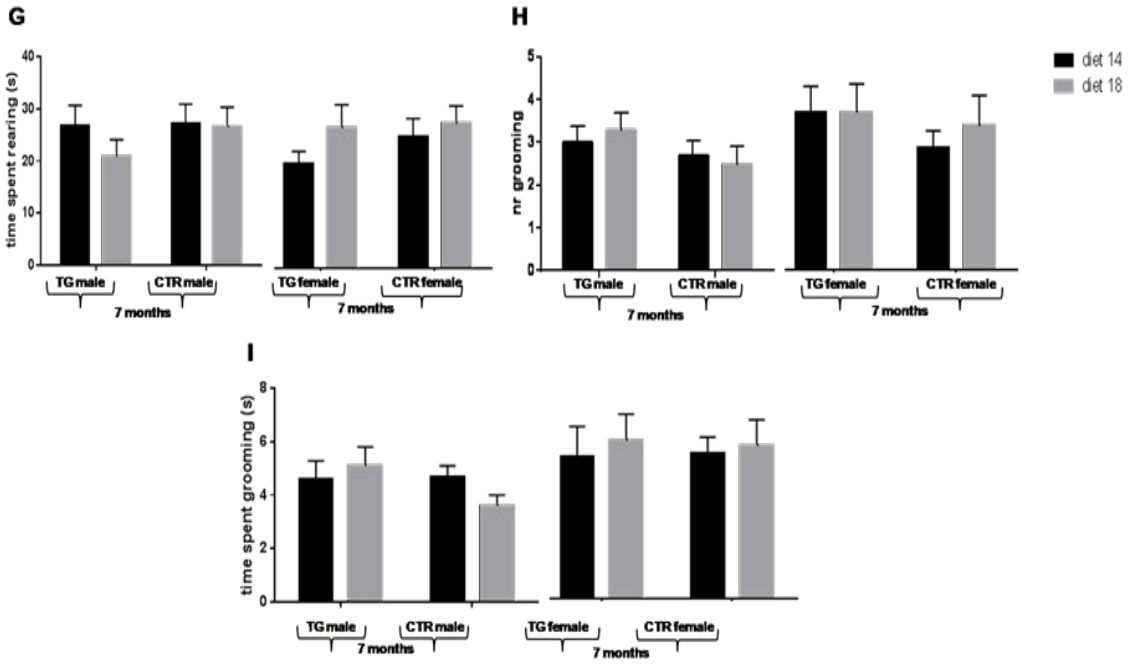

Figure 17. Locomotor and exploratory activity at 7 months of age in TG and CTR mice fed with different diets. A-C) Locomotor activity. Any significant effect of diets was found for parameters analyzed as total number of crossing, number of internal and external crossing. **D-I)** Exploratory activity. Any significant effect of diets was found for parameters analyzed as number of rearing, number of grooming, time spent for rearings and time spent for grooming.

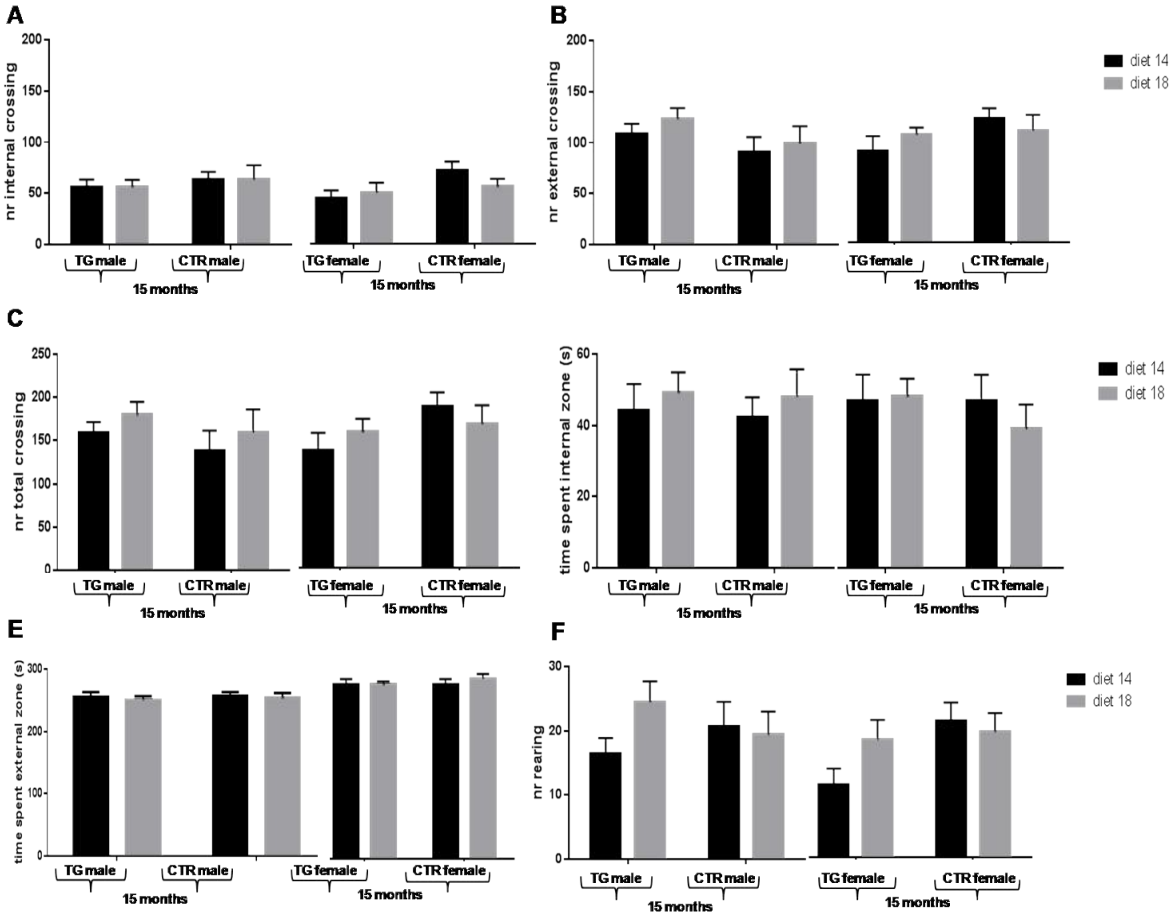
A
nr internal crossing
200
150
100
50
0
TG male
CTR male
TG female
CTR female
15 months
15 months
B
nr external crossing
200
150
100
50
0
TG male
CTR male
TG female
CTR female
15 months
15 months
diet 14
diet 18
C
nr total crossing
250
200
150
100
50
0
TG male
CTR male
TG female
CTR female
15 months
15 months
time spent internal zone (s)
60
40
20
0
TG male
CTR male
TG female
CTR female
15 months
15 months
diet 14
diet 18
E
time spent external zone (s)
300
200
100
0
TG male
CTR male
TG female
CTR female
15 months
15 months
F
nr rearing
30
20
10
0
TG male
CTR male
TG female
CTR female
15 months
15 months
diet 14
diet 18

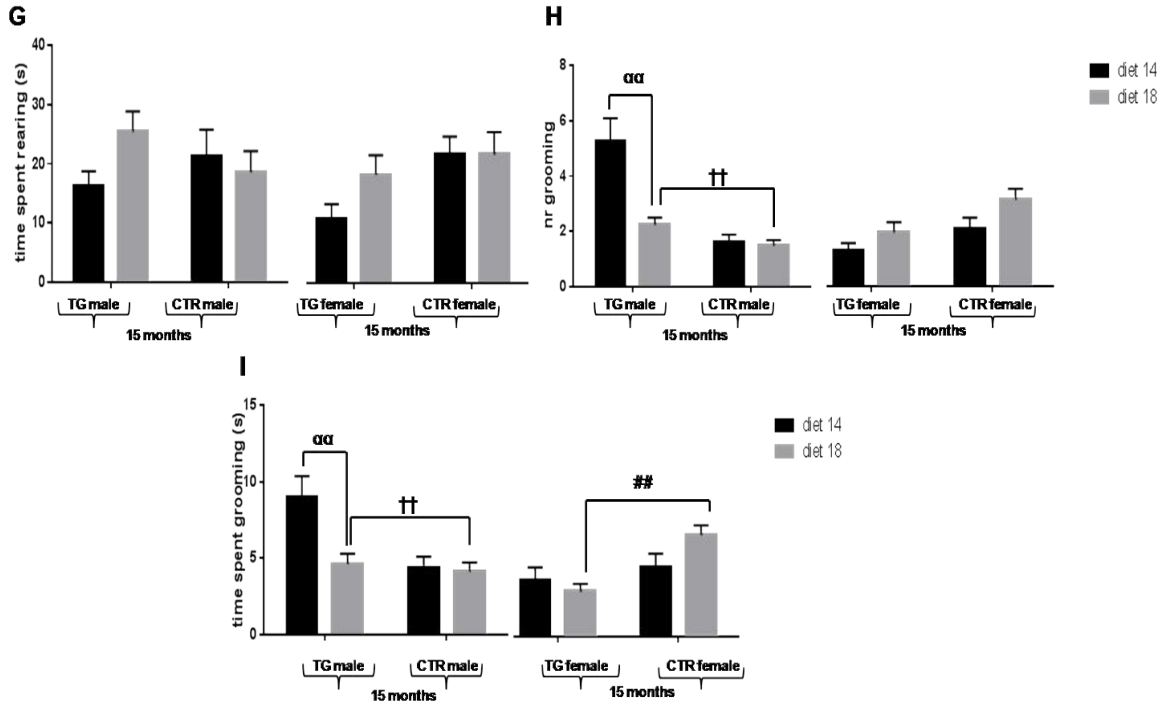

Figure 18. Locomotor and exploratory activity at 15 months of age in TG and CTR mice fed with different diets. A-C) Locomotor activity. Any significant effect of diets was found for parameters analyzed as total number of crossing, number of internal and external crossing. **D-I)** Exploratory activity. A significant diet effect and genotype effect for measures of number of grooming and time spent for grooming in male TG mice fed with different diets was found. Data were shown as mean ± SEM. DIET 14: TG male vs CTR male mice †† P< 0.001, DIET 18: TG female vs CTR female mice ## P< 0.001. TG male diet 18 vs TG male diet 14 mice αα P< 0.001.

4.5.4 Immunohistochemistry

Sections of both P301L TG and CTR mice brains were screened with phospho-specific antibodies for AT8 and AT100 (Fig. 20 and Fig. 22 respectively), in order to understand if different diets (**diet 18**: 18% protein and 5% and **diet 14**: 14% protein and 3.5% fat) can improve the progression of tauopathy. Immunostaining applied to cortex and hippocampus with AT8 antibody revealed that, regardless of diets administrated, in P301L TG mice the phosphorylation of Tau was present at both 7 and 15 months of age (**diet 14**: Fig. 19A-H, 21A-H, **diet 18**: Fig. 19I-P, 21I-P). These brain areas were subsequently quantified by AT8-immunoreactive cell counts (Fig. 20A-B and 22A-B). At 7 months of age for both male and female mice fed with different diets, a significant genotype effect in the cortex was detected (diet 14: TG vs CTR mice $P<0.0001$, diet 18: TG male vs CTR male mice $P<0.001$, TG female vs CTR female mice $P<0.0001$; Fig. 19A) and in the hippocampus (diet 14: TG vs CTR mice $P<0.0001$, diet 18: TG male vs CTR male mice $P<0.0001$, TG female vs CTR female mice $P<0.001$; Fig. 19B). A significant diet effect in the cortex of male and female TG mice was detected (TG male diet 14 vs TG male diet 18 $P<0.001$ and TG female diet 14 vs TG female diet 18 $P<0.05$; Fig. 19B).

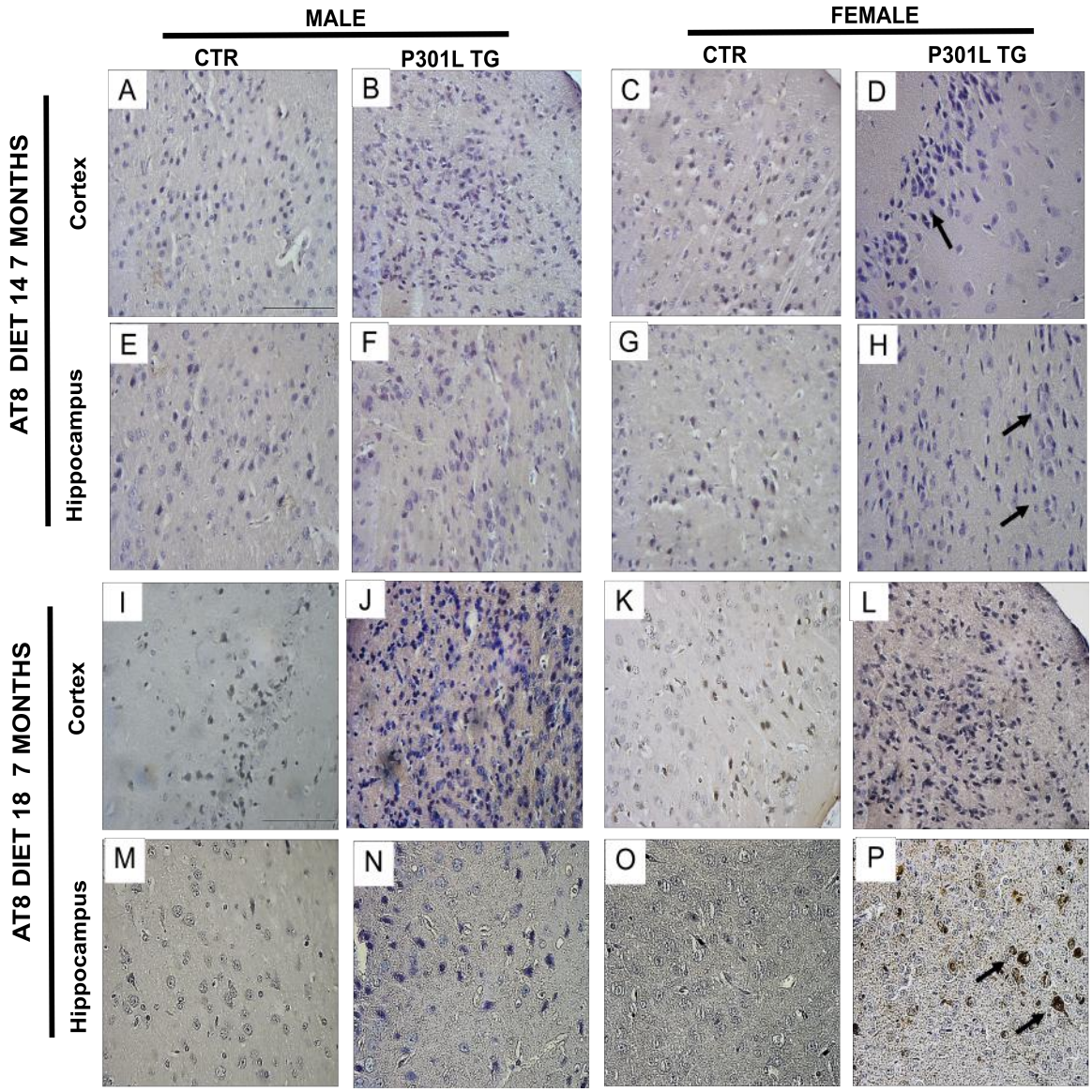

Figure 19. AT8 immunoreactivity in TG and CTR mice fed with different diets at 7 month of age. PSer202–Thr205 (AT8)-stained sections revealed the accumulation of abnormal Tau conformation and phosphorylation in 7-month-old males and females (P301L TG mice and CTR mice) fed with diet 14 and 18 in cortex (**A-D**, **I-L**) and in hippocampus (**E-H**,**M-P** note the arrows pointing to the most representative aspects in TG mice). Representative sections are shown of 4 animals used per each group. Scale bar: 40 μm.

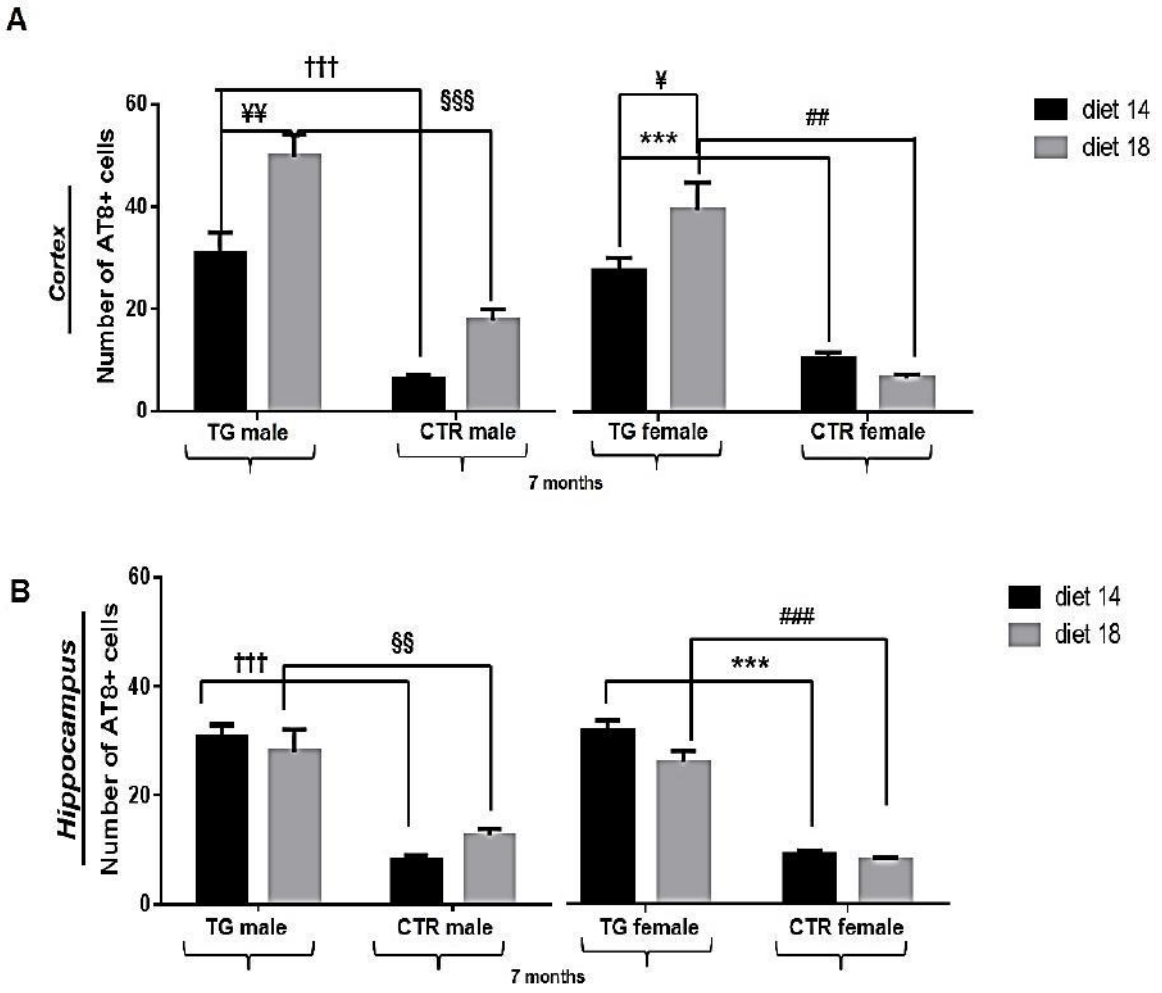

Figure 20. Quantification of AT8 immunoreactive cell counts in TG and CTR mice fed with different diets at 7 month of age. A-B) Quantification of AT8 immunoreactive cells in hippocampus and in the cortex showed a significantly increased number of AT8+ cells in TG mice compared to CTR mice at 7 months of age. A significant diet effect in the cortex of male and female TG mice was detected, as shown by a significantly increase of AT8+ cells TG mice fed with diet 18 compared to TG mice fed with diet 14. Data were shown as mean ± SEM.DIET 14: TG male vs CTR male mice ††† P< 0.0001, TG female vs CTR female mice *** P< 0.0001. DIET 18: TG male vs CTR male mice §§ P< 0.001, §§§ P< 0.0001, TG female vs CTR female mice ## P< 0.001, ### P< 0.0001. TG male diet 18 vs TG male diet 14 ¥¥ P< 0.001, TG female diet 18 vs TG female diet 14 ¥ P< 0.05.

At 15 months of age for both male and female mice fed with different diets a significant genotype effect in the cortex was detected (diet 14: TG vs CTR mice P<0.0001, diet 18: TG vs CTR mice P<0.0001; Fig. 22A) and in the hippocampus (diet 14: TG vs CTR mice P<0.0001, diet 18: TG male vs CTR male mice P<0.0001, TG female vs CTR female mice P<0.001; Fig. 22B). Any significant diet effect in the cortex and in hippocampus of TG mice fed with different diets was detected (P>0.05, Fig. 22A-B).

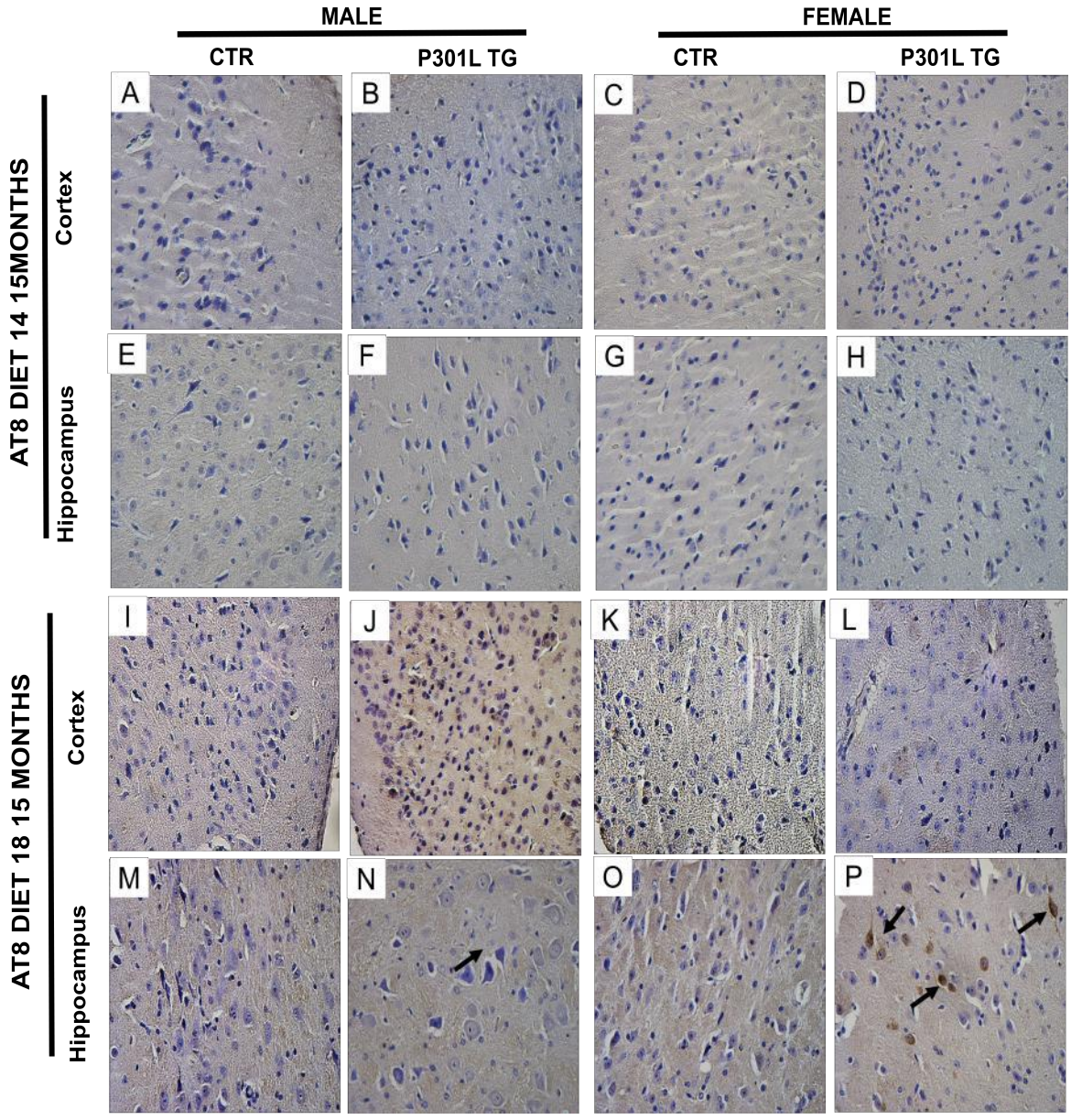

Figure 21. AT8 immunoreactivity in TG and CTR mice fed with different diets at 15 month of age. PSer202–Thr205 (AT8)-stained sections revealed the accumulation of abnormal Tau conformation and phosphorylation in 15-month-old males and females (P301L TG mice and CTR mice) fed with diet 14 and 18 in cortex (**A-D, I-L**) and in hippocampus (**E-H**, **M-P** note the arrows pointing to the most representative aspects in TG mice). Representative sections are shown of 4 animals used per each group. Scale bar: 40 μm.

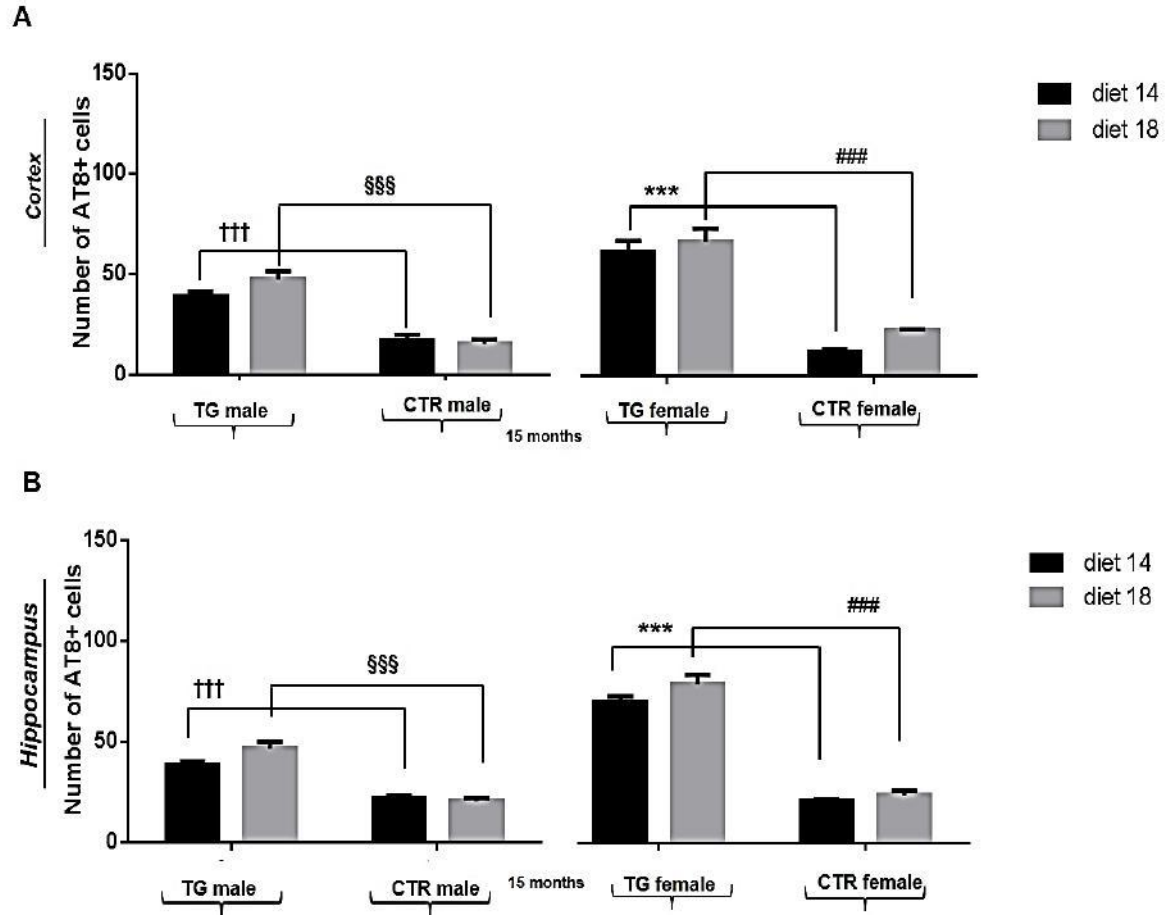

Figure 22. Quantification of AT8 immunoreactive cell counts in TG and CTR mice fed with different diets at 15 month of age. A-B) Quantification of AT8 immunoreactive cells in hippocampus and in the cortex showed a significantly increased number of AT8+ cells in TG mice compared to CTR mice at 15 months of age. Data were shown as mean ± SEM. DIET 14: TG male vs CTR male mice ††† P< 0.0001, TG female vs CTR female mice *** P< 0.0001. DIET 18: TG male vs CTR male mice, §§§ P< 0.0001, TG female vs CTR female mice ### P< 0.0001.

Immunostaining applied to cortex and hippocampus with AT100 antibody revealed that, regardless of diets administrated, in P301L TG mice the phosphorylation of Tau was present at both 7 and 15 months of age (diet 14: Fig. 23A-H, 25A-H, diet 18: Fig. 23I-P, 25I-P). These brain areas were subsequently quantified by AT100-immunoreactive cell counts (Fig. 24A-B and 26A-B). At 7 months of age for both male and female mice fed with different diets a significant genotype effect in the cortex was detected (diet 14: TG vs CTR mice P<0.0001, diet 18: TG male vs CTR male mice P<0.001, TG female vs CTR female mice P<0.0001; Fig. 24A) and in the hippocampus (both male and female mice diet 14: TG vs CTR mice P<0.0001, diet 18: TG vs CTR mice P<0.0001; Fig. 24B). A significant diet effect in the hippocampus of male TG mice was detected (TG male diet 14 vs diet 18 P<0.0001; Fig. 24B).

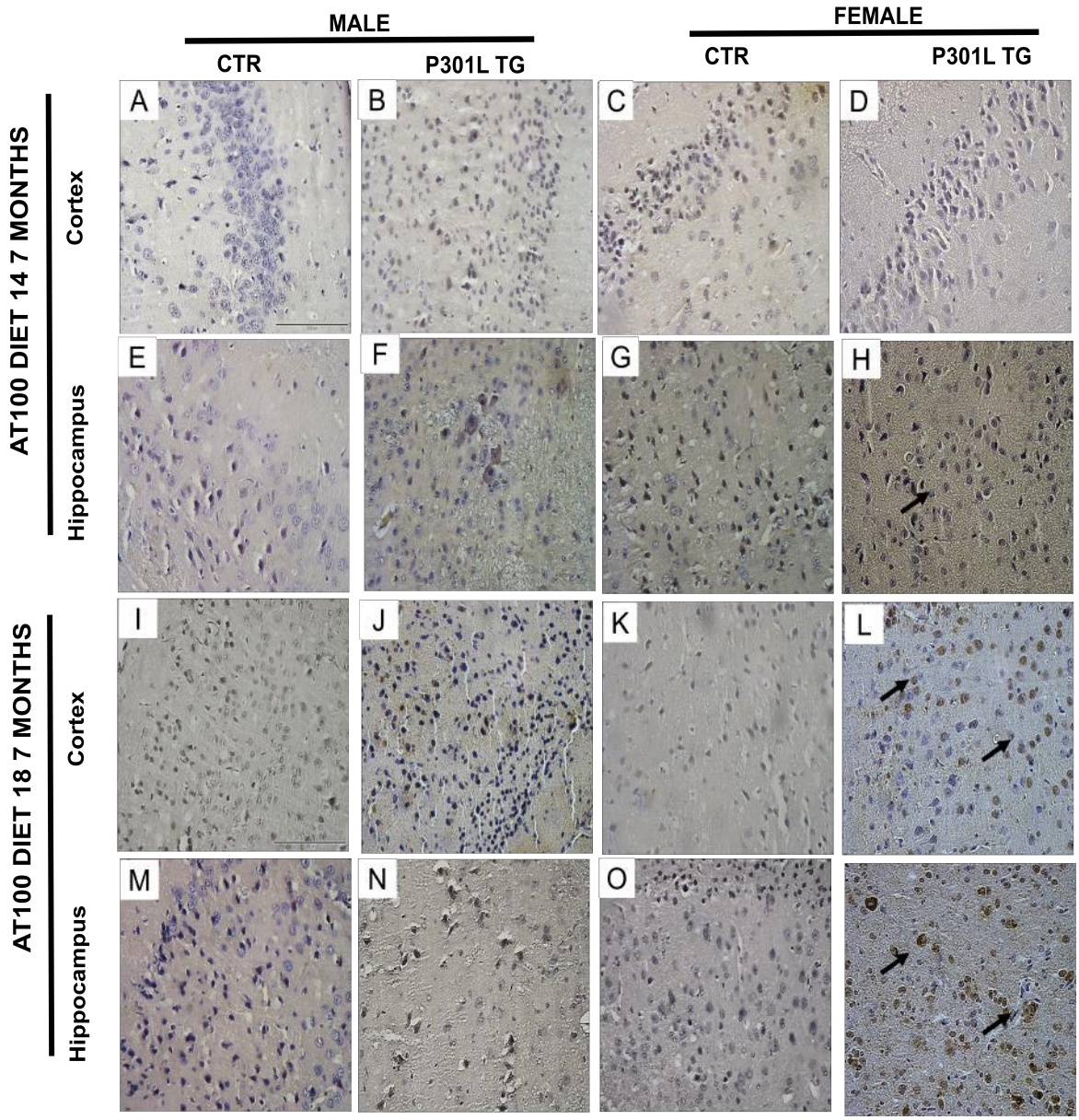

Figure 23. AT100 immunoreactivity in TG and CTR mice fed with different diets at 7 month of age. PThr212-PSer214 (AT100)-stained sections revealed the accumulation of abnormal Tau conformation and phosphorylation in 7-month-old males and females (P301L TG mice and CTR mice) fed with diet 14 and 18 in cortex (**A-D**, **I-L**) and in hippocampus (**E-H**, **M-P** note the arrows pointing to the most representative aspects in TG mice). Representative sections are shown of 4 animals used per each group. Scale bar: 40 μm.

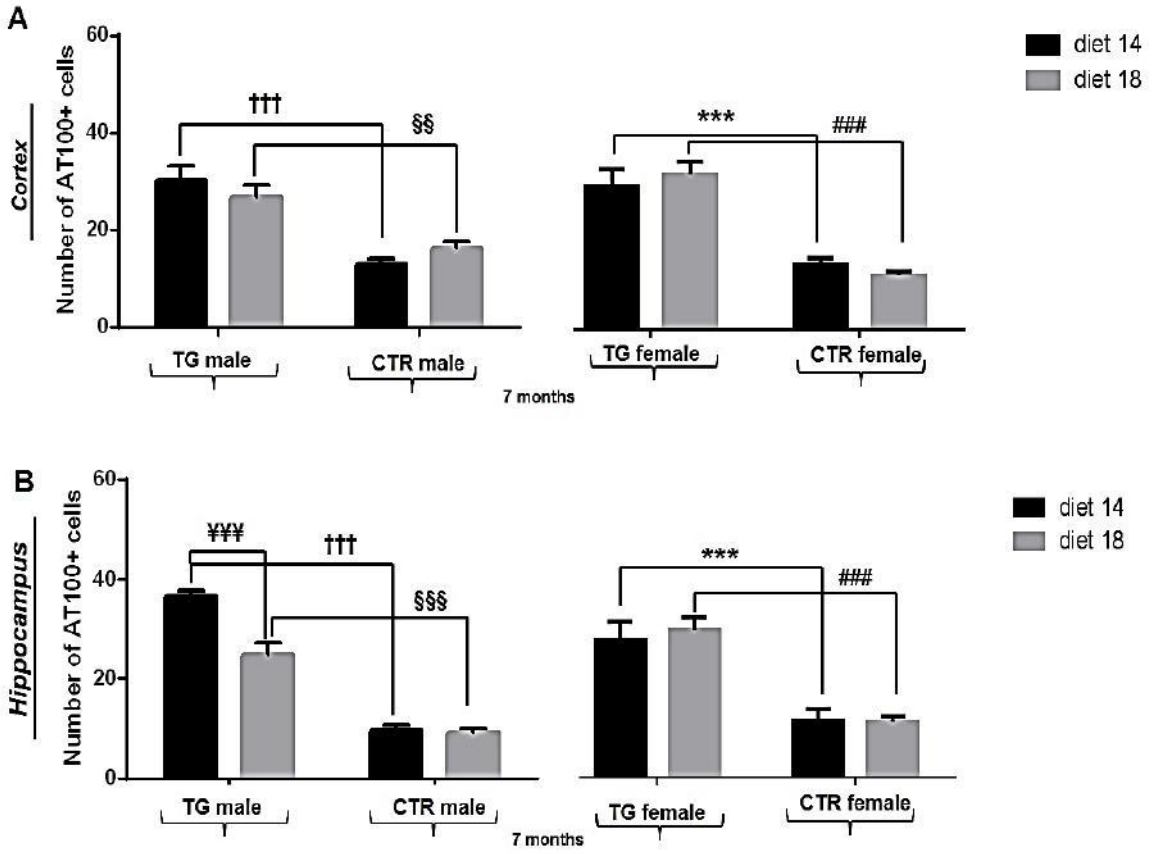

Figure 24. Quantification of AT100 immunoreactive cell counts in TG and CTR mice fed with different diets at 7 month of age. A-B) Quantification of AT100 immunoreactive cells in hippocampus and in the cortex showed a significantly increased number of AT100+ cells in TG mice compared to CTR mice at 7 months of age. A significant diet effect in the hippocampus of male TG mice was detected, as shown by a significantly increase of AT100+ cells TG mice fed with diet 14 compared to TG mice fed with diet 18. Data were shown as mean ± SEM. DIET 14: TG male vs CTR male mice ††† P< 0.0001, TG female vs CTR female mice *** P< 0.0001. DIET 18: TG male vs CTR male mice §§ P< 0.001, §§§ P< 0.0001, TG female vs CTR female mice ### P< 0.0001. TG male diet 18 vs diet 14 ¥¥¥ P< 0.0001.

At 15 months of age for both male and female mice fed with different diets a significant genotype effect in the cortex was detected (diet 14: TG vs CTR mice P<0.0001, diet 18: TG male vs CTR male mice P<0.001, TG female vs CTR female mice P<0.0001; Fig. 26A) and in the hippocampus (both male and female mice diet 14: TG vs CTR mice P<0.0001, diet 18: TG vs CTR mice P<0.0001; Fig. 26B). A significant diet effect in the cortex and in the hippocampus of female TG mice was detected (TG female diet 14 vs diet 18 P<0.0001; Fig. 26B).

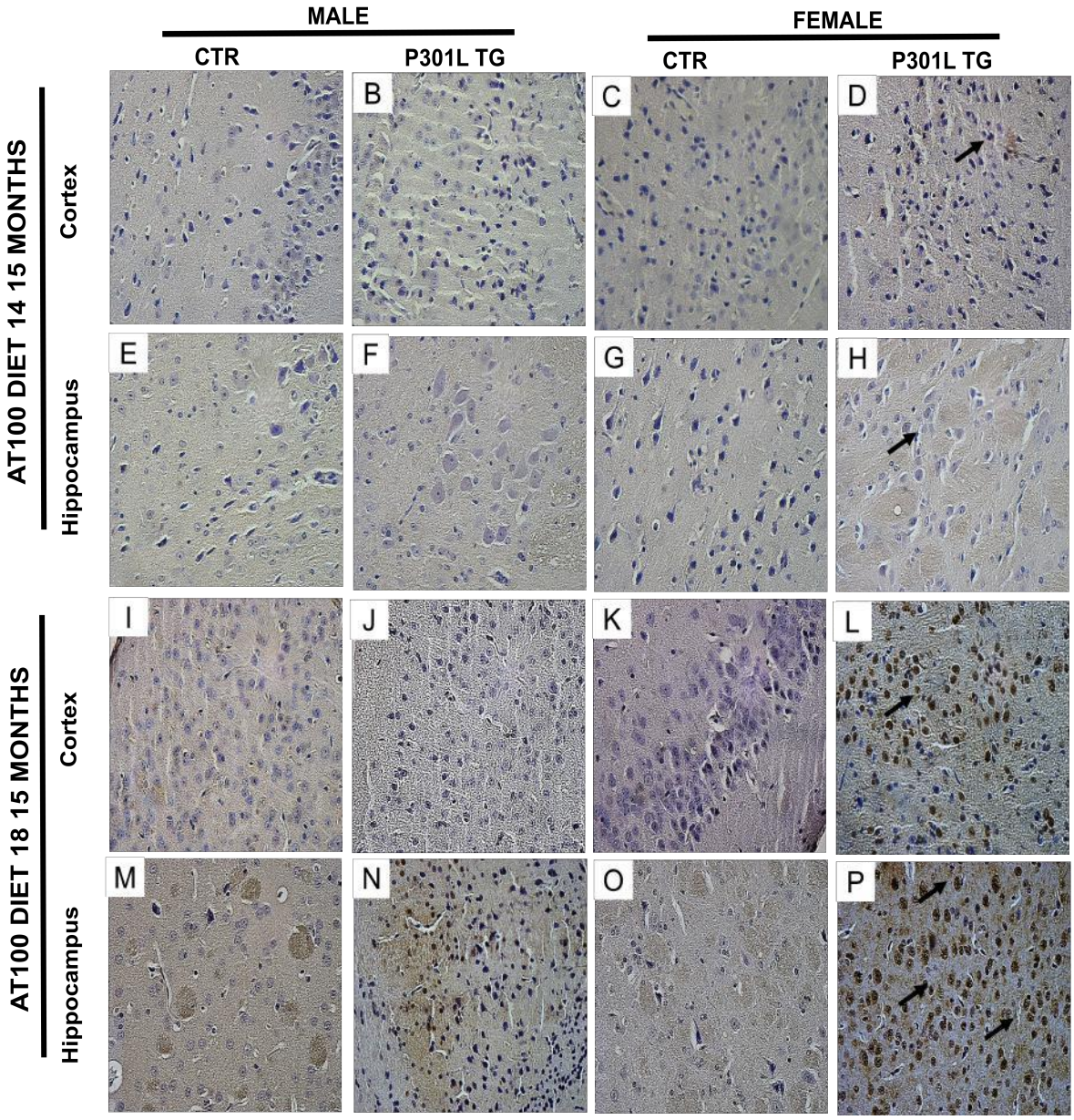

Figure 25. AT100 immunoreactivity in TG and CTR mice fed with different diets at 15 month of age. PThr212-PSer214 (AT100)-stained sections revealed the accumulation of abnormal Tau conformation and phosphorylation in 15-month-old males and females (P301L TG mice and CTR mice) fed with diet 14 and 18 in cortex (**A-D**, **I-L**) and in hippocampus (**E-H**, **M-P** note the arrows pointing to the most representative aspects in TG mice). Representative sections are shown of 4 animals used per each group. Scale bar: 40 μm.

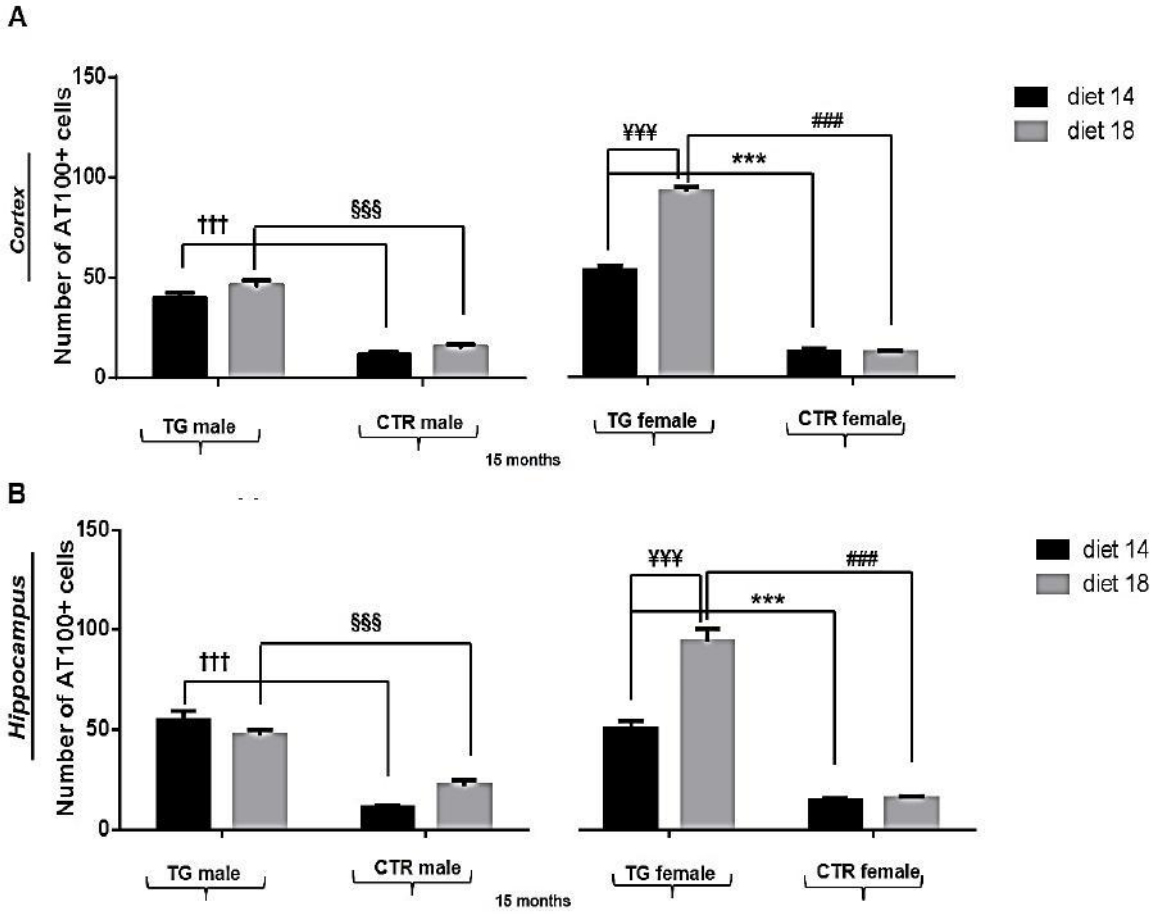

Figure 26. Quantification of AT100 immunoreactive cell counts in TG and CTR mice fed with different diets at 15 month of age. A-B) Quantification of AT100 immunoreactive cells in hippocampus and in the cortex showed a significantly increased number of AT100+ cells in TG mice compared to CTR mice at 15 months of age. A significant diet effect in the cortex and in the hippocampus of female TG mice was detected, as shown by a significantly increase of AT100+ cells TG mice fed with diet 18 compared to TG mice fed with diet 14. Data were shown as mean ± SEM. DIET 14: TG male vs CTR male mice ††† P< 0.0001, TG female vs CTR female mice *** P< 0.0001. DIET 18: TG male vs CTR male mice §§§ P< 0.0001, TG female vs CTR female mice ### P< 0.0001. TG female diet 18 vs diet 14 ¥¥¥ P< 0.0001.

In order to describe the neurodegeneration aspects, sections of both P301L TG and CTR mice brains fed with different diets were treated with neuronal nuclei (NeuN) antibody to value the survival of neuronal populations and with TUNEL to value apoptotic neurons. Immunostaining of cortex and hippocampus with NeuN revealed, regardless of diets administrated, a loss of neurons in TG mice compared to CTR mice at 7 months of age, with an abnormal neuronal morphology and a decrease in cell size confirmed also at 15 months of age (Fig. 27A-H, 29A-H). The NeuN+ cells were stained by the brown color of immunostochemystry (Fig. 27A-H).

NeuN-immunopositive cells in the cortex and in the hippocampus were quantified; at 7 months of age a significant genotype effect was found between female TG and CTR mice fed with different diets in the cortex (diet 14: $P< 0.0001$; diet 18: $P< 0.0001$, Fig. 28A) and in the hippocampus (diet 14: $P< 0.0001$; diet 18: $P< 0.0001$, Fig. 28B). A significant diet effect in the cortex of female TG mice was detected (TG female diet 14 vs diet 18 $P<0.0001$; Fig. 28A). At 15 months of age a significant genotype effect was found between female TG and CTR mice fed with different diets in the cortex (diet 14: $P< 0.001$; diet 18: $P< 0.0001$, Fig. 30A) and in the hippocampus (diet 18: $P< 0.001$, Fig. 30B). Any significant diet effect in the cortex and hippocampus of TG and CTR mice was detected (Fig. 30A-B).

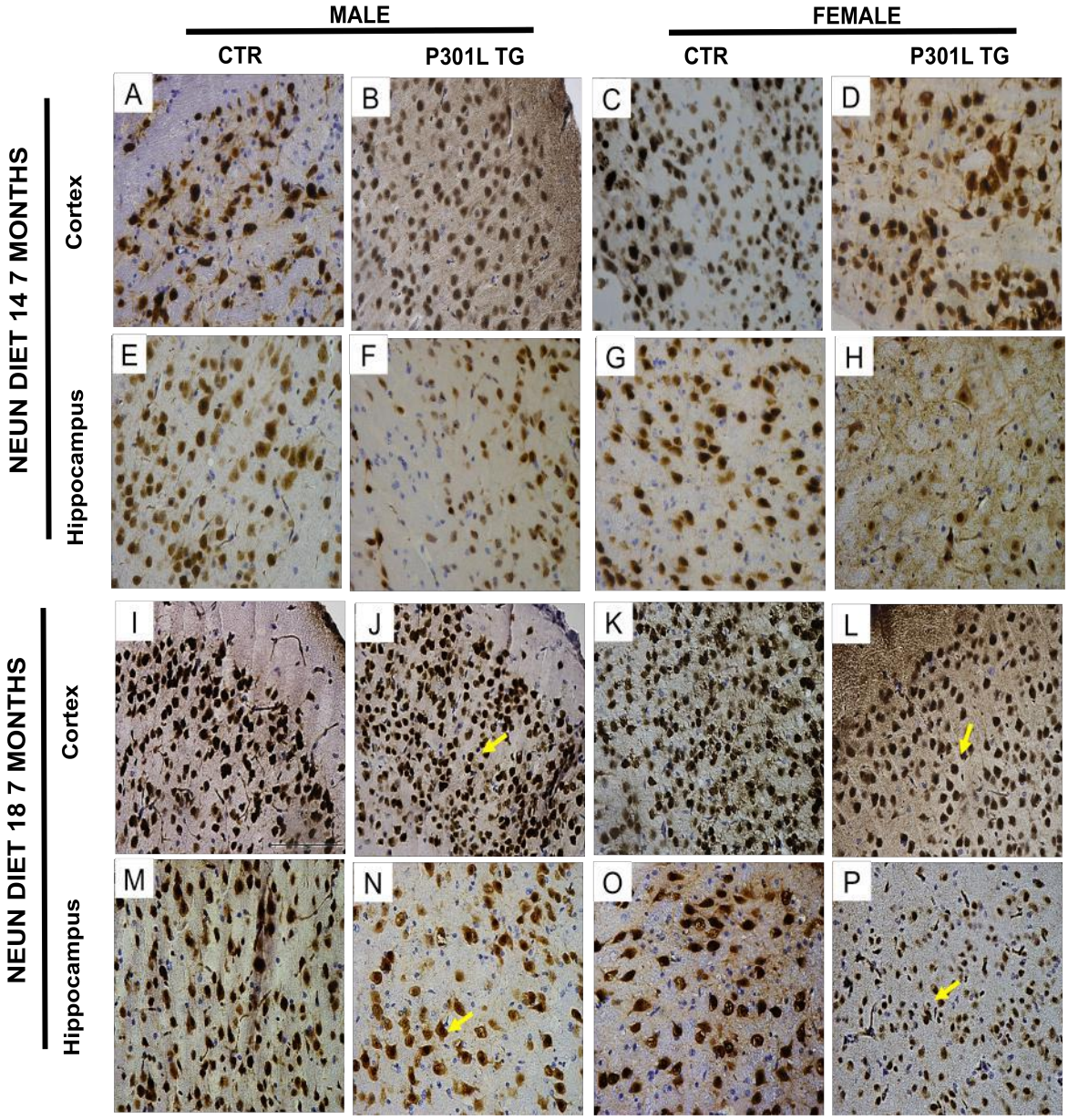

Figure 27. NeuN immunoreactivity in TG and CTR mice fed with different diets at 7 month of age. NeuN-stained sections revealed the accumulation of abnormal tau conformation and phosphorylation in 7-month-old males and females (P301L TG mice and CTR mice) fed with diet 14 and 18 in cortex (**A-D**, **I-L**) and in hippocampus (**E-H**, **M-P** note the arrows pointing to the most representative aspects in TG mice). Representative sections are shown of 4 animals used per each group. Scale bar: 40 μm.

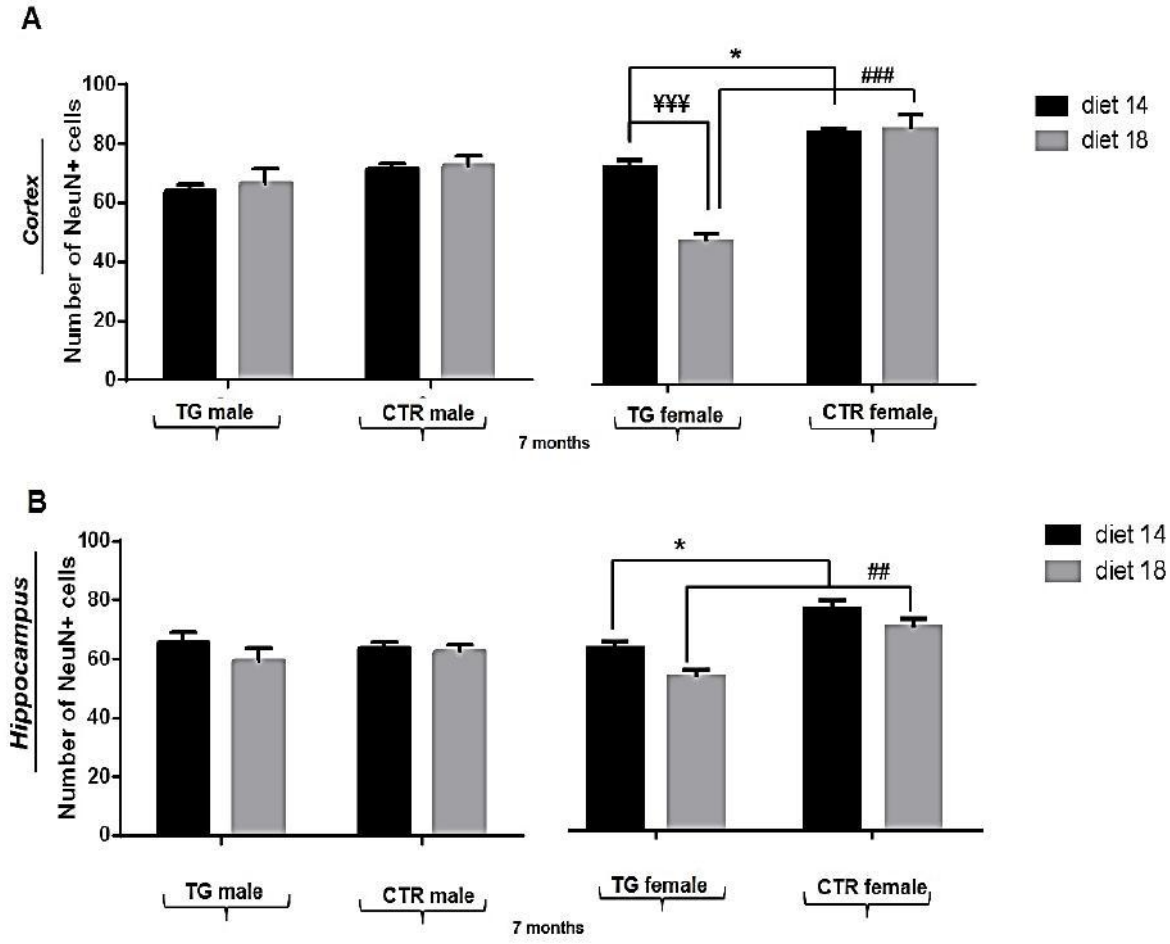

Figure 28. Quantification of NeuN immunoreactive cell counts in TG and CTR mice fed with different diets at 7 month of age. A-B) Quantification of NeuN immunoreactive cells in hippocampus and in the cortex showed a significantly decreased number of NeuN+ cells in TG female mice compared to relative CTR mice at 7 months of age. A significant diet effect in the cortex of female TG mice was detected, as shown by a significantly increase of NeuN+ cells TG mice fed with diet 14 compared to TG mice fed with diet 18. Data were shown as mean ± SEM. DIET 14: TG female vs CTR female mice * P< 0.05. DIET 18: TG female vs CTR female mice ## P< 0.001, ### P< 0.0001. TG female diet 18 vs diet 14 ¥¥¥ P< 0.0001.

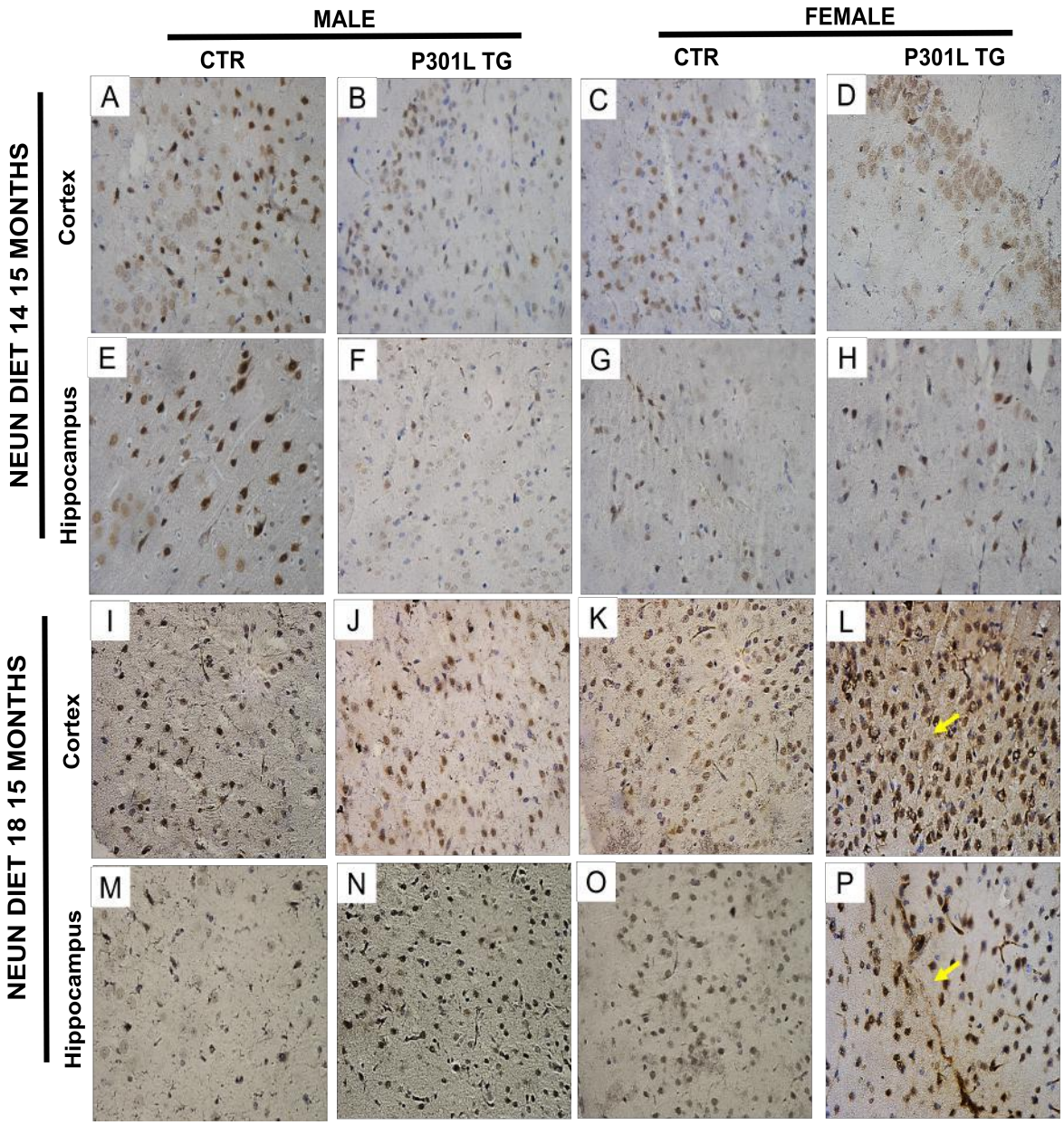

Figure 29. NeuN immunoreactivity in TG and CTR mice fed with different diets at 15 month of age. NeuN-stained sections revealed the accumulation of abnormal tau conformation and phosphorylation in 15-month-old males and females (P301L TG mice and CTR mice) fed with diet 14 and 18 in cortex (**A-D, I-L**) and in hippocampus (**E-H, M-P** note the arrows pointing to the most representative aspects in TG mice). Representative sections are shown of 4 animals used per each group. Scale bar: 40 μm.

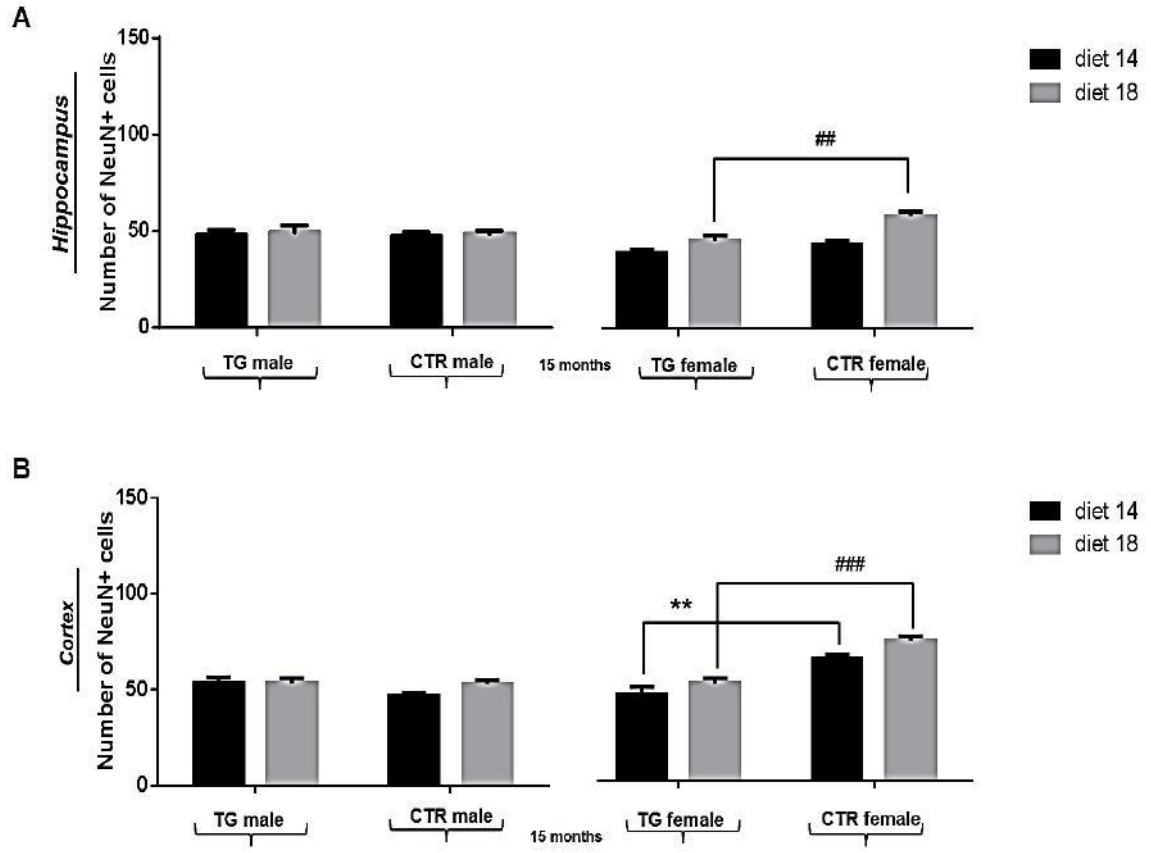

Figure 30. Quantification of NeuN immunoreactive cell counts in TG and CTR mice fed with different diets at 15 month of age. A-B) Quantification of NeuN immunoreactive cells in hippocampus and in the cortex showed a significantly decreased number of NeuN+ cells in TG female mice compared to relative CTR mice at 15 months of age. Any significant diet effect was detected. Data were shown as mean ± SEM. DIET 14: TG female vs CTR female mice ** P< 0.0001. DIET 18: TG female vs CTR female mice ## P< 0.001, ### P< 0.0001.

Immunostaining of cortex and hippocampus with TUNEL revealed, regardless of diets administrated, an increase of neurons in TG mice compared to CTR mice at 7 months of age, with an abnormal neuronal morphology and a decrease in cell size confirmed also at 15 months of age (Fig. 31A-H, 33A-H). At 7 months of age a significant genotype effect was detected in the cortex of TG female mice compared to relative CTR mice (diet 14: P<0.0001, diet 18: P< 0.0001; Fig. 32A) and in hippocampus (diet 14: P<0.001, diet 18: P< 0.001; Fig. 32B). Any significant diet effect in the cortex and hippocampus of TG and CTR mice was detected (Fig. 32A-B). At 15 months of age a significant genotype effect was found both male and female TG and CTR mice fed with different diets in the cortex (male diet 14: P< 0.001; diet 18: P< 0.001; female diet 14: P< 0.0001; diet 18: P< 0.0001; Fig. 34A) and in the hippocampus (male diet 14: P< 0.001; diet 18: P< 0.001; female diet 14: P< 0.0001; diet 18: P< 0.0001 Fig. 34B). A significant diet effect in the cortex of female TG mice was detected (TG female diet 14 vs diet 18 P<0.05; Fig. 34A).

Immunostaining of cortex and hippocampus with TUNEL revealed, regardless of diets administrated, an increase of neurons in TG mice compared to CTR mice at 7 months of age, with an abnormal neuronal morphology and a decrease in cell size confirmed also at 15 months of age (Fig. 31A-H, 33A-H). At 7 months of age a significant genotype effect was detected in the cortex of TG female mice compared to relative CTR mice (diet 14: $P< 0.0001$, diet 18: $P< 0.0001$; Fig. 32A) and in hippocampus (diet 14: $P< 0.001$, diet 18: $P< 0.001$; Fig. 32B). Any significant diet effect in the cortex and hippocampus of TG and CTR mice was detected (Fig. 32A-B). At 15 months of age a significant genotype effect was found both male and female TG and CTR mice fed with different diets in the cortex (male diet 14: $P< 0.001$; diet 18: $P<0.001$; female diet 14: $P< 0.0001$; diet 18: $P< 0.0001$; Fig. 34A) and in the hippocampus (male diet 14: $P< 0.001$; diet 18: $P< 0.001$; female diet 14: $P< 0.0001$; diet 18: $P< 0.0001$; Fig. 34B). A significant diet effect in the cortex of female TG mice was detected (TG female diet 14 vs diet 18 $P< 0.05$; Fig. 34A).

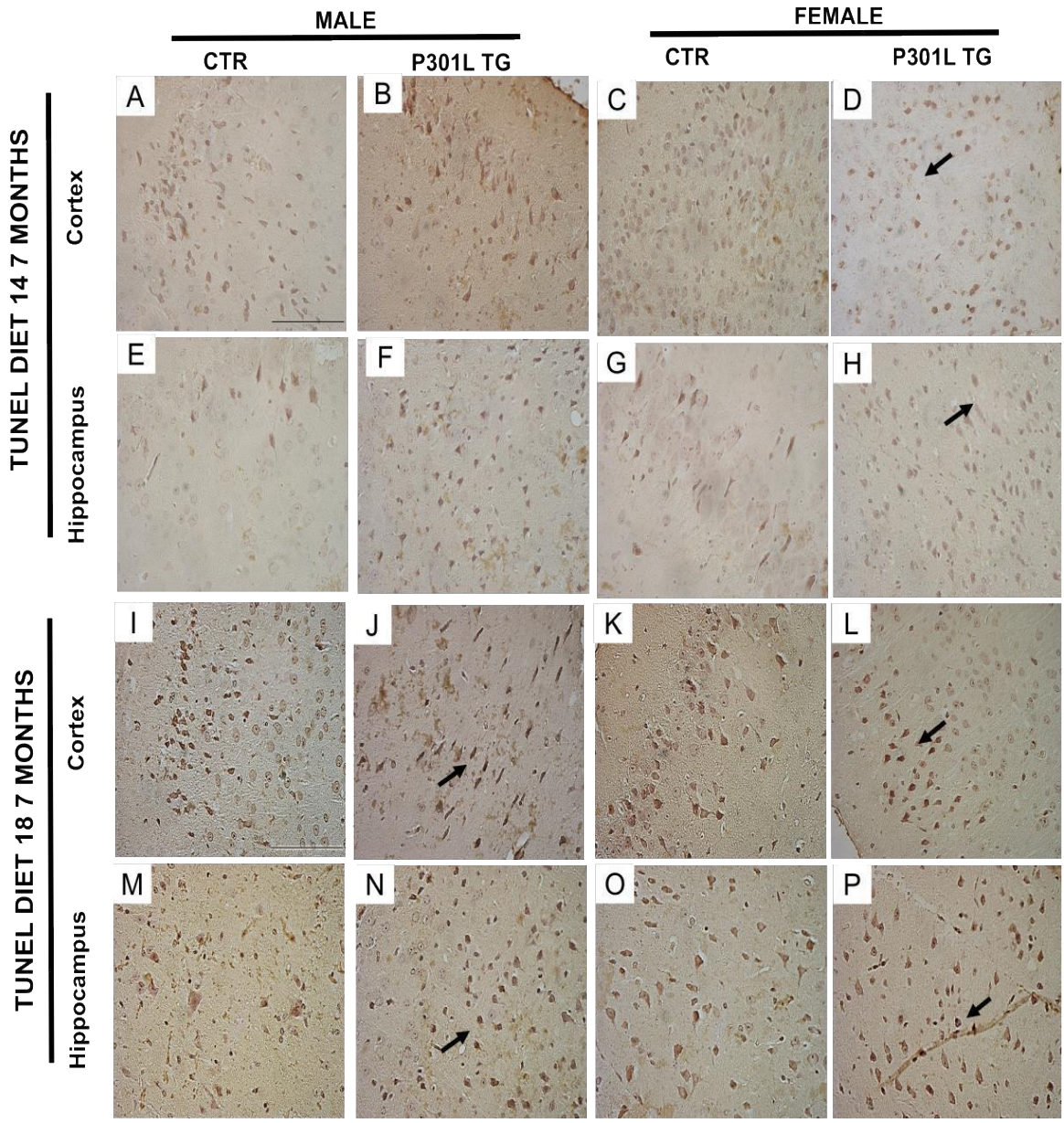

Figure 31. TUNEL immunoreactivity in TG and CTR mice fed with different diets at 7 month of age. TUNEL stained sections revealed the accumulation of abnormal Tau conformation and phosphorylation in 7-month-old males and females (P301L TG mice and CTR mice) fed with diet 14 and 18 in cortex (**A-D, I-L**) and in hippocampus (**E-H, M-P** note the arrows pointing to the most representative aspects in TG mice). Representative sections are shown of 4 animals used per each group. Scale bar: 40 μm.

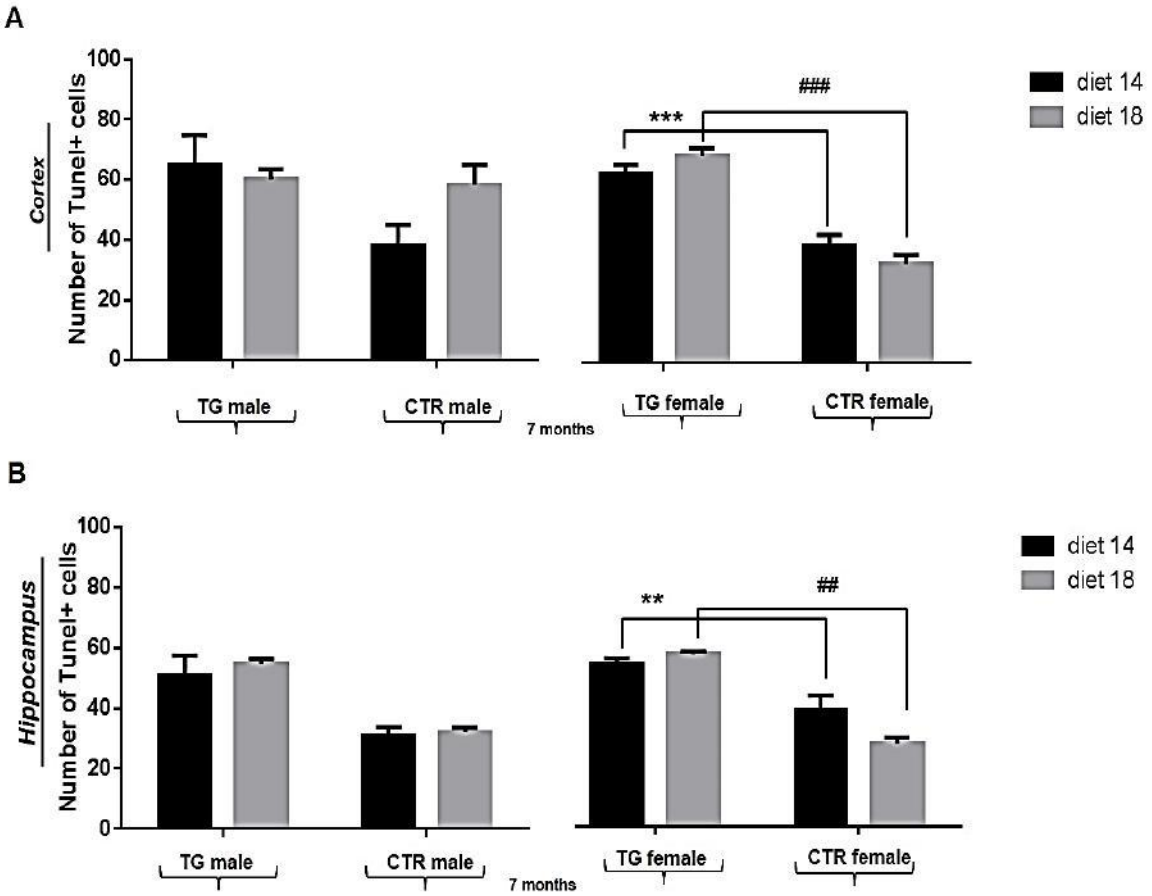

Figure 32. Quantification of TUNEL immunoreactive cell counts in TG and CTR mice fed with different diets at 7 month of age. A-B) Quantification of TUNEL immunoreactive cells in hippocampus and in the cortex showed a significantly increased number of TUNEL+ cells in TG mice compared to CTR mice at 7 months of age. Any significant diet effect in the cortex and hippocampus of TG and CTR mice was detected. DIET 14: TG female vs CTR female mice ** P< 0.001, *** P< 0.0001. DIET 18: TG female vs CTR female mice ## P< 0.001, ### P< 0.0001. Data were shown as mean ± SEM.

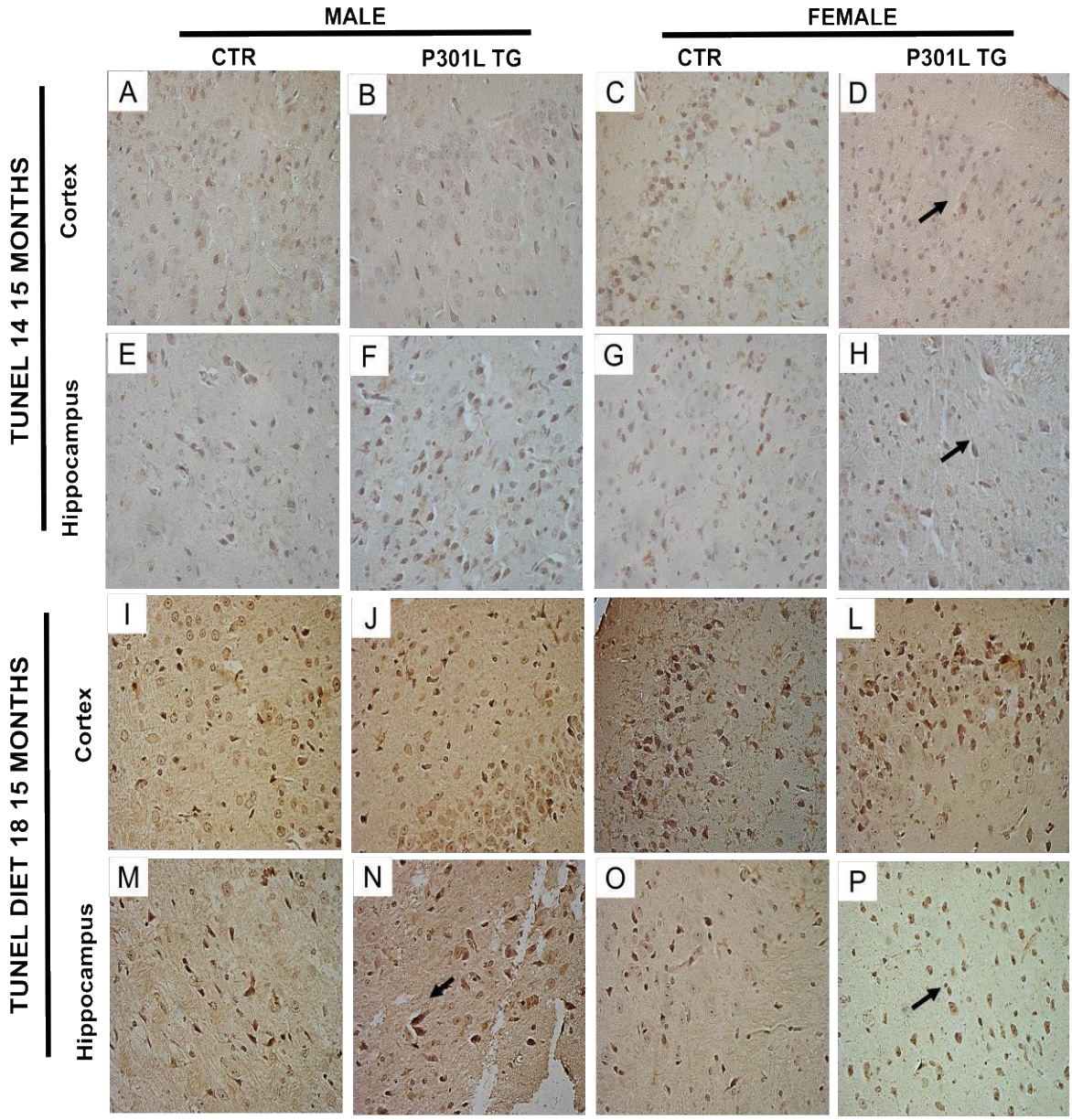

Figure 33. TUNEL immunoreactivity in TG and CTR mice fed with different diets at 15 month of age. TUNEL stained sections revealed the accumulation of abnormal Tau conformation and phosphorylation in 15-month-old males and females (P301L TG mice and CTR mice) fed with diet 14 and 18 in cortex (**A-D, I-L**) and in hippocampus (**E-H, M-P** note the arrows pointing to the most representative aspects in TG mice). Representative sections are shown of 4 animals used per each group. Scale bar: 40 μm.

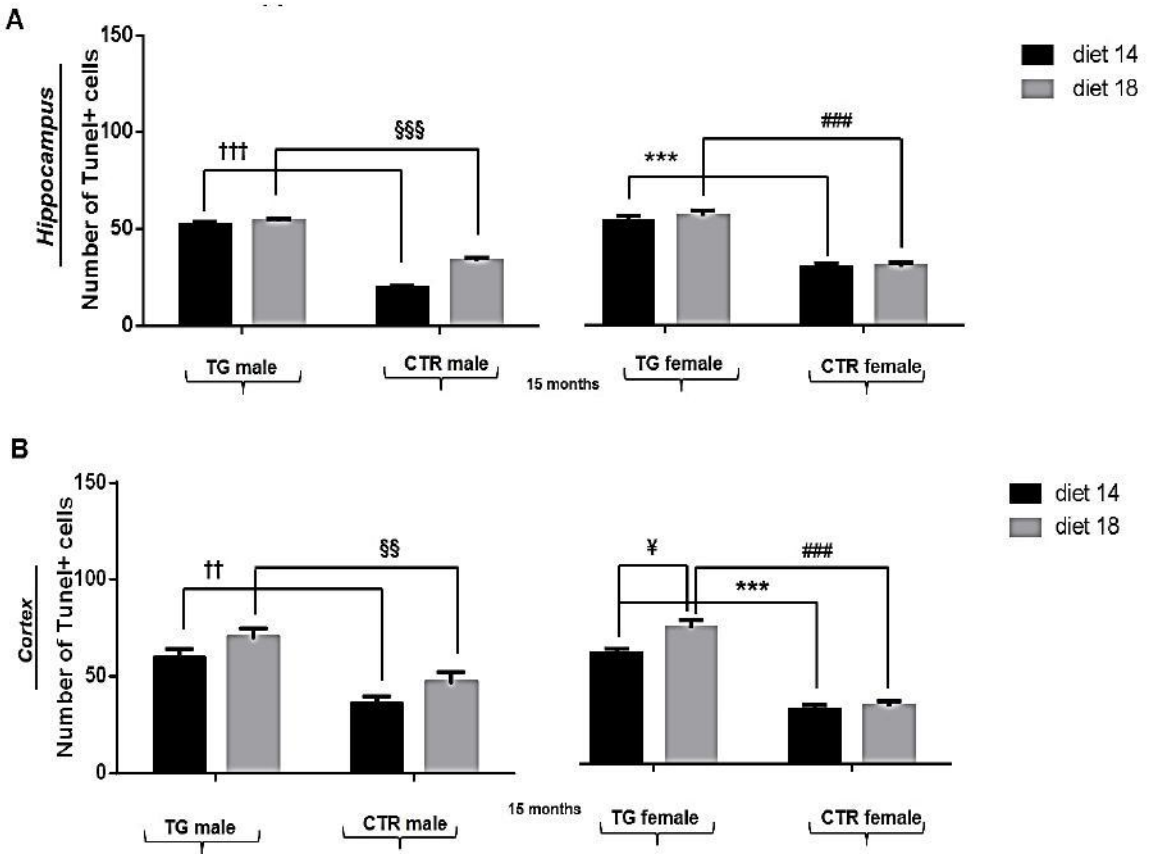

Figure 34. Quantification of TUNEL immunoreactive cell counts in TG and CTR mice fed with different diets at 15 month of age. A-B) Quantification of TUNEL immunoreactive cells in hippocampus and in the cortex showed a significantly increased number of TUNEL+ cells in TG mice compared to CTR mice at 15 months of age. A significant diet effect in the hippocampus of female TG mice was detected, as shown by a significantly increase of TUNEL+ cells TG mice fed with diet 18 compared to TG mice fed with diet 14. DIET 14: TG male vs CTR male mice †† P< 0.001, ††† P< 0.0001, TG female vs CTR female mice *** P< 0.0001. DIET 18: TG male vs CTR male mice §§ P< 0.001, §§§ P< 0.0001, TG female vs CTR female mice ### P< 0.0001. TG female diet 18 vs diet 14 ¥ P< 0.05. Data were shown as mean ± SEM.

In order to analyze the neurodegeneration aspects correlated to hyperphosphorylation of Tau, sections of P301L TG and CTR mice brain fed with different diets were immunostained with neurofilaments (NFTs), aggregates of actin filaments that in the physiological state are needed to support the organization and function of cytoskeleton, but in pathological conditions are enriched in hyperphosphorylated Tau and beta amyloid forming the so-called neurofibrillary tangles, typical hallmarks of neurodegenerative diseases. Immunostaining of cortex and hippocampus with NFTs revealed a pathological state in TG mice compared to CTR mice at 7 months of age (Fig. 35), with an increase of the number of NFTs+ cells confirmed also at 15 months of age (Fig. 36).

From the qualitative point of view, no significant effect of diets between TG and CTR was detected.

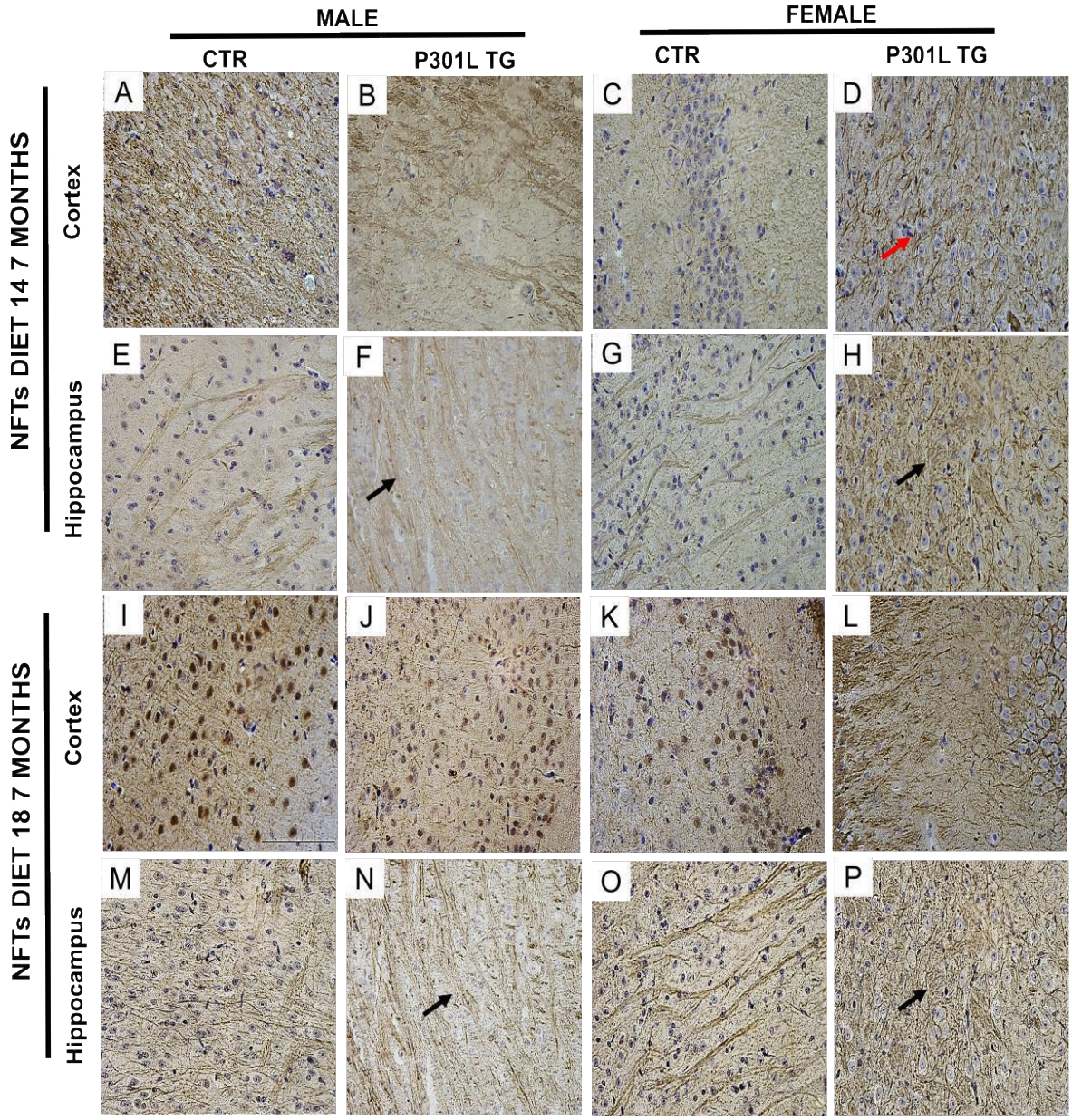

Figure 35. NFTs immunoreactivity in TG and CTR mice fed with different diets at 7 month of age. NFTs stained sections revealed the accumulation of neurofilaments in 7-month-old males and females (P301L TG mice and CTR mice) fed with diet 14 and 18 in cortex (**A-D**, **I-L**) and in hippocampus (**E-H**, **M-P** note the arrows pointing to the most representative aspects in TG mice). Representative sections are shown of 4 animals used per each group. Scale bar: 40 μm.

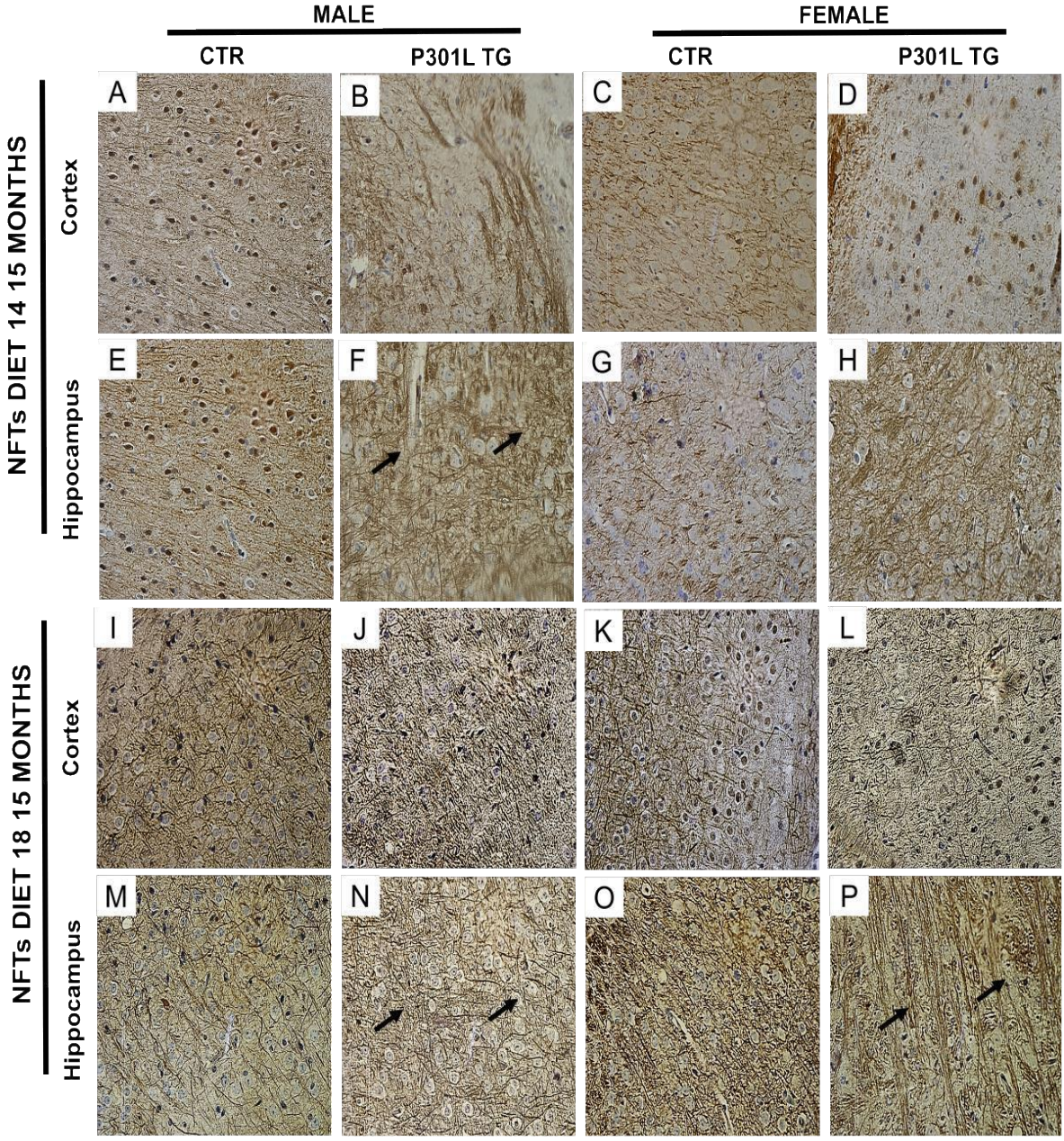

Figure 36. NFTs immunoreactivity in TG and CTR mice fed with different diets at 15 month of age. NFTs stained sections revealed the accumulation of neurofilaments in 15-month-old males and females (P301L TG mice and CTR mice) fed with diet 14 and 18 in cortex (**A-D**, **I-L**) and in hippocampus (**E-H**, **M-P** note the arrows pointing to the most representative aspects in TG mice). Representative sections are shown of 4 animals used per each group. Scale bar: 40 μm.

To analyze gliosis coronal sections of P301L TG and CTR mice brain fed with different diets were immunostained with glial fibrillary acid protein (GFAP) (Fig. 37-38). Immunostaining of cortex and hippocampus with GFAP revealed a state of gliosis in TG mice compared to CTR mice at 7 months of age (Fig. 37), with an increase of the number of GFAP+ cells confirmed also at 15 months of age (GFAP) (Fig. 38).

An increase in the number of astroglial GFAP-positive cells was observed in the hippocampal area and in the cortex of 15-month-oldP301L TG mice compared to 7-month-oldP301L TG mice. The number of GFAP-positive cells increases with age in both CTR and TG mice.

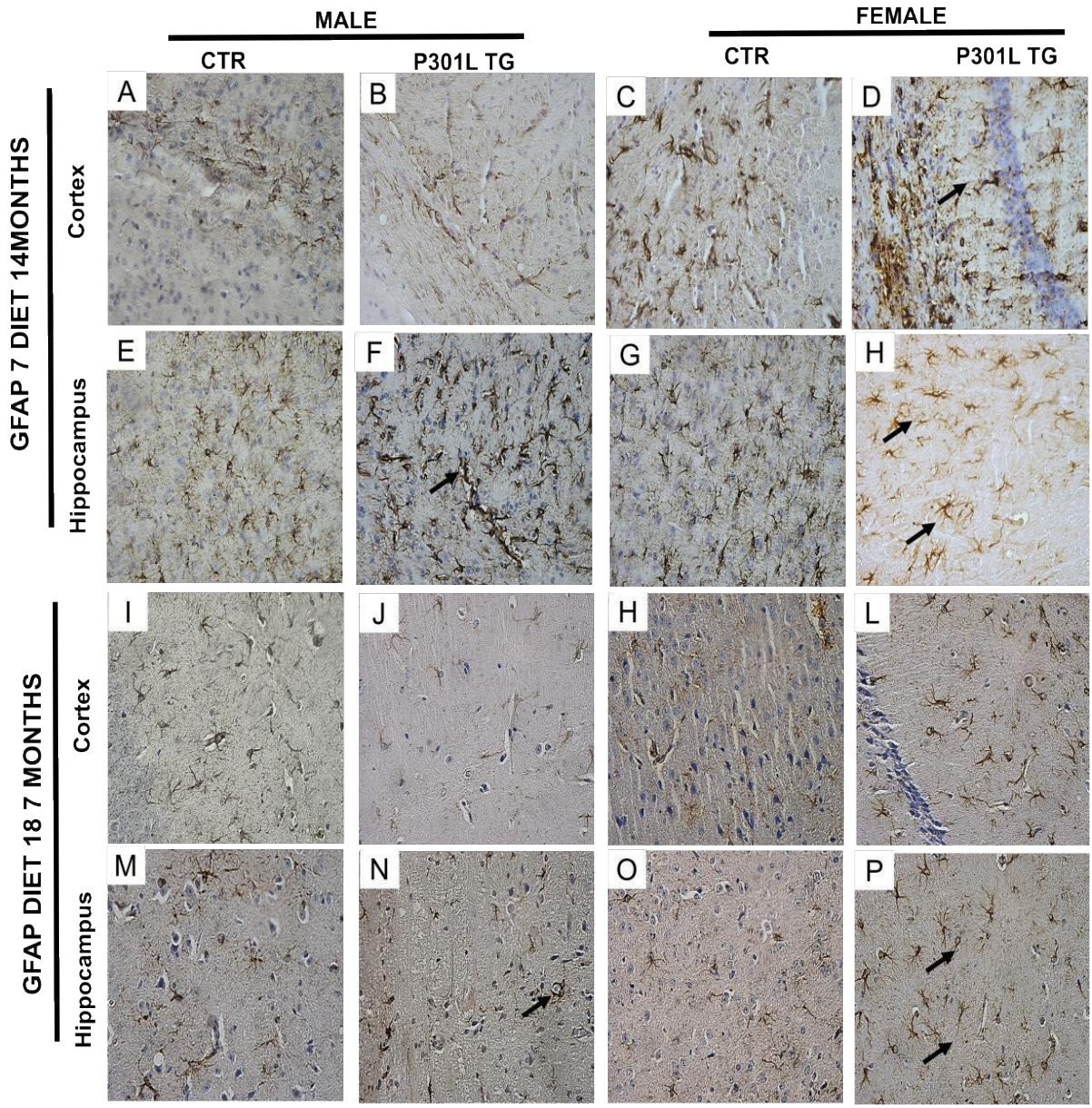

Figure 37. GFAP immunoreactivity in TG and CTR mice fed with different diets at 7 month of age. GFAP stained sections revealed a state of gliosis in 7-month-old males and females (P301L TG mice and CTR mice) fed with diet 14 and 18 in cortex (**A-D**, **I-L**) and in hippocampus (**E-H**, **M-P** note the arrows pointing that show an increase state of gliosis in TG mice). Representative sections are shown of 4 animals used per each group. Scale bar: 40 μm.

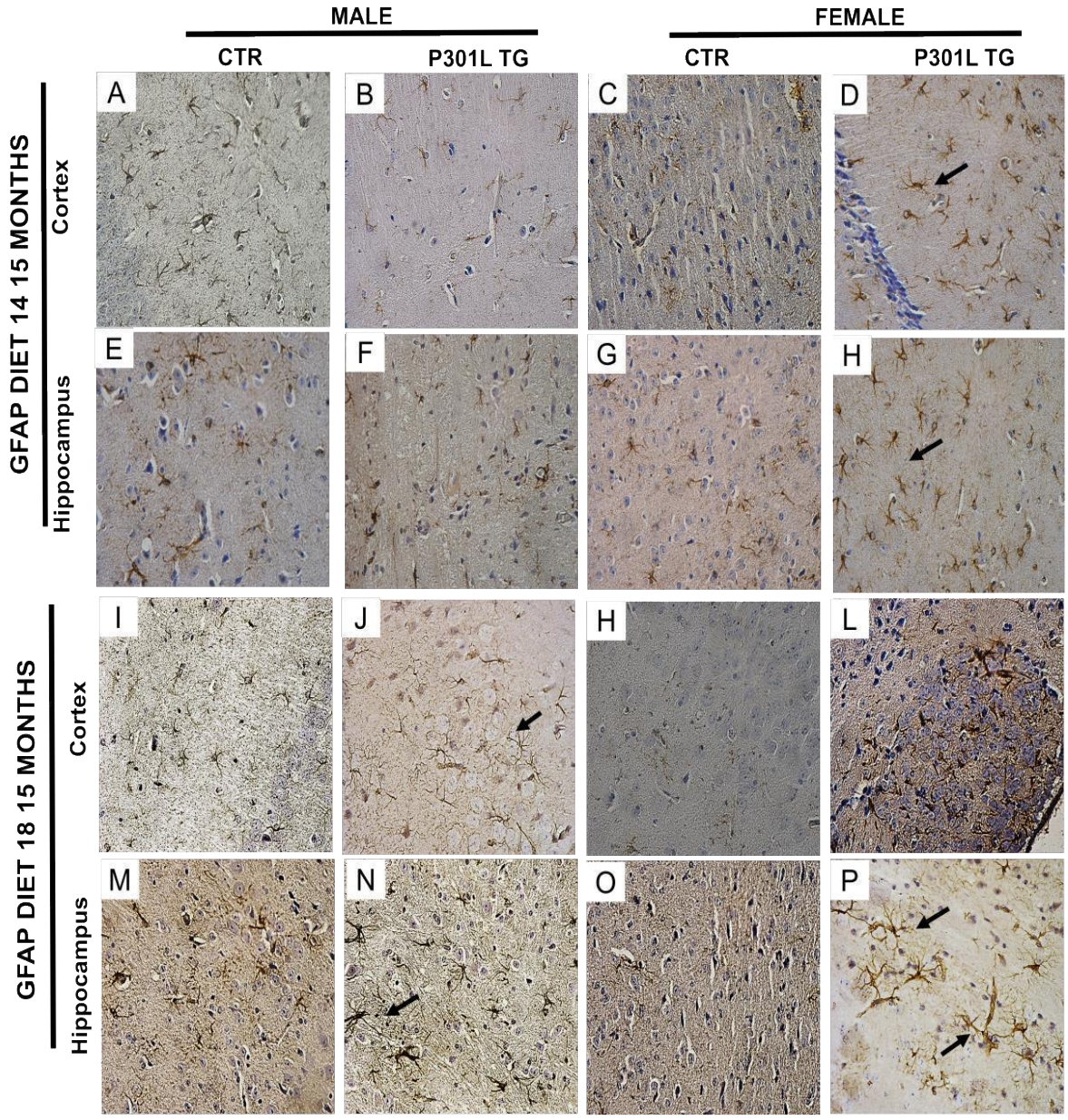

Figure 38. GFAP immunoreactivity in TG and CTR mice fed with different diets at 15 month of age. GFAP stained sections revealed a state of gliosis in 15-month-old males and females (P301L TG mice and CTR mice) fed with diet 14 and 18 in cortex (**A-D**, **I-L**) and in hippocampus (**E-H**, **M-P** note the arrows pointing that show an increase state of gliosis in TG mice). Representative sections are shown of 4 animals used per each group. Scale bar: 40 μm.

4.6 DISCUSSION

Neurodegenerative diseases are complex diseases often caused by a combination of genetic and environmental risk factors, as age, sex and nutrition. The pathological mechanisms need to be clarified in order to develop therapeutically strategy to slow or spot the tauopathies. Because the underlying pathologies may start years before the cognitive and behavioral impairments are clinically evident, application of the knowledge on preventive nutritional strategies warrants early identification of the disease to be able to intervene and delay, or even prevent its onset.

In the present study, we evaluated how two different diets (low protein-fat diet and high protein-fat diet) can interact with genotype, sex and age of P301L TG mice model of tauophaty and can reduce the progression of Tau pathology. In our previous work, we characterized P301L model that replicates the impairments found in patients affected by tauophaty in a way age-gender-dependent, founding that females had strong cognitive impairment and this was strongly correlated with an increase in P-Tau, in both cerebral cortex and hippocampus, as well as astrogliosis.

In this work, using P301L model, administrating the same diet (growth diet) to P301L TG and CTR mice until 12 weeks of age, we confirmed a gender-genotype interaction with a significantly decrease of body weight gain in female TG mice compared to CTR mice. Analyzing food and water consumptions, any difference between TG and CTR mice was detected for food consumption, while water consumption was significantly increased in TG than CTR mice. From 12 weeks of age, mice were randomized and fed with different diets (diet 18 high protein-fat diet and diet 14 low protein-fat diet), but a genotype effect overbeared diet effects. CTR mice, regardless of diets administrated, significantly ate and drank more than TG mice; male TG and CTR mice fed with diet 18 ate and drank more of mice fed with diet 14. Concerning nutrition as preventive care of tauophaty, lifespan of TG mice was significantly reduced than CTR mice; lifespan of female mice fed with diet 14 was significantly higher than female mice fed with diet 18.

Several evidences show that nutrition profoundly influences lifespan [24]; dietary restriction has been the central focus of most research, with numerous studies showing that caloric restriction can improve age-related health and prolong lifespan across a wide range of taxa ranging from yeasts to humans. More recently, the "constitutive tradeoff" models have been superseded by the idea that macronutrients differentially facilitate survival and give rise to life-history tradeoffs that constrain trait evolution [25-26].

Experiments in Drosophila have shown that the balance of macronutrients, rather than total calorie intake, is a key nutritional factor that influences lifespan, and the appearance of a resource-based tradeoff arises because of the different nutritional requirements of this biological function. Such experiments have shown that intake of total calories per se is not responsible for prolonging life, but, rather, the restriction of protein relative to carbohydrate may be the key under ad libitum feeding conditions [27-28].

In order to investigate the correlation between nutrition-cognitive impairment and exploratory locomotor performance, we found a highly significantly genotype effect that overbeared diet effects on cognitive and locomotor performances, with a further decrease at 15 months compared to 7 months of age, more pronounced in female than male TG mice. This strong genotype effect was also confirmed with the accumulation of hyperphosphorylated Tau in the cortex and in the hippocampus and correlated with a significantly decrease of aggregates of Tau in TG mice fed with diet 14 compared with TG mice fed with diet 18 at 7 months of age. This genotype effect was also found in the increase of distribution of neurofilaments in TG mice compared to CTR mice at 7 and 15 months of age, but any significant diet effect was found. Recent study suggests that the high-fat diet in Alzheimer's disease background induces the expression and exon 10 inclusion of Tau in the brain of female mice [29]; the excessive incorporation of fatty acids in the neuronal membrane increases fluidity of neuronal membranes and herewith improves neurotransmission and signaling via increased receptor binding and enhancement of the number and affinity of receptors and function of ion channels [30-31-32-33].

We also detected a major water consumption of water in mice fed with diet 18 (high protein-fat diet), more increased in TG than CTR mice. One mechanism linking the intake of high total fat and saturated fat intake to cognitive impairment may be through the development of insulin resistance characterized by growth body weight and excessive consumption of water [34-35]. Insulin resistance leads to deficiencies in energy metabolism and increased oxidative stress, correlated in our mouse model with a high state of astrogliosis [36]. For the neuronal loss we found a female-genotype effect located in the cortex and hippocampus of TG mice, with a significantly increase of number of neurons in TG mice fed with diet 14 compared with TG mice fed with diet 18 at 7 months of age and a correlated decrease of number of death neurons in TG mice fed with diet 14 compared with TG mice fed with diet 18 at 15 months of age. In the cortex and hippocampus, we also detected GFAP-positive cells at 7 months of age, with an increase of the number of GFAP+ cells age-gender-dependent, revealing a state of astrogliosis age-dependent more pronounced in females than

in males, with a qualitative increase of GFAP+ cells in TG mice compared to CTR mice, not yet identified.

In summary, we found an improvement of pathological conditions associated with our mouse model of tauophaty administrating a low fat-protein diet, occurred with an increased lifespan, a reduction of food and water consumption, a reduction of aggregates of hyperphosphorylated Tau and neuronal loss, more pronounced in female than male TG mice at 7 months of age, since 15 months of age a time point which pathological conditions are too severe. The importance of a correct dietary intake can be a useful tool for intervene in early identification of the neurodegenerative disease before the cognitive and behavioral impairments are clinically evident, in order to delay or even prevent the onset of tauophaty and neurodegenerative diseases.

4.7 ACKNOWLEDGMENTS

We thank D. Corna and I. Bertani for technical help.

4.8 REFERENCES

1. Iqbal K, Alonso Adel C, Chen S, Chohan MO, El-Akkad E, Gong CX et al. Tau pathology in Alzheimer disease and other Tauopathies. Biochim BiophysActa. 2005 Jan 3; 1739(2-3):198-210.
2. Nasreddine ZS, Loginov M, Clark LN, Lamarche J, Miller BL, Lamontagne A et al. From genotype to phenotype: a clinical pathological, and biochemical investigation of frontotemporal dementia and Parkinsonism (FTDP-17) caused by the P301L Tau mutation. Ann Neurol. 1999 Jun; 45(6):704-15.
3. Grundke-Iqbal I, Iqbal K, Tung YC, Quinlan M, Wisniewski HM, et al. (1986) Abnormal phosphorylation of the microtubule-associated protein Tau in Alzheimer cytoskeletal pathology. Proc Natl Acad Sci USA 83: 4913–4917.
4. Rosenberg KJ, Ross JL, Feinstein HE, Feinstein SC, Israelachvili J (2008) Complementary dimerization of microtubule-associated Tau protein: Implications for microtubule bundling and Tau-mediated pathogenesis. Proc Natl Acad Sci USA 105: 7445–7450
5. Bourre JM, Dumont O, Durand G. Dose-effect of dietary oleic acid: oleic acid is conditionally essential for some organs. Reprod Nutr Dev. 2004 Jul-Aug; 44(4):371-80.

6. Bourre JM. The role of nutritional factors on the structure and function of the brain: an update on dietary requirements. Rev Neurol (Paris). 2004 Sep; 160(8-9):767-92. Review.
7. Weih M, Wiltfang J, Kornhuber J. Non-pharmacologic prevention of Alzheimer's disease: nutritional and life-style risk factors. J Neural Transm. 2007 Sep; 114(9):1187-97.
8. Bourre JM. Effects of nutrients (in food) on the structure and function of the nervous system: update on dietary requirements for brain. Part 1: micronutrients J Nutr Health Aging. 2006 Sep-Oct; 10(5):377-85. Review.
9. Bourre JM. Effects of nutrients (in food) on the structure and function of the nervous system: update on dietary requirements for brain. Part 2: macronutrients. J Nutr Health Aging. 2006 Sep-Oct; 10(5):386-99.
10. Schroeder JE, Richardson JC, Virley DJ Dietary manipulation and caloric restriction in the development of mouse models relevant to neurological diseases. Biochim Biophys Acta. 2010 Oct; 1802(10):840-6.
11. Luchsinger JA, Tang MX, Shea S, Mayeux R Caloric intake and the risk of Alzheimer disease. Arch Neurol. 2002 Aug; 59(8):1258-63.
12. Borchelt DR, Davis J, Fischer M, Lee MK, Slunt HH, Ratovitsky T. et al. A vector for expressing foreign genes in the brains and hearts of transgenic mice. Genet Anal. 1996 Dec; 13(6):159-63.
13. Clarke JR, Cammarota M, Gruart A, Izquierdo I and Delgado-García JM (2010) Plastic modifications induced by object recognition memory processing. Proc Natl AcadSci USA 107, 2652–2657.
14. Ennaceur A and Delacour J (1988) A new one-trial test for neurobiological studies of memory in rats. 1: Behavioral data. Behav Brain Res 31, 47–59.
15. Seibenhener ML, Wooten MC. Use of the Open Field Maze to Measure Locomotor and Anxiety-like Behavior in Mice. J Vis Exp. 2015 Feb 6 ;(96).
16. Crawley JN (2007) What's wrong with my mouse?: behavioral phenotyping of transgenic and knockout mice. Hoboken, N.J.: Wiley-Interscience. Xvi, 523 p.
17. Carbone L1, Carbone ET, Yi EM, Bauer DB, Lindstrom KA, Parker JM, Austin JA, Seo Y, Gandhi AD, Wilkerson JD. Assessing cervical dislocation as a humane euthanasia method in mice. J Am Assoc Lab Anim Sci. 2012 May; 51(3):352-6.
18. Angus DW1, Baker JA, Mason R, Martin IJ. The potential influence of CO2, as an agent for euthanasia, on the pharmacokinetics of basic compounds in rodents. Drug Metab Dispos. 2008 Feb; 36(2):375-9. Epub 2007 Nov 15.

19. Cras, P., Smith, M. A., Richey, P. L., Siedlak, S. L., Mulvihill, P. and Perry, G. (1995) Extracellular neurofibrillary tangles reflect neuronal loss and provide further evidence of extensive protein cross-linking in Alzheimer disease. Acta Neuropathologica 89, 291 – 295.
20. Fukutani, Y., Kobayashi, K., Nakamura, I., Watanabe, K., Isaki, K. and Cairns, N. J. (1995) Neurons, intracellular and extracellular neurofibrillary tangles in subdivisions of the hippocampal cortex in normal ageing and Alzheimer's disease. Neurosci. Lett. 200, 57 –60.
21. Goedert, M. (1999) Filamentous nerve cell inclusions in neurodegenerative diseases: Tauopathies and alpha-synucleinopathies. Philos. Trans. R. Soc. Lond. B Biol. Sci. 354, 1101 – 1118.
22. Bondareff, W., Mountjoy, C. Q., Roth, M. and Hauser, D. L. (1989) Neurofibrillary degeneration and neuronal loss in Alzheimer's disease. Neurobiol. Aging 10, 709 – 715.
23. Ludvigson AE, Luebke JI, Lewis J., Peters A. Structural abnormalities in the cortex of the rTg4510 mouse model of Tauopathy: a light and electron microscopy study. Brain Struct Funct. 2011 Mar; 216(1):31-42.
24. Solon-Biet SM1, Walters KA2, Simanainen UK2, McMahon AC1, Ruohonen K3, Ballard JW4, Raubenheimer D5, Handelsman DJ2, Le Couteur DG1, Simpson SJ6. Macronutrient balance, reproductive function, and lifespan in aging mice. Proc Natl Acad Sci U S A. 2015 Mar 17; 112(11):3481-6.
25. Lee KP, Simpson SJ, Clissold FJ, Brooks R, Ballard JW, Taylor PW, Soran N, Raubenheimer D Lifespan and reproduction in Drosophila: New insights from nutritional geometry. Proc Natl Acad Sci U S A. 2008 Feb 19; 105(7):2498-503.
26. Tatar MThe plate half-full: status of research on the mechanisms of dietary restriction in Drosophila melanogaster. Exp Gerontol. 2011 May; 46(5):363-8.
27. Nakagawa S, Lagisz M, Hector KL, Spencer HG Comparative and meta-analytic insights into life extension via dietary restriction. Aging Cell. 2012 Jun; 11(3):401-9.
28. Piper MD, Partridge L, Raubenheimer D, Simpson SJ Dietary restriction and aging: a unifying perspective. Cell Metab. 2011 Aug 3; 14(2):154-60.
29. Takalo M, Haapasalo A, Martiskainen H, Kurkinen KM, Koivisto H, Miettinen P, Khandelwal VK, Kemppainen S, Kaminska D, Mäkinen P, Leinonen V, Pihlajamäki J, Soininen H, Laakso M, Tanila H, Hiltunen M. High-fat diet increases Tau expression in the brain of T2DM and AD mice independently of peripheral metabolic status. J Nutr Biochem. 2014 Jun; 25(6):634-41.

30. Kitajka K, Puskás LG, Zvara A, Hackler L Jr, Barceló-Coblijn G, Yeo YK, Farkas T. The role of n-3 polyunsaturated fatty acids in brain: modulation of rat brain gene expression by dietary n-3 fatty acids. Proc Natl Acad Sci U S A. 2002 Mar 5; 99(5):2619-24.
31. Zérouga M, Beaugé F, Niel E, Durand G, Bourre JM. Interactive effects of dietary (n-3) polyunsaturated fatty acids and chronic ethanol intoxication on synaptic membrane lipid composition and fluidity in rats.Biochim Biophys Acta. 1991 Nov 27; 1086(3):295-304.
32. Bourre JM, Dumont O, Piciotti M, Clément M, Chaudière J, Bonneil M, Nalbone G, Lafont H, Pascal G, Durand G. Essentiality of omega 3 fatty acids for brain structure and function. World Rev Nutr Diet. 1991; 66:103-17.
33. Bourre JM, Durand G, Pascal G, Youyou A. Brain cell and tissue recovery in rats made deficient in n-3 fatty acids by alteration of dietary fat.J Nutr. 1989 Jan; 119(1):15-22.
34. Winocur G, Greenwood CE.Studies of the effects of high fat diets on cognitive function in a rat model. Neurobiol Aging. 2005 Dec; 26 Suppl 1:46-9. Epub 2005 Oct 10. Review.
35. Winocur G, Greenwood CE, Piroli GG, Grillo CA, Reznikov LR, Reagan LP, McEwen BS. Memory impairment in obese Zucker rats: an investigation of cognitive function in an animal model of insulin resistance and obesity. Behav Neurosci. 2005 Oct; 119(5):1389-95.
36. Chitturi S, Farrell GC. Etiopathogenesis of nonalcoholic steatohepatitis. Semin Liver Dis 2001; 21:27–41; Brewer GJ

CHAPTER 5

A low fat-protein diet improves the oxidative damage in young and aged Tau P301L mice model of tauophaty

Submitted for publication to Histology and Histopathology (December 2015)

5. A low fat-protein diet improves the oxidative damage in young and aged Tau P301L mice model of tauophaty

AUTHORS: L. Buccarello[1], G. Grignaschi[2], A. Di Giancamillo[1], C. Domeneghini[1]

[1]Department of Health, Animal Science and Food Safety, Università degli Studi di Milano, Milan, Italy

[2]Department of Animal welfare, IRCCS-Mario Negri Institute for Pharmacological Research, Milan, Italy

5.1 ABSTRACT

Accumulating evidence shows nutritional factors influence the risk of developing and progression of neurodegenerative diseases. A greater understanding of these mechanisms is showed by studies of oxidative stress, a prominent and early feature in Tau pathology. Several studies showed as a high fat diets induce oxidative stress, which may be involved in neurodegenerative diseases as tauophaty. In this study, young and old male and female transgenic P301L-Tau mice were studied in comparison with CTR mice fed with different diets (low fat-protein diet and high fat-protein diet) to investigate the oxidative damage and to investigate how diets can interact and improve a possible condition of oxidative stress. Immunostaining with oxidative stress markers (acrolein, nitrotyrosine, NOS2 and NOS3) in the cortex and hippocampus of TG and CTR mice revealed a significant interaction genotype-oxidative stress in TG mice, regardless of diets administrated, more pronounced at 15 months of age compared to 7 months of age. This effect was also confirmed with the quantification of immunoreactive cell counts for each oxidative stress markers that revealed a significant increase of number of immunoreactive cell counts in TG mice compared to CTR mice. At 15 months of age, immunohistochemical analysis and quantification cell counts correlated to oxidative marker used, had shown a significant diet effect in the cortex and hippocampus of TG mice, highlighted by a decrease of immunopositive cells in TG mice fed with low fat-protein diet (diet 14) compared to TG mice fed with high fat-protein diet (diet 18). This diet effect was more pronounced in female TG mice compared to male TG mice. We demonstrated an oxidative damage associated with P301LTG model in a way age-gender-dependent and an improvement of oxidative damage in TG mice fed with a low fat-protein diet, more pronounced in female than male TG mice. Results suggests that nutritional factors may have protective effects in the onset and development of tauopathies by reducing oxidative stress, leading to the development of preventive treatments for tauopathies.

Keywords:

AD: Alzheimer disease, AGEs: glycation end products, CTR: control, DHA: docosahexaenoic acid, GSK-3b: glycogen synthase kinase-3b, NFTs: neurofilaments, PUFAs: Polyunsaturated fatty acids, ROS: reactive oxygen, RNS: reactive nitrogen, TG: transgenic.

5.2 INTRODUCTION

A greater understanding of the mechanisms involved in nutritional influences on neurodegenerative risk and progression could help to better inform possible interventional strategies. Among the mechanisms most studied as a contributory cause of neurodegenerative diseases, oxidative stress plays a key role. Oxidative stress occurs when the intracellular capacity for removing free radicals is exceeded, leading to modification of DNA, lipids, polysaccharides, and proteins, and to changes in redox homeostatic balance. Oxidative stress is a prominent and early feature in tauopathies, in particular in AD pathology [1].

Tauopathies are currently considered to be groups of neurodegenerative diseases presenting in adults with aggregates of abnormal Tau in neurons and glial cells. Tau is a neuronal protein that stabilizes microtubules and axoplasmic transport, establishes neuronal polarity, mediates axonal outgrowth and dendritic positioning, and protects DNA from heat damage and oxidative stress [2]. A pathological hallmark of tauopathies is the deposition of excessive amounts of hyperphosphorylated Tau in neurons and glial cells in affected brain areas, as temporal cortex, hippocampus and cerebellum. Hyperphosphorylation of Tau is thought to suppress its ability to stabilize microtubules, resulting in axonal degeneration and eventual cell death [3]. Several transgenic animal models of tauopathies have been generated in order to understand the effects of Tau not only on Tau phosphorylation and aggregation and their effects on cytoskeletal stability and axonal transport, but also to learn about putative alterations of metabolic pathways the defects of which underlie cellular malfunction and eventual neuronal death in tauopathies. Increased inflammatory responses, increased oxidative stress, abnormal mitochondrial function, and abnormal autophagy have been described in P301S transgenic mice [4-5-6]. A number of reports have established damage from reactive oxygen species (ROS) not only in the lesions of AD, but also in neuronal populations affected in the neurodegenerative disease [7-8-9].

Persistent oxidative stress leads to reactive oxygen (ROS) and reactive nitrogen (RNS) species formation, as occur in AD [10]. ROS and RNS exacerbate oxidative stress by attacking organelles such as mitochondria.

Their molecular attacks result in formation of stable adducts with DNA, RNA, lipids, and proteins, still further compromising neuronal integrity [11]. Oxidation of amino acids leads to formation of advanced glycation end products (AGEs) or advanced oxidation protein products, and protein unfolding, rendering them inactive and vulnerable to cleavage. Oxidation of aliphatic side-chains yields peroxides and carbonyls (aldehydes and ketone) that can attack other molecules and generate radicals, as well as AGE accumulation. Oxidative stress and its responses can activate pro- inflammatory networks that exacerbate organelle dysfunction and pro-apoptosis mechanisms and activate or dis-inhibit GSK-3b, which promotes Tau phosphorylation. Interestingly, many of the pathogenic factors such as oxidative damage, mitochondrial dysfunction, and accumulation of hyperphosphorylated Tau are found at synaptic terminals in AD brain and models, and are associated with synaptic dysfunction. This is important because synaptic damage is a critical factor in cognitive decline during aging and progression of tauopathies as AD [12].

There is good evidence linking oxidative stress with synaptic dysfunction and loss [12-13-14]. A mouse model of AD showed loss of postsynaptic proteins was associated with increased oxidation [14]. This effect may involve loss of the omega-3 fatty acid docosahexaenoic acid (DHA), which is highly vulnerable to oxidative damage, showing as a dietary deficiency of DHA may be a relevant and modifiable risk factor in AD and emphasizing the importance of a healthy diet regime as a preventive therapy for neurodegenerative disease [14]. Several nutrients are of special interest in tauopathies, particularly those required for the maintenance of neuronal integrity, including antioxidants and fatty acids; changes in the composition and levels of fatty acids also have important implications on neuronal integrity during the development of neurodegenerative diseases. Polyunsaturated fatty acids (PUFAs), such as DHA, are essential to support neuronal integrity and brain function; an excess of these nutrients supplied by a high fat diet could support the development of neurodegenerative disease [15]. Accumulating evidence suggests that diet and nutrition status influence neuronal membrane integrity, oxidative status and risk for tauopathies; maintaining a healthy diet, designed to support neuronal membrane integrity and to reduce the oxidative damage, may reduce the risk of developing neurodegenerative diseases.

In our first study, we demonstrated that the P301L TG mice replicates the impairments found in patients affected by Tauophaty in a way age-gender-dependent, with cognitive and behavioral impairment more pronounced in female than male P301L TG mice. In our previous study, we demonstrated that a low fat-protein diet might play an important role to improve the lifespan and cognitive activity in a transgenic mouse model of Tauophaty (P301L), with a major improvement in female than male P301L TG mice.

In this study, young and old male and female transgenic P301L-Tau mice were studied in comparison with CTR mice fed with different diets (low fat-protein diet and high fat-protein diet) to investigate the oxidative damage in this model of Tauophaty and to explore the possible mechanisms through which diets can interact and improve a possible condition of oxidative stress. Together, these results add new perspectives to our understanding how dietary intake can delay or even prevent the oxidative damage in AD and other Tau-related pathologies, in order to prevent tauophaty and neurodegenerative diseases with a correct nutrition.

5.3 MATERIALS AND METHODS

5.3.1 Animals and Diets

Four hundred mice were used in this study. Two hundred were hemizygous Tau transgenic mice of mixed gender with a mutant form (P301L) of human Tau protein including four-repeats without amino terminal inserts, and driven by the mouse prion promoter 6 (MoPrP) [16]. Two hundred age-compatible wild type mice (B6D2F1) of mixed gender served as controls. Mice originated from Taconic Laboratories, USA, were bred at IRCCS Mario Negri Institute of Pharmacological Research in a Specific Pathogen free (SPF) facility with a regular 12:12 h light/dark cycle (lights on 07:00 a.m.), at a constant room temperature of 22 ± 2 °C, and relative humidity approximately 55 ± 10%. Animals were housed (n= 4 per group) in standard mouse cages, until three months of ages all animals were fed with standard rodent chow (diet 1: 18% protein and 5% fat, Harlan Lab. Tekland global diet), then animals were divided into two experimental groups, balanced for body weight and sex. The first group was fed with a standard rodent chow (diet 1: 18% protein and 5% fat, Harlan Lab. Tekland global diet), and the second group was fed with a low protein diet (diet 2: 14% protein and 3.5% fat Harlan Lab. Tekland global diet). Since the animals were bred in a SPF facility, where all materials introduced are sterilized, we had to use an autoclavable diet manufactured with high quality ingredients and supplemented with additional vitamins to ensure nutritional adequacy after autoclaving.

The diet 1 is a fixed formula, autoclavable diet designed to support gestation, lactation, and growth of rodents. This diet does not contain alfalfa, thus lowering the occurrence of natural phytoestrogens. Typical isoflavone concentrations (daidzein + genistein aglycone equivalents) range from 150 to 250 mg/kg. Exclusion of alfalfa reduces chlorophyll, improving optical imaging clarity. Absence of animal protein and fishmeal minimizes the presence of nitrosamines (Fig. 1).

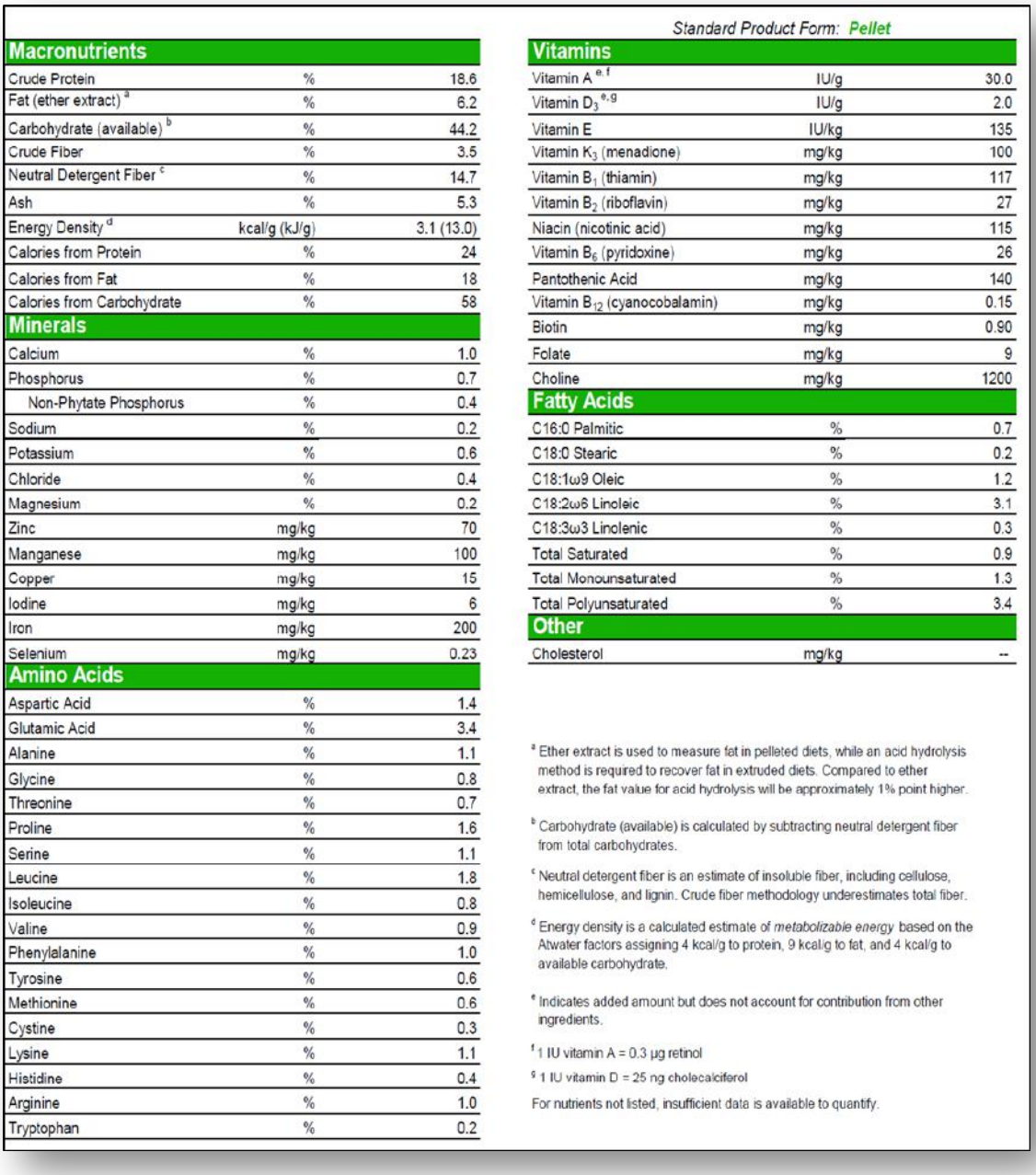

Standard Product Form: Pellet

Macronutrients		
Crude Protein	%	18.6
Fat (ether extract) [a]	%	6.2
Carbohydrate (available) [b]	%	44.2
Crude Fiber	%	3.5
Neutral Detergent Fiber [c]	%	14.7
Ash	%	5.3
Energy Density [d]	kcal/g (kJ/g)	3.1 (13.0)
Calories from Protein	%	24
Calories from Fat	%	18
Calories from Carbohydrate	%	58
Minerals		
Calcium	%	1.0
Phosphorus	%	0.7
Non-Phytate Phosphorus	%	0.4
Sodium	%	0.2
Potassium	%	0.6
Chloride	%	0.4
Magnesium	%	0.2
Zinc	mg/kg	70
Manganese	mg/kg	100
Copper	mg/kg	15
Iodine	mg/kg	6
Iron	mg/kg	200
Selenium	mg/kg	0.23
Amino Acids		
Aspartic Acid	%	1.4
Glutamic Acid	%	3.4
Alanine	%	1.1
Glycine	%	0.8
Threonine	%	0.7
Proline	%	1.6
Serine	%	1.1
Leucine	%	1.8
Isoleucine	%	0.8
Valine	%	0.9
Phenylalanine	%	1.0
Tyrosine	%	0.6
Methionine	%	0.6
Cystine	%	0.3
Lysine	%	1.1
Histidine	%	0.4
Arginine	%	1.0
Tryptophan	%	0.2

Vitamins		
Vitamin A [e, f]	IU/g	30.0
Vitamin D_3 [e, g]	IU/g	2.0
Vitamin E	IU/kg	135
Vitamin K_3 (menadione)	mg/kg	100
Vitamin B_1 (thiamin)	mg/kg	117
Vitamin B_2 (riboflavin)	mg/kg	27
Niacin (nicotinic acid)	mg/kg	115
Vitamin B_6 (pyridoxine)	mg/kg	26
Pantothenic Acid	mg/kg	140
Vitamin B_{12} (cyanocobalamin)	mg/kg	0.15
Biotin	mg/kg	0.90
Folate	mg/kg	9
Choline	mg/kg	1200
Fatty Acids		
C16:0 Palmitic	%	0.7
C18:0 Stearic	%	0.2
C18:1ω9 Oleic	%	1.2
C18:2ω6 Linoleic	%	3.1
C18:3ω3 Linolenic	%	0.3
Total Saturated	%	0.9
Total Monounsaturated	%	1.3
Total Polyunsaturated	%	3.4
Other		
Cholesterol	mg/kg	--

[a] Ether extract is used to measure fat in pelleted diets, while an acid hydrolysis method is required to recover fat in extruded diets. Compared to ether extract, the fat value for acid hydrolysis will be approximately 1% point higher.

[b] Carbohydrate (available) is calculated by subtracting neutral detergent fiber from total carbohydrates.

[c] Neutral detergent fiber is an estimate of insoluble fiber, including cellulose, hemicellulose, and lignin. Crude fiber methodology underestimates total fiber.

[d] Energy density is a calculated estimate of *metabolizable energy* based on the Atwater factors assigning 4 kcal/g to protein, 9 kcal/g to fat, and 4 kcal/g to available carbohydrate.

[e] Indicates added amount but does not account for contribution from other ingredients.

[f] 1 IU vitamin A = 0.3 µg retinol

[g] 1 IU vitamin D = 25 ng cholecalciferol

For nutrients not listed, insufficient data is available to quantify.

Figure 1: Composition of diet 1: 18% protein and 5% fat (Harlan Tekland global diet)

The diet 2 is a fixed formula, autoclavable diet designed to promote longevity and normal body weight in rodents. Diet 2 does not contain alfalfa or soybean meal, thus minimizing the occurrence of natural phytoestrogens. Typical isoflavone concentrations (daidzein + genistein aglycone equivalents) range from non-detectable to 20 mg/kg.

Exclusion of alfalfa reduces chlorophyll, improving optical imaging clarity. Absence of animal protein and fishmeal minimizes the presence of nitrosamines (Fig. 2).

Standard Product Form: Pellet

Macronutrients		
Crude Protein	%	14.3
Fat (ether extract) [a]	%	4.0
Carbohydrate (available) [b]	%	48.0
Crude Fiber	%	4.1
Neutral Detergent Fiber [c]	%	18.0
Ash	%	4.7
Energy Density [d]	kcal/g (kJ/g)	2.9 (12.1)
Calories from Protein	%	20
Calories from Fat	%	13
Calories from Carbohydrate	%	67
Minerals		
Calcium	%	0.7
Phosphorus	%	0.6
Non-Phytate Phosphorus	%	0.3
Sodium	%	0.1
Potassium	%	0.6
Chloride	%	0.3
Magnesium	%	0.2
Zinc	mg/kg	70
Manganese	mg/kg	100
Copper	mg/kg	15
Iodine	mg/kg	6
Iron	mg/kg	175
Selenium	mg/kg	0.23
Amino Acids		
Aspartic Acid	%	0.9
Glutamic Acid	%	2.9
Alanine	%	0.9
Glycine	%	0.7
Threonine	%	0.5
Proline	%	1.2
Serine	%	0.7
Leucine	%	1.4
Isoleucine	%	0.6
Valine	%	0.7
Phenylalanine	%	0.7
Tyrosine	%	0.4
Methionine	%	0.4
Cystine	%	0.3
Lysine	%	0.7
Histidine	%	0.4
Arginine	%	0.8
Tryptophan	%	0.2

Vitamins		
Vitamin A [e, f]	IU/g	17.0
Vitamin D_3 [e, g]	IU/g	1.2
Vitamin E	IU/kg	150
Vitamin K_3 (menadione)	mg/kg	58
Vitamin B_1 (thiamin)	mg/kg	64
Vitamin B_2 (riboflavin)	mg/kg	16
Niacin (nicotinic acid)	mg/kg	84
Vitamin B_6 (pyridoxine)	mg/kg	17
Pantothenic Acid	mg/kg	76
Vitamin B_{12} (cyanocobalamin)	mg/kg	0.09
Biotin	mg/kg	0.57
Folate	mg/kg	5
Choline	mg/kg	1030
Fatty Acids		
C16:0 Palmitic	%	0.5
C18:0 Stearic	%	0.1
C18:1ω9 Oleic	%	0.7
C18:2ω6 Linoleic	%	2.0
C18:3ω3 Linolenic	%	0.1
Total Saturated	%	0.6
Total Monounsaturated	%	0.7
Total Polyunsaturated	%	2.1
Other		
Cholesterol	mg/kg	--

[a] Ether extract is used to measure fat in pelleted diets, while an acid hydrolysis method is required to recover fat in extruded diets. Compared to ether extract, the fat value for acid hydrolysis will be approximately 1% point higher.

[b] Carbohydrate (available) is calculated by subtracting neutral detergent fiber from total carbohydrates.

[c] Neutral detergent fiber is an estimate of insoluble fiber, including cellulose, hemicellulose, and lignin. Crude fiber methodology underestimates total fiber.

[d] Energy density is a calculated estimate of *metabolizable energy* based on the Atwater factors assigning 4 kcal/g to protein, 9 kcal/g to fat, and 4 kcal/g to available carbohydrate.

[e] Indicates added amount but does not account for contribution from other ingredients.

[f] 1 IU vitamin A = 0.3 µg retinol

[g] 1 IU vitamin D = 25 ng cholecalciferol

For nutrients not listed, insufficient data is available to quantify.

Figure 2: Composition of diet 2: 14% protein and 3.5% fat (Harlan Tekland global diet)

5.3.2 Ethics Statement

Procedures involving animals and their care were in accordance to the national and international laws and policies (EEC Council Directive 86/609, OJ L 358, 1 Dec.12, 1987; NIH Guide for the Care and use of Laboratory Animals, U.S. National Research Council, 2011). The Mario Negri Institute for Pharmacological Research (IRCCS, Milan, Italy) Animal Care and Use Committee (IACUC) approved the experiments, which were conducted according to the institutional guidelines, which are in compliance with Italian laws (D.L. no. 116, G.U. suppl. 40, Feb. 18, 1992, Circular No.8, G.U., Juli14, 1994). The scientific project was approved by Italian Ministry of Health (Permit Number: 71/2014 B).

5.3.3 Study Design

The first point of our study was to characterize the transgenic mouse model of tauophaty that replicates the impairments found in patients affected by tauophaty in a way age-gender-dependent showing that females were more affected than males. Subsequently we investigated the effect of two different diets (high fat-protein and low fat-protein diets) on the onset and progression of tauophaty, finding that a low fat-protein diet may play an important role to improve the lifespan and cognitive activity in a transgenic mouse model of tauophaty (P301L), with a major improvement in female than male P301L TG mice.

The aim of this study was to investigate the oxidative damage in this model of tauophaty and to explore the possible mechanisms through which diets can interact and improve a possible condition of oxidative stress. After the weaning, all animals were fed with the same diet (diet 1 required for the growth of the mice); at 3 months of age the animals were divided into two experimental groups: the first group fed with diet 1 and the second group fed with diet 2. Mice were further divided into two separate groups for studying either behavior or metabolic profile linked to different diets administered; in the first group (n=240) body weight, food and water consumption and survival rates were analyzed (data shown previously).

In the second group (n=160), based on data in the literature [17-18], two time points were defined at 7 and 15 months of age (the first time point the symptoms of the disease were evident expressed, the second time point: maximum survival for mice affected by tauophaty), cognitive and locomotor aspects were evaluated utilizing behavioral tests.

To investigate the possible condition of oxidative stress and to investigate the possible mechanisms through which diets can interact and improve a possible condition of oxidative stress, animals were sacrificed after the behavioral tests and the brain were analyzed for immunohistochemical (IHC) studies, labeling the oxidative stress assessments as acrolein (alpha, beta-unsaturated aldehyde byproduct of lipid peroxidation), nitrotyrosine (marker for peroxynitrite formation in vivo), NOS2 and NOS3 (nitric oxide synthases the enzymes responsible for synthesis of NO identified the first in neurons and the second in endothelial cells).

At both time points (7 and 15 months) n=12 animals were sacrificed for IHC analyses as described below.

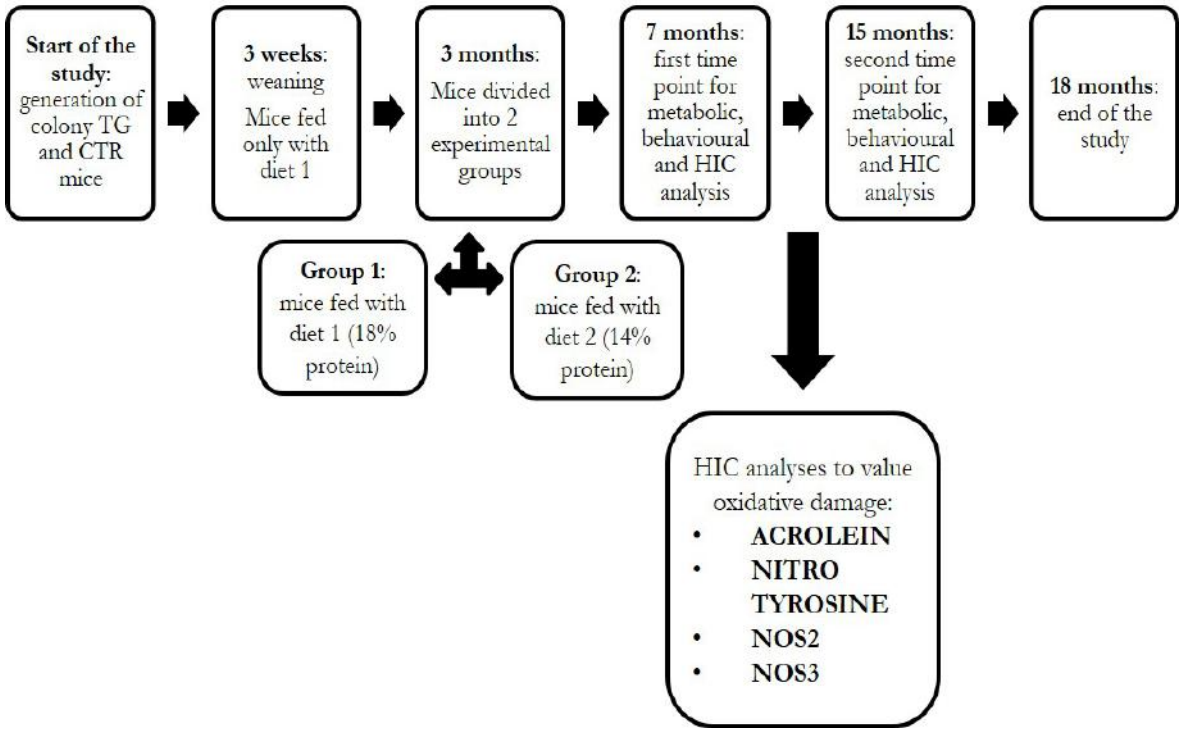

Figure 3: Experimental design of the study. In the study were set three time points: 3 months of age related to the administration of two different diets (diet 1 and diet 2), 7 and 15 months of age related to manifestation of the neurodisease and maximum survival of TG animals (time points for behavioral tests). After behavioral tests, HIC analysis and neuronal counts were conducted to value a condition of oxidative damage.

5.3.4 Immunohistochemistry

At the end of behavioral tests animals were euthanized by cervical dislocation [17-18]; brains were removed and fixed in 10% formalin for 24–48 h with the usual procedure and embedded in paraffin.

After deparaffinization, brain coronal sections (3 µm thick; three slices per mouse) were stained for immunohistochemistry utilizing different antibodies: acrolein, nitrotyrosine, NOS2 and NOS3 (see table 1). Acrolein, a reactive alpha, beta-unsaturated aldehyde, is a common environmental pollutant, a metabolite of the anticancer drug cyclophosphamide, and a byproduct of lipid peroxidation.
An increase in acrolein production has been proposed as a marker for Alzheimer's disease, diabetic glomerular lesions, and atherosclerosis.
Acrolein is a potent inhibitor of cell proliferation at nonlethal doses and may act through effects on redox-regulated transcription factors.
Nitric oxide (NO) is a product of the enzymatic conversion of arginine to citrulline by nitric oxide synthase. NO reacts rapidly with superoxide to form peroxynitrite. At physiological pH and in the presence of transition metals, peroxynitrite undergoes heterolytic cleavage to form hydroxyl anion and nitronium ion, the latter of which nitrates protein tyrosine residues. Thus, the presence of nitrotyrosine on proteins can be used as a marker for peroxynitrite formation in vivo. The presence of nitrotyrosine has been detected in various inflammatory processes including atherosclerotic plaques.
Nitric oxide (NO) has a broad range of biological activities and has been implicated in signaling pathways in phylogenetically different species. Nitric oxide synthases (NOSs), the enzymes responsible for synthesis of NO, contain an N-terminal oxygenase domain and a C-terminal reductase domain. NOS activity requires homodimerization as well as three cosubstrates (L-arginine, NADPH and O2) and five cofactors or prosthetic groups (FAD, FMN, calmodulin, tetrahydrobiopterin and heme).
Several distinct NOS isoforms have been described and been shown to represent the products of three distinct genes. These include two constitutive Ca2+/CaM-dependent forms of NOS, including NOS1 (also designated ncNOS) whose activity was first identified in neurons, and NOS3 (also designated ecNOS), first identified in endothelial cells. The inducible form of NOS, NOS2 (also designated iNOS), is Ca2+-independent and is expressed in a broad range of cell types. The sections were incubated for 1 h at room temperature with blocking solutions [NITRO TYROSINE and ACROLEIN: 3% Triton X-100 plus 1% NGS; NOS2 and NOS3: before antigen unmasking with citrate buffer PH 6 for 15 min in microwave; 0.1% Triton X-100 plus 1.5% NGS] and then overnight at 4°C with the primary antibodies.
After incubation with the biotinylated secondary antibody (1:200; 1 h at room temperature; Vector Laboratories, Burlingame, CA), the sections were then incubated for 30 minutes at room temperature with the avidin-biotin-peroxidase complex (Vector Laboratories) and diaminobenzidine (Sigma).

The sections were then lightly counterstained with hematoxylin. The specificity of the immunostaining was verified by incubating sections with PBS instead of the specific primary antibodies.

Table 1: primary antibodies

Antibody	Species	Specificity		Use	Dilution	Source, type
Acrolein	Mouse	Neurons		Oxidative damage	1:500	ABCam, mAb IgG1
Nitrotyrosine	Mouse	Neurons		Oxidative damage	1:500	ABCam, mAb IgG1
NOS2	Mouse	Neurons		Oxidative damage	1:50	Genetex, mAbIgG1
NOS3	Rabbit	Neurons		Oxidative damage	1:50	Genetex, mAbIgG

5.3.4 Neuronal Counts

The brain areas most affected by the toxic role of Tau, characterized by the presence of aggregates of hyperphosphorylated Tau, deposition of neurofibrillary tangles, axonal dilatations, neuronal and synaptic loss, are hippocampus, entorhinal cortex, CA1 pyramidal layer and the basal forebrain [19-20-21-22-23]. In our tauophaty mouse model the accumulation of oxidative species were quantified in the cortex and in the hippocampus (brain coronal sections). Immunoreactive cells were counted by image analysis software in 3 fields using an Olympus Bx51 light microscope (Olympus, Italy) equipped with a digital camera (at x400 each field represented a tissue section area of about 0.036 mm2). Following manual tracing of the cortex and hippocampus at the same stereotactic level in all mice, the number of positive cells were manually tagged, counted and oxidative damage scoring system was used. Grading is based on quantification of immunoreactive positive cells.

Oxidative damage scoring (histological) was as follows:

0=normal (no oxidative damage)

1=mild presence of oxidative damage (corresponding to 25% of immunoreactive positive cells)

2=moderate presence of oxidative damage (corresponding to 50% of immunoreactive positive cells)

3=severe presence of oxidative damage (corresponding to 75% of immunoreactive positive cells)

4=total presence of oxidative damage (corresponding to 100% of immunoreactive positive cells).

Every section was individually examined for the presence or absence of positive signaling in the nucleus neuronal (acrolein, nitrotyrosine, NOS2 and NOS3). The observer was not aware of the origin of the sections.

5.3.5 Statistical Analysis

Statistical analyses were performed using Graph Pad Prism 6 program. Neuronal counts data were analyzed using two-way ANOVA, followed by Tukey's *post hoc* test.

5.4 RESULTS

5.4.1 Immunohistochemistry and Neuronal Counts

Sections of both P301L TG and CTR mice brains were screened with acrolein, nitrotyrosine, NOS2 and NOS3 (Fig.4-6-8-10-12 respectively), in order to understand if oxidative damage was present and if different diets (diet 18: 18% protein and 5% and diet 14: 14% protein and 3.5% fat) can improve a hypothetical condition of oxidative status and progression of tauophaty. Immunostaining applied to cortex and hippocampus with acrolein antibody revealed that, regardless of diets administrated, in P301L TG mice the oxidative status was present at both 7 and 15 months of age (diet 14: Fig. 4B-F-D-H, Fig. 6B-F-D-H, diet 18: Fig. 4J-N-L-P,Fig. 6J-N-L-P).

These brain areas were subsequently quantified by acrolein immunoreactive cell counts (Fig. 5A-B and 7A-B). At 7 months of age for both male and female mice fed with different diets, a significant genotype effect in the cortex was detected (diet 14: TG female vs CTR female mice $P<0.0001$, diet 18: TG female vs CTR female mice $P<0.001$; Fig. 5A) and in the hippocampus (diet 18: TG male vs CTR male mice $P<0.0001$, TG female vs CTR female mice $P<0.0001$; Fig. 5B). At 7 month of age, any significant diet effect in the cortex of male and female TG mice was detected ($P>0.05$). At 15 months of age for both male and female mice fed with different diets, a significant genotype effect in the cortex was detected (diet 14: TG male vs CTR male mice $P<0.05$, TG female vs CTR female mice $P<0.0001$, diet 18: TG male vs CTR male mice $P<0.0001$, TG female vs CTR female mice $P<0.0001$; Fig. 7A) and in the hippocampus (diet 14: TG male vs CTR male mice $P<0.05$, TG female vs CTR female mice $P<0.0001$; diet 18: TG male vs CTR male mice $P<0.0001$, TG female vs CTR female mice $P<0.0001$Fig. 6B). A significant diet effect in the cortex and hippocampus of female TG mice was detected (cortex: TG diet 14 vs TG diet 18 $P<0.05$; hippocampus: TG diet 14 vs TG diet 18 $P<0.00001$; Fig. 6B).

Also in the hippocampus of CTR female mice a significant diet effect was detected (CTR diet 14 vs CTR diet 18 $P<0.05$; Fig. 6B).

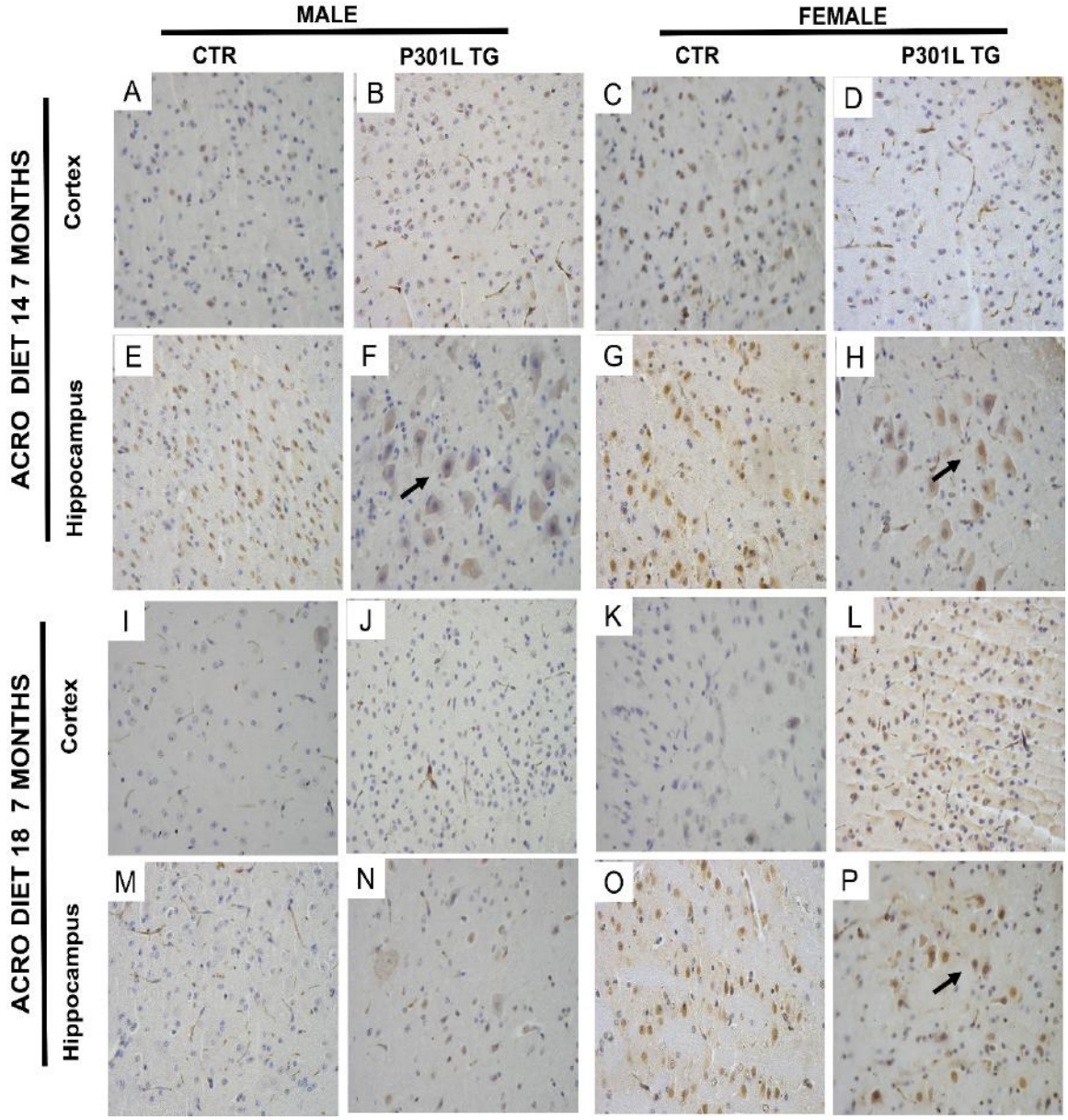

Figure 4. Acrolein immunoreactivity in TG and CTR mice fed with different diets at 7 month of age. Acrolein stained sections revealed the positive signal in 7-month-old males and females (P301L TG mice and CTR mice) fed with diet 14 and 18 in cortex (**A-D**, **I-L**) and in hippocampus (**E-H**, **M-P** note the arrows pointing to the most representative aspects in TG mice). Representative sections are shown of 4 animals used per each group. Scale bar: 40 μm.

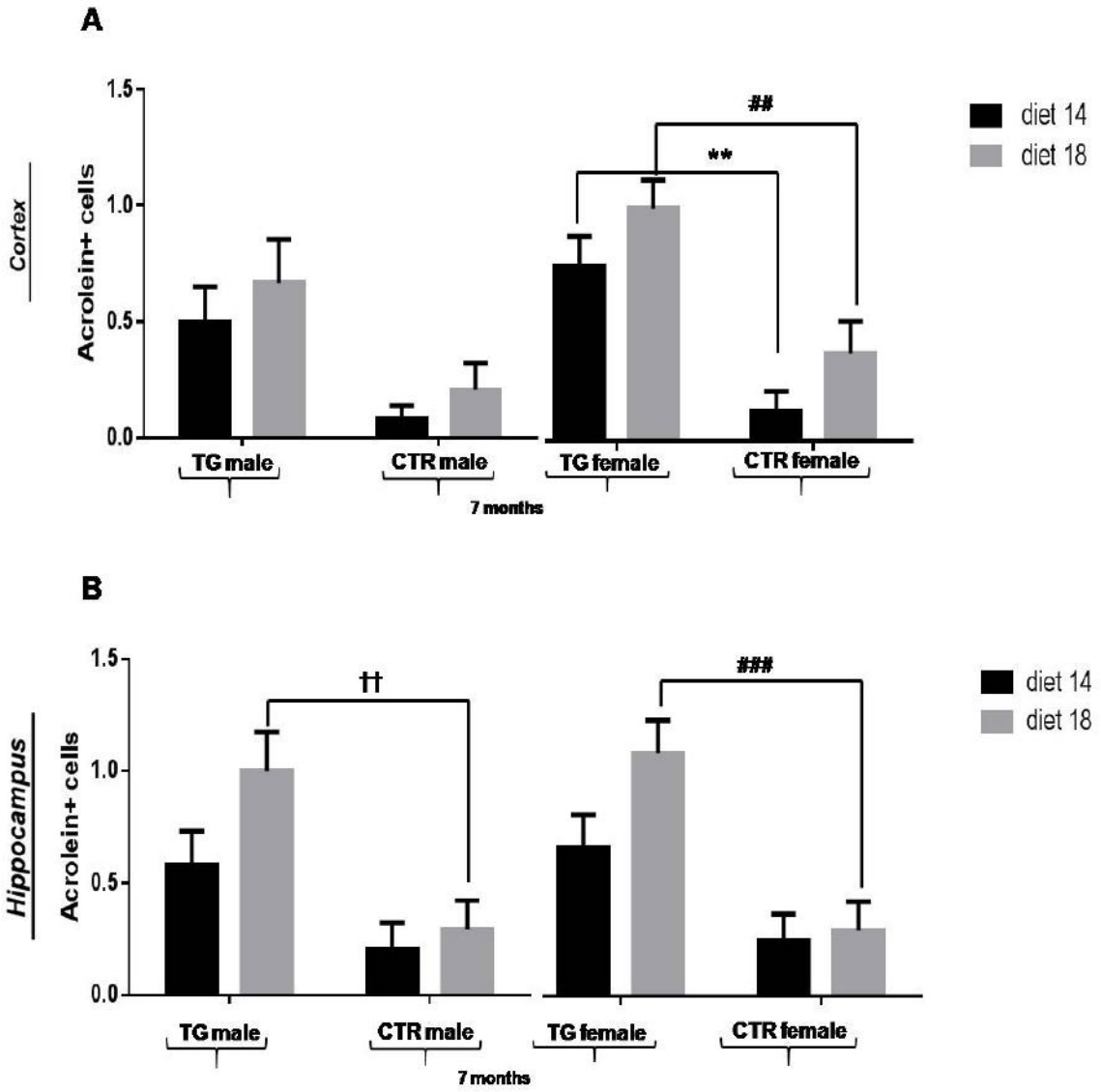

Figure 5. Quantification of Acrolein immunoreactive cell counts in TG and CTR mice fed with different diets at 7 month of age. A-B) Quantification of Acrolein immunoreactive cells in the cortex and in hippocampus showed a significantly increased number of Acrolein+ cells in TG mice compared to CTR mice, regardless of diet administrated, at 7 months of age. Any significant diet effect in the cortex and hippocampus of male and female TG mice was detected. Data were shown as mean ± SEM.DIET 14: TG female vs CTR female mice ** P< 0.001. DIET 18: TG male vs CTR male mice †† P< 0.001, TG female vs CTR female mice ### P< 0.0001.

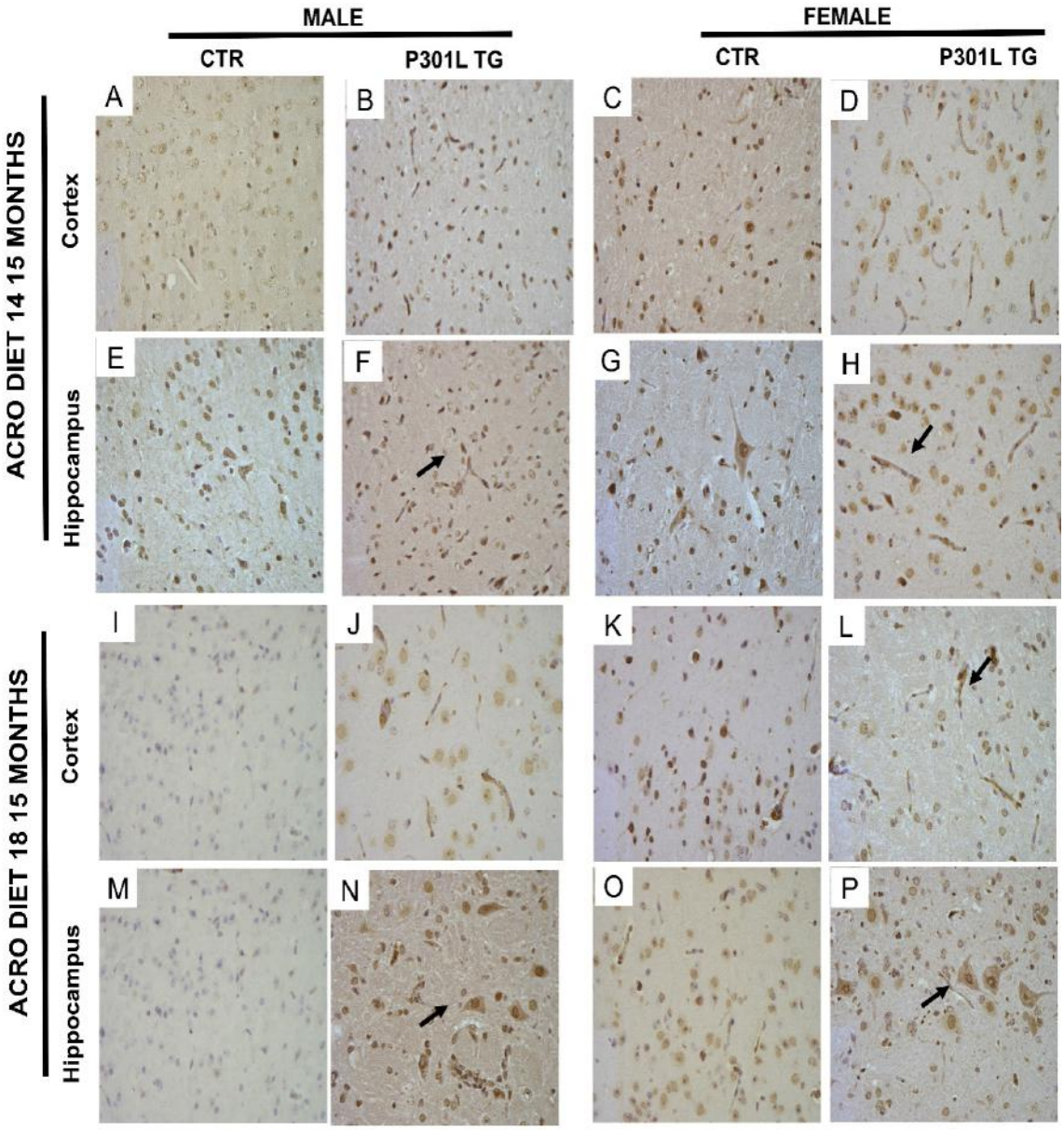

Figure 6. Acrolein immunoreactivity in TG and CTR mice fed with different diets at 15 month of age. Acrolein stained sections revealed the positive signal in 7-month-old males and females (P301L TG mice and CTR mice) fed with diet 14 and 18 in cortex (**A-D**, **I-L**) and in hippocampus (**E-H**, **M-P** note the arrows pointing to the most representative aspects in TG mice). Representative sections are shown of 4 animals used per each group. Scale bar: 40 μm.

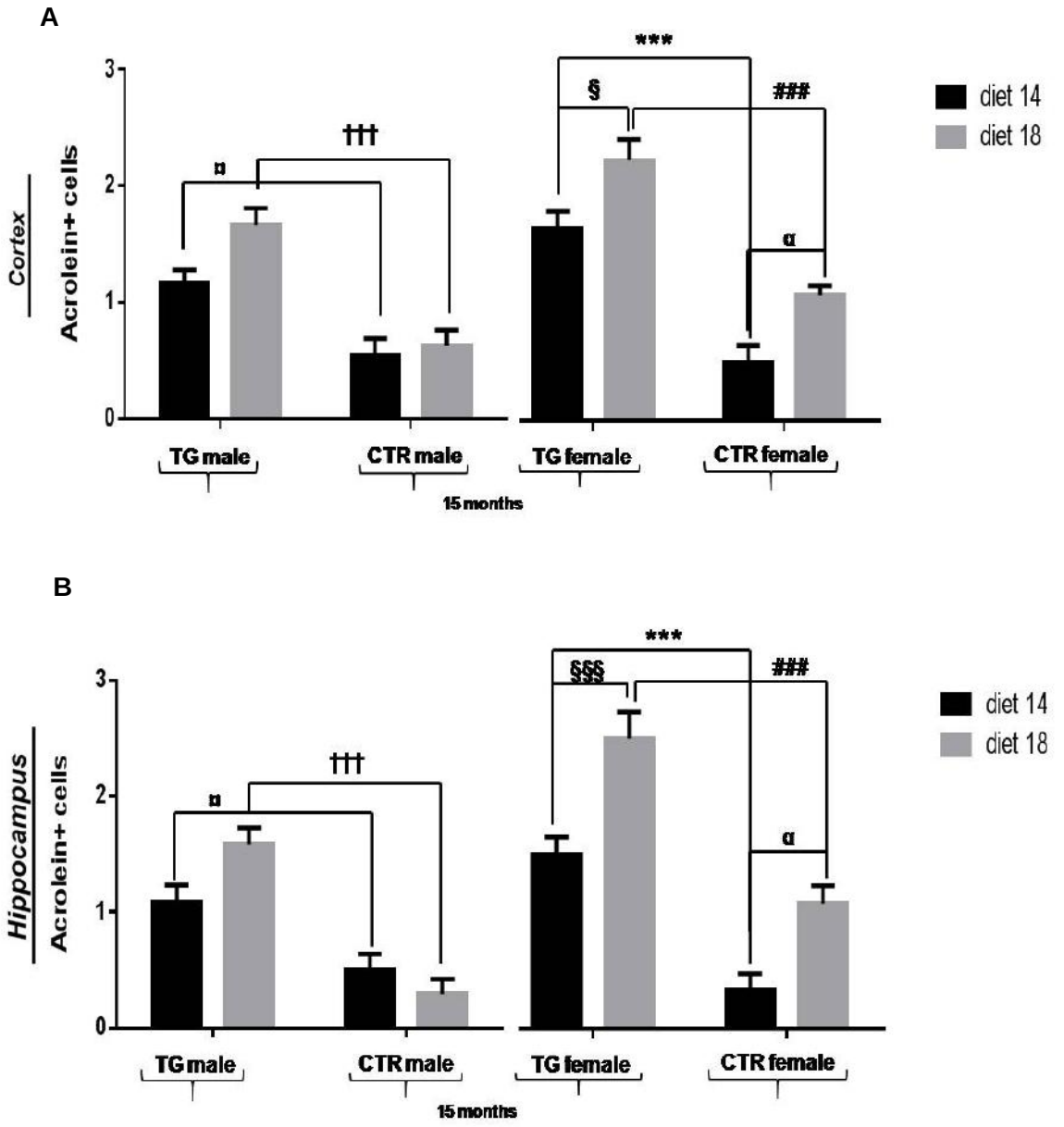

Figure 7. Quantification of Acrolein immunoreactive cell counts in TG and CTR mice fed with different diets at 15 month of age. A-B) Quantification of acrolein immunoreactive cells in hippocampus and in the cortex showed a significantly increased number of acrolein+ cells in TG mice compared to CTR mice at 15 months of age. A significant diet effect in the cortex and hippocampus of female TG mice was detected, as shown by a significantly increase of acrolein+ cells TG mice fed with diet 18 compared to TG mice fed with diet 14. DIET 18: TG male vs CTR male mice ††† P< 0.0001, TG female vs CTR female mice ### P< 0.0001. DIET 14: TG male vs CTR male mice ¤ P< 0.05, TG female vs CTR female mice *** P< 0.0001. TG female diet 18 vs TG female diet 14 § P< 0.05, §§§ P< 0.0001; CTR female diet 18 vs CTR female diet 14 α P< 0.05. Data were shown as mean ± SEM.

Immunostaining applied to cortex and hippocampus with nitrotyrosine antibody revealed that, regardless of diets administrated, in P301L TG mice the oxidative status was present at both 7 and 15 months of age (diet 14: Fig. 8B-F-D-H, Fig. 10B-F-D-H, diet 18: Fig. 8J-N-L-P, Fig. 10J-N-L-P).

These brain areas were subsequently quantified by nitrotyrosine immunoreactive cell counts (Fig. 9A-B and 11A-B). At 7 months of age for both male and female mice, regardless of diets administrated, a significant genotype effect in the cortex was detected (diet 14: TG female vs CTR female mice $P<0.05$, diet 18: TG female vs CTR female mice $P<0.0001$; Fig. 9A) and in the hippocampus (diet 18: TG male vs CTR male mice $P<0.0001$, Fig. 9B). At 7 month of age, in the hippocampus of TG male mice a significant diet effect was detected (TG diet 14 vs TG diet 18 $P<0.05$; Fig. 9B).

At 15 months of age for both male and female mice fed with different diets, a significant genotype effect in the cortex was detected (diet 14: TG male vs CTR male mice $P<0.001$, diet 18: TG female vs CTR female mice $P<0.0001$, Fig. 11A) and in the hippocampus (diet 14: TG female vs CTR female mice $P<0.0001$; diet 18: TG male vs CTR male mice $P<0.0001$, TG female vs CTR female mice $P<0.0001$; Fig. 11B).

A significant diet effect in the cortex and hippocampus of TG mice was detected (cortex: TG male mice diet 14 vs diet 18 $P<0.05$, TG female mice diet 14 vs diet 18 $P<0.0001$; hippocampus: TG male mice diet 14 vs TG diet 18 $P<0.0001$; Fig. 11B).

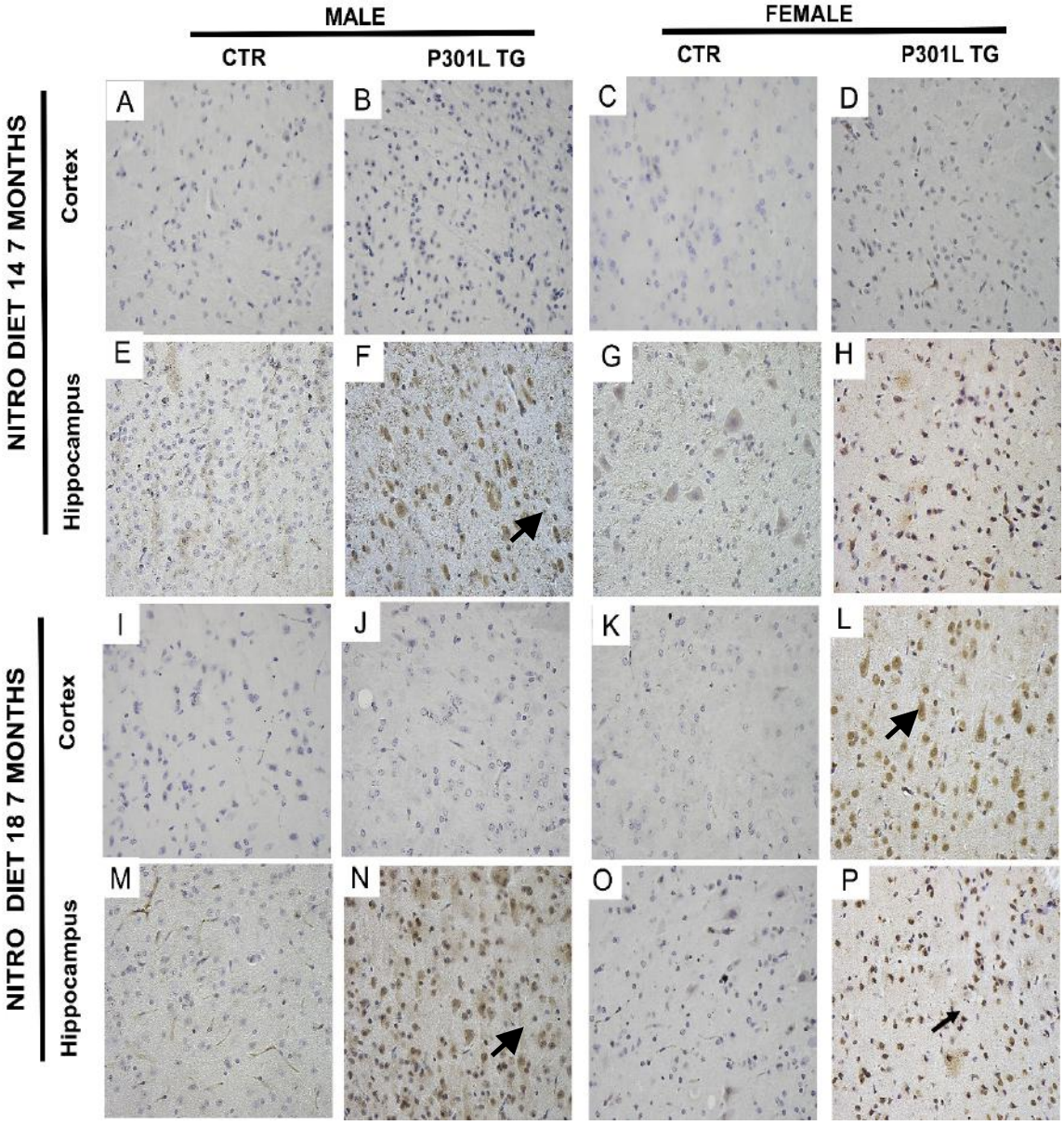

Figure 8. Nitrotyrosine immunoreactivity in TG and CTR mice fed with different diets at 7 month of age. Nitrotyrosine stained sections revealed the positive signal in 7-month-old males and females (P301L TG mice and CTR mice) fed with diet 14 and 18 in cortex (**A-D**, **I-L**) and in hippocampus (**E-H**, **M-P** note the arrows pointing to the most representative aspects in TG mice). Representative sections are shown of 4 animals used per each group. Scale bar: 40 μm.

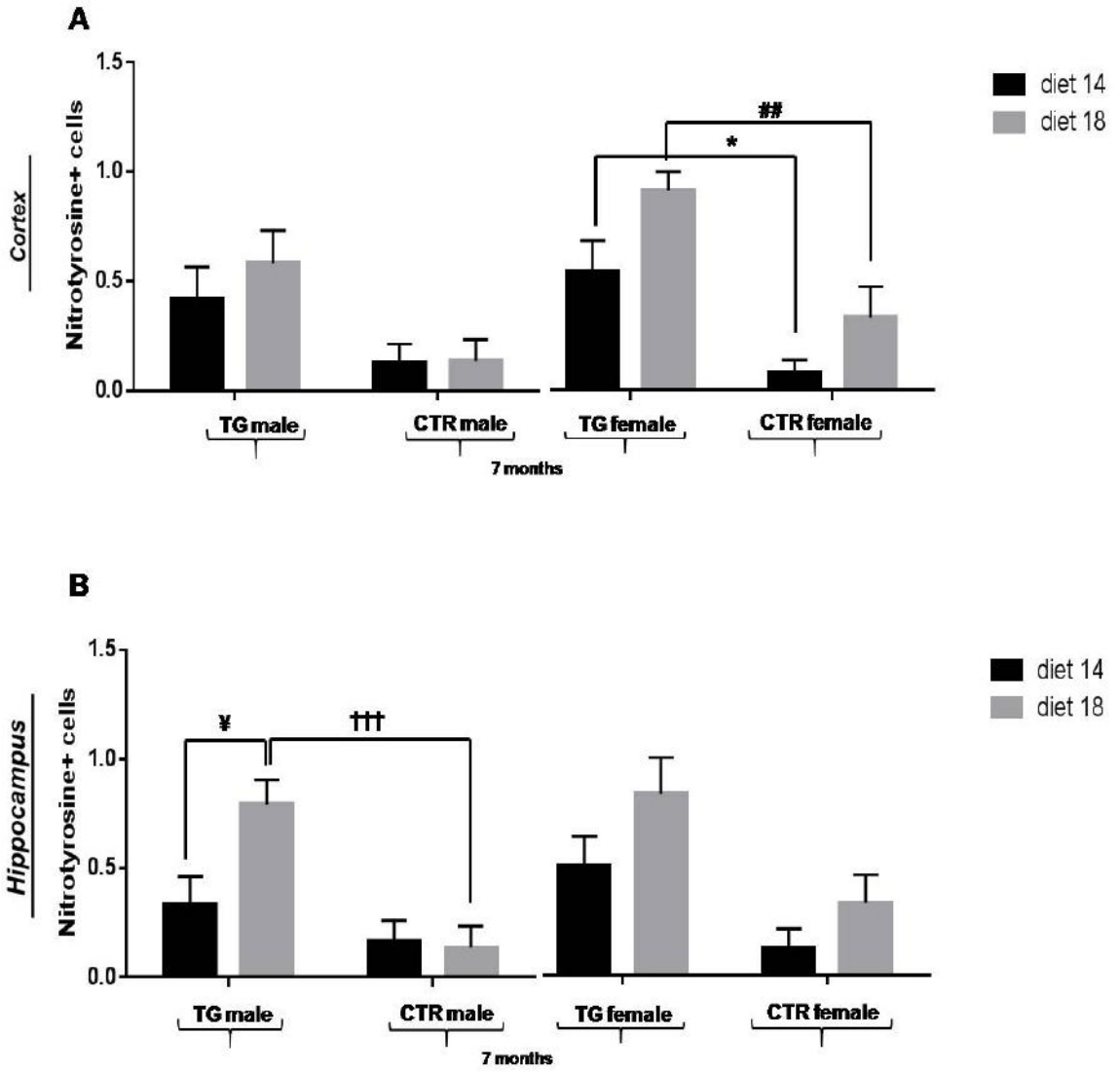

Figure 9. Quantification of nitrotyrosine immunoreactive cell counts in TG and CTR mice fed with different diets at 7 month of age. A-B) Quantification of nitrotyrosine immunoreactive cells in the cortex and in hippocampus showed a significantly increased number of nitrotyrosine+ cells in TG mice compared to CTR mice, regardless of diets administrated, at 7 months of age. A significant diet effect in hippocampus of male TG mice was detected, as shown by a significantly increase of nitrotyrosine+ cells TG mice fed with diet 18 compared to TG mice fed with diet 14. DIET 18: TG male vs CTR male mice ††† P< 0.0001, TG female vs CTR female mice ## P< 0.001. DIET 14: TG female vs CTR female mice * P< 0.05. TG male diet 18 vs TG male diet 14 ¥ P< 0.05. Data were shown as mean ± SEM.

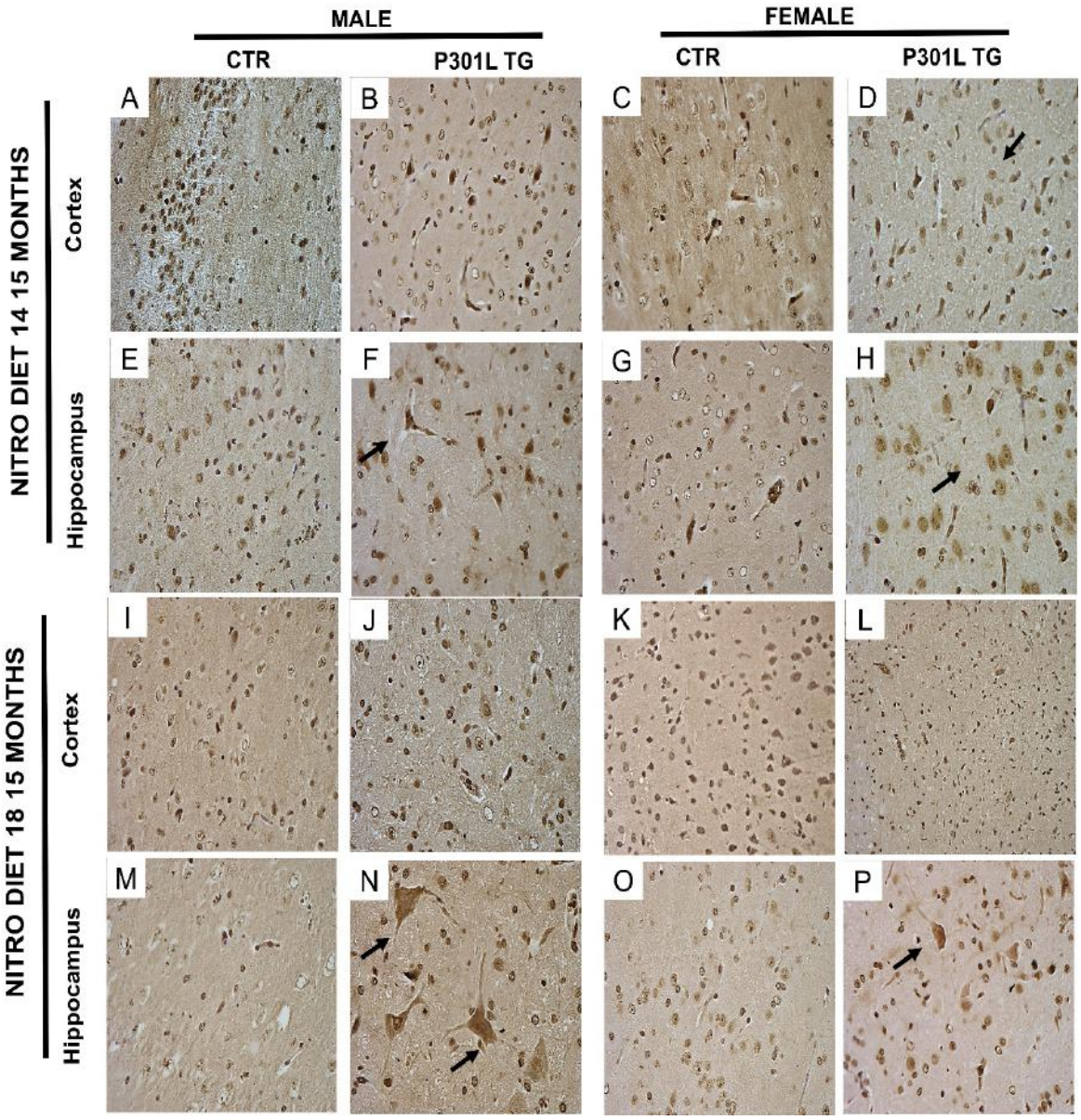

Figure 10. Nitrotyrosine immunoreactivity in TG and CTR mice fed with different diets at 15 month of age. Nitrotyrosine stained sections revealed the positive signal in 15-month-old males and females (P301L TG mice and CTR mice) fed with diet 14 and 18 in cortex (**A-D**, **I-L**) and in hippocampus (**E-H**, **M-P** note the arrows pointing to the most representative aspects in TG mice). Representative sections are shown of 4 animals used per each group. Scale bar: 40 μm.

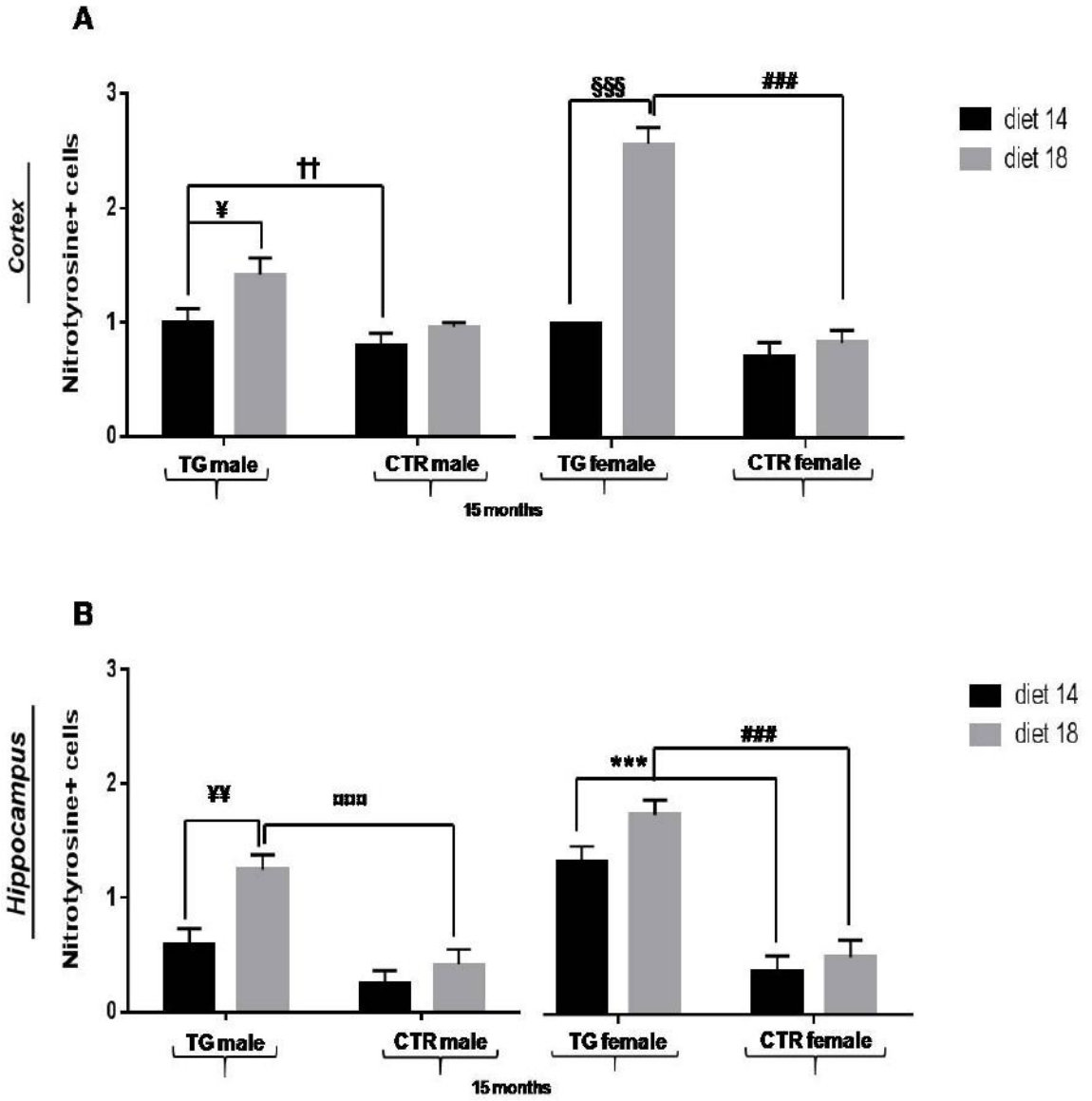

Figure 11. Quantification of nitrotyrosine immunoreactive cell counts in TG and CTR mice fed with different diets at 15 month of age. A-B) Quantification of nitrotyrosine immunoreactive cells in the cortex and in hippocampus showed a significantly increased number of nitrotyrosine+ cells in TG mice compared to CTR mice, regardless of diets administrated, at 15 months of age. A significant diet effect in the cortex and in hippocampus of male and female TG mice was detected, as shown by a significantly increase of nitrotyrosine+ cells TG mice fed with diet 18 compared to TG mice fed with diet 14. DIET 18: TG male vs CTR male mice ¤¤¤ P< 0.0001, TG female vs CTR female mice ### P< 0.0001. DIET 14: TG male vs CTR male mice ††† P< 0.0001, TG female vs CTR female mice *** P< 0.0001. TG male diet 18 vs TG male diet 14 ¥ P< 0.05, ¥¥ P<0.001. TG female diet 18 vs TG female diet 14 §§§ P< 0.0001 Data were shown as mean ± SEM.

Immunostaining applied to cortex and hippocampus with NOS2 antibody revealed that, regardless of diets administrated, in P301L TG mice the oxidative status was present at 15, but not at 7 months of age (diet 14: Fig. 12B-F-D-H, Fig. 14B-F-D-H, diet 18: Fig. 12J-N-L-P, Fig. 14J-N-L-P). These brain areas were subsequently quantified by NOS2 immunoreactive cell counts (Fig. 13A-B and 15A-B). At 7 months of age for both male and female mice fed with different diets, any significant genotype and diet effect in the cortex and in hippocampus was detected ($P>0.05$).

At 15 months of age for both male and female mice fed with different diets, a significant genotype effect in the cortex was detected (diet 14: TG male vs CTR male mice $P<0.0001$, TG female vs CTR female mice $P<0.0001$; diet 18: TG male vs CTR male mice $P<0.0001$, TG female vs CTR female mice $P<0.0001$, Fig. 15A) and in the hippocampus (diet 14: TG male vs CTR male mice $P<0.0001$, TG female vs CTR female mice $P<0.0001$; diet 18: TG male vs CTR male mice $P<0.0001$, TG female vs CTR female mice $P<0.0001$, Fig. 15B). A significant diet effect in the cortex of TG female mice (TG female mice diet 14 vs diet 18 $P<0.0001$) and in the hippocampus of TG male mice (TG male mice diet 14 vs TG diet 18 $P<0.05$; Fig. 15B) was detected.

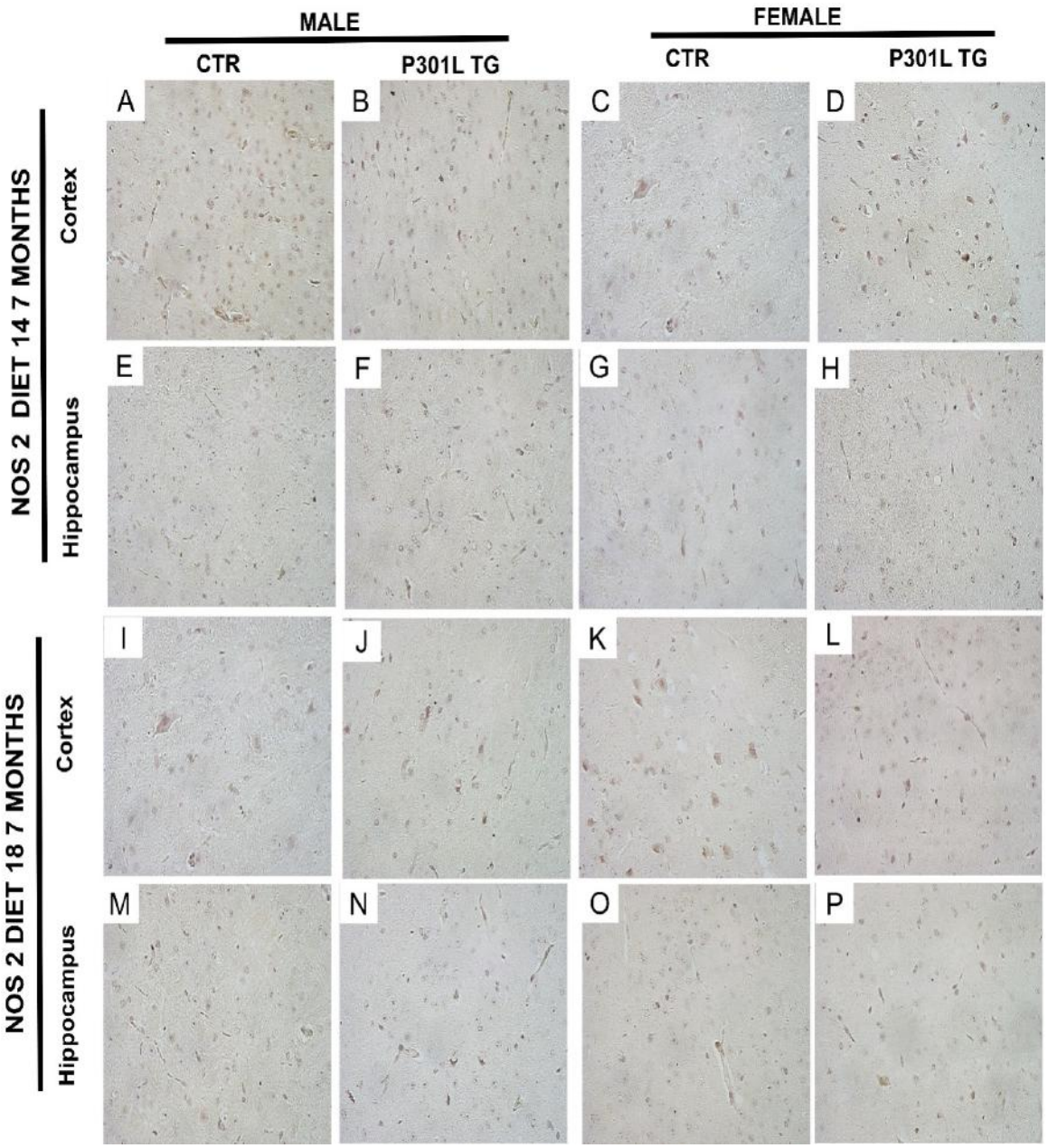

Figure 12. NOS2 immunoreactivity in TG and CTR mice fed with different diets at 7 month of age. NOS2 stained sections revealed the positive signal in 7-month-old males and females (P301L TG mice and CTR mice) fed with diet 14 and 18 in cortex (**A-D**, **I-L**) and in hippocampus (**E-H**, **M-P** note the arrows pointing to the most representative aspects in TG mice). Representative sections are shown of 4 animals used per each group. Scale bar: 40 μm.

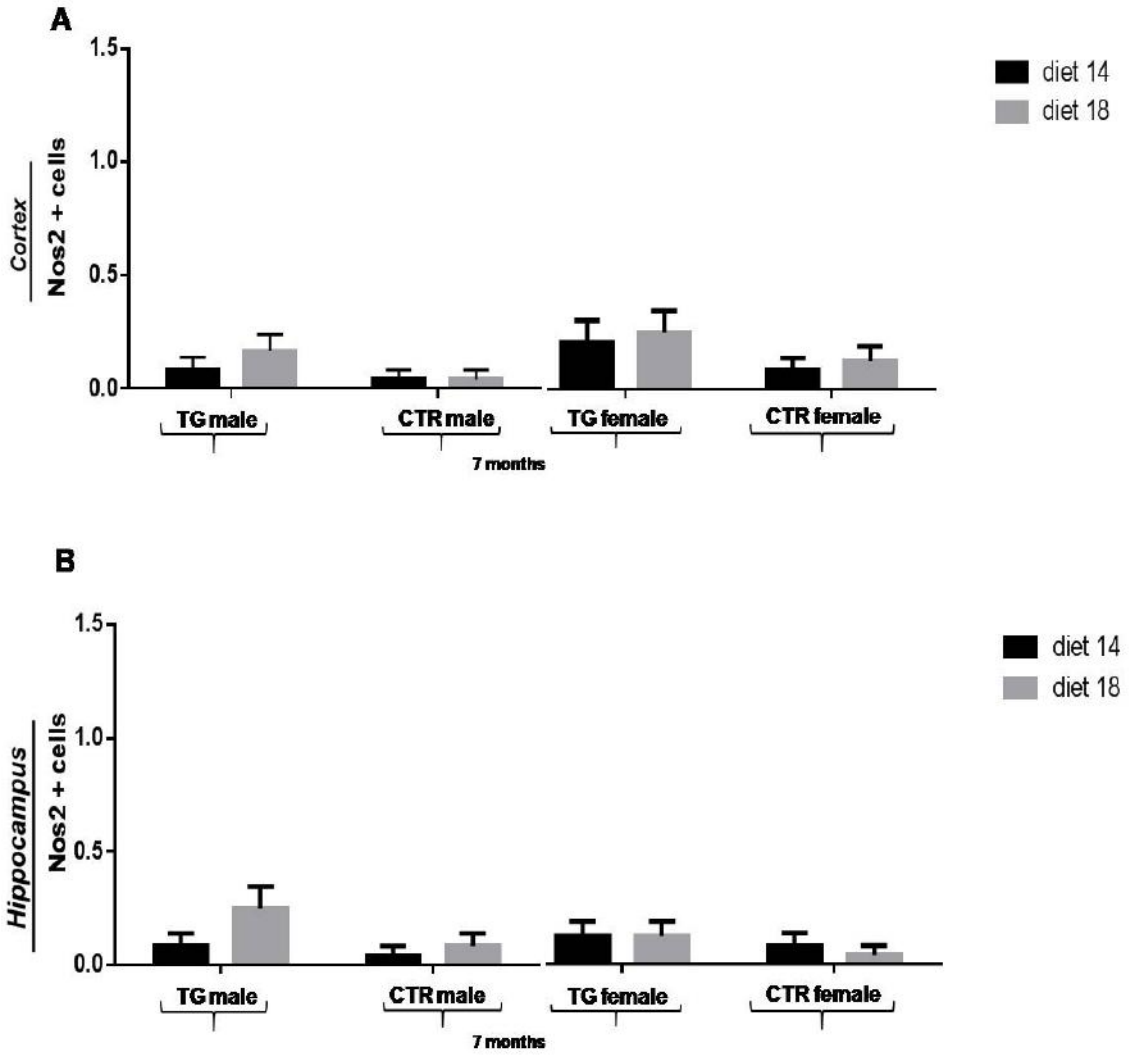

Figure 13. Quantification of NOS2 immunoreactive cell counts in TG and CTR mice fed with different diets at 7 month of age. A-B) Quantification of NOS2 immunoreactive cells in the cortex and in hippocampus showed any significant difference between TG and CTR mice fed with different diets.

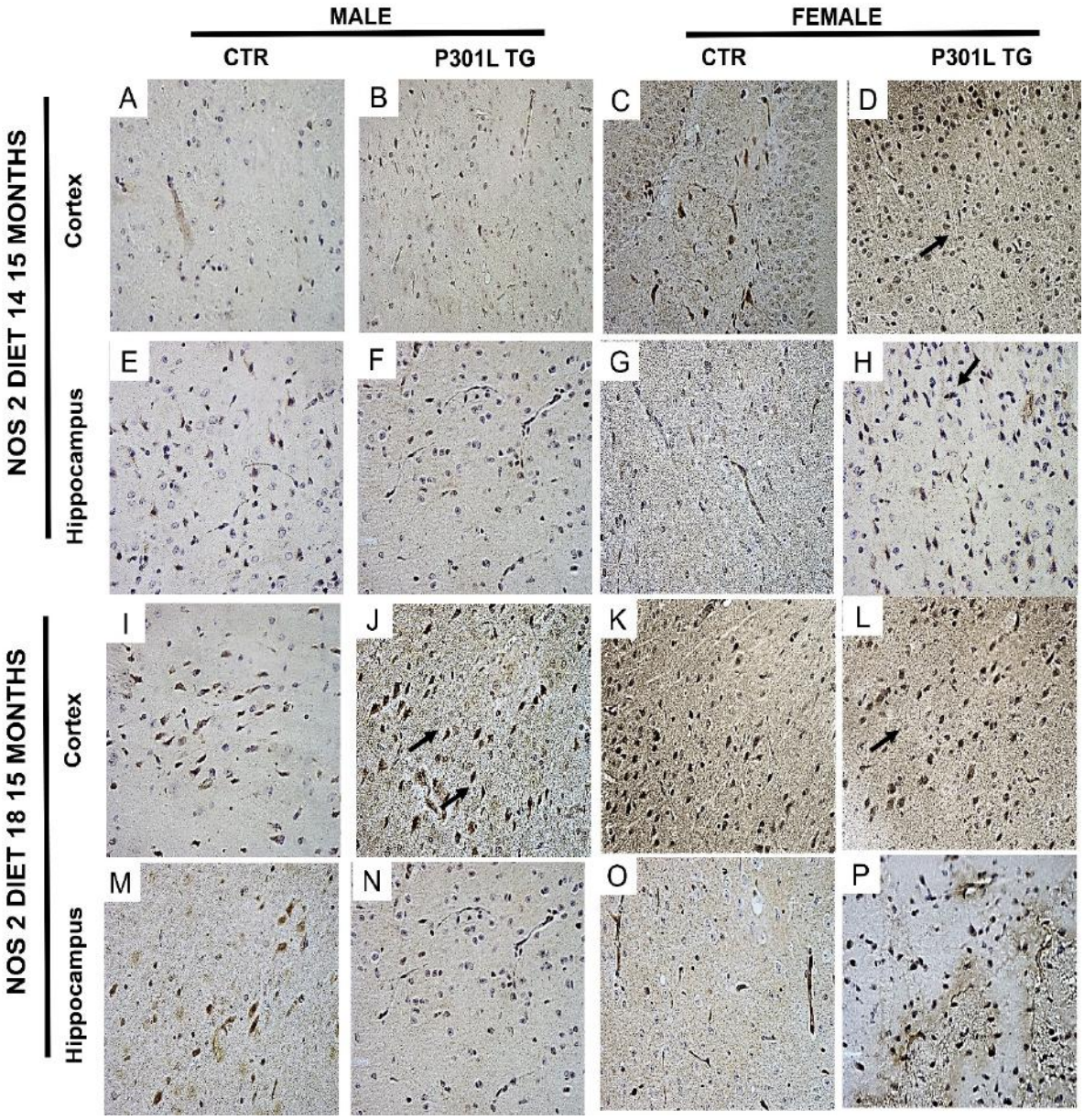

Figure 14. NOS2 immunoreactivity in TG and CTR mice fed with different diets at 15 month of age. NOS2 stained sections revealed the positive signal in 15-month-old males and females (P301L TG mice and CTR mice) fed with diet 14 and 18 in cortex (**A-D**, **I-L**) and in hippocampus (**E-H**, **M-P** note the arrows pointing to the most representative aspects in TG mice). Representative sections are shown of 4 animals used per each group. Scale bar: 40 μm.

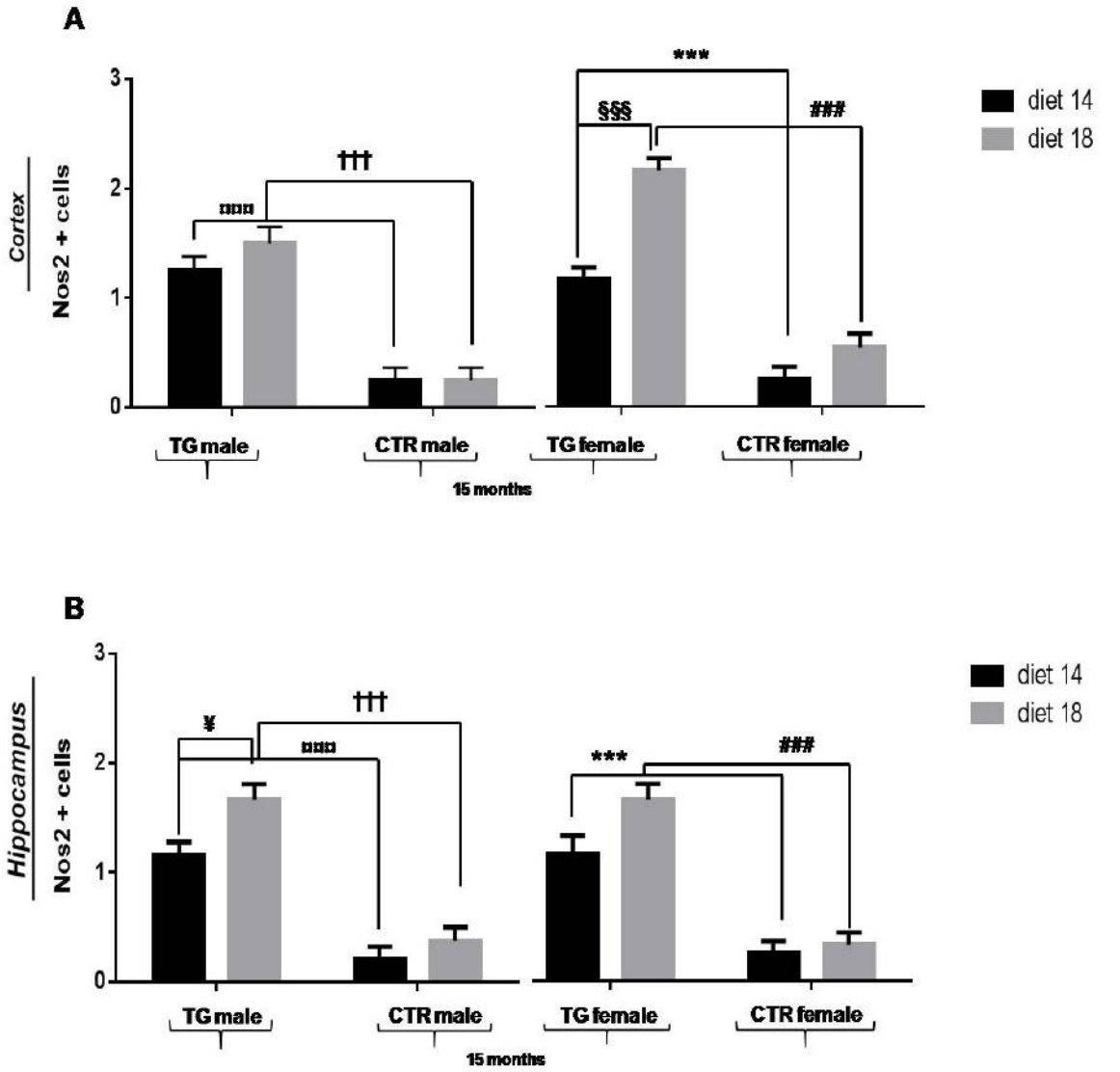

Figure 15. Quantification of NOS2 immunoreactive cell counts in TG and CTR mice fed with different diets at 15 month of age. A-B) Quantification of Nos2 immunoreactive cells in the cortex and in hippocampus showed a significantly increased number of NOS2+ cells in TG mice compared to CTR mice, regardless of diets administrated, at 15 months of age. A significant diet effect in the cortex and in hippocampus of female and male TG mice was detected, as shown by a significantly increase of Nos2+ cells TG mice fed with diet 18 compared to TG mice fed with diet 14. DIET 18: TG male vs CTR male mice ††† P< 0.0001, TG female vs CTR female mice ### P< 0.0001. DIET 14: TG male vs CTR male mice ¤¤¤ P< 0.0001, TG female vs CTR female mice *** P< 0.0001. TG male diet 18 vs TG male diet 14 ¥ P< 0.05; TG female diet 18 vs TG female diet 14 §§§ P< 0.0001 Data were shown as mean ± SEM.

Immunostaining applied to cortex and hippocampus with NOS3 antibody revealed that, regardless of diets administrated, in P301L TG mice the oxidative status was present both at 7 and 15months of age (diet 14: Fig. 16B-F-D-H, Fig. 18B-F-D-H, diet 18: Fig. 16J-N-L-P,Fig. 18J-N-L-P).

These brain areas were subsequently quantified by NOS3 immunoreactive cell counts (Fig. 17A-B and 19A-B). At 7 months of age for both male and female mice, regardless diets administrated, a significant genotype effect in the cortex was detected (diet 14: TG female vs CTR female mice $P<0.0001$; diet 18: TG male vs CTR male mice $P<0.0001$, TG female vs CTR female mice $P<0.0001$, Fig. 17A) and in the hippocampus (diet 14: TG male vs CTR male mice $P<0.0001$, TG female vs CTR female mice $P<0.0001$; diet 18: TG male vs CTR male mice $P<0.05$, TG female vs CTR female mice $P<0.0001$, Fig. 17B).

A significant diet effect in the cortex of TG mice (TG female mice diet 14 vs diet 18 $P<0.001$, TG male mice diet 14 vs TG diet 18 $P<0.05$; Fig. 17B) was detected. At 15 months of age for both male and female mice fed with different diets, a significant genotype effect in the cortex was detected (diet 14: TG male vs CTR male mice $P<0.0001$, TG female vs CTR female mice $P<0.0001$; diet 18: TG male vs CTR male mice $P<0.0001$, TG female vs CTR female mice $P<0.0001$, Fig. 19A) and in the hippocampus (diet 14: TG female vs CTR female mice $P<0.0001$; diet 18: TG male vs CTR male mice $P<0.0001$, TG female vs CTR female mice $P<0.0001$, Fig. 19B). A significant diet effect in the cortex and hippocampus of TG female mice (cortex: TG mice diet 14 vs diet 18 $P<0.0001$, hippocampus: TG mice diet 14 vs diet 18 $P<0.05$; Fig. 19B) was detected.

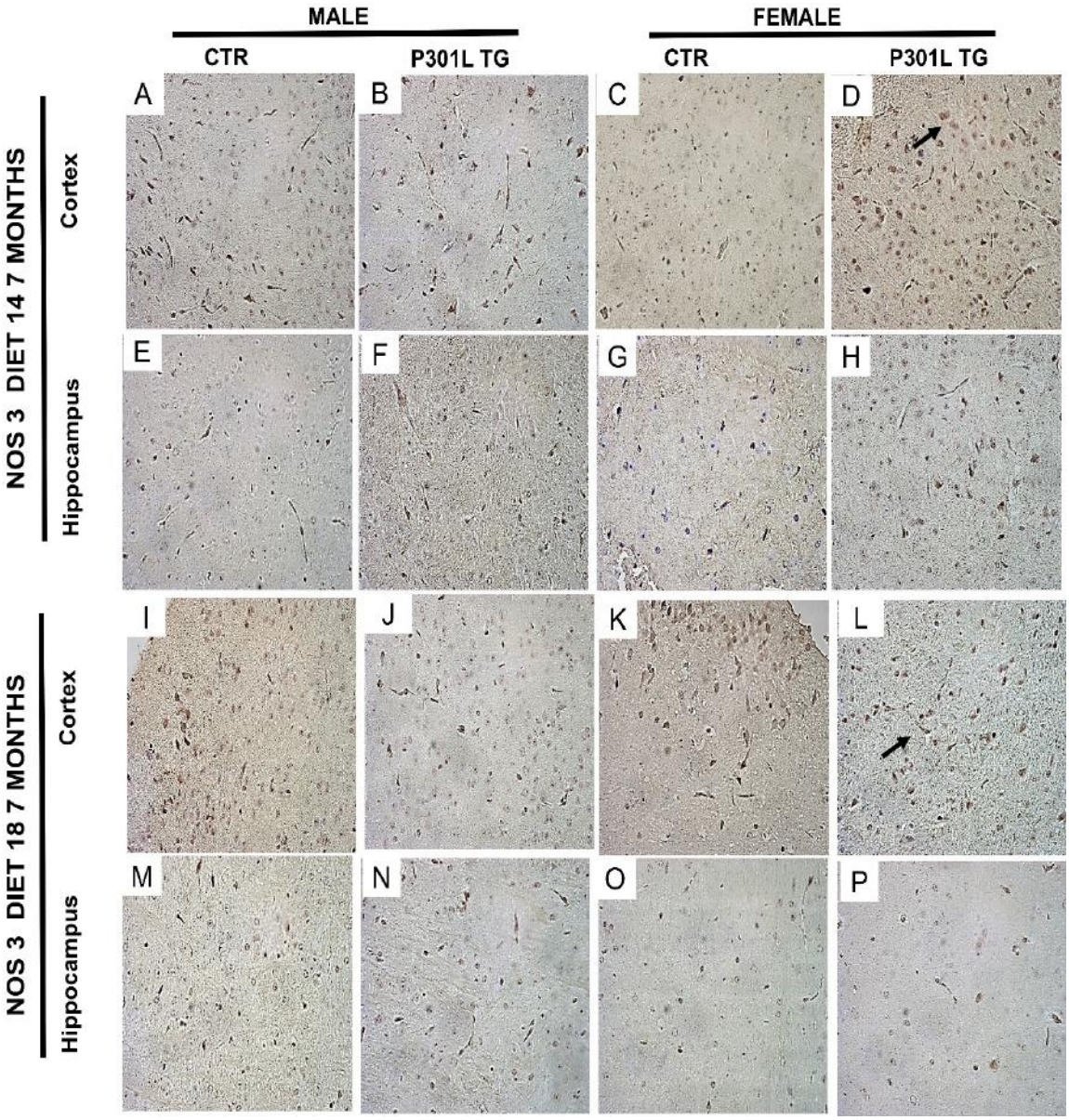

Figure 16. NOS3 immunoreactivity in TG and CTR mice fed with different diets at 7 month of age. NOS3 stained sections revealed the positive signal in 7-month-old males and females (P301L TG mice and CTR mice) fed with diet 14 and 18 in cortex (**A-D**, **I-L**) and in hippocampus (**E-H**, **M-P** note the arrows pointing to the most representative aspects in TG mice). Representative sections are shown of 4 animals used per each group. Scale bar: 40 μm.

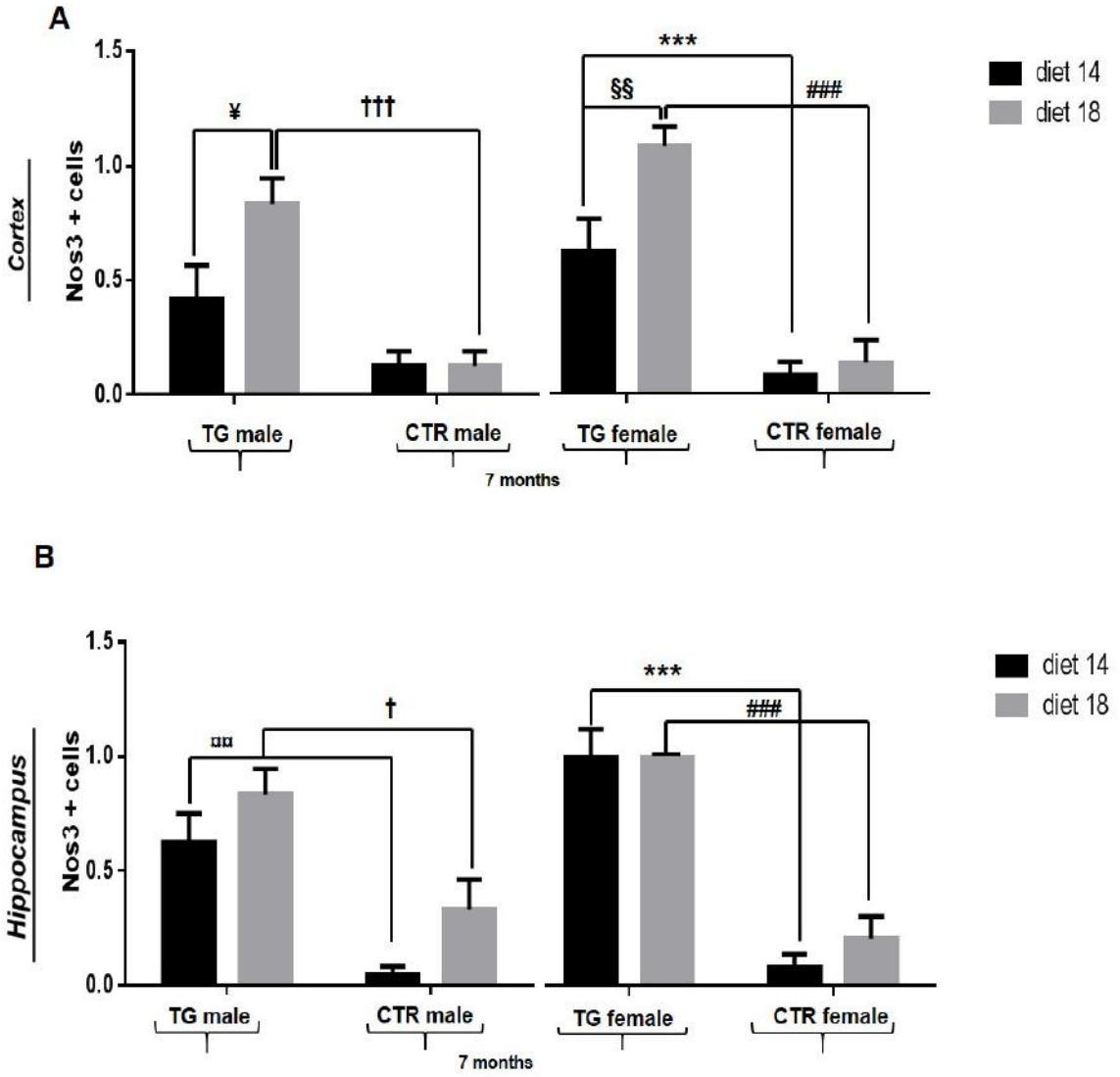

Figure 17. Quantification of NOS3 immunoreactive cell counts in TG and CTR mice fed with different diets at 7 month of age. A-B) Quantification of NOS3 immunoreactive cells in the cortex and in hippocampus showed a significantly increased number of NOS3+ cells in TG mice compared to CTR mice, regardless of diets administrated, at 7 months of age. A significant diet effect in the cortex of male and female TG mice was detected, as shown by a significantly increase of NOS3+ cells TG mice fed with diet 18 compared to TG mice fed with diet 14. DIET 18: TG male vs CTR male mice ††† P< 0.0001, TG female vs CTR female mice ### P< 0.0001. DIET 14: TG male vs CTR male mice ¤¤ P< 0.001, TG female vs CTR female mice *** P< 0.0001. TG male diet 18 vs TG male diet 14 ¥ P< 0.05; TG female diet 18 vs TG female diet 14 §§ P< 0.001. Data were shown as mean ± SEM.

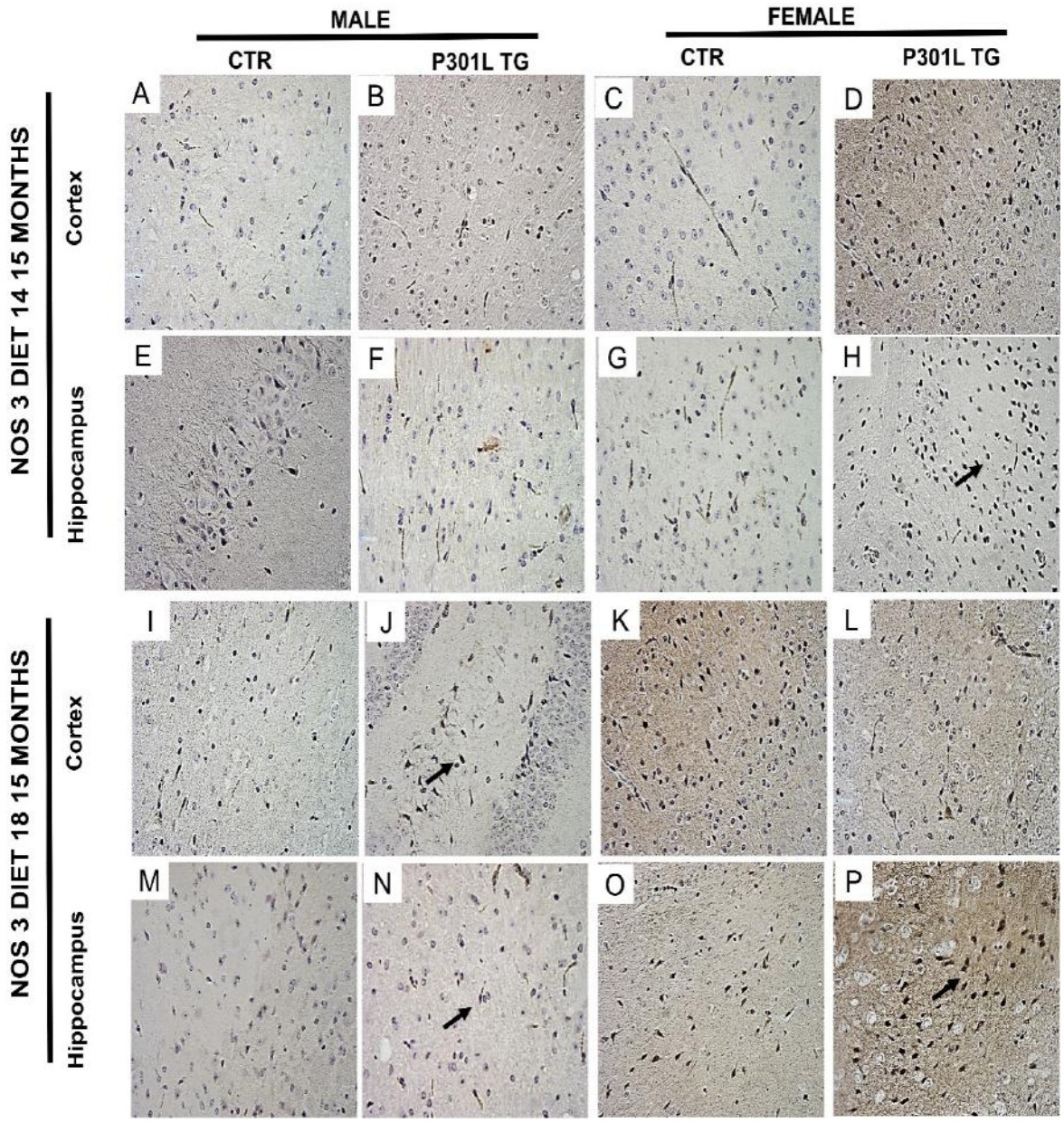

Figure 18. NOS3 immunoreactivity in TG and CTR mice fed with different diets at 15 month of age. NOS3 stained sections revealed the positive signal in 15-month-old males and females (P301L TG mice and CTR mice) fed with diet 14 and 18 in cortex (**A-D**, **I-L**) and in hippocampus (**E-H**, **M-P** note the arrows pointing to the most representative aspects in TG mice). Representative sections are shown of 4 animals used per each group. Scale bar: 40 μm.

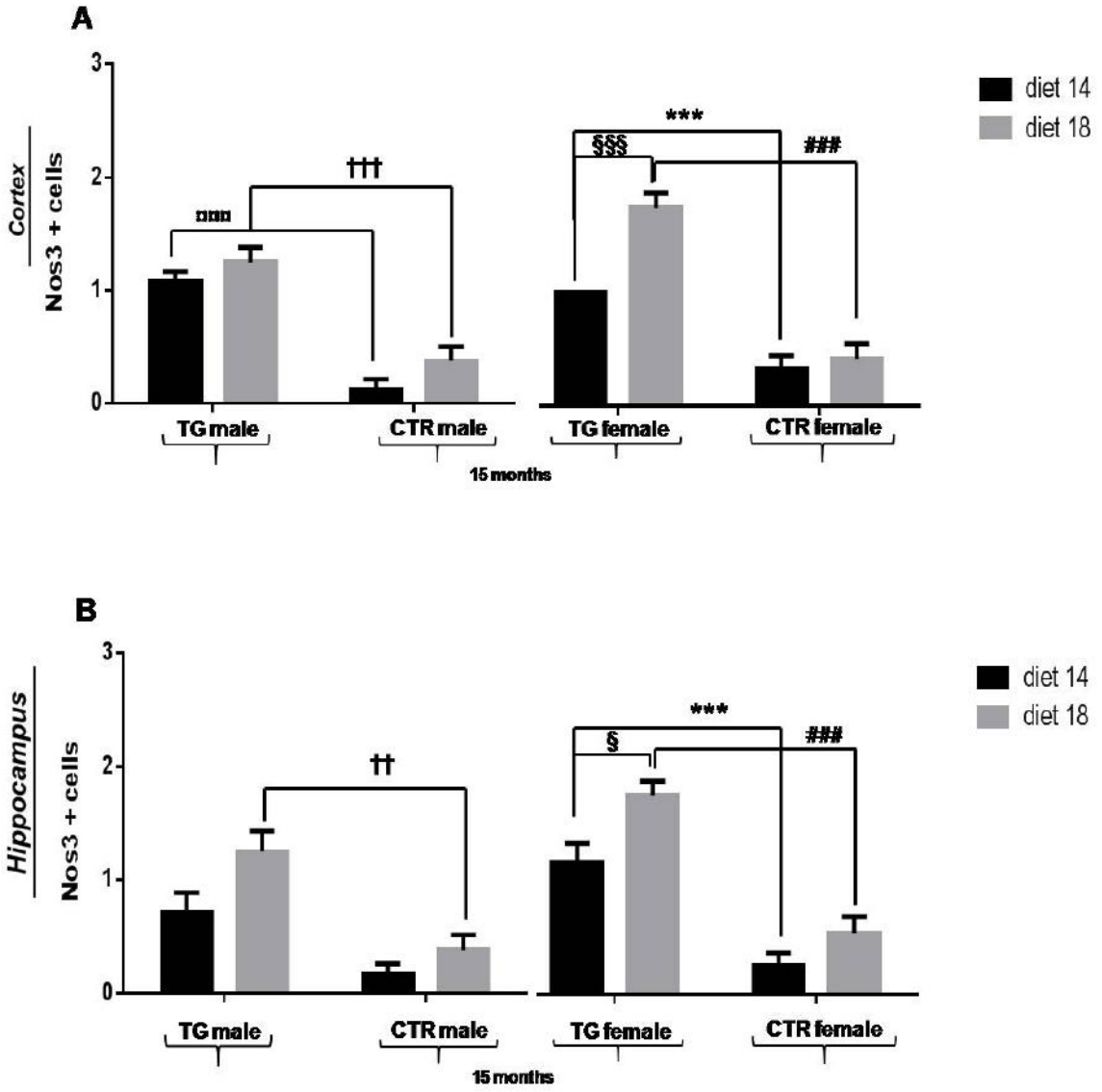

Figure 19. Quantification of NOS3 immunoreactive cell counts in TG and CTR mice fed with different diets at 15 month of age. A-B) Quantification of Nos3 immunoreactive cells in the cortex and in hippocampus showed a significantly increased number of NOS3+ cells in TG mice compared to CTR mice, regardless of diets administrated, at 15 months of age. A significant diet effect in the cortex and hippocampus of female TG mice was detected, as shown by a significantly increase of Nos3+ cells TG mice fed with diet 18 compared to TG mice fed with diet 14. DIET 18: TG male vs CTR male mice †† P< 0.001, ††† P< 0.0001, TG female vs CTR female mice ### P< 0.0001. DIET 14: TG male vs CTR male mice ¤¤¤ P< 0.0001, TG female vs CTR female mice *** P< 0.0001. TG female diet 18 vs TG female diet 14 § P< 0.05; TG female diet 18 vs TG female diet 14 §§§ P< 0.0001. Data were shown as mean ± SEM.

After detected an oxidative damage in the mouse model of tauophaty used in this study, confirming a greater increase of oxidative damage in females than males TG mice (as described in the first article on the characterization of P301L line used in this project), a possible correlation increase of age- oxidative damage was investigated too.

The cortex and hippocampus of male and female TG mice fed with different diets at 7 and 15 months of age were quantified by acrolein, nitrotyrosine, NOS2 and NOS3 immunoreactive cell counts; for each antibody used, a significant interaction oxidative damage-time was found, regardless of diet administrated, as shown by the increase of antibody-immunopositive cells numbers in 15-month-old TG mice (both male and female) compared to 7-month-old TG mice in the cortex and in the hippocampus (P<0.0001; Fig. 20A-B, 21A-B, 22A-B,23 A-B). For each antibody used, also a significant interaction diet-oxidative damage-time was found, as shown by the increase of antibody-immunopositive cells numbers in 15-month-old TG mice (both male and female) fed with diet 18 compared to 7-month-old TG mice fed with diet 14 in the cortex and in the hippocampus (P<0.0001,Fig. 20A-B, 21A-B, 22A-B, 23 A-B).

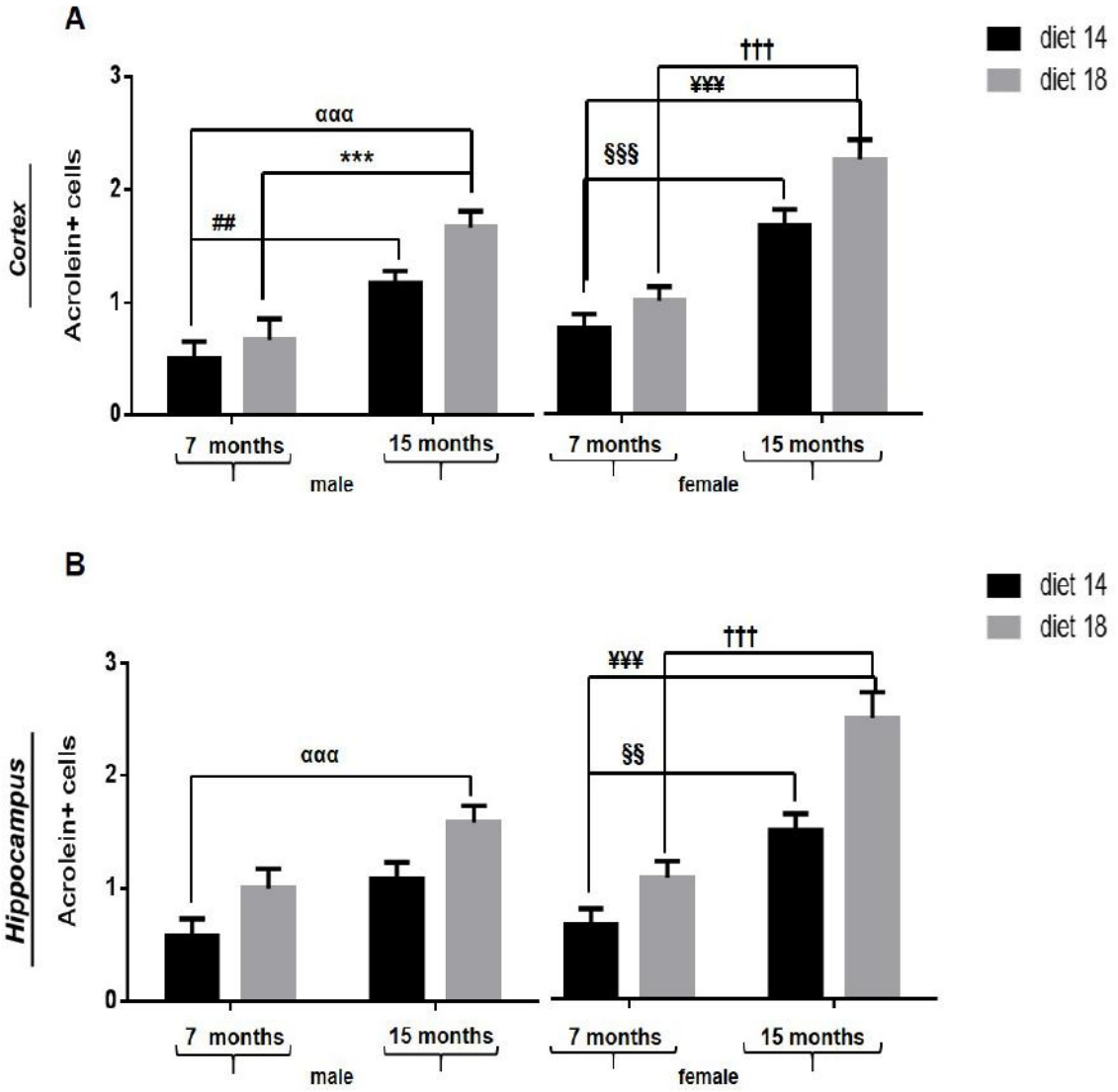

Figure 20. Quantification of acrolein immunoreactive cell counts in TG mice fed with different diets at 7 and 15 month of age. A-B) Quantification of acrolein immunoreactive cells in the cortex

and in hippocampus showed a significantly interaction oxidative damage-time shown by an increase of number of acrolein+ cells in 15-months-old TG mice compared to 7-months-old TG mice, regardless of diets administrated. A significant diet-oxidative damage-time interaction in the cortex and hippocampus of TG mice was detected, as shown by a significantly increase of acrolein+ cells 15-months-old TG mice fed with diet 18 compared to 7-months-old TG mice fed with diet 14. DIET 18: 7-month-old vs 15-month-old TG male mice *** P< 0.0001, 7-month-old vs 15-month-old TG female mice ††† P< 0.0001. DIET 14: 7-month-old vs 15-month-old TG male mice ## P<0.001, 7-month-old vs 15-month-old TG female mice §§§ P< 0.0001.15-month-old TG mice diet 18 vs 7-month-old TG mice diet 14 male ααα P< 0.0001, female ¥¥¥ P< 0.0001. Data were shown as mean ± SEM.

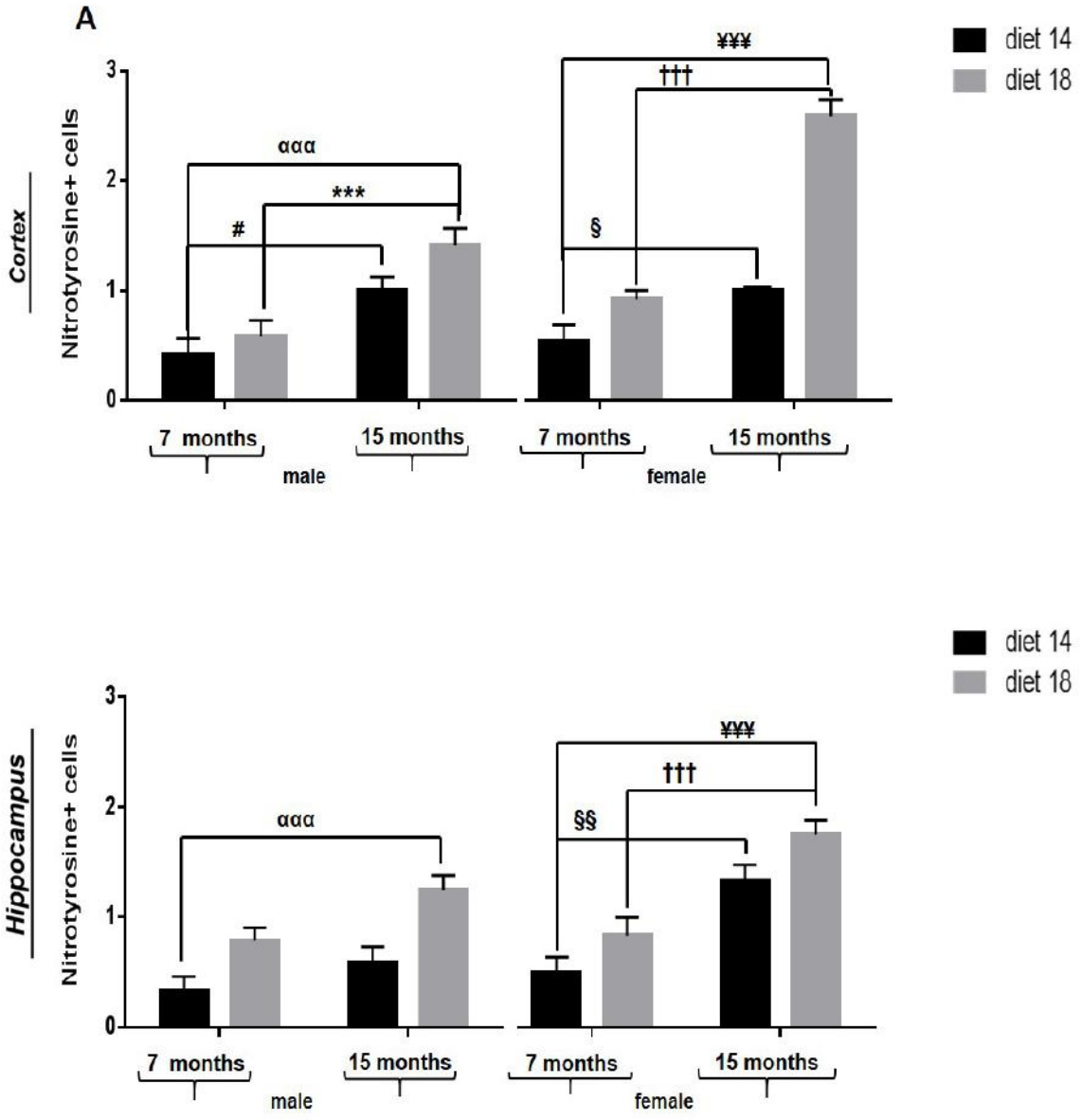

Figure 21. Quantification of nitrotyrosine immunoreactive cell counts in TG mice fed with different diets at 7 and 15 month of age. A-B) Quantification of nitrotyrosine immunoreactive cells in the cortex and in hippocampus showed a significantly interaction oxidative damage-time shown by an increase of number of nitrotyrosine+ cells in 15-months-old TG mice compared to 7-months-old TG mice, regardless of diets administrated. A significant diet-oxidative damage-time interaction in the cortex and hippocampus of TG mice was detected, as shown by a significantly increase of acrolein+

cells 15-months-old TG mice fed with diet 18 compared to 7-months-old TG mice fed with diet 14. DIET 18: 7-month-old vs 15-month-old TG male mice *** P< 0.0001, 7-month-old vs 15-month-old TG female mice ††† P< 0.0001. DIET 14: 7-month-old vs 15-month-old TG male mice # P< 0.05, 7-month-old vs 15-month-old TG female mice §§ P< 0.001. 15-month-old TG mice diet 18 vs 7-month-old TG mice diet 14 male ααα P< 0.0001, female ¥¥¥ P< 0.0001. Data were shown as mean ± SEM.

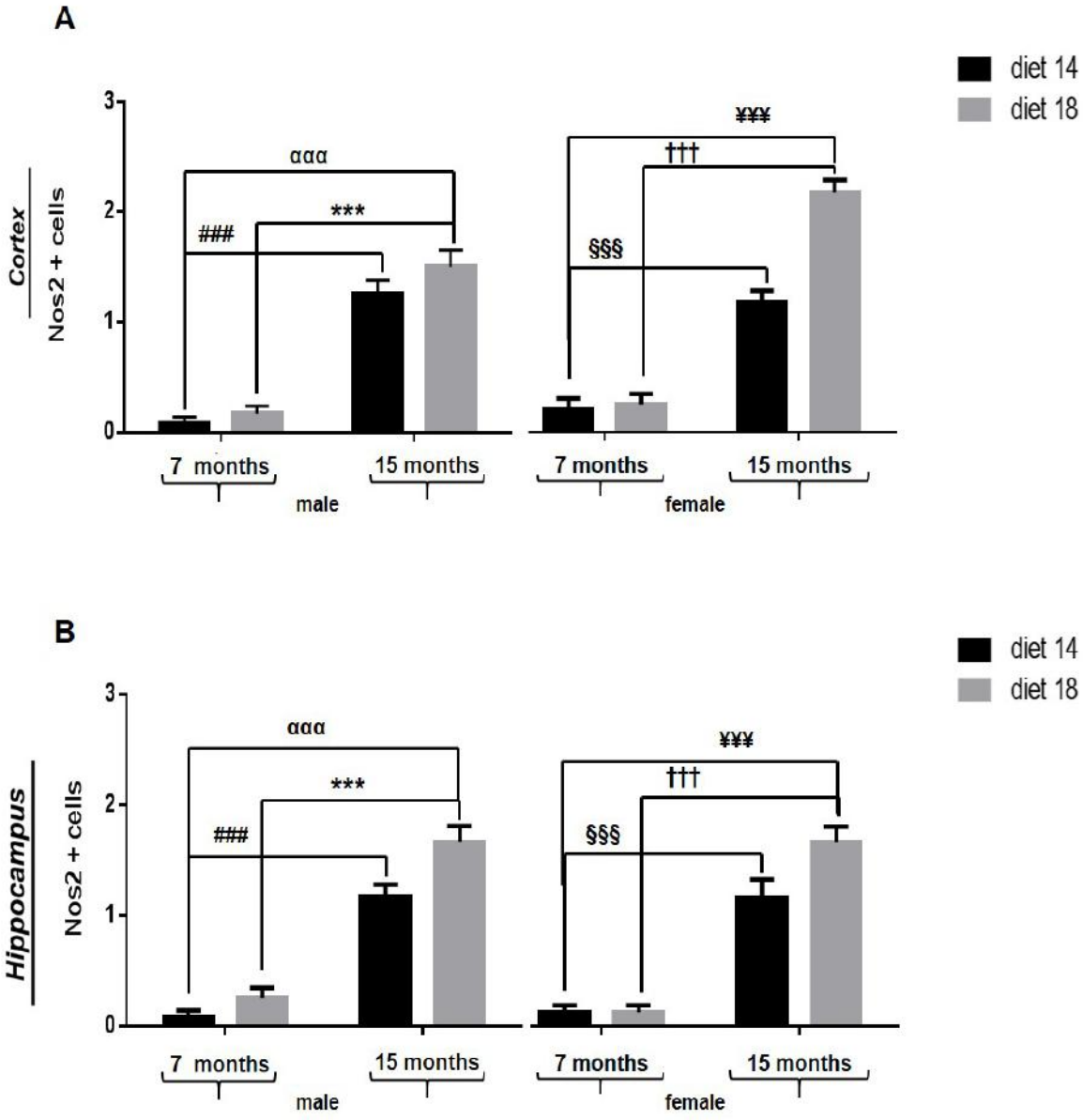

Figure 22. Quantification of NOS2 immunoreactive cell counts in TG mice fed with different diets at 7 and 15 month of age. A-B) Quantification of NOS2 immunoreactive cells in the cortex and in hippocampus showed a significantly interaction oxidative damage-time shown by an increase of number of NOS2+ cells in 15-months-old TG mice compared to 7-months-old TG mice, regardless of diets administrated. A significant diet-oxidative damage-time interaction in the cortex and hippocampus of TG mice was detected, as shown by a significantly increase of acrolein+ cells 15-months-old TG mice fed with diet 18 compared to 7-months-old TG mice fed with diet 14. DIET 18: 7-month-old vs 15-month-old TG male mice *** P< 0.0001, 7-month-old vs 15-month-old TG female mice ††† P< 0.0001. DIET 14: 7-month-old vs 15-month-old TG male mice ### P< 0.0001, 7-month-old vs 15-month-old TG female mice §§§ P< 0.0001. 15-month-old TG mice diet 18 vs 7-

month-old TG mice diet 14 male ααα P< 0.0001, female ¥¥¥ P< 0.0001. Data were shown as mean ± SEM.

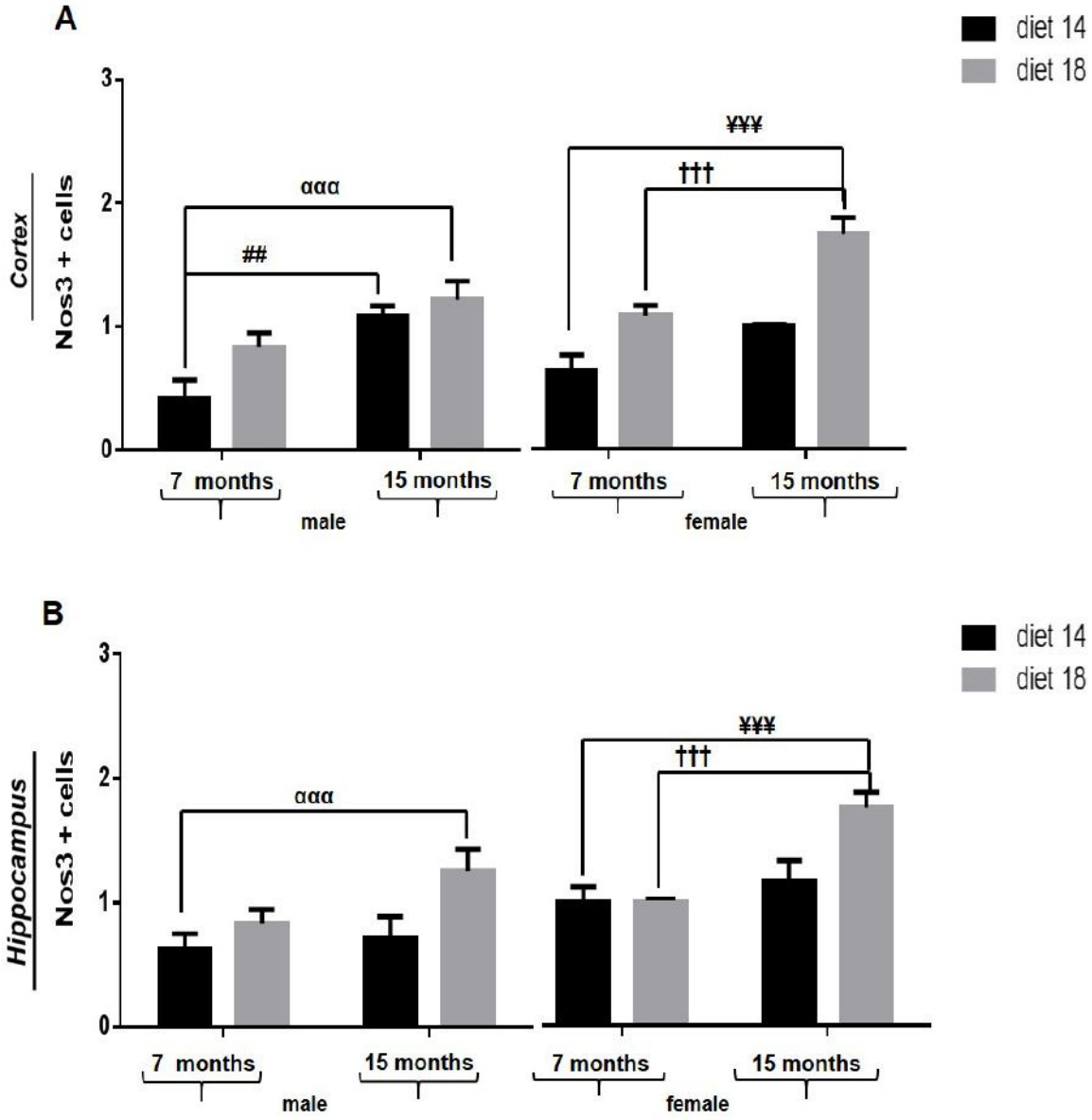

Figure 23. Quantification of NOS3 immunoreactive cell counts in TG mice fed with different diets at 7 and 15 month of age. A-B) Quantification of NOS3 immunoreactive cells in the cortex and in hippocampus showed a significantly interaction oxidative damage-time shown by an increase of number of NOS3+ cells in 15-months-old TG mice compared to 7-months-old TG mice, regardless of diets administrated. A significant diet-oxidative damage-time interaction in the cortex and hippocampus of TG mice was detected, as shown by a significantly increase of acrolein+ cells 15-months-old TG mice fed with diet 18 compared to 7-months-old TG mice fed with diet 14. DIET 18: 7-month-old vs 15-month-old TG female mice ††† P< 0.0001. DIET 14: 7-month-old vs 15-month-old TG male mice ## P< 0.001. 15-month-old TG mice diet 18 vs 7-month-old TG mice diet 14 male ααα P< 0.0001, female ¥¥¥ P< 0.0001. Data were shown as mean ± SEM.

5.5 DISCUSSION

Tauopathies are neurodegenerative disease characterized by agglomerates of hyperphosphorylated Tau and neurofibrillary tangles, typical hallmarks of most neurodegenerative disease, as AD. Although the pathological mechanisms driving Tau to hyperphosphorylation and oligomerization in vivo are poorly understood [19], the oxidative stress is an important player in the pathogenesis of neurodegenerative diseases [20]. Increased oxidative stress has been implicated in the process of aging, thus is a major contributing risk factor in the progression of neurodegeneration. The brain is highly susceptible to oxidative imbalance due to its high-energy demand, high oxygen consumption, rich abundance of easily peroxidable polyunsaturated fatty acids, high level of potent ROS catalyst iron, and relative paucity of antioxidants and related enzymes [21]. Hippocampus, basal forebrain and cortex are the brain areas that are involved in learning and memory formation and are the most vulnerable areas susceptible to oxidative stress [22-23]. Thus, in an obvious way oxidative imbalance subsequently leads to oxidative stress mediated damage to the biomolecules that is widely reported in pathogenesis of various neurodegenerative disorders, as tauopathies.

In our previous works, we characterized P301L model that replicates the impairments found in patients affected by tauophaty in a way age-gender-dependent, we investigated the effects of two different diets (high fat-protein diet and low fat-protein diet) on cognitive and behavioral impairments in this mouse model of tauophaty, founding an improvement of pathological conditions administrating a low fat-protein diet, occurred with an increased lifespan, a reduction of food and water consumption, a reduction of aggregates of hyperphosphorylated Tau and neuronal loss.

In this study, young and old male and female transgenic P301L-Tau mice fed with different diets (low fat-protein diet and high fat-protein diet) were studied in comparison with CTR mice to investigate the oxidative damage in this model of Tauophaty and to explore the possible mechanisms through which diets can interact and improve a possible condition of oxidative damage. All oxidative stress markers used in this project for brain immunohistochemical studies (acrolein, nitrotyrosine, NOS2 and NOS3) revealed a significant interaction genotype-oxidative damage in TG mice, regardless of diets administrated, more pronounced at 15 months of age compared to 7 months of age. This effect was also confirmed with the quantification of immunoreactive cell counts for each oxidative stress markers that revealed a significant increase of number of immunoreactive cell counts in TG mice compared to CTR mice. In particular, immunostaining of acrolein, a byproduct of lipid peroxidation, reveled a higher

increase of immunopositive cells in TG mice compared to CTR mice at 7 months of age that was found to be doubled at 15 months of age.

Several studies had shown as oxidative damage has an important role in the development of many tauopathies [24-25-26], but very little is known about oxidative stress in FTLD (disease which has affected the animal model used in this study). A study carried out on human patients affected by FTLD had revealed, using anti-HNE (4-Hydroxynonenal) antibodies and MS (Mowse scores), an increased lipoxidative damage in the frontal cortex, identifying astrocytes as targets of lipoxidative damage, GFAP as a target of lipoxidation, and that astrocytes were crucial elements of oxidative stress responses in FTLD [27]. After detected an oxidative damage in the mouse model of Tauophaty used in this study, we investigated a possible interaction between diets and oxidative damage, valuating if diets can improve this pathological condition.

At 7 months of age, immunostaining applied to cortex and hippocampus of CTR and TG mice with acrolein and NOS2 antibodies revealed any significant interaction diet- oxidative damage. In the same brain areas, immunostaining with nitrotyrosine antibody revealed in the hippocampus of TG male mice a significant diet effect, highlighted by a decrease of nitrotyrosine+ cells in TG mice fed with low fat-protein diet (diet 14) compared to TG mice fed with high fat-protein diet (diet 18). Immunostaining with NOS3 antibody revealed in the cortex of TG mice (both males and females) a significant diet effect, highlighted by a decrease of NOS3+ cells in TG mice fed with low fat-protein diet (diet 14) compared to TG mice fed with high fat-protein diet (diet 18).

At 15 months of age, for each oxidative marker used for immunohistochemistry in this study, a significant diet effect in the cortex and hippocampus of TG mice was detected, highlighted by a decrease of immunopositive cells in TG mice fed with low fat-protein diet (diet 14) compared to TG mice fed with high fat-protein diet (diet 18). This diet effect was more pronounced in female TG mice compared to male TG mice, confirming a genotype-gender effect showed in previous works.

After detected an oxidative damage in the mouse model of Tauophaty used in this study, found an improvement of oxidative status in TG mice fed with low fat-protein diet, a possible correlation increase of age- oxidative damage was investigated too. The cortex and hippocampus of male and female TG mice fed with different diets at 7 and 15 months of age were quantified by acrolein, nitrotyrosine, NOS2 and NOS3 immunoreactive cell counts; for each antibody used, a significant interaction oxidative damage-time was found, regardless of diet administrated, as shown by the increase of antibody-immunopositive cells

numbers in 15-month-old TG mice (both male and female) compared to 7-month-old TG mice in the cortex and in the hippocampus.

For each oxidative marker used, also a significant interaction diet-oxidative damage-time was found, as shown by the increase of antibody-immunopositive cells numbers in 15-month-old TG mice (both male and female) fed with diet 18 compared to 7-month-old TG mice fed with diet 14 in the cortex and in the hippocampus.

Several studies showed as high fat diets induce oxidative stress that may be involved in neurodegenerative diseases, in particular the hippocampus is the primary region of the brain for spatial learning and memory, as well as for neurogenesis that continues into adulthood, and it is susceptible to the effects of high-fat diets [28]. Previous research has clarified that a high-fat diet can impair hippocampal synaptic plasticity as well as hippocampus-dependent learning and memory [29]. The central role of lipids in maintaining neuronal integrity has clear implications for dietary management for neurodegenerative diseases prevention and management. A high ratio of saturated/unsaturated fatty acids in the diet leads to an increase in LDL and a decrease in high-density lipoprotein cholesterol; this change may significantly alter the oxidative status in the brain, and consequently oxidative stress causes increased Tau phosphorylation, facilitates the conformational conversion and assembly of Tau fibrils, and impairs the proteasomal and lysosomal activity that may lead to progressive accumulation of protein deposits [30-31].

In summary, we found an oxidative damage associated with our mouse model of Tauophaty in a way age-gender-dependent, confirming that female TG mice were more affected by Tauophaty then male TG mice. Administering different diets to TG and CTR mice, we found an improvement of oxidative damage associated with our mouse model of tauophaty administrating a low fat-protein diet, occurred with a decreased of immunopositive cells numbers correlated to oxidative markers used for immunohistochemistry (acrolein, nitrotyrosine, NOS2 and NOS3), more pronounced in female than male TG mice. Oxidative stress plays a central role in the development of neurodegenerative disease, contributing to loss of neuronal integrity in tauopathies as AD.

A correct dietary intake, consisting of nutrients with antioxidant properties, low fat and protein, may have protective effects in the onset and development of tauopathies by reducing oxidative stress, particularly when used in combination.

Moreover, preventing or reducing the oxidative damage with a low fat-protein diet in this model, may represent a system to study the correlation between nutrition and pathological mechanisms underlying tauopathies and could finally lead to the development of preventive treatments for tauopathies, like AD.

5.6 ACKNOWLEDGMENTS

We thank D. Corna for technical help.

5.7 REFERENCES

1. Clark TA, Lee HP, Rolston RK, Zhu X, Marlatt MW, Castellani RJ, Nunomura A, Casadesus G, Smith MA, Lee HG, Perry G (2010) Oxidative stress and its implications for future treatments and management of Alzheimer disease. Int J Biomed Sci 6, 225-227.
2. Noble W, Hanger DP, Miller CC, Lovestone S. The importance of Tau phosphorylation for neurodegenerative diseases. Front Neurol. 2013 Jul 1; 4:83.
3. Rodríguez-Martín T, Cuchillo-Ibáñez I, Noble W, Nyenya F, Anderton BH, Hanger DP.Tau phosphorylation affects its axonal transport and degradation. Neurobiol Aging. 2013 Sep; 34(9):2146-57.
4. Yoshiyama Y, Higuchi M, Zhang B, et al. Synapse loss and microglial activation precede tangles in a P301S Tauopathy mouse model. Neuron 2007; 53:337–51.
5. Bellucci A,Westwood AJ, Ingram E, Casamenti F, Goedert M, Spillantini MG. Induction of inflammatory mediators and microglial activation in mice transgenic for mutant human P301S Tau protein. Am J Pathol 2004; 165:1643–52.
6. Ozcelik S, Fraser G, Castets P, et al. Rapamycin attenuates the progression of Tau pathology in P301S Tau transgenic mice. PLoS One 2013; 8:e62459.
7. Sayre LM, Zelasko DA, Harris PLR, Perry G,Salomon RG, Smith MA, 4-Hydroxynonenalderivedadvanced lipid peroxidation end productsare increased in Alzheimer's disease, J Neurochem 68 (1997) 2092–2097.
8. Smith MA, Taneda S, Richey PL, Miyata S, YanS-D, Stern D, Sayre LM, Monnier VM, Perry G, Advanced Maillard reaction products areassociated with Alzheimer disease pathology,Proc Natl Acad Sci USA 91 (1994) 5710–5714.
9. Smith MA, Harris PLR, Sayre LM, Perry G, Iron accumulation in Alzheimer disease is a source ofredox-generated free radicals, Proc Natl Acad SciUSA 94 (1997) 9866–9868.
10. Markesbery WR, Carney JM. Oxidative alterations in Alzheimer's disease. Brain Pathol 1999; 9:133–46.
11. Reddy VP, Zhu X, Perry G, Smith MA. Oxidative stress in diabetes and Alzheimer's disease. J Alzheimers Dis 2009; 16:763–74.

12. Reddy PH, Beal MF (2008) Amyloid beta, mitochondrial dysfunction and synaptic damage: Implications for cognitive decline in aging and Alzheimer's disease. Trends Mol Med14, 45-53.
13. Ansari MA, Scheff SW (2010) Oxidative stress in theprogression of Alzheimer disease in the frontal cortex. J Neuropathol Exp Neurol 69, 155-167.
14. Calon F, Lim GP, Yang F, Morihara T, Teter B, Ubeda O, Rostaing P, Triller A, Salem N Jr, Ashe KH, Frautschy SA,Cole GM (2004) Docosahexaenoic acid protects from dendritic pathology in an Alzheimer's disease mouse model.Neuron 43, 633-645.
15. Morris MC, Tangney CC (2014) Dietary fat composition and dementia risk. Neurobiol Aging 35 (Suppl 2), S59-S64.
16. Sontag E, Nunbhakdi-Craig V, Lee G, Bloom GS, Mumby MC. Regulation of the phosphorylation state and microtubule-binding activity of Tau by protein phosphatase 2A. Neuron. 1996; 17:1201–7.
17. Lewis, J, McGowan, E, Rockwood, J, Melrose, H, Nacaraju, P, Van Slegtenhorst M. et al. (2000) Neurofibrillary tangles, amyotrophy and progressive motor disturbance in mice expressing mutant (P301L) Tau protein. Nature Genetics 25:402-406.
18. Lewis, J, Dickson D.W, Lin, W-L, Chisholm L, Corral A, Jones, G. et al. (2001) Enhanced neurofibrillary degeneration in transgenic mice expressing mutant Tau and APP. Science. 93:1487-1491.
19. Zaheer S, Thangavel R, Wu Y, Khan MM, Kempuraj D, Zaheer A. Enhanced expression of glia maturation factor correlates with glial activation in the brain of triple transgenic Alzheimer's disease mice. Neurochem Res. 2013 Jan; 38(1):218-25.
20. Sutherland GT, Chami B, Youssef P, Witting PK Oxidative stress in Alzheimer's disease: Primary villain or physiological by-product? Redox Rep. 2013; 18(4):134-41.
21. Wataya T, Nunomura A, Smith MA, Siedlak SL, Harris PL, Shimohama S, Szweda LI, Kaminski MA, Avila J, Price DL, Cleveland DW, Sayre LM, Perry G.High molecular weight neurofilament proteins are physiological substrates of adduction by the lipid peroxidation product hydroxynonenal. J Biol Chem. 2002 Feb 15; 277(7):4644-8.
22. Mattson MP, Guo ZH, Geiger JD.Secreted form of amyloid precursor protein enhances basal glucose and glutamate transport and protects against oxidative impairment of glucose and glutamate transport in synaptosomes by a cyclic GMP-mediated mechanism.J Neurochem. 1999 Aug; 73(2):532-7.
23. Mattson MP, Pedersen WA, Duan W, Culmsee C, Camandola S.Cellular and molecular mechanisms underlying perturbed energy metabolism and

neuronal degeneration in Alzheimer's and Parkinson's diseases. Ann N Y Acad Sci. 1999; 893:154-75. Review.
24. Albers DS, Augood SJ, Park LC, et al. Frontal lobe dysfunction in progressive supranuclear palsy: Evidence for oxidative stress and mitochondrial impairment. J Neurochem 2000; 74:878-81.
25. Odetti P, Garibaldi S, Norese R, et al. Lipoperoxidation is selectively involved in progressive supranuclear palsy. J Neuropathol Exp Neurol 2000; 59:393-97.
26. Martinez A, Dalfó E, Muntane G, et al. Glycolitic enzymes are targets of oxidation in aged human frontal cortex and oxidative damage of these proteins is increased in progressive supranuclear palsy. J Neural Transm 2008; 115:59-66.
27. Martínez A, Carmona M, Portero-Otin M, Naudí A, Pamplona R, Ferrer I Type-dependent oxidative damage in frontotemporal lobar degeneration: cortical astrocytes are targets of oxidative damage.J Neuropathol Exp Neurol. 2008 Dec; 67(12):1122-36.
28. Y. Tozuka, E. Wada, K. Wada Diet-induced obesity in female mice leads to peroxidized lipid accumulations and impairment of hippocampal neurogenesis during the early life of their offspring. FASEB J, 23 (6) (2009), pp. 1920–1934.
29. S.A. Farr, K.A. Yamada, D.A. Butterfield, H.M. Abdul, L. Xu, N.E. Miller, et al. Obesity and hypertriglyceridemia produce cognitive impairment Endocrinology, 149 (5) (2008), pp. 2628–2636.
30. Zhu X, Lee HG, Casadesus G, Avila J, Drew K, Perry G, Smith MA (2005) Oxidative imbalance in Alzheimer's disease. Mol Neurobiol 31, 205-217.
31. Sutherland GT, Chami B, Youssef P, Witting PK (2013) Oxidative stress in Alzheimer's disease: Primary villain orphysiological by-product? Redox Rep 18, 134-141.

CHAPTER 6

A high fat-protein diet induces nonalcoholic fatty liver disease (NAFLD) in young and aged P301L TG mice model of tauophaty

This paper is at present (December 2015) being composed for a submission to an international journal

Chapter 6: A high fat-protein diet induces nonalcoholic fatty liver disease (NAFLD) in young and aged P301L TG mice model of tauophaty

AUTHORS: L. Buccarello[1], G. Grignaschi[2], A. Di Giancamillo[1], C. Domeneghini[1]

1 Department of Health, Animal Science and Food Safety, Università degli Studi di Milano, Milan, Italy

2 Department of Animal welfare, IRCCS-Mario Negri Institute for Pharmacological Research, Milan, Italy

6.1 ABSTRACT

Growing evidence supports the concept that insulin resistance and metabolic dysfunction are mediators of tauopathies as AD, and tauopathies could be regarded as a metabolic disease mediated by brain insulin and IGF resistance. In particular, a crosslink between insulin resistance-dysregulates lipid metabolism and oxidative stress seems to be the cause of hepatic dysfunctions as fibrosis or steatosis including nonalcoholic fatty liver disease (NAFLD). In this study we investigated in males and females P301L TG mice and B6D2F1 control mice at 7 and 15 months of age fed with different diets a possible condition of nonalcoholic fatty liver disease (NAFLD) valuating macroscopy, histology and immunohistochemical profiles (H&E and Sirius Red) of liver and spleen removed from each experimental group. We also evaluated the concentration of molecules and enzymes related to hepatic activity as cholesterol, triglycerides, alanine aminotransferase and aspartate aminotransferase in plasma of TG and CTR mice at 7 and 15 months of age. Macroscopy analysis revealed a significant difference in the aspect, size and weight in liver and spleen removed from TG mice compared to CTR mice, regardless of diet administrated, in a way age-dependent. At 15 months of age, these alterations were also correlated to a significant diet effect showed by significative increase of size and weight of tissues removed from TG mice fed with high fat-protein diet compared to TG mice fed with low fat-protein diet. Immunohistochemical analysis (H&E immunostaining and Sirius red) of liver and spleen removed from TG and CTR mice replicated the previous results revealing an age-dependent lobular inflammatory infiltrate with increased vascularity and a state of fibrosis in P301L TG mice, more pronounced in TG mice fed with high fat-protein diet. These results were confirmed by biochemical analysis on plasma that showed, except for the measurement of total cholesterol (which values were included into reference intervals of values for biochemical analytes), a high increase of the median levels of triglycerides, AST and ALT in TG mice, more pronounced in TG mice fed with high fat-protein diet. In summary, in this study we demonstrated a correlation between hyperphosphorylated Tau, insulin/IGF

resistance and high fat-protein diet consumption in P301L TG mice expressed on peripheral organs as hepatic insulin resistance and fatty accumulation in the liver, which induced nonalcoholic fatty liver disease.

Keywords:

AD: Alzheimer disease, ALT: alanine aminotransferase, AST: aspartate aminotransferase CTR: control, FFA: free fatty acid, NAFLD: nonalcoholic fatty liver disease, NFTs: neurofilaments, IGF: insulin growth factor, ROS: reactive oxygen, RNS: reactive nitrogen, TG: transgenic.

6.2 BACKGROUND

During necropsy analysis performed after the behavioral tests in P301L TG and B6D2F1 CTR mice fed with different diets (diet 18: high fat-protein diet and diet 14: low fat-protein diet), we observed an alteration of the size of the liver and spleen in TG mice fed with a high fat-protein diet at 7 and 15 months of age. This apparent condition of hepatomegaly was associated to an increase of body weight, food and water consumption in TG mice fed with high fat-protein diet. Based on data obtained in our previous works, the mouse model of tauophaty used in this study showed:

1) a gender-genotype interaction, with a strong cognitive impairment in female than male mice, strongly correlated with an increase in P-Tau, in both cerebral cortex and hippocampus, as well as astrogliosis;
2) an improvement of pathological conditions administrating a low fat-protein diet, occurred with an increased lifespan, a reduction of food and water consumption, a reduction of aggregates of hyperphosphorylated tau and neuronal loss in both cerebral cortex and hippocampus, more pronounced in female than male TG mice;
3) a strong oxidative damage associated to tauophaty in a way age-gender-dependent, with a strong oxidative damage in female than male mice; an improvement of oxidative damage administrating a low fat-protein diet was also detected, with a decreased of oxidative markers in both cerebral cortex and hippocampus, more pronounced in female than male TG mice.

6.3 INTRODUCTION

Growing evidence supports the concept that insulin resistance and metabolic dysfunction are mediators of tauopathies as AD [1-2], and tauopathies could be regarded as a metabolic disease mediated by brain insulin and IGF resistance [3-4]. In fact, AD shares many features in common with systemic insulin resistance diseases including, reduced insulin-stimulated growth and survival signaling, increased oxidative stress, pro-inflammatory cytokine activation, mitochondrial dysfunction, and impaired energy metabolism [5-6-7]. Human postmortem studies showed that brain insulin resistance with reduced insulin receptor expression and insulin receptor binding were consistently present in AD brains and worsen with disease progression [3-4], and that insulin signaling impairments were associated with deficits in IGF-1 and IGF-2 networks [4].

Tau gene expression [8] and phosphorylation [9] are regulated by insulin and IGF, and impairments in insulin/IGF signaling contribute to tau hyper-phosphorylation due to over activation of specific kinases, e.g. GSK-3b [9-10] and reductions in tau gene expression [7-8-11]. Attendant failure to generate sufficient normal tau protein, vis-a-vis accumulation of hyperphosphorylated insoluble fibrillary tau likely promotes cytoskeletal collapse, neurite retraction, and synaptic disconnection. Moreover, decreased signaling through phosphoinositol-3-kinase (PI3K), Akt [9], and increased activation of GSK-3β correlate with brain insulin and IGF resistance. Therefore, impairments in signaling through these pathways could account for the reductions in neuronal survival, myelin maintenance, synaptic integrity, neuronal plasticity, mitochondrial function, and cellular stress management in AD.

Insulin stimulates lipogenesis, which results in increased triglyceride storage in the liver [12-13]. Independent studies have shown that cognitive impairment and neuropsychiatric dysfunction occur with steatohepatitis and hepatic insulin resistance of various etiologies [14-15-16]. Mechanistically, inflammation in the setting of hepatic steatosis increases ER stress, oxidative damage, mitochondrial dysfunction, and lipid peroxidation, which together drive hepatic insulin resistance. Insulin resistance dysregulates lipid metabolism and promotes lipolysis [17-18], which increases production of toxic lipids, including ceramides, which further impair insulin signaling, mitochondrial function, and cell viability [18-19]. Liver disease worsens because ER stress and mitochondrial dysfunction exacerbate insulin resistance, lipolysis, and ceramide accumulation [81–83], generating nonalcoholic fatty liver disease (NAFLD). Nonalcoholic fatty liver disease (NAFLD) is characterized by insulin resistance, which results in elevated serum concentration of free fatty acids (FFAs). Circulating FFAs provide the substrate for triacylglycerol formation in the liver, and may be directly cytotoxic.

Hepatocyte apoptosis is a key histologic feature of NAFLD, and correlates with progressive inflammation and fibrosis. The hallmark in the pathogenesis of the NAFDL is the accumulation of triglycerides (TGs) in hepatocytes, which is followed by increased susceptibility to hepatocyte injury. The pathogenesis is thought to involve the "two‐hits" hypothesis [20]; the "first hit" is characterized by accumulation of TGs derived from the esterification of free fatty acid (FFA) and glycerol. The latter arises from an imbalance of supply, formation, consumption and hepatic oxidation and disposal of TG [21]. The sources of FFAs are diet, adipose tissue lipolysis, and de novo lipogenesis. Donnely et al. [22] demonstrated that in NAFLD, the major sources of FFA are adipose tissue lipolysis (59%) and de novo lipogenesis (26%) and less so from diet (15%). The increased influx of FFA from adipose tissue in NAFLD is attributed to impaired suppression of lipolysis in adipose tissue by insulin due to insulin resistance [21-22]. Following accumulation of TG in hepatocytes, there is increased susceptibility to inflammatory injury, and this constitutes the "second hit" in the pathogenetic pathway. The injury is mediated by increased expression of inflammatory cytokines and adipokines, oxidative stress and mitochondrial dysfunction, endoplasmic reticulum stress and gut‐derived endotoxemia from bacterial overgrowth among others [8-9]. Fibrosis is the final stage or the "third hit" resulting from an imbalance between the rate of hepatocyte death and hepatocyte regeneration. There is inhibition of hepatocyte proliferation due to oxidative stress.

Metabolic syndrome is a cluster of disease processes centered on insulin resistance, visceral obesity, hypertension, and dyslipidemia [23]. Metabolic syndrome is frequently associated with NAFLD/NASH, pro-inflammatory and pro-thrombotic states [23]. Studies have linked peripheral insulin resistance [24], visceral obesity [25], and metabolic syndrome [26-27-28] to brain atrophy, cognitive impairment, and impaired executive function [29]. The aggregate findings in humans and experimental models suggest that peripheral/systemic insulin resistance disease states serve as cofactors in the pathogenesis and progression of neurodegeneration.

Based on the data in the literature, we decided to investigate a possible condition of nonalcoholic fatty liver disease (NAFLD) in mouse model of tauophaty used in this study evaluating: macroscopy and histology of various tissues such as liver and spleen, the concentration of molecules and enzymes related to hepatic activity as cholesterol, triglycerides, alanine aminotransferase and aspartate aminotransferase in plasma of males and females P301L TG mice and B6D2F1 CTR mice at 7 and 15 months of age fed with different diets.

6.3 MATERIALS AND METHODS

6.3.1 Animals and Diets

Four hundred mice were used in this study. Two hundred were hemizygous tau transgenic mice of mixed gender with a mutant form (P301L) of human tau protein including four-repeats without amino terminal inserts, and driven by the mouse prion promoter 6 (MoPrP) [30]. Two hundred age-compatible wild type mice (B6D2F1) of mixed gender served as controls. Mice originated from Taconic Laboratories, USA, were bred at IRCCS Mario Negri Institute of Pharmacological Research in a Specific Pathogen free (SPF) facility with a regular 12:12 h light/dark cycle (lights on 07:00 a.m.), at a constant room temperature of 22 ± 2 °C, and relative humidity approximately 55 ± 10%. Animals were housed (n= 4 per group) in standard mouse cages, until three months of ages all animals were fed with standard rodent chow (diet 1: 18% protein and 5% fat, Harlan Lab. Tekland global diet), then animals were divided into two experimental groups, balanced for body weight and sex.

The first group was fed with a standard rodent chow (diet 1: 18% protein and 5% fat, Harlan Lab. Tekland global diet), and the second group was fed with a low protein diet (diet 2: 14% protein and 3.5% fat Harlan Lab. Tekland global diet). Since the animals were bred in a SPF facility, where all materials introduced are sterilized, we had to use an autoclavable diet manufactured with high quality ingredients and supplemented with additional vitamins to ensure nutritional adequacy after autoclaving (Fig. 1-2).

Standard Product Form: **Pellet**

Macronutrients		
Crude Protein	%	18.6
Fat (ether extract) [a]	%	6.2
Carbohydrate (available) [b]	%	44.2
Crude Fiber	%	3.5
Neutral Detergent Fiber [c]	%	14.7
Ash	%	5.3
Energy Density [d]	kcal/g (kJ/g)	3.1 (13.0)
Calories from Protein	%	24
Calories from Fat	%	18
Calories from Carbohydrate	%	58
Minerals		
Calcium	%	1.0
Phosphorus	%	0.7
Non-Phytate Phosphorus	%	0.4
Sodium	%	0.2
Potassium	%	0.6
Chloride	%	0.4
Magnesium	%	0.2
Zinc	mg/kg	70
Manganese	mg/kg	100
Copper	mg/kg	15
Iodine	mg/kg	6
Iron	mg/kg	200
Selenium	mg/kg	0.23
Amino Acids		
Aspartic Acid	%	1.4
Glutamic Acid	%	3.4
Alanine	%	1.1
Glycine	%	0.8
Threonine	%	0.7
Proline	%	1.6
Serine	%	1.1
Leucine	%	1.8
Isoleucine	%	0.8
Valine	%	0.9
Phenylalanine	%	1.0
Tyrosine	%	0.6
Methionine	%	0.6
Cystine	%	0.3
Lysine	%	1.1
Histidine	%	0.4
Arginine	%	1.0
Tryptophan	%	0.2

Vitamins		
Vitamin A [e, f]	IU/g	30.0
Vitamin D_3 [e, g]	IU/g	2.0
Vitamin E	IU/kg	135
Vitamin K_3 (menadione)	mg/kg	100
Vitamin B_1 (thiamin)	mg/kg	117
Vitamin B_2 (riboflavin)	mg/kg	27
Niacin (nicotinic acid)	mg/kg	115
Vitamin B_6 (pyridoxine)	mg/kg	26
Pantothenic Acid	mg/kg	140
Vitamin B_{12} (cyanocobalamin)	mg/kg	0.15
Biotin	mg/kg	0.90
Folate	mg/kg	9
Choline	mg/kg	1200
Fatty Acids		
C16:0 Palmitic	%	0.7
C18:0 Stearic	%	0.2
C18:1ω9 Oleic	%	1.2
C18:2ω6 Linoleic	%	3.1
C18:3ω3 Linolenic	%	0.3
Total Saturated	%	0.9
Total Monounsaturated	%	1.3
Total Polyunsaturated	%	3.4
Other		
Cholesterol	mg/kg	--

[a] Ether extract is used to measure fat in pelleted diets, while an acid hydrolysis method is required to recover fat in extruded diets. Compared to ether extract, the fat value for acid hydrolysis will be approximately 1% point higher.

[b] Carbohydrate (available) is calculated by subtracting neutral detergent fiber from total carbohydrates.

[c] Neutral detergent fiber is an estimate of insoluble fiber, including cellulose, hemicellulose, and lignin. Crude fiber methodology underestimates total fiber.

[d] Energy density is a calculated estimate of *metabolizable energy* based on the Atwater factors assigning 4 kcal/g to protein, 9 kcal/g to fat, and 4 kcal/g to available carbohydrate.

[e] Indicates added amount but does not account for contribution from other ingredients.

[f] 1 IU vitamin A = 0.3 µg retinol

[g] 1 IU vitamin D = 25 ng cholecalciferol

For nutrients not listed, insufficient data is available to quantify.

Figure 1: Composition of diet 1: 18% protein and 5% fat (Harlan Tekland global diet)

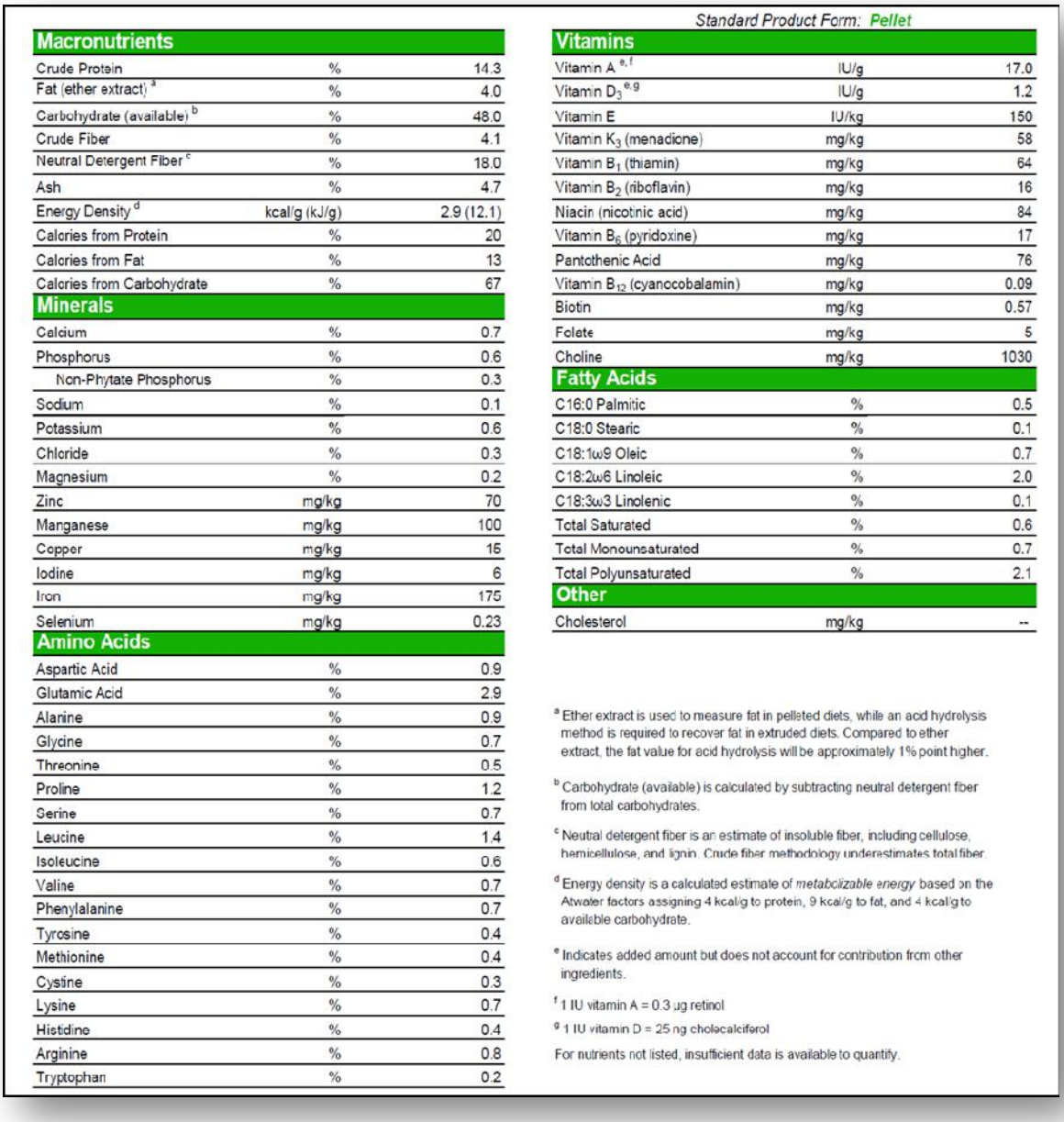

Standard Product Form: Pellet

Macronutrients		
Crude Protein	%	14.3
Fat (ether extract) [a]	%	4.0
Carbohydrate (available) [b]	%	48.0
Crude Fiber	%	4.1
Neutral Detergent Fiber [c]	%	18.0
Ash	%	4.7
Energy Density [d]	kcal/g (kJ/g)	2.9 (12.1)
Calories from Protein	%	20
Calories from Fat	%	13
Calories from Carbohydrate	%	67
Minerals		
Calcium	%	0.7
Phosphorus	%	0.6
Non-Phytate Phosphorus	%	0.3
Sodium	%	0.1
Potassium	%	0.6
Chloride	%	0.3
Magnesium	%	0.2
Zinc	mg/kg	70
Manganese	mg/kg	100
Copper	mg/kg	15
Iodine	mg/kg	6
Iron	mg/kg	175
Selenium	mg/kg	0.23
Amino Acids		
Aspartic Acid	%	0.9
Glutamic Acid	%	2.9
Alanine	%	0.9
Glycine	%	0.7
Threonine	%	0.5
Proline	%	1.2
Serine	%	0.7
Leucine	%	1.4
Isoleucine	%	0.6
Valine	%	0.7
Phenylalanine	%	0.7
Tyrosine	%	0.4
Methionine	%	0.4
Cystine	%	0.3
Lysine	%	0.7
Histidine	%	0.4
Arginine	%	0.8
Tryptophan	%	0.2

Vitamins		
Vitamin A [e,f]	IU/g	17.0
Vitamin D_3 [e,g]	IU/g	1.2
Vitamin E	IU/kg	150
Vitamin K_3 (menadione)	mg/kg	58
Vitamin B_1 (thiamin)	mg/kg	64
Vitamin B_2 (riboflavin)	mg/kg	16
Niacin (nicotinic acid)	mg/kg	84
Vitamin B_6 (pyridoxine)	mg/kg	17
Pantothenic Acid	mg/kg	76
Vitamin B_{12} (cyanocobalamin)	mg/kg	0.09
Biotin	mg/kg	0.57
Folate	mg/kg	5
Choline	mg/kg	1030
Fatty Acids		
C16:0 Palmitic	%	0.5
C18:0 Stearic	%	0.1
C18:1ω9 Oleic	%	0.7
C18:2ω6 Linoleic	%	2.0
C18:3ω3 Linolenic	%	0.1
Total Saturated	%	0.6
Total Monounsaturated	%	0.7
Total Polyunsaturated	%	2.1
Other		
Cholesterol	mg/kg	--

[a] Ether extract is used to measure fat in pelleted diets, while an acid hydrolysis method is required to recover fat in extruded diets. Compared to ether extract, the fat value for acid hydrolysis will be approximately 1% point higher.

[b] Carbohydrate (available) is calculated by subtracting neutral detergent fiber from total carbohydrates.

[c] Neutral detergent fiber is an estimate of insoluble fiber, including cellulose, hemicellulose, and lignin. Crude fiber methodology underestimates total fiber.

[d] Energy density is a calculated estimate of *metabolizable energy* based on the Atwater factors assigning 4 kcal/g to protein, 9 kcal/g to fat, and 4 kcal/g to available carbohydrate.

[e] Indicates added amount but does not account for contribution from other ingredients.

[f] 1 IU vitamin A = 0.3 µg retinol

[g] 1 IU vitamin D = 25 ng cholecalciferol

For nutrients not listed, insufficient data is available to quantify.

Figure 2: Composition of diet 2: 14% protein and 3.5% fat (Harlan Tekland global diet)

6.3.2 Ethics Statement

Procedures involving animals and their care were in accordance to the national, international laws and policies (EEC Council Directive 86/609, OJ L 358, 1 Dec.12, 1987; NIH Guide for the Care and use of Laboratory Animals, U.S. National Research Council, 2011). The Mario Negri Institute for Pharmacological Research (IRCCS, Milan, Italy) Animal Care and Use Committee (IACUC) approved the experiments, which were conducted according to the institutional guidelines, which are in compliance with Italian laws (D.L. no. 116, G.U. suppl. 40, Feb. 18, 1992, Circular No.8, G.U., Juli14,

1994). The scientific project was approved by Italian Ministry of Health (Permit Number: 71/2014 B).

6.3.3 Study Design

The first point of our study was to characterize the transgenic mouse model of tauophaty, that replicates the impairments found in patients affected by tauophaty in a way age-gender-dependent showing that females were more affected than males, and subsequently investigate the effect of two different diets (high fat-protein and low fat-protein diets) on the onset and progression of tauophaty, finding that a low fat-protein diet may play an important role to improve the lifespan and cognitive activity in a transgenic mouse model of tauophaty (P301L), with a major improvement in female than male P301L TG mice.

The aim of this study was to investigate a possible condition of nonalcoholic fatty liver disease (NAFLD) due to alteration of insulin signaling in this model of tauophaty and to explore the possible mechanisms through which diets can interact and improve this pathological condition. After the weaning, all animals were fed with the same diet (diet 1 required for the growth of the mice); at 3 months of age the animals were divided into two experimental groups: the first group fed with diet 1 and the second group fed with diet 2.

Based on data in the literature [17-18], two time points were defined at 7 and 15 months of age (the first time point the symptoms of the disease were evident expressed, the second time point: maximum survival for mice affected by tauophaty); in the previous works we evaluated metabolic profiles and cognitive and locomotor aspects utilizing behavioral tests. To investigate the possible condition of nonalcoholic fatty liver disease (NAFLD) and to investigate the possible mechanisms through which diets can interact and improve a possible condition of oxidative stress, animals were sacrificed after the behavioral tests and different tissues were used for morphometry and immunohistochemistry (H&E and Sirius red). Blood samples were collected for biochemical analysis. At both time points (7 and 15 months) n=5 animals for each experimental group were sacrificed for IHC and biochemical analyses as described below.

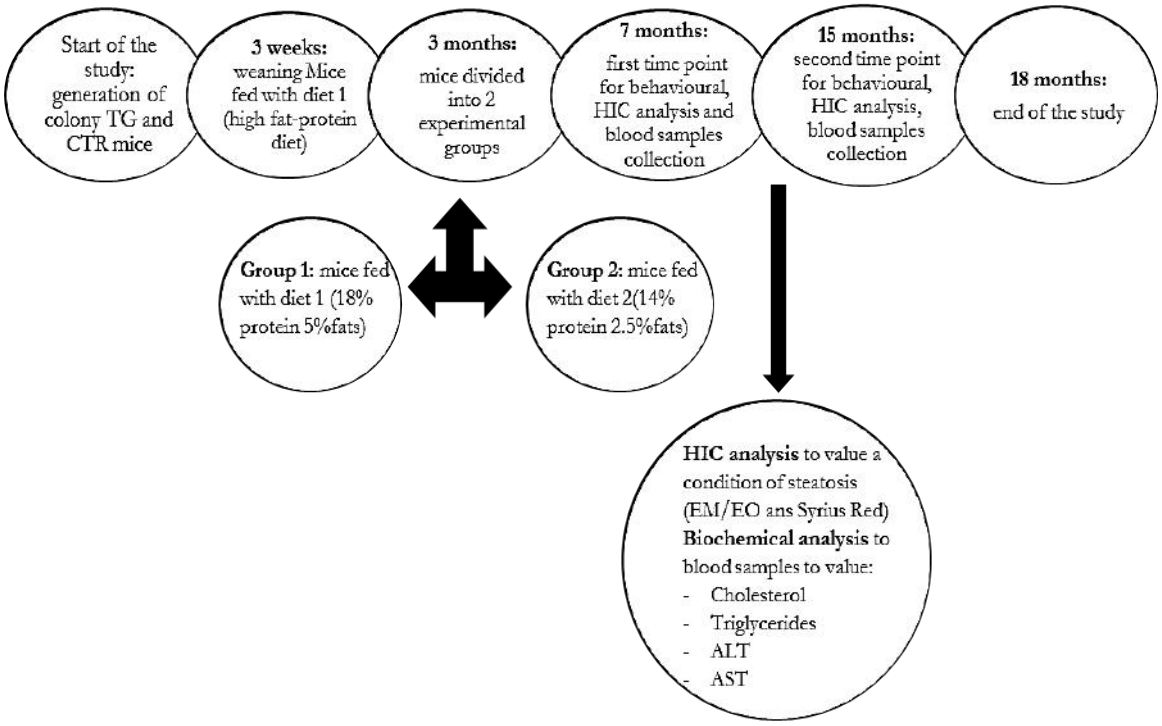

Figure 3: Experimental design of the study. In the study were set three time points: 3 months of age related to the administration of two different diets (diet 1 and diet 2), 7 and 15 months of age related to manifestation of the neuro disease and maximum survival of TG animals (time points for behavioral tests After behavioral tests HIC and biochemical analysis were conducted to value a condition of nonalcoholic fatty liver disease (NAFLD).

6.3.4 Histopathology: collection of mouse tissue and sera

At the end of behavioral tests (7 and 15 months of age) TG and CTR mice fed with different diets were euthanized by cervical dislocation [31-32]; the peripheral blood samples were collected from mice under isoflurane inhalation anesthesia by sterile cardiac puncture. Intestine, stomach, kidney, liver and spleen were promptly dissected from the animals and measured after removal. The spleen and the left hepatic lobe was divided into sections for fixation in 10% buffered formalin, embedded in paraffin and used for different staining (Sirius red Staining and hematoxylin and eosin staining).

6.3.5 Sirius Red Staining

After deparaffinization, spleen and liver sections (3 μm thick; three slices per mouse) were stained with Sirius Red. Sections were stained in Wiegert's hematoxylin for 8 minutes, and then washed for 10 minutes in running tap water. The sections were incubated for 1 h at room temperature with in picro-sirius red (0.5 gr/500 ml) and washed in two changes of acidified water, removing the water from the slides by vigorous shaking.

The sections were dehydrated in three changes of 100% ethanol, cleared in xylene and mounted in a resinous medium.

6.3.6 Hematoxylin and Eosin (H&E) Staining

After deparaffinization, spleen and liver sections (3 µm thick; three slices per mouse) were stained with Hematoxylin and Eosin using this protocol. Sections were stained within Harris hematoxylin solution for 8 minutes then were washed in running tap water for 5 minutes. Sections were differentiated in 1% acid alcohol for 30 seconds, washed in running tap water for 1 minute and bluinged in 0.2% ammonia water or saturated lithium carbonate solution for 30 seconds to 1 minute. Sections were washed in running tap water for 5 minutes, rinsed in 95% alcohol (10 dips) and counterstained in eosin-phloxine solution for 30 seconds to 1 minute. Finally, the sections were dehydrated in three changes of 100% ethanol, cleared in xylene and mounted in a resinous medium.

6.3.7 Cholesterol, Triglycerides, Alanine Aminotransferase And Aspartate Aminotransferase Measurements

Plasma of CTR and TG mice fed with different diets at 7 and 15 months of age (n=5 animals per each experimental group) were collected to value the concentration of cholesterol, triglycerides, alanine aminotransferase and aspartate aminotransferase using specific kit of Biochemicals System (for Triglycerides cod. TG383, for ALAT GPT cod. ALO20XL, for ASAT GOT cod. ASO70XL and for cholesterol total cod. C20TS).

6.3.8 Statistical Analysis

Statistical analyses were performed using Graph Pad Prism 6 program. Biochemical data (cholesterol, triglycerides, ALT, AST) were analyzed using two-way ANOVA, followed by Tukey's *post hoc* test.

6.4 RESULTS

6.4.1 Histopathology

At 7 and 15 months of age intestine (duodenum), stomach, kidney, liver and spleen of TG and CTR mice fed with different diets were dissected from the animals and measured after removal. At 7 months of age macroscopy analysis revealed a difference both in the aspect and size in liver and spleen of TG mice compared to CTR mice, regardless of diet administrated (Fig.4 and table 1). The assessment of the weight of tissues removed revealed a difference in the weight of liver and spleen between TG and CTR mice ($P= 0.06$, Fig. 5A-B; Fig. 6A-B), but any statistically significant effect of diet was found ($P> 0.05$, Fig. 5C-D).

Based on these data, we decided to investigate in terms of immunohistochemical analysis, liver and spleen of animals for each experimental group at 7 months of age. Sections of both P301L TG and CTR mice liver and spleen were staining with hematoxylin and eosin and Sirius red (Fig.7-8), in order to understand if inflammation was present and if different diets (diet 18: 18% protein and 5% and diet 14: 14% protein and 3.5% fat) can improve the pathological condition. H&E immunostaining applied to liver and spleen revealed that, regardless of diets administrated, in P301L TG mice the inflammation with increased vascularity and an initial state of fibrosis was present at 7 months of age (liver: Fig. 7B-D-F-H, spleen: Fig. 7J-L-N-P).

This result was also confirmed with Sirius red immunostaining applied to liver and spleen of TG and CTR mice, showing a strong positive signal of collagen presence in TG mice compare to CTR mice (liver: Fig. 8B-D-F-H, spleen: Fig. 8J-L-N-P).

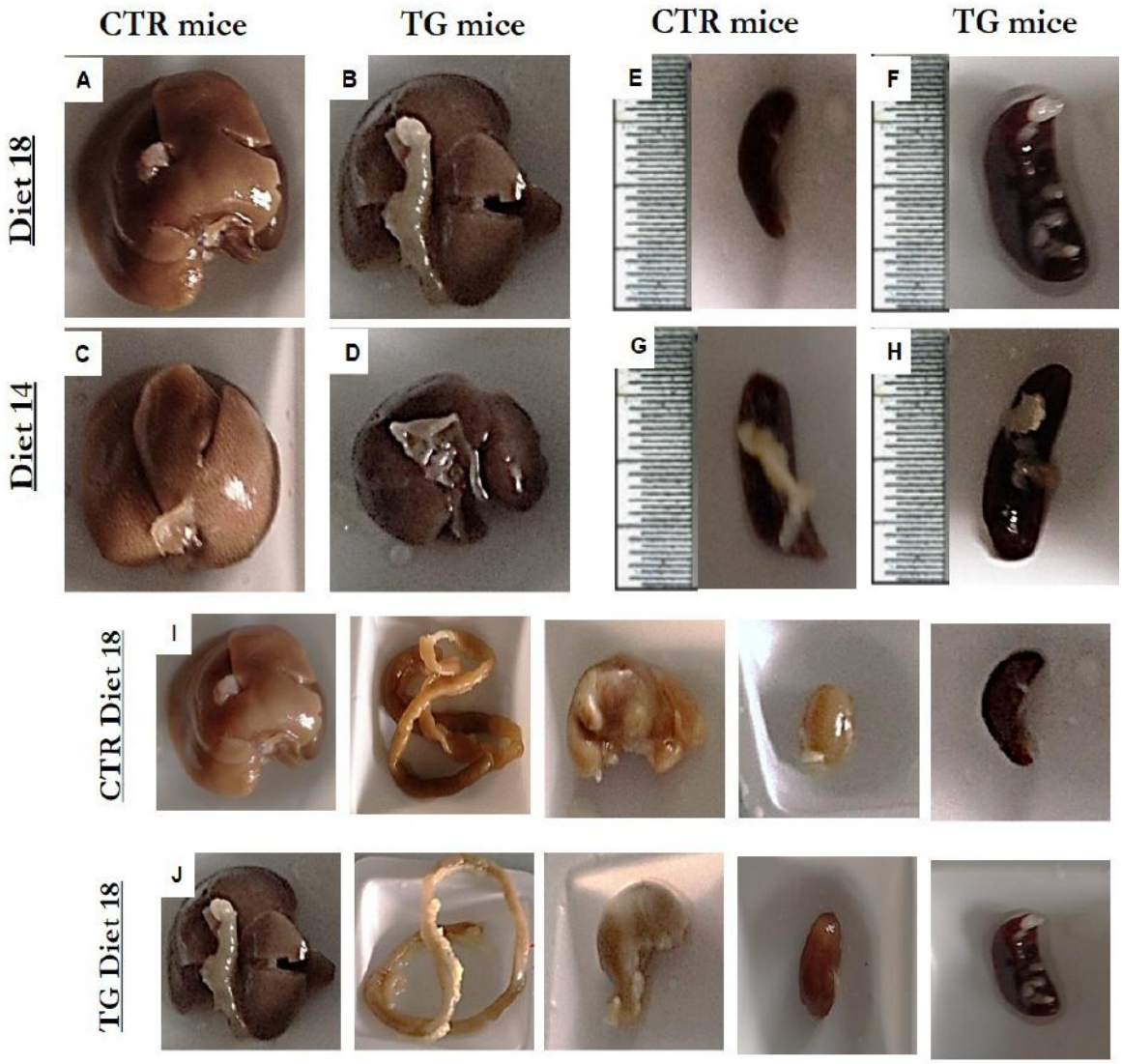

Figure 4. Gross anatomy of mouse liver and spleen in TG and CTR mice fed with different diets at 7 month of age. Detailed front **(A-D)** view of excised liver and spleen **(E-H)** in TG and CTR mice fed with different diets. **I-J)** Detailed view of excised tissues (liver, intestine, stomach, kidney and spleen) removed from CTR mice **(I)** and TG mice **(J)** fed with high fat-protein diet (diet 18).

		Diet 18				Diet 14		
	CTR male	**CTR female**	**TG male**	**TG female**	**CTR male**	**CTR female**	**TG male**	**TG female**
Liver (cm)	2 x 1.3	1.9 x 1.3	3 x 2.2	2.5 x 1.8	1.8 x 1.5	2 x 1.2	2.6 x 2	2.6 x 2
Intestine (cm)	1	1.1	1.1	1.2	1.3	1	1.1	1.2
Stomach (cm)	1.2 x 1	1.3 x 1.2	1.6 x 1.2	1.4 x 1.2	1.4 x 1.3	1.1 x 1.3	1.8 x 1.3	1.2 x 1.3
Kidney (cm)	0.7 x 0.9	0.9 x 0.8	1 x 0.9	1 x 0.8	0.7 x 0.8	0.8 x 0.9	1 x 0.9	1 x 1.2
Spleen (cm)	1.2 x 1	0.9 x 1	1.8 x 1	1.9 x 1.1	1.3 x 1.2	1.1 x 1.3	1.4 x 1	1.6 x 1

Table 1: Valuation of size tissues in TG and CTR mice fed with different diets at 7 months of age. Valuation of intestine, stomach, kidney, liver and spleen size in male and female CTR and TG mice at 7 months of age. Values are mean of size of 5 animals for each experimental groups.

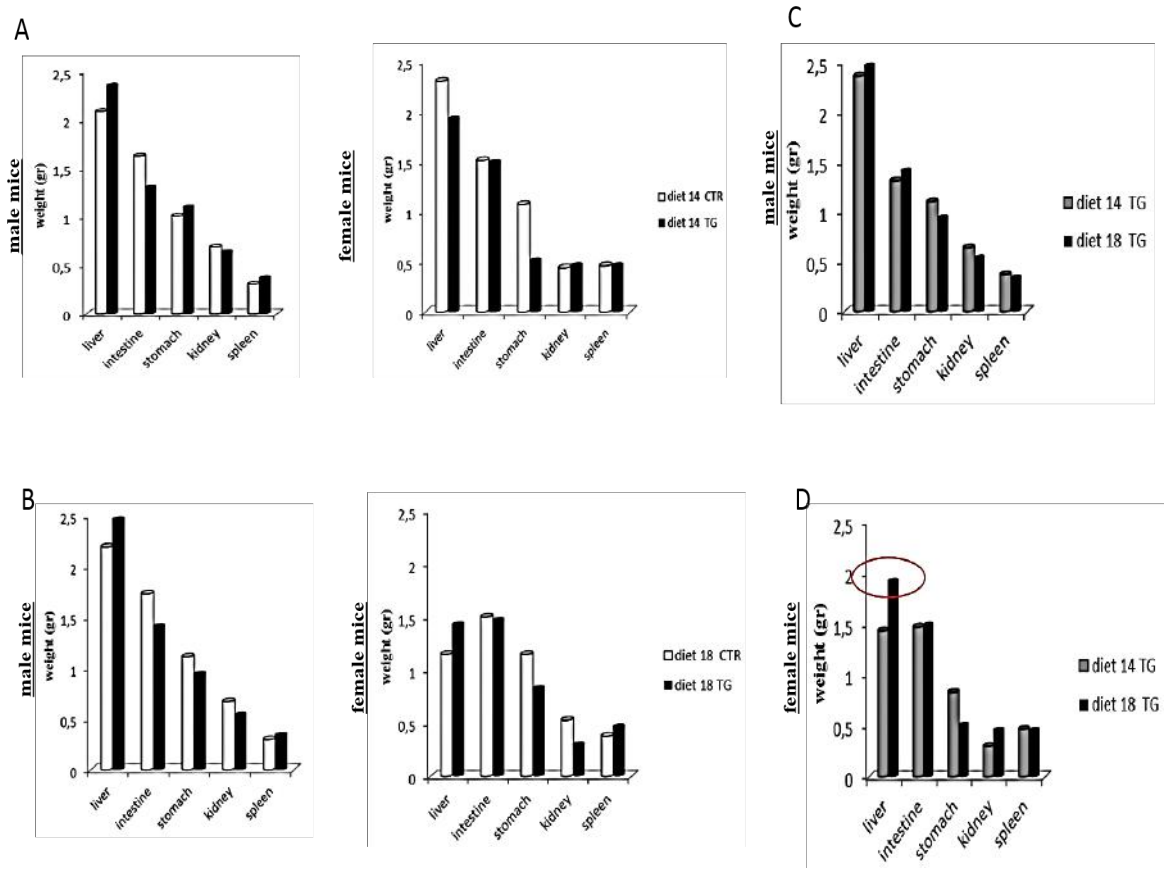

Figure 5: Valuation of weight tissues in TG and CTR mice fed with different diets at 7 months of age. A-B) Valuation of intestine, stomach, kidney, liver and spleen weights in male and female CTR and TG mice fed with different diets at 7 months of age. **C-D)** Valuation of intestine, stomach, kidney, liver and spleen weights only in male and female TG mice fed with different diets showed any diet effect (n= 5 mice per each experimental group).

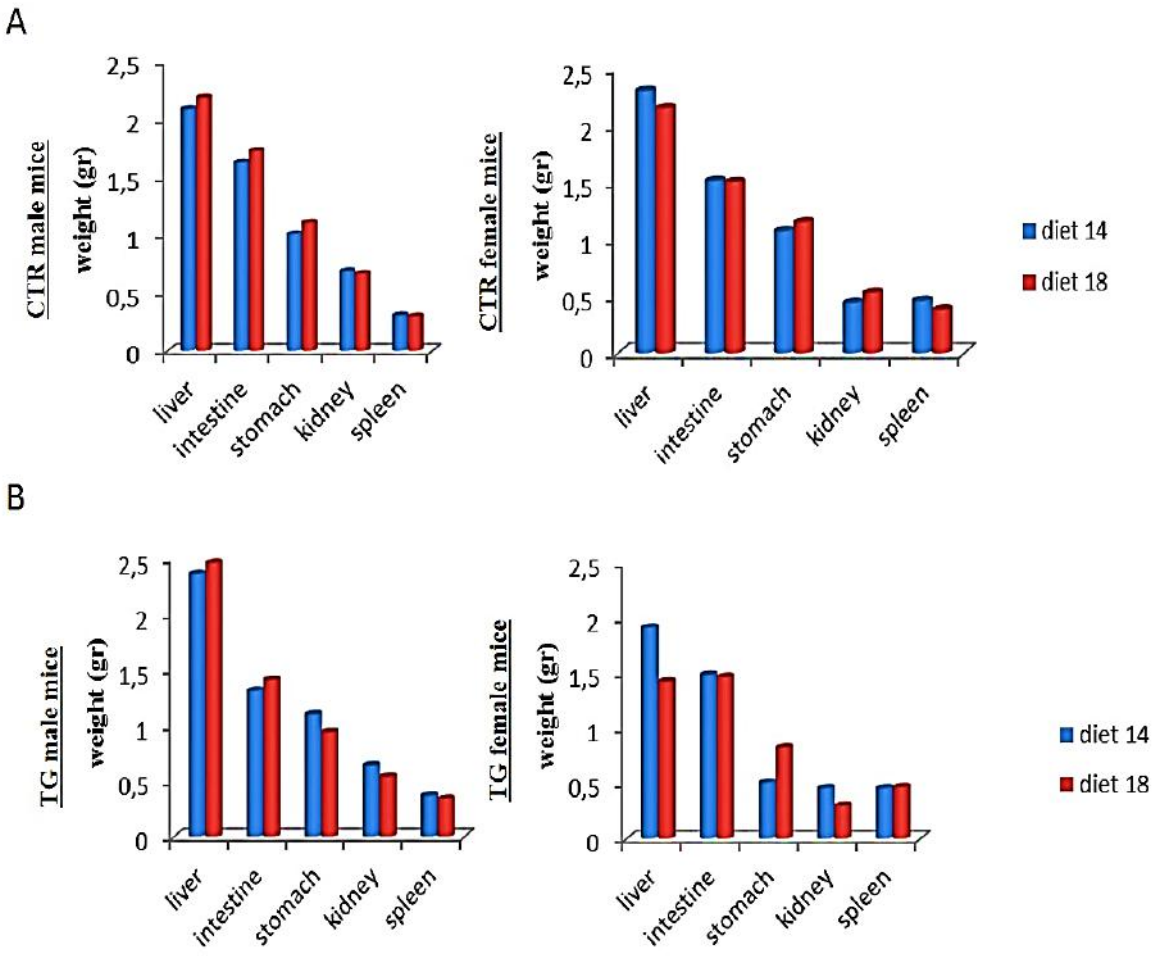

Figure 6: Valuation of weight tissues in TG and CTR mice fed with different diets at 7 months of age. A) Valuation of intestine, stomach, kidney, liver and spleen weight in male and female CTR and **B)** TG mice revealed any diet effect at 7 months of age.

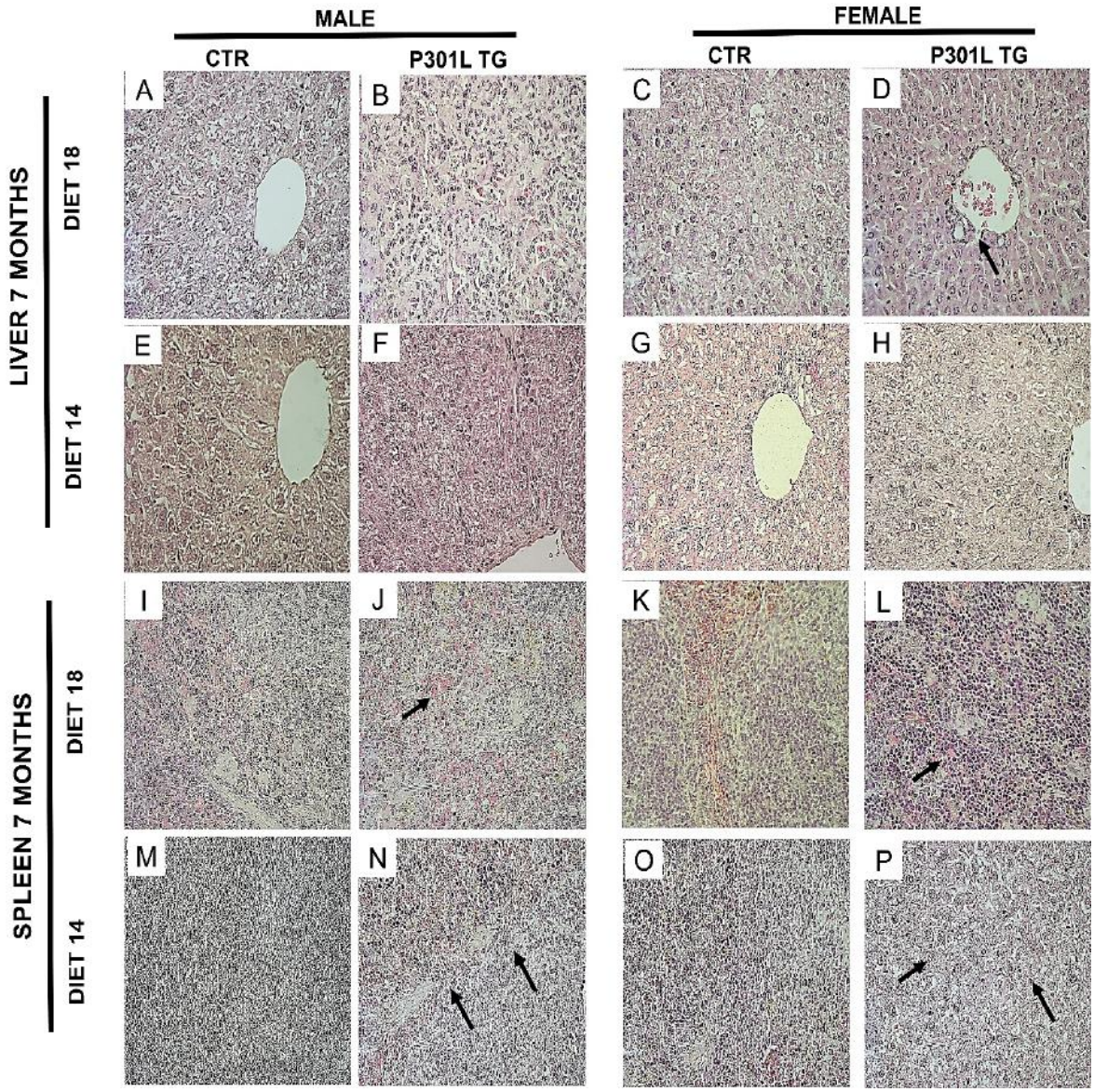

Figure 7. Hematoxylin and Eosin (H&E) staining of liver and spleen in TG and CTR mice fed with different diets at 7 month of age. H&E stained sections revealed a condition of inflammation in 7-month-old males and females (P301L TG mice) fed with diet 14 and 18 in liver (**A-H**) and in spleen (**I-P** note the arrows pointing to the most representative aspects in TG mice). Representative sections are shown of 5 animals used per each group. Scale bar: 40 μm.

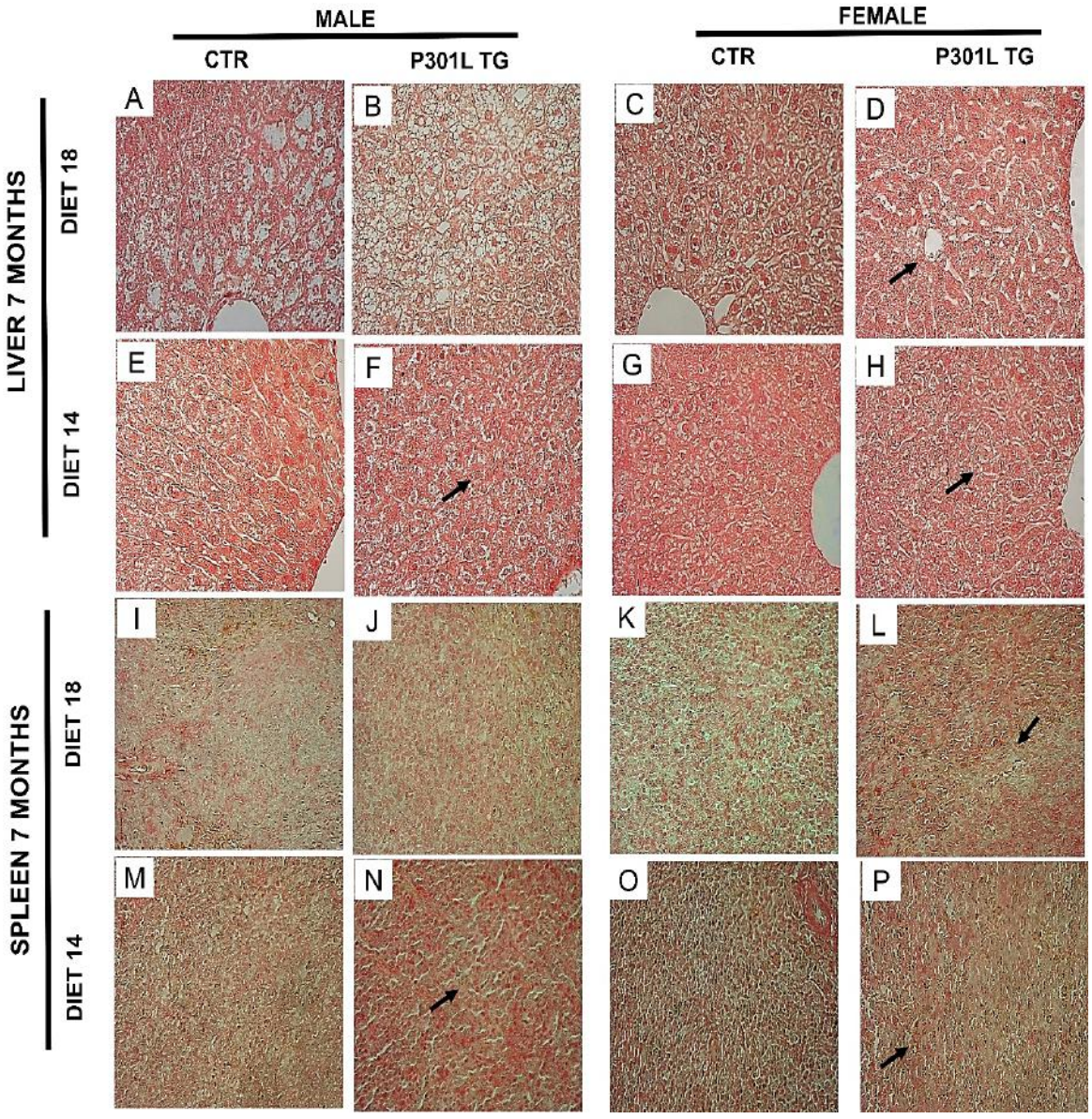

Figure 8. Sirius red staining of liver and spleen in TG and CTR mice fed with different diets at 7 month of age. Sirius red stained sections revealed the positive signal in 7-month-old males and females (P301L TG mice and CTR mice) fed with diet 14 and 18 in liver (**A-H**) and in spleen (**I-P** note the arrows pointing to the most representative aspects in TG mice). Representative sections are shown of 5 animals used per each group. Scale bar: 40 μm.

At 15 months of age macroscopy analysis revealed a strong difference both in the aspect and size in liver and spleen of TG mice compared to CTR mice, with a strong diet effect showing by an increase of size and alteration of aspect of tissues in TG mice fed with high fat-protein diet (Fig. 9 and table 2).

The assessment of the weight of tissues removed revealed a significant genotype effect, showing by an increase in the weight of liver and intestine in TG mice compared to CTR mice ($P<0.0001$, Fig. 10A-B), and a significant diet effect showing by an increase in the weight of liver and intestine in TG mice fed with high fat-protein diet compared to TG mice fed with low fat-protein diet ($P<0.0001$, Fig. 10C-D). Consequently, we decided to investigate in terms of immunohistochemical analysis, liver and spleen of animals for each experimental group at 15 months of age. Sections of both P301L TG and CTR mice liver and spleen were staining with hematoxylin and eosin and Sirius red (Fig. 12-13), in order to understand if inflammation was present and if different diets (diet 18: 18% protein and 5% and diet 14: 14% protein and 3.5% fat) can improve the pathological condition. H&E immunostaining applied to liver and spleen revealed that in P301L TG mice a severe inflammation with increased vascularity and an advanced state of fibrosis was present at 15 months of age (liver: Fig. 12B-D-F-H, spleen: Fig. 12J-L-N-P).

This effect was more pronounced in TG mice fed with high fat-protein diet compared to TG mice fed with low fat-protein diet; an initial state of inflammation was also detected in CTR mice fed with high fat-protein diet. These results were also confirmed with Sirius red immunostaining applied to liver and spleen of TG and CTR mice, revealing a strong positive signal of collagen presence in TG mice compare to CTR mice (liver: Fig. 13B-D-F-H, spleen: Fig. 13J-L-N-P). Comparing the images of TG mice fed with different diets, an increase of collagen aggregates in TG mice fed with high fat-protein diet compared to TG mice fed with low fat-protein diet was detected.

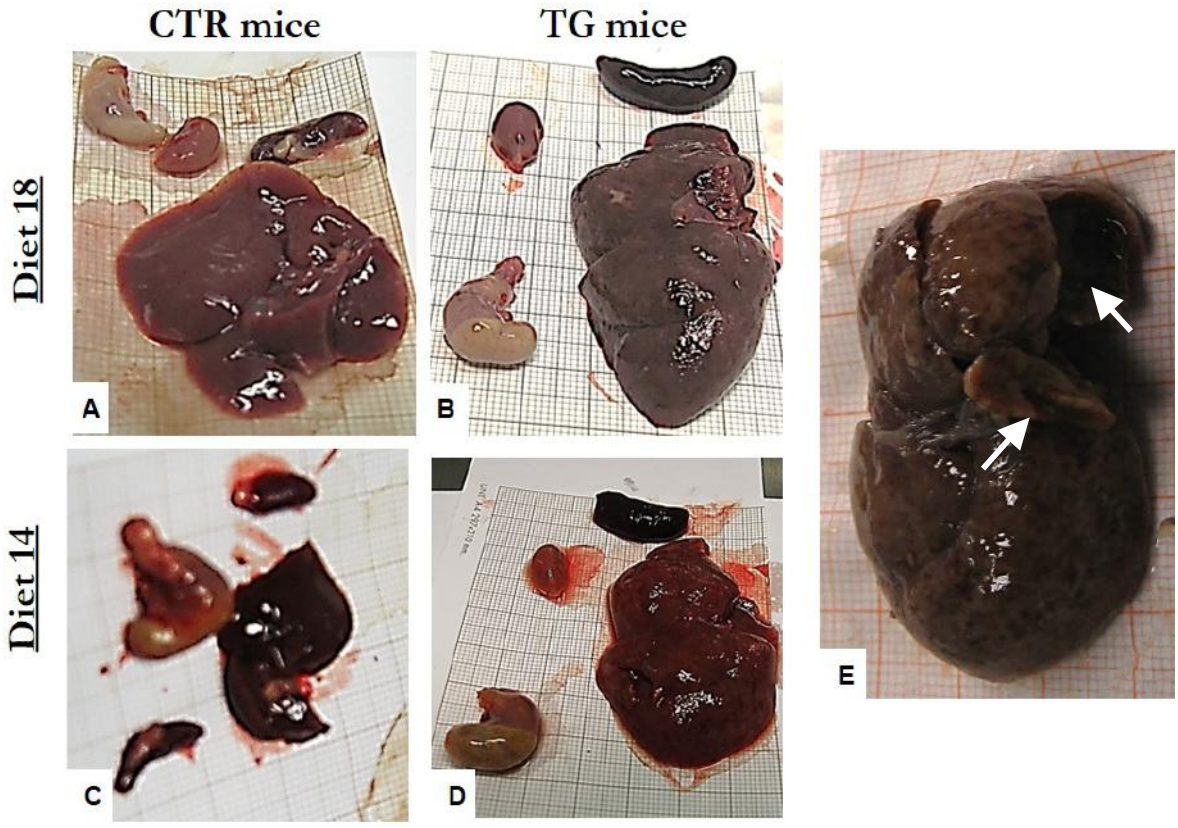

Figure 9. Gross anatomy of mouse liver, spleen, stomach and kidney in TG and CTR mice fed with different diets at 15 month of age. A-D) Detailed view of excised tissues (liver, spleen, stomach and kidney) in TG and CTR mice fed with different diets (diet 18 A-B, diet 14. **E)** Detailed view of liver removed from TG mice fed with high fat- protein diet that shows a strong state of fibrosis.

		Diet 18				Diet 14		
	CTR male	**CTR female**	**TG male**	**TG female**	**CTR male**	**CTR female**	**TG male**	**TG female**
Liver (cm)	4 x 3.4	3.7 x 3	7 x 4.5	4.5 x 3.2	2.6 x 2.2	2 x 1.2	6 x 3.5	2.6 x 4
Intestine (cm)	1	1.1	1.2	1.1	1.1	1	1.3	1.2
Stomach (cm)	1.7 x 1.1	1.3 x 1.2	2 x 1.8	2.4 x 1.2	1.9 x 2	1.5 x 1.3	2.3 x 1.5	2.5 x 1.8
Kidney (cm)	1.2 x 0.8	0.9 x 0.8	1.5 x 1	1.3 x 0.8	1.2 x 1	1.2 x 1	1.6 x 1.2	1.2 x 0.8
Spleen (cm)	0.5 x 1.3	0.9 x 1	1.9 x 1.5	1.9 x 1.2	0.8 x 1.2	0.5 x 1.2	1.4 x 1.9	0.9 x 1.4

Table 2: Valuation of size tissues in TG and CTR mice fed with different diets at 15 months of age. Valuation of intestine, stomach, kidney, liver and spleen size in male and female CTR and TG mice at 15 months of age. Values are mean of size of 5 animals for each experimental group.

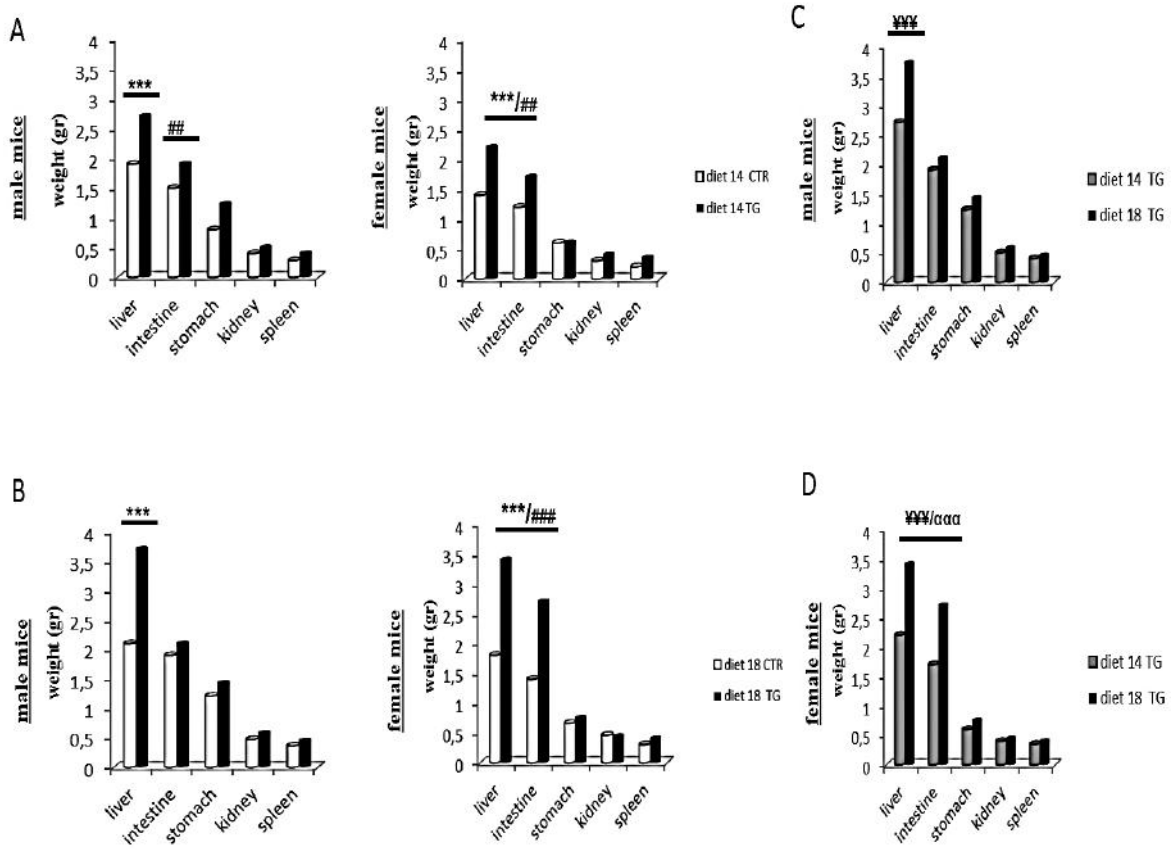

Figure 10: Valuation of weight tissues in TG and CTR mice fed with different diets at 15 months of age. A-B) Valuation of intestine, stomach, kidney, liver and spleen weights in male and female CTR and TG mice fed with different diets at 15 months of age showed a significant genotype effect for the weight measurements of liver and intestine. **C-D)** Valuation of intestine, stomach, kidney, liver and spleen weights only in male and female TG mice fed with different diets revealed a significant diet effect for the weight measurements of liver and intestine, showing by an increase of weight in TG mice fed with high fat- protein diet (diet 18). DIET 18: TG vs CTR mice *** P< 0.0001. DIET 14: TG vs CTR mice ## P< 0.001, ### P< 0.0001. Liver: TG mice diet 18 vs TG mice diet 14 ¥¥¥ P< 0.0001; intestine: TG mice diet 18 vs TG mice diet 14 ααα P< 0.0001 (n= 5 mice per each experimental group).

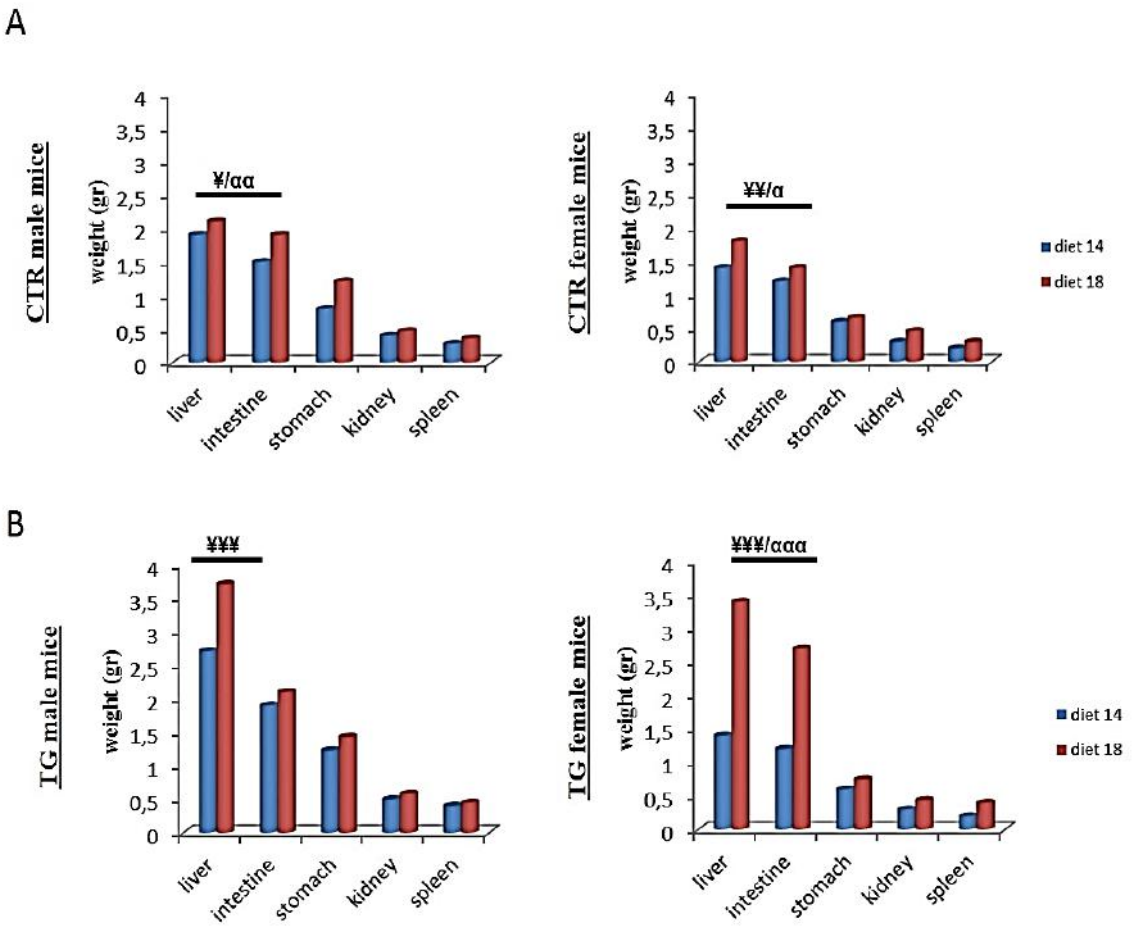

Figure 11: Valuation of weight tissues in TG and CTR mice fed with different diets at 15 months of age. A) Valuation of intestine, stomach, kidney, liver and spleen weight in male and female CTR and **B)** TG mice revealed a significant diet for the weight measurements of liver and intestine, showing by an increase of weight in TG mice fed with high fat- protein diet (diet 18) at 15 months of age. Liver: CTR mice diet 18 vs CTR mice diet 14 ¥ P< 0.05, ¥¥ P< 0.001; TG mice diet 18 vs TG mice diet 14 ¥¥¥ P< 0.0001; intestine: CTR mice diet 18 vs CTR mice diet 14 α P< 0.05, αα P< 0.001; TG mice diet 18 vs TG mice diet 14 ααα P< 0.0001 (n= 5 mice per each experimental group).

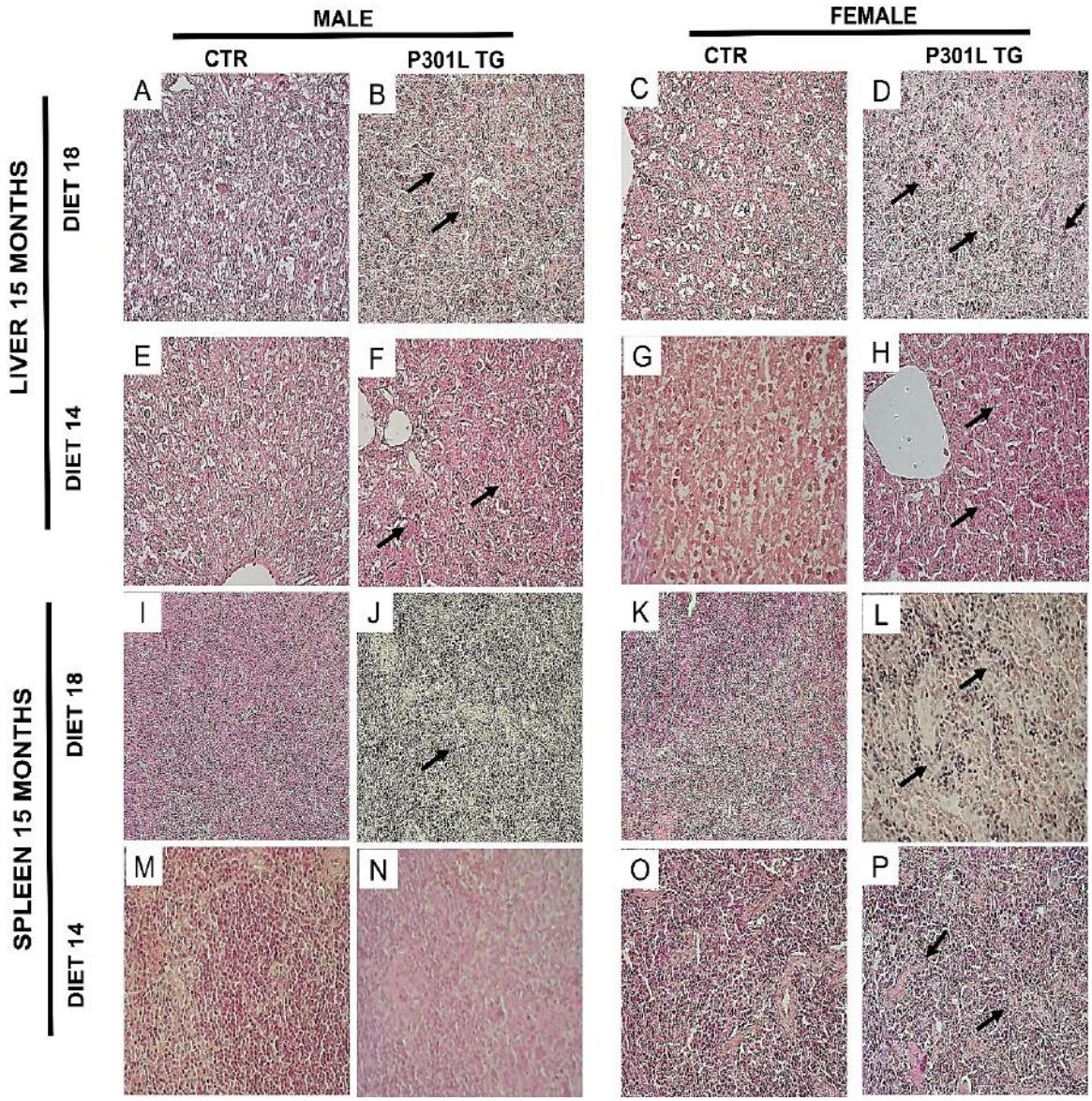

Figure 12. Hematoxylin and Eosin (H&E) staining of liver and spleen in TG and CTR mice fed with different diets at 15 month of age. H&E stained sections revealed the positive signal in 15-month-old males and females (P301L TG mice and CTR mice) fed with diet 14 and 18 in liver (**A-H**) and in spleen (**I-P** note the arrows pointing to the most representative aspects in TG mice). Representative sections are shown of 5 animals used per each group. Scale bar: 40 μm.

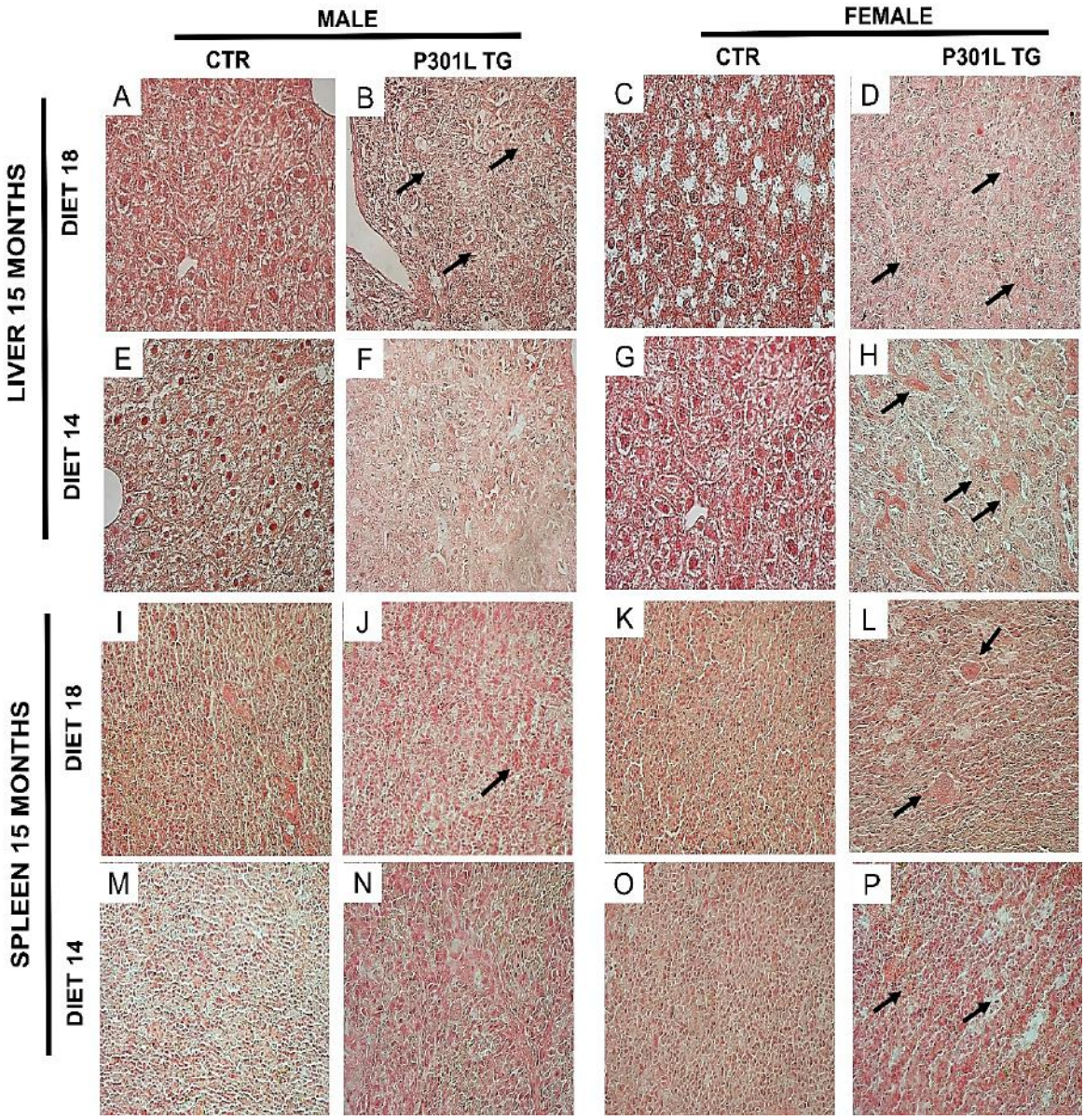

Figure 13. Sirius red staining of liver and spleen in TG and CTR mice fed with different diets at 15 month of age. Sirius red stained sections revealed the positive signal in 15-month-old males and females (P301L TG mice and CTR mice) fed with diet 14 and 18 in liver (**A-H**) and in spleen (**I-P** note the arrows pointing to the most representative aspects in TG mice). Representative sections are shown of 5 animals used per each group. Scale bar: 40 μm

6.4.2 Cholesterol, Triglycerides, Alanine Aminotransferase and Aspartate Aminotransferase Measurements

Based on previous data related to histopathology analysis, plasma of TG and CTR mice fed with different diets (n=5 animals per each experimental group) were collected to value the concentration of total cholesterol, triglycerides, alanine aminotransferase (ALT) and aspartate aminotransferase (AST) in order to explore tauophaty-related metabolic modifications in mouse model used in this study and to understand if diets can interact with this metabolic syndrome. The measurement of concentration of cholesterol total had shown any significant difference between TG mice fed with different diets at 7 and 15 months of age (Fig. 14). Median levels of total cholesterol measured in both TG and CTR mice, regardless of diet administrated, were included in age-related reference intervals (median and 2.5th–97.5th percentiles ranges) for biochemical analytes published in literature (see table 3) [33].

Analyte	Mouse Strain						Inter strain differences[a]
	C57BL/6J		129SV/EV		C3H/HeJ		
	Male	Female	Male	Female	Male	Female	
GLU mmol/L	7.4 [b]	7.1	6.7	6.6	7.5 [b]	6.6	129SV/EV $p<0.05$
	5.6–9.1	5.2–12.2	4.1–9.9	4.7–8.4	6.3–8.6	5.6–8.3	
LPS U/L	901	1177 [b]	991	1090	969	1057	
	649–1646	788–1624	689–1201	777–1419	536–1372	634–1541	
TAG mmol/L	2.2 [c]	1.2	1.8	1.6	2.3	2.3	C3H/HeJ $p<0.001$
	1.1–2.9	0.6–1.8	0.9–4.5	0.7–4.8	1.7–6.0	1.0–3.8	
Chol mmol/L	2.6 [b]	2.1	3.2	3.1	3.5	3.4	C3H/HeJ $p<0.001$
	1.8–3.9	1.3–3.4	2.2–5.3	2.1–4.1	2.8–5.2	2.2–3.6	
LDH U/L	1888	1837	2430	2240		2067	
	1590–2610	843–3150	2212–3150	1752–3150	>2250 [b d]	1829–2250	
CK U/L	327	319	398	544	324	464	
	209–635	105–649	138–615	199–964	206–660	204–921	
Crea µmol/L	10.2	10.2	12.4	12.4	10.2	10.2	
	8.8–13.2	8.8–13.2	8.8–20.5	8.8–20.5	8.8–12.3	8.8–12.4	
BUN mmol/L	9.0 [b]	7.8	10.0 [b]	7.8	8.3 [b]	7.5	
	7.8–11.5	6.8–10.0	6.8–13.2	6.5–10.3	7.4–12.9	6.6–10.0	
UA mmol/L	0.3	0.2	0.2	0.2	0.2	0.2	
	0.1–0.6	0.1–0.7	0.1–0.3	0.1–0.3	0.1–0.6	0.1–0.5	
GGT U/L	6.9	7	6.8	6.9	7	8.4	
	6–8	6–8	6–8	6–8	6–8	6–10	
AST U/L	75	91 [b]	98	104	116	121	C57BL/6J $p<0.001$
	55–91	51–122	71–201	69–194	67–160	80–172	
ALT U/L	61	55	64	63	67	80	
	46–70	42–73	45–84	46–114	39–115	56–107	
ALP U/L	84	145 [c]	86	142 [b]	120	200 [c]	
	67–128	103–217	68–179	97–287	75–137	126–240	
t-Bil µmol/L	7.2	7.9	5.9	3.9	9.6	9.6	129SV/EV $p<0.05$
	5.1–11.9	3.4–14.3	1.7–19.1	1.7–14.3	3.4–11.9	3.4–13.9	
c- Bil µmol/L [e]	0–1.7	0–5.1	0–5.1	0–3.4	0–6.8	0–6.8	
CHE U/L	4450	6880 [c]	5540	7550 [c]	5350	6790 [b]	
	3870–6130	5660–9770	4440–6830	5870–8620	3690–9790	5420–9560	
TP g/L	63	66	61	57	62	53	
	47–72	45–83	43–65	48–68	49–74	25–71	
Alb g/L	33	34	29	27	31	31	
	22–42	20–47	18–31	20–36	22–39	24–41	
CRP mg/L [e]	0–0.7	0–0.7	0–2.8	0–1.4	0–0.7	0–2.3	
Na^+ mmol/L	179.2	179.8	180.9	178.6	184.4	182.1	
	151.0–254.8	149.0–281.4	147.0–253.4	148.0–253.4	151.0–247.8	150.0–245.0	
K^+ mmol/L	6.6	6.6	8.2	7.9	8.6	8.1	C57BL/6J $p<0.05$
	5.2–14.5	4.0–14.0	4.9–10.3	5.0–9.5	5.8–13.1	6.0–13.4	
Cl^- mmol/L	131.1	137.4	128.7	131.1	131.1	132.2	
	109.0–179.2	110.0–204.4	106.0–179.2	110.0–184.8	110.0–172.2	110.0–177.8	
Ca^{++} mmol/L	2.4	2.5	2.8	2.8	2.6	2.7	C57BL/6J $p<0.05$
	2.2–2.6	2.3–3.5	2.3–3.4	2.3–3.0	2.2–2.9	2.3–2.9	
Mg^{++} mmol/L	1.3	1.3	1.2	1.3	1.3	1.3	
	1.1–1.7	1.2–1.8	1.0–1.4	0.9–1.4	0.9–1.8	1.0–1.9	

Table 3. Serum biochemical analytes (median and 2.5th–97.5th percentiles interval) measured in aged 4–8 months C57BL/6J, 129SV/EV and C3H/HeJ mouse strains. [1]

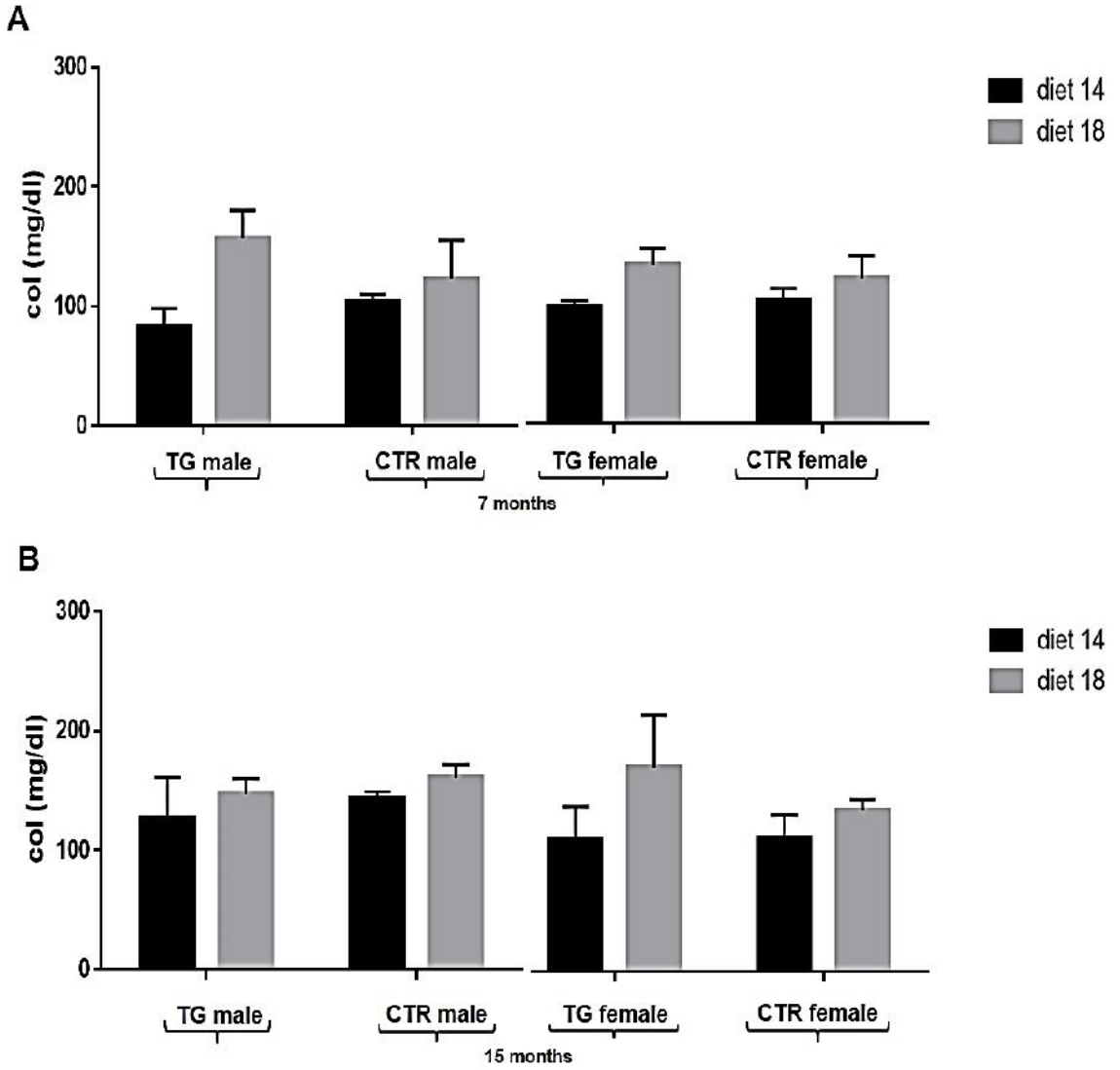

Figure 14: Biochemical median values of total cholesterol in TG and CTR mice at 7 and 15 months of age. A) Total cholesterol median values calculated in TG and CTR mice fed with different diets at 7 and **B)** 15 months of age showed any significant difference between experimental groups.

The measurement of concentration of triglycerides had shown at 7 months of age a significant genotype effect between TG and CTR male mice fed with diet 14 ($P < 0.05$, Fig. 15A) and a significant diet effect between TG male mice fed with diet 14 and diet 18 ($P < 0.0001$, Fig. 15A). At 15 months of age any significant difference between TG and CTR mice were detected ($P > 0.05$, Fig. 15B), but median levels of triglycerides measured in TG mice, regardless of diet administrated, were higher compared to value included in reference intervals for biochemical analytes (table 3), revealing an altered metabolic condition associated to tauophaty in mouse model used in this study.

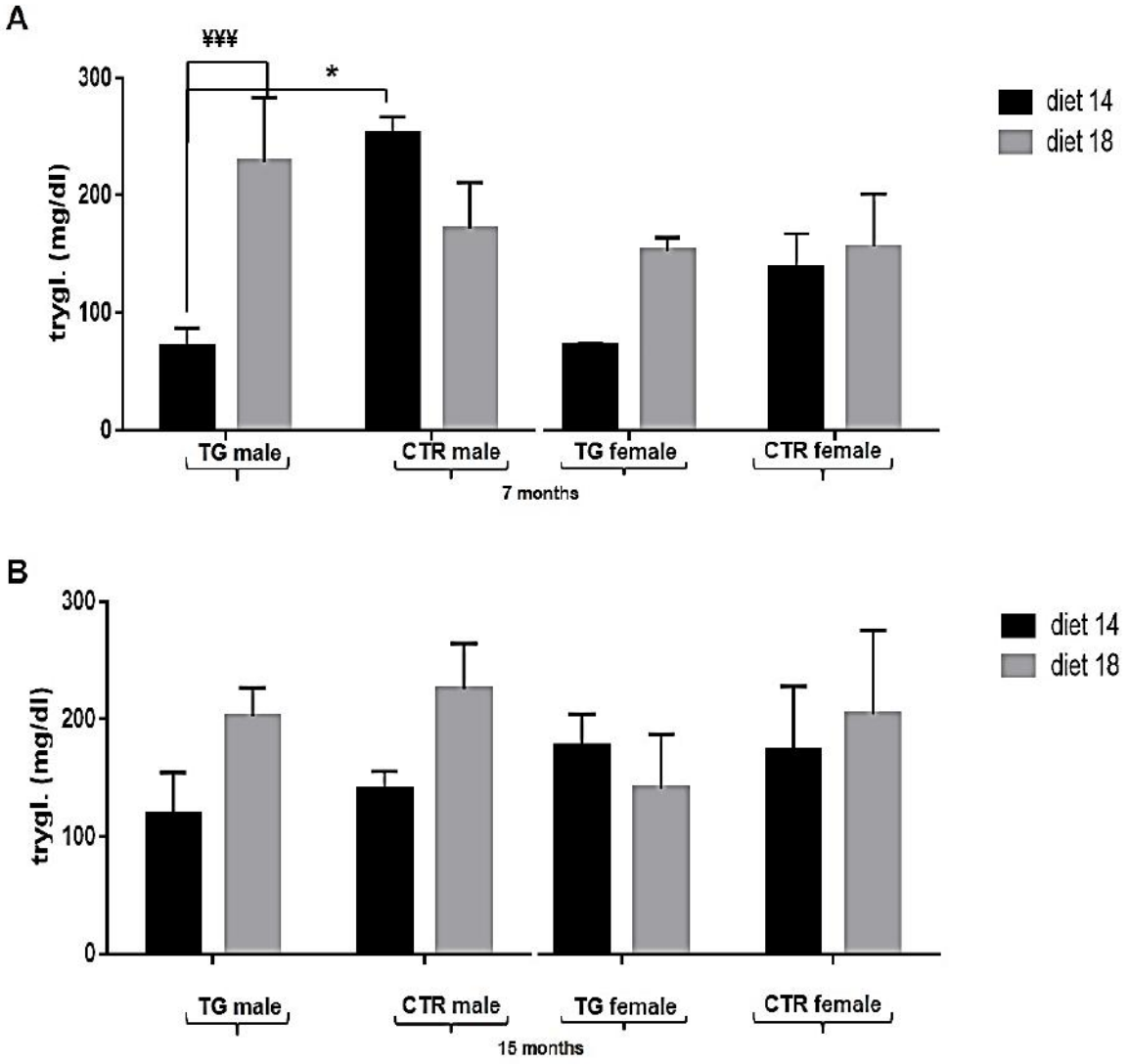

Figure 15: Biochemical median values of triglycerides in TG and CTR mice at 7 and 15 months of age. A) Triglycerides median values calculated in TG and CTR mice fed with different diets at 7 and **B**) 15 months of age showed a significant difference between TG and CTR male mice fed with diet 14 and a significant diet effect between TG male mice fed with diet 14 and diet 18. TG male mice diet 14 vs CTR male mice diet 14 ¥¥¥ P< 0.0001; TG male mice diet 18 vs TG male mice diet 14 * P< 0.05. Data were shown as mean ± SEM (n= 5 mice per each experimental group).

The measurement of concentration of ALT had shown at 7 months of age a significant genotype effect between TG and CTR male mice fed with diet 14 (P< 0.05, Fig. 16A) and a significant diet effect between TG male mice fed with diet 14 and diet 18 (P< 0.0001, Fig. 16A). At 15 months of age a significant diet effect between TG and CTR mice fed with different diets were detected (TG male mice fed with diet 14 vs diet 18 and CTR male mice fed with diet 14 vs diet 18 P< 0.05, Fig. 16B), but median levels of ALT measured in TG mice, regardless of diet administrated, were higher compared to value included in

reference intervals for biochemical analytes (table 3), revealing an altered metabolic condition associated to tauophaty in mouse model used in this study.

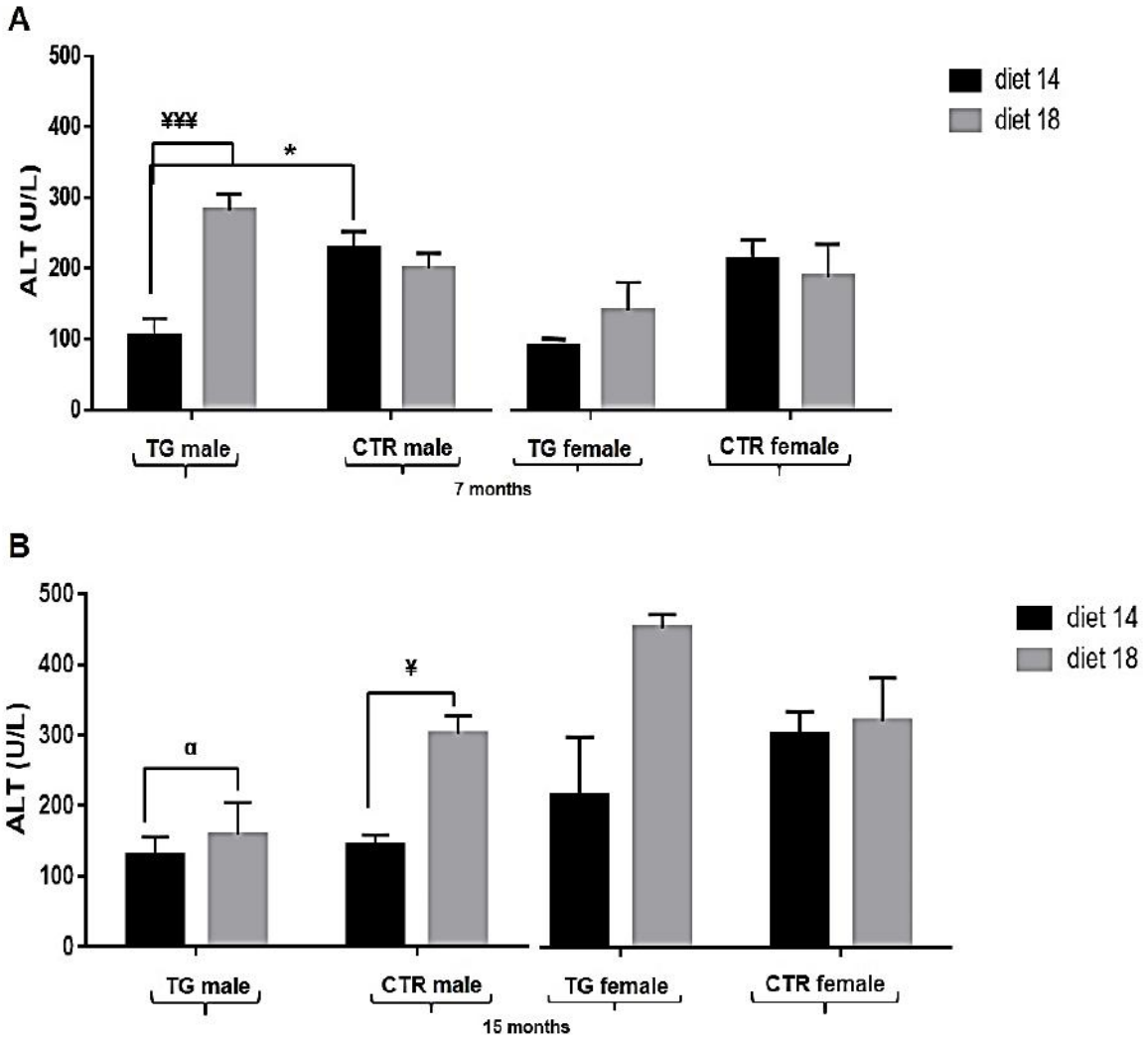

Figure 16: Biochemical median values of ALT in TG and CTR mice at 7 and 15 months of age. A) ALT median values calculated in TG and CTR mice fed with different diets at 7 and **B)** 15 months of age showed a significant difference between TG and CTR male mice fed with diet 14 and a significant diet effect between TG male mice fed with diet 14 and diet 18. 7 months: TG male mice diet 14 vs CTR male mice diet 14 ¥¥¥ P< 0.0001; TG mice diet 18 vs TG mice diet 14 * P< 0.05. 15 months: TG male mice diet 18 vs TG mice diet 14 α P< 0.05; CTR male mice diet 14 vs CTR male mice diet 18 ¥ P< 0.05. Data were shown as mean ± SEM (n= 5 mice per each experimental group).

The measurement of concentration of AST had shown at 7 months of age a significant genotype effect between male and female TG and CTR male mice fed with diet 14 (P< 0.05, Fig. 17A) and any significant diet effect between experimental group (P> 0.05, Fig. 17A). At 15 months of age a significant diet effect between TG and CTR mice fed with different diets were detected (TG male mice fed with diet 14 vs diet 18 and CTR male mice fed with diet 14 vs diet 18 P< 0.05, Fig. 16B), and a significant genotype effect between female TG and

CTR male mice fed with diet 18 (P< 0.05, Fig. 17B). Median levels of AST measured in TG mice, regardless of diet administrated, were higher compared to value included in reference intervals for biochemical analytes (table 3), revealing an altered metabolic condition associated to tauophaty in mouse model used in this study.

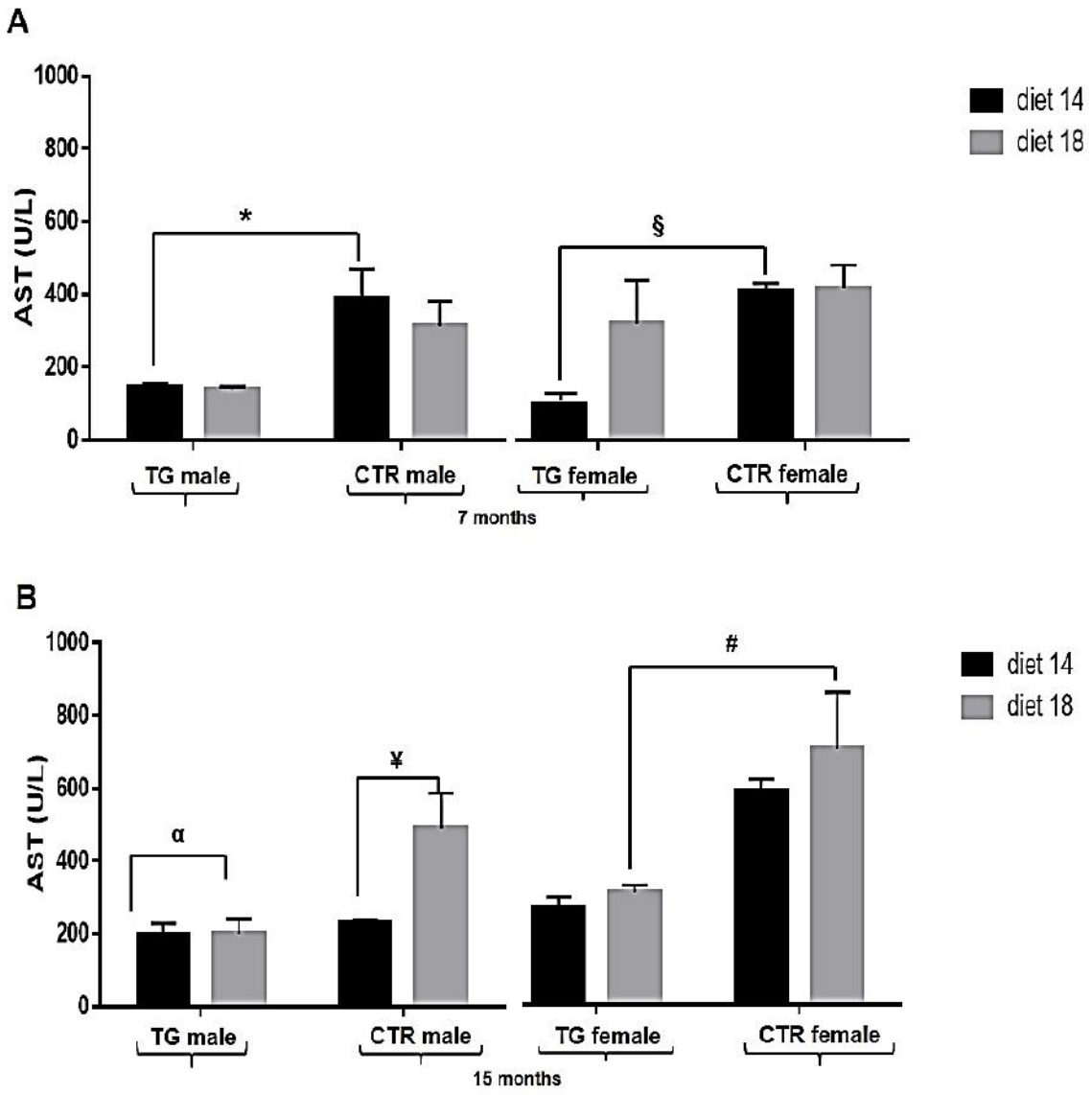

Figure 17: Biochemical median values of AST in TG and CTR mice at 7 and 15 months of age. A) ALT median values calculated in TG and CTR mice fed with different diets at 7 and **B)** 15 months of age showed a significant difference between male and female TG and CTR mice fed with diet 14 and a significant diet effect between TG male mice fed with diet 14 and diet 18 and CTR male mice fed with diet 14 and diet 18. 7 months: TG male mice diet 14 vs CTR male mice diet 14 * P< 0.05; TG female mice diet 14 vs CTR female mice diet 14 § P< 0.05. 15 months: TG mice diet 18 vs TG mice diet 14 α P< 0.05. TG female mice diet 18 vs CTR female mice diet 18 # P< 0.05; CTR male mice diet 14 vs CTR male mice diet 18 ¥ P< 0.05. Data were shown as mean ± SEM (n= 5 mice per each experimental group).

6.5 DISCUSSION

Growing evidence supports the concept that insulin resistance and metabolic dysfunction are mediators of tauopathies as AD [1-2], and tauopathies could be regarded as a metabolic disease mediated by brain insulin and IGF resistance [3-4]. In particular, a crosslink between insulin resistance-dysregulates lipid metabolism and oxidative stress seems to be the cause of hepatic dysfunctions as fibrosis or steatosis including nonalcoholic fatty liver disease (NAFLD).

In our previous works we characterized P301LTG line, a mouse model of tauophaty used in our studies, that replicate both cognitive and behavioral impairment found in patient affected by tauophaty, strongly correlated with an increase in P-Tau, astrogliosis and oxidative damage in both cerebral cortex and hippocampus, more pronounced in female than male TG mice at 7 and 15 months of age. Investigating the effects of different diets (high and low fat-protein diets) on neurodegeneration aspects of this mouse model, we found an improvement of pathological conditions administrating a low fat-protein diet, occurred with an increased lifespan, a reduction of food and water consumption, a reduction of aggregates of P-Tau and neuronal loss in both cerebral cortex and hippocampus, more pronounced in female than male TG mice. During necropsy analysis performed after the behavioral tests in TG and CTR mice, we observed an alteration of the size of the liver and spleen in TG mice fed with a high fat-protein diet at 7 and 15 months of age. This apparent condition of hepatomegaly was associated to an increase of body weight, food and water consumption in TG mice fed with high fat-protein diet. Consequently, in this study we decided to investigate this pathological condition, assuming it can be nonalcoholic fatty liver disease (NAFLD), in P301L TG and CTR mice at 7 and 15 months of age fed with different diets evaluating: macroscopy and histopathology of various tissues such as liver and spleen, the concentration of cholesterol, triglycerides, alanine aminotransferase and aspartate aminotransferase in plasma of TG and CTR mice.

At 7 and 15 months of age macroscopy analysis revealed a difference both in the aspect and size in tissues (in particular liver, spleen and intestine) removed from TG mice compared to CTR mice, regardless of diet administrated, most pronounced at 15 months of age. In the second time point, these alterations were also correlated to a significant diet effect showed by an increase of size and alterations of tissues removed from TG mice fed with high fat-protein diet compared to TG mice fed with low fat-protein diet. Macroscopy results were confirmed by the assessment of the weight of tissues removed from TG and CTR mice fed with different diets both at 7 and 15 months of age.

In particular, at 15 months of age, a significant genotype effect and diet effect for the weight of liver and intestine removed from TG mice fed with high fat-protein diet was found, replicating previous results obtained.

Immunohistochemical analysis (H&E immunostaining and Sirius red) of liver and spleen removed from TG and CTR mice at 7 and 15 months of age revealed that, regardless of diets administrated, in P301L TG mice a lobular inflammatory infiltrate with increased vascularity and an initial state of fibrosis correlated to collagen infiltration was present at 7 months of age. At 15 months of age, a severe lobular inflammatory infiltrate and fibrosis in TG mice was found. This pathological state was more pronounced in TG mice fed with high fat-protein diet compared to TG mice fed with low fat-protein diet and an initial state of inflammation was also detected in CTR mice fed with high fat-protein diet.

In order to understand the causes that have generated these alterations in the liver and spleen of mouse model used in this study, plasma of TG and CTR mice were collected to value the concentration of molecules and enzymes related to hepatic activity as total cholesterol, triglycerides, alanine aminotransferase (ALT) and aspartate aminotransferase (AST) at 7 and 15 months of age. The measurement of concentration of cholesterol total had shown any significant difference between TG mice fed with different diets at 7 and 15 months of age. The measurement of concentration of triglycerides had shown at 7 months of age a significant genotype effect between TG and CTR male mice fed with diet 14, showing by an increase of triglycerides concentration in plasma of TG mice compared to CTR mice, and a significant diet effect showing by an increase of triglycerides concentration in TG mice fed with diet 18 compared to TG mice fed with diet 14. At 15 months of age any significant difference between TG and CTR mice were detected, but median levels of triglycerides measured in plasma of TG mice were higher compared to value included in reference intervals for biochemical analytes published in literature.

The measurement of concentration of ALT and AST had shown at 7 months of age a significant genotype effect between TG and CTR mice fed with diet 14 and a significant diet effect showing by an increase of ALT concentration in TG mice fed with diet 18 compared to TG mice fed with diet 14. At 15 months of age a significant diet effect in both CTR and TG mice was detected, showing by an increase of ALT and AST concentration in mice fed with diet 18 compared to mice fed with diet 14 and a significant genotype effect between female TG and CTR mice fed with diet 18 for AST analysis.

Therefore the biochemical results obtained showed that, except for the measurement of total cholesterol (which values were included into reference intervals of values for biochemical analytes), the median levels of triglycerides,

AST and ALT measured in plasma of TG mice were higher compared both to median levels measured in CTR mice both to values included in reference intervals for biochemical analytes, revealing a pathological condition in the liver associated to tauophaty in mouse model used in this study. This hepatic pathological condition was more severe in TG mice fed with high fat-protein diet, assuming an interaction between tauophaty and an excessive consumption of fats that could lead to lipotoxicity, resulting in accumulation of fats in the liver, hepatic inflammation and fibrosis. Several studies in literature described this pathological condition as nonalcoholic fatty liver disease (NAFLD), a metabolic syndrome (of which fatty liver disease is considered the hepatic manifestation) overloads tissues with lipids, leading to toxic effects such as apoptosis, insulin resistance, maladaptive autophagy, and oxidative stress [34].

NAFLD is considered a "collateral pathology" in neurodegenerative diseases, AD in particular, being the result of hepatic insulin resistance caused by deficits in brain insulin/IGF signaling due to the combined effects of insulin/IGF resistance and deficiency [35-36]. P301L TG line is used in literature for the study of its main features, as neurofibrillary tangles and hyperphosphorylated Tau, and for the study of diet effects in the brain and mitochondrial functions, not on peripheral organs [37-38].

In summary, in this study we demonstrated a correlation between hyperphosphorylated Tau, insulin/IGF resistance and high fat-protein diet consumption in P301L TG mice expressed on peripheral organs as hepatic insulin resistance and fatty accumulation in the liver, which induced nonalcoholic fatty liver disease. This correlation was confirmed by a condition of hepatomegaly characterized by the presence of lobular inflammatory infiltrate and deposits of collagen in liver and spleen, an increase of weight and size of liver and spleen, an increase of body weight due to hepatomegaly and not for the accumulation of adipose tissue, the excessive water consumption, the highest increase of median levels of triglycerides, AST and ALT in P301L TG mice fed with high-fat protein diet.

Since tauophaty defined a metabolic disease mediated by brain insulin and IGF resistance, the mouse model P301L TG used in this study could represent a valuable tool to study not only the eziopathogenesis of tauophaty, but also metabolic dysfunctions that occurred in peripheral organs neurodegenerative diseases. Moreover, preventing or reducing IGF resistance and consequently the accumulation of fats in the liver in this model may represent a system to study molecular mechanism of metabolic syndrome related to neurodegenerative disease and could finally lead to the development of potential treatments not only for tauophaty, but also for its collateral pathology as NAFLD.

6.6 ACKNOWLEDGMENTS

We thank D. Corna and Dr. Marsella for technical help.

6.7 REFERENCES

1. Frolich L, Blum-Degen D, Bernstein HG, Engelsberger S, Humrich J, Laufer S, et al. Brain insulin and insulin receptors in aging and sporadic Alzheimer's disease. J Neural Transm 1998; 105:423–38.
2. Hoyer S. Glucose metabolism and insulin receptor signal transduction in Alzheimer disease. Eur J Pharmacol 2004; 490:115–25.
3. Rivera EJ, Goldin A, Fulmer N, Tavares R, Wands JR, de la Monte SM. Insulin and insulin-like growth factor expression and function deteriorate with progression of Alzheimer's disease: link to brain reductions in acetylcholine. J Alzheimers Dis 200; 8:247–68.
4. Steen E, Terry BM, Rivera EJ, Cannon JL, Neely TR, Tavares R, et al. Impaired insulin and insulin-like growth factor expression and signaling mechanisms in Alzheimer's disease – is this type 3 diabetes. J Alzheimers Dis 200; 7:63–80.
5. De la Monte SM, Longato L, Tong M, Wands JR. Insulin resistance and neurodegeneration: roles of obesity, type 2 diabetes mellitus and non-alcoholic steatohepatitis. Curr Opin Investig Drugs 2009; 10:1049–60.
6. De la Monte SM. Therapeutic targets of brain insulin resistance in sporadic Alzheimer's disease. Front Biosci 2012; E4:1582–605.
7. Dela Monte SM, Re E, Longato L, Tong M. Dysfunctional pro-ceramide, ER stress, and insulin/IGF signaling networks with progression of Alzheimer's disease. J Alzheimers Dis 2012; 30: S217–29.
8. De la Monte SM, Tong M, Bowling N, Moskal P. si-RNA inhibition of brain insulin or insulin-like growth factor receptors causes developmental cerebellar abnormalities: relevance to fetal alcohol spectrum disorder. Mol Brain2011; 4:13.
9. Schubert M, Gautam D, Surjo D, Ueki K, Baudler S, Schubert D, et al. Role for neuronal insulin resistance in neurodegenerative diseases. Proc Natl Acad Sci USA 2004; 101:3100–5.
10. Bhat R, Xue Y, Berg S, Hellberg S, Ormo M, Nilsson Y, et al. Structural insights and biological effects of glycogen synthase kinase 3-specific inhibitor ARA014418.J Biol Chem 2003; 278:45937–45.
11. De la Monte SM, Chen GJ, Rivera E, Wands JR. Neuronal thread protein regulation and interaction with microtubule-associated proteins in SHSy5yneuronal cells. Cell Mol Life Sci 2003; 60:2679–91.

12. Capeau J. Insulin resistance and steatosis in humans. Diabetes Metab. 2008; 34(6 Pt 2):649–657.
13. Leonard BL, Watson RN, Loomes KM, Phillips AR, Cooper GJ. Insulin resistance in the Zucker diabetic fatty rat: A metabolic characterization of obese and lean phenotypes. Acta Diabetol. 2005; 42(4):162–170.
14. Tong M, Longato L, de la Monte SM. Early limited nitrosamine exposures exacerbate high fat diet-mediated type2 diabetes and neurodegeneration. BMC Endocr Dis 2010; 10:4.
15. Perry W, Hilsabeck RC, Hassanein TI. Cognitive dysfunction in chronic hepatitis C: a review. Dig Dis Sci 2008; 53:307–21.
16. Weiss JJ, Gorman JM. Psychiatric behavioral aspects of comanagement of hepatitis C virus and HIV. Curr HIV/AIDS Rep 2006; 3:176–81.
17. Tong M, Neusner A, Longato L, Lawton M, Wands JR, De la Monte SM. Nitrosamine exposure causes insulin resistance diseases: relevance to type2 diabetes mellitus, non-alcoholic steatohepatitis, and Alzheimer's disease. J Alzheimers Dis 2009; 17:827–44.
18. Kao Y, Youson JH, Holmes JA, Al-Mahrouki A, Sheridan MA. Effects of insulin on lipid metabolism of larvae and metamorphosing landlocked sea lamprey, Petromyzon marinus. Gen Comp Endocrinol 1999; 114:405–14.
19. Holland WL, Summers SA. Sphingolipids, insulin resistance, and metabolic disease: new insights from in vivo manipulation of sphingolipid metabolism. Endocr Rev 2008; 29:381–402.
20. Dowman JK, Tomlinson JW, Newsome PN. Pathogenesis of non alcoholic fatty liver disease. QJM 2010; 103:71‑83.
21. Schreuder TC, Verwer BJ, van Nieuwkerk CM, Mulder CJ. Nonalcoholic fatty liver disease: An overview of current insights in pathogenesis, diagnosis and treatment. World J Gastroenterol 2008; 14:2474‑86.
22. Donnelly KL, Smith CI, Schwarzenberg SJ, Jessurun J, Boldt MD, Parks EJ. Sources of fatty acids stored in liver and secreted via lipoproteins in patients with nonalcoholic fatty liver disease. J Clin Invest 2005; 115:1343-51.
23. Kassi E, Pervanidou P, Kaltsas G, Chrousos G. Metabolic syndrome: definitions and controversies. BMC Med 2011; 9:48.
24. Tan ZS, Beiser AS, Fox CS, Au R, Himali JJ, Debette S, et al. Association of metabolic dysregulation with volumetric brain magnetic resonance imaging and cognitive markers of subclinical brain aging in middle-aged adults: the Framingham offspring study. Diabetes Care 2011; 34:1766–70.
25. Debette S, Beiser A, Hoffmann U, Decarli C, O'Donnell CJ, Massaro JM, et al. Visceral fat is associated with lower brain volume in healthy middle-aged adults. Ann Neurol 2010; 68:136–44.

26. Hassenstab JJ, Sweat V, Bruehl H, Convit A. Metabolic syndrome is associated with learning and recall impairment in middle age. Dement Geriatr Cogn Disord 2010; 29:356–62.
27. Frisardi V, Solfrizzi V, Capurso C, Imbimbo BP, Vendemiale G, Seripa D, et al. Is insulin resistant brain state a central feature of the metabolic-cognitive syndrome? J Alzheimers Dis 2010; 21:57–63.
28. Yates KF, Sweat V, Yau PL, Turchiano MM, Convit A. Impact of metabolic syndrome on cognition and brain: a selected review of the literature. Arterioscler Thromb Vasc Biol 2012; 32:2060–7.
29. Burns JM, Honea RA, Vidoni ED, Hutfles LJ, Brooks WM, Swerd low RH. Insulin is differentially related to cognitive decline and atrophy in Alzheimer's disease and aging. Biochim Biophys Acta 2012; 1822:333–9.
30. Sontag E, Nunbhakdi-Craig V, Lee G, Bloom GS, Mumby MC. Regulation of the phosphorylation state and microtubule-binding activity of Tau by protein phosphatase 2A. Neuron. 1996; 17:1201–7.
31. Lewis, J., McGowan, E., Rockwood, J., Melrose, H., Nacaraju, P., Van Slegtenhorst, M. et al. (2000) Neurofibrillary tangles, amyotrophy and progressive motor disturbance in mice expressing mutant (P301L) tau protein. Nature Genetics 25:402-406.
32. Lewis, J., Dickson, D.W., Lin, W-L., Chisholm, L., Corral, A., Jones, G. et al. (2001) Enhanced neurofibrillary degeneration in transgenic mice expressing mutant tau and APP. Science. 93:1487-1491.
33. Cristina Mazzaccara, Giuseppe Labruna, Gennaro Cito, Marzia Scarfo`, Mario De Felice, Lucio Pastore, Lucia Sacchetti Age-Related Reference Intervals of the Main Biochemical and Hematological Parameters in C57BL/6J, 129SV/EV and C3H/HeJ Mouse Strains.
34. Mlinar B. and Marc J. New insights into adipose tissue dysfunction in insulin resistance. Clinical chemistry and laboratory medicine: CCLM/FESCC49, 1925-°©-1935(2011).
35. De la Monte SM, Tong M. Brain metabolic dysfunction at the core of Alzheimer's disease. Biochem Pharmacol. 2014 Apr 15; 88(4):548-59.
36. Kraegen EW, Cooney GJ. Free fatty acids and skeletal muscle insulin resistance. Curr Opin Lipidol 2008; 19:235–41.
37. Delic V, Brownlow M, Joly-Amado A, Zivkovic S, Noble K, Phan TA, Ta Y, Zhang Y, Bell SD, Kurien C, Reynes C, Morgan D, Bradshaw PC. Caloric restriction does not restore brain mitochondrial function in P301L tau mice, but it does decrease mitochondrial F0F1-ATPase activity.Mol Cell Neurosci. 2015 Jul; 67:46-54.
38. Glöckner F, Meske V, Lütjohann D, Ohm TG. Dietary cholesterol and its effect on tau protein: a study in apolipoprotein E-deficient and P301L human tau mice. J Neuropathol Exp Neurol. 2011 Apr;70(4):292-301.

CHAPTER 7

General Discussion

7.1 GENERAL DISCUSSION

The aim of this study, during three years of my PhD, was to investigate the effects of two different diets in a mouse model of neurodegenerative disease. The mouse model chosen for this study is P301L TG affected by tauophaty, a rare disease that manifests the typical hallmarks of Alzheimer disease, a pathology that affects 60% of the human population.

The hallmarks of tauophaty are neurofibrillary tangles consist of hyperphosphorylated tau, neurofilaments and beta amyloid in the brain, causing alteration of axonal transport, synaptic dysfunctions and neuronal loss leading to cognitive and behavioral impairments. We decided to use two different diets characterized by the different protein and fat content (diet 1: 18% protein and 5% fat, diet 2: 14% protein and 3.5% fat) based on data in literature that underling the adverse effects of a high fat-protein diet on brain functionality, influence neuronal membrane integrity, oxidative status and risk for tauopathies. Based on the manifestation of symptoms of disease described by Lewis et al. in this mouse model, we established two experimental time points at 7 and 15 months of age (the first time point the symptoms of the disease were evident expressed, the second time point: maximum survival for mice affected by tauophaty).

In this study we investigated at 7 and 15 months of age the effects of different diets on P301L TG and CTR mice valuating metabolic, behavioral and cognitive activities; for the metabolic activities we analyzed survival rate, body weight gain and food and water consumption of animals. For behavioral activities we valuated mnemonic, locomotor and exploratory performances of animals; for cognitive activities we investigated the cognitive impairment (identifying agglomerates of hyperphosphorylated tau, neuronal loss, astrogliosis and oxidative damage) using immunohistochemical analysis and neuronal counts.

We started the study characterizing P301L TG mouse model that replicated the impairments found in patients affected by tauophaty in a way age-gender-dependent underling an important interaction between gender and pathology until now yet never reported in tauophaty models. Female TG mice had strong cognitive impairment strongly correlated with an increase in P-Tau, in both cerebral cortex and hippocampus, as well as astrogliosis. After characterization of P301L TG model, we evaluated how two different diets (low protein-fat diet and high protein-fat diet) can interact with genotype, sex and age of P301L TG mice and can improve Tau pathology.

Administrating a low fat-protein diet we found an improvement of pathological conditions associated with our mouse model of tauophaty, occurred with an increased lifespan, a reduction of food and water consumption, a reduction of aggregates of hyperphosphorylated tau and neuronal loss, more pronounced in female than male TG mice at 7 months of age, since 15 months of age a time point which pathological conditions are too severe.

Since oxidative damage is a neuropathological hallmark of tauopathies and strictly correlated to nutrition, we decided to investigate the oxidative damage in this model of tauophaty and to explore the possible mechanisms through which diets can interact and improve a possible condition of oxidative stress. We found an oxidative damage associated with our mouse model of tauophaty in a way age-gender-dependent, confirming an increase of oxidative damage in female TG mice. Administrating a low fat-protein diet we found an improvement of oxidative damage in TG mice, occurred with a decreased of immunopositive cells numbers correlated to oxidative markers used for immunohistochemistry, more pronounced in female than male TG mice. During necropsy analysis performed after the behavioral tests in TG and CTR mice fed with different diets, we observed an alteration of the size of the liver and spleen in TG mice fed with a high fat-protein diet at 7 and 15 months of age. This apparent condition of hepatomegaly was associated to an increase of body weight, food and water consumption in TG mice fed with high fat-protein diet.

Based on our previous data and literature, we assumed that P301L mice could be affected by nonalcoholic fatty liver disease (NAFLD), a metabolic syndrome correlated to neurodegenerative disease caused by insulin/IGF resistance, accumulation of fats in liver, hepatic inflammation and fibrosis. So we decided to investigate this pathological condition in TG and CTR mice at 7 and 15 months of age fed with different diets evaluating: macroscopy and histopathology of various tissues such as liver and spleen, the concentration of cholesterol, triglycerides, alanine aminotransferase and aspartate aminotransferase in plasma of these animals. We found a correlation between hyperphosphorylated Tau, insulin/IGF resistance and high fat-protein diet consumption in TG mice fed with a high fat-protein diet at 7 and 15 months of age expressed on peripheral organs as hepatic insulin resistance and fatty accumulation in the liver, which induced nonalcoholic fatty liver disease.

This correlation was confirmed by a condition of hepatomegaly characterized by the presence of lobular inflammatory infiltrate and deposits of collagen in liver and spleen, an increase of weight and size of liver and spleen, an increase of

body weight due to hepatomegaly and not for the accumulation of adipose tissue, the excessive water consumption, the highest increase of median levels of triglycerides, AST and ALT in P301L TG mice fed with high-fat protein diet.

7.2 CONCLUDING REMARKS AND FUTURE PROSPECTIVES

In conclusion, in this study we demonstrated the importance of interaction between nutrition and neurodegeneration and the role that different diets can have on the onset and development of tauophaty, obtaining an improvement of pathological conditions administrating a low fat-protein diet. Also an improvement of welfare, represented by an increase in survival, both in control and transgenic animals fed with a low fat-protein diet was detected. We found an important interaction between tauophaty and consumption of high fat-protein diet that lead to the onset of metabolic syndrome as nonalcoholic fatty liver disease.

Since this important interaction between tauophaty and consumption of high fat-protein until now yet never reported in tauophaty models, a more detailed investigation on the possible mechanisms of action that leading to metabolic syndrome will be performed. In particular, we will investigate the insulin/IGF signaling on brain and peripheral organs, valuating the concentration of insulin/glucagon on plasma and in liver and pancreas of P301L TG mice. Results obtained in this study suggest that P301L-Tau model could represent a valuable tool to study the role and the mechanisms through hyperphosphorylation and Tau aggregation leading to cognitive and memory impairment. Using the influence of nutrition for preventing or reducing the accumulation of hyperphosphorylated tau in this model could finally lead to the development of preventive potential treatments for tauopathies.

CHAPTER 8

Summary

Effects of different diets in a mouse model of neurodegeneration

Abstract

Tauopathies are neurodegenerative disorders characterized by the accumulation of abnormal Tau protein leading to cognitive and/or motor dysfunction; several studies suggest that dietary manipulations are increasingly viewed as possible approaches to treating neurodegenerative diseases. The mouse model chosen for this study was P301L; mice expressing P301L mutant Tau mimics features of human tauopathies and provides a model for investigating the neuropathogenesis of diseases. In this study we investigate at 7 and 15 months of age the effects of different diets (high fat-protein diet and low fat-protein diet) on P301L TG and CTR mice valuating metabolic, behavioral and cognitive activities; for the metabolic activities we analyzed survival rate, body weight gain and food and water consumption of animals. For behavioral activities we valuated mnemonic, locomotor and exploratory performances of animals; for cognitive activities we investigated the cognitive impairment (identifying agglomerates of hyperphosphorylated tau, neuronal loss, astrogliosis and oxidative damage) using immunohistochemical analysis and neuronal counts. We characterized P301L TG mouse model (trial 1-3) that replicated the impairments found in patients affected by tauophaty in a way age-gender-dependent showing in female TG mice a strong cognitive impairment strictly correlated with an increase in P-Tau, in both cerebral cortex and hippocampus, as well as astrogliosis and oxidative damage. We found an improvement of pathological conditions in TG mice administrating a low fat-protein diet in a way age-gender-dependent (trial 2-3), occurred with an increased lifespan, a reduction of food and water consumption, a reduction of aggregates of P-Tau, neuronal loss, astrogliosis and oxidative damage. We found an interaction between tauophaty and consumption of high fat-protein expressed on peripheral organs as hepatic insulin resistance and fatty accumulation in the liver, which induced nonalcoholic fatty liver disease in TG mice (trial 4). The correlation between P-Tau, insulin/IGF resistance and high fat-protein diet consumption was expressed by a condition of hepatomegaly characterized by the presence of lobular inflammatory infiltrate and deposits of collagen in liver and spleen, an increase of weight and size of liver and spleen, the highest increase of median levels of triglycerides, AST and ALT in P301L TG mice fed with high-fat protein diet in a

way age-gender-dependent. In summary, we demonstrated the importance of interaction between nutrition and neurodegeneration and the role that different diets can have on the onset and development of tauophaty, obtaining an improvement of pathological conditions administrating a low fat-protein diet. Results obtained in this study suggest that P301L-Tau model could represent a valuable tool to study the role and the mechanisms through hyperphosphorylation and Tau aggregation leading to cognitive and memory impairment. Using the influence of nutrition for preventing or reducing the accumulation of hyperphosphorylated tau in this model could finally lead to the development of preventive potential treatments for tauopathies.

CHAPTER 9

References

9. REFERENCES

1. Pick A. On the relations of senile brain atrophy for aphasia. (1892) Prager Med Wochenschr 16: 765-767.
2. Alzheimer A. About strange illness of later ages. (1911) Z ges Neurol Psychiat 4: 356-385.
3. Rewcastle NB, Ball MJ Electron microscopic structure of the inclusion bodies in Pick's disease. Neurology (1968) 18:1205–1213.
4. Pollock NJ, Mirra SS, Binder LI, Hansen LA, Wood JG Filamentous aggregates in Pick's disease, progressive supranuclear palsy, and Alzheimer's disease share antigenic determinants with microtubule-associated protein tau. (1986) Lancet II: 1211.
5. Probst A, Tolnay M, Langui D, Goedert M, Spillantini MG. Pick's disease: hyperphosphorylated tau segregates to the somatoaxonal compartment. (1996) Acta Neuropathol (Berl) 92:588–596.
6. Alzheimer A. About a rare disease of the cortex. Generic Z Psychiatr Psych Judiciary (1907) Med 64:146–148.
7. Spillantini MG, Goedert M (1998) Tau protein pathology in neurodegenerative diseases. Trends Neurosci 21:428–433.
8. Rocca WA, Hofman A, Brayne C, Breteler MM, Clarke M, Copeland JR, Dartigues JF, Engedal K, Hagnell O, Heeren TJ, et al. Frequency and distribution of Alzheimer's disease in Europe: a collaborative study of 1980-1990 prevalence findings. The EURODEM-Prevalence Research Group. Ann Neurol. 1991 Sep; 30(3):381-90.
9. Onorato M, Mulvihill P, Connolly J, Galloway P, Whitehouse P, Perry G. Alteration of neuritic cytoarchitecture in Alzheimer disease. Prog Clin Biol Res. 1989; 317:781-9. Review.
10. Braak H, Braak E. On areas of transition between entorhinal allocortex and temporal isocortex in the human brain. Normal morphology and lamina-specific pathology in Alzheimer's disease. Acta Neuropathol. 1985; 68(4):325-32.
11. Hyman BT, Trojanowski JQ. Consensus recommendations for the postmortem diagnosis of Alzheimer disease from the National Institute on Aging and the Reagan Institute Working Group on diagnostic criteria for the neuropathological assessment of Alzheimer disease. J Neuropathol Exp Neurol. 1997 Oct; 56(10):1095-7.
12. Holzer M, Holzapfel HP, Zedlick D, Brückner MK, Arendt T. Abnormally phosphorylated tau protein in Alzheimer's disease:

heterogeneity of individual regional distribution and relationship to clinical severity. Neuroscience. 1994 Nov; 63(2):499-516.
13. Hodges JR, Davies R, Xuereb J, Kril J, Halliday G. Survival in frontotemporal dementia. Neurology. 2003 Aug 12; 61(3):349-54.
14. Neary D, Snowden JS, Gustafson L, Passant U, Stuss D, Black S, Freedman M, Kertesz A, Robert PH, Albert M, Boone K, Miller BL, Cummings J, Benson DF. Frontotemporal lobar degeneration: a consensus on clinical diagnostic criteria. Neurology. 1998 Dec; 51(6):1546-54. Review.
15. Poorkaj P, Grossman M, Steinbart E, Payami H, Sadovnick A, Nochlin D, Tabira T, Trojanowski JQ, Borson S, Galasko D, Reich S, Quinn B, Schellenberg G, Bird TD. Frequency of tau gene mutations in familial and sporadic cases of non-Alzheimer dementia. Arch Neurol. 2001 Mar; 58(3):383-7.
16. Poorkaj P, Kas A, D'Souza I, Zhou Y, Pham Q, Stone M, Olson MV, Schellenberg GD. A genomic sequence analysis of the mouse and human microtubule-associated protein tau. Mamm Genome. 2001 Sep; 12(9):700-12.
17. Mackenzie IR, Baker M, Pickering-Brown S, Hsiung GY, Lindholm C, Dwosh E, Gass J, Cannon A, Rademakers R, Hutton M, Feldman HH. The neuropathology of frontotemporal lobar degeneration caused by mutations in the progranulin gene. Brain. 2006 Nov; 129(Pt 11):3081-90.
18. Hodges JR, Davies RR, Xuereb JH, Casey B, Broe M, Bak TH, Kril JJ, Halliday GM. Clinicopathological correlates in frontotemporal dementia. Ann Neurol. 2004 Sep; 56(3):399-406.
19. Spillantini MG, Goedert M, Crowther RA, Murrell JR, Farlow MR, Ghetti B. Familial multiple system tauopathy with presenile dementia: a disease with abundant neuronal and glial tau filaments. Proc Natl Acad Sci U S A. 1997 Apr 15; 94(8):4113-8.
20. Bugiani O, Murrell JR, Giaccone G, Hasegawa M, Ghigo G, Tabaton M, Morbin M, Primavera A, Carella F, Solaro C, Grisoli M, Savoiardo M, Spillantini MG, Tagliavini F, Goedert M, Ghetti B. Frontotemporal dementia and corticobasal degeneration in a family with a P301S mutation in tau. J Neuropathol Exp Neurol. 1999 Jun; 58(6):667-77.
21. Sperfeld AD, Collatz MB, Baier H, Palmbach M, Storch A, Schwarz J, Tatsch K, Reske S, Joosse M, Heutink P, Ludolph AC. FTDP-17: an

early-onset phenotype with parkinsonism and epileptic seizures caused by a novel mutation. Ann Neurol. 1999 Nov;46(5):708-15.

22. Hogg M, Grujic ZM, Baker M, Demirci S, Guillozet AL, Sweet AP, Herzog LL, Weintraub S, Mesulam MM, LaPointe NE, Gamblin TC, Berry RW, Binder LI, de Silva R, Lees A, Espinoza M, Davies P, Grover A, Sahara N, Ishizawa T, Dickson D, Yen SH, Hutton M, Bigio EH. The L266V tau mutation is associated with frontotemporal dementia and Pick-like 3R and 4R tauopathy. Acta Neuropathol. 2003 Oct; 106(4):323-36.
23. Van Swieten JC, Stevens M, Rosso SM, Rizzu P, Joosse M, de Koning I, Kamphorst W, Ravid R, Spillantini MG, Niermeijer, Heutink P. Phenotypic variation in hereditary frontotemporal dementia with tau mutations. Ann Neurol. 1999 Oct; 46(4):617-26.
24. Bugiani O. Pathogenesis of Alzheimer's disease and dementia. Rev Neurol (Paris). 1999; 155 Suppl 4: S28-32. Review.
25. Harada A, Oguchi K, Okabe S, Kuno J, Terada S, Ohshima T, Sato-Yoshitake R, Takei Y, Noda T, Hirokawa N. Altered microtubule organization in small-calibre axons of mice lacking tau protein. Nature. 1994 Jun 9;369(6480):488-91
26. Ebneth A, Godemann R, Stamer K, Illenberger S, Trinczek B, Mandelkow E. Overexpression of tau protein inhibits kinesin-dependent trafficking of vesicles, mitochondria, and endoplasmic reticulum: implications for Alzheimer's disease. J Cell Biol. 1998 Nov 2; 143(3):777-94.
27. Neve RL, Selkoe DJ, Kurnit DM, Kosik KS. A cDNA for a human microtubule associated protein 2 epitope in the Alzheimer neurofibrillary tangle. Brain Res. 1986 Nov; 387(2):193-6.
28. Goedert M, Spillantini MG, Jakes R, Rutherford D, Crowther RA. Multiple isoforms of human microtubule-associated protein tau: sequences and localization in neurofibrillary tangles of Alzheimer's disease. Neuron. 1989 Oct; 3(4):519-26.
29. Goedert M, Crowther RA. Amyloid plaques, neurofibrillary tangles and their relevance for the study of Alzheimer's disease. Neurobiol Aging. 1989 Sep-Oct; 10(5):405-6; discussion 412-4.
30. Goedert M, Jakes R, Spillantini MG, Crowther RA, Cohen P, Vanmechelen E, Probst A, Götz J, Bürki K. Tau protein in Alzheimer's disease. Biochem Soc Trans. 1995 Feb; 23(1):80-5. Review.

31. Ingelson M1, Vanmechelen E, Lannfelt L. Microtubule-associated protein tau in human fibroblasts with the Swedish Alzheimer mutation. Neurosci Lett. 1996 Dec 6; 220(1):9-12.
32. Thurston VC, Zinkowski RP, Binder LI. Tau as a nucleolar protein in human non neural cells in vitro and in vivo. Chromosoma. 1996 Jul; 105(1):20-30.
33. Mandell JW, Banker GA. A spatial gradient of tau protein phosphorylation in nascent axons.J Neurosci. 1996 Sep 15; 16(18):5727-40.
34. Al-Bassam J, Ozer RS, Safer D, Halpain S, Milligan RA. MAP2 and tau bind longitudinally along the outer ridges of microtubule protofilaments. J Cell Biol. 2002 Jun 24; 157(7):1187-96.
35. Kar S, Fan J, Smith MJ, Goedert M, Amos LA. Repeat motifs of tau bind to the insides of microtubules in the absence of taxol. EMBO J. 2003 Jan 2; 22(1):70-7.
36. Knops J, Kosik KS, Lee G, Pardee JD, Cohen-Gould L, McConlogue L. Overexpression of tau in a non-neuronal cell induces long cellular processes. J Cell Biol. 1991 Aug; 114(4):725-33.
37. Goedert M, Spillantini MG. Tau gene mutations and neurodegeneration. Biochem Soc Symp. 2001 ;(67):59-71. Review.
38. Iqbal K, Liu F, Gong CX, Alonso Adel C, Grundke-Iqbal I. Mechanisms of tau-induced neurodegeneration. Acta Neuropathol. 2009 Jul; 118(1):53-69. Review.
39. Noble W, Hanger DP, Miller CC, Lovestone S. The importance of tau phosphorylation for neurodegenerative diseases. Front Neurol. 2013 Jul 1; 4:83. eCollection 2013.
40. Goedert M, Hasegawa M, Jakes R, Lawler S, Cuenda A, Cohen P. Phosphorylation of microtubule-associated protein tau by stress-activated protein kinases. FEBS Lett. 1997 Jun 2;409(1):57-62.
41. Drewes G1, Lichtenberg-Kraag B, Döring F, Mandelkow EM, Biernat J, Goris J, Dorée M, Mandelkow E. Mitogen activated protein (MAP) kinase transforms tau protein into an Alzheimer-like state. EMBO J. 1992 Jun;11(6):2131-8.
42. Geddes JF1, Hughes AJ, Lees AJ, Daniel SE. Pathological overlap in cases of Parkinsonism associated with neurofibrillary tangles. A study of recent cases of post encephalitic Parkinsonism and comparison with progressive supranuclear palsy and Guamanian parkinsonism-dementia complex. Brain. 1993 Feb; 116 (Pt 1):281-302.

43. Goedert, M., Jakes, R., Qi, Z., Wang, J. H. and Cohen, P. Protein phosphatase 2A is the major enzyme in brain that dephosphorylates tau protein phosphorylated by proline directed protein kinases or cyclic AMP-dependent protein kinase. (1995) J. Neurochem. 65, 2804 – 2807.
44. Gong, C. X., Lidsky, T., Wegiel, J., Zuck, L., Grundke-Iqbal, I. and Iqbal, K. Phosphorylation of microtubule-associated protein tau is regulated by protein phosphatase 2A in mammalian brain. Implications for neurofibrillary degeneration in Alzheimer s disease. (2000) J. Biol. Chem. 275, 5535–5544.
45. Sontag, E., Nunbhakdi Craig, V., Lee, G., Brandt, R., Kamibayashi, C., Kuret, J., White, C. L., Mumby, M. C. and Bloom, G. S. Molecular interactions among protein phosphatase 2A, tau, and microtubules-implications for the regulation of tau phosphorylation and the development of tauopathies. (1999) J. Biol. Chem. 274, 25490 – 25498.
46. Goedert, M., Satumtira, S., Jakes, R., Smith, M. J., Kamibayashi, C.,White, C. L., 3rd and Sontag, E. Reduced binding of protein phosphatase 2A to tau protein with frontotemporal dementia and parkinsonism linked to chromosome 17 mutations. (2000) J. Neurochem. 75, 2155 – 2162.
47. Kovacs GG, Botond G, Budka H. Protein coding of neurodegenerative dementias: the neuropathological basis of biomarker diagnostics. Acta Neuropathol. 2010 Apr; 119(4):389-408. Review.
48. Delacourte A, Buée L. Tau pathology: a marker of neurodegenerative disorders. Curr Opin Neurol. 2000 Aug; 13(4):371-6. Review.
49. Stamer K, Vogel R, Thies E, Mandelkow E, Mandelkow EM. Tau blocks traffic of organelles, neurofilaments, and APP vesicles in neurons and enhances oxidative stress. J Cell Biol. 2002 Mar 18; 156(6):1051-63.
50. Goedert M. Tau gene mutations and their effects. Mov Disord. 2005 Aug; 20 Suppl 12: S45-52.
51. Zilka N, Korenova M, Novak M. Misfolded tau protein and disease modifying pathways in transgenic rodent models of human tauopathies. Acta Neuropathol. 2009 Jul;118(1):71-86. Review.
52. Salehi A, Delcroix JD, Mobley WC. Traffic at the intersection of neurotrophic factor signaling and neurodegeneration. Trends Neurosci. 2003 Feb; 26(2):73-80.
53. J.P. Brion, G. Tremp, J.N. Octave, Transgenic expression of this shortest human tau affects its compartmentalization and its

phosphorylation as in the pretangle stage of Alzheimer's disease, Am. J. Pathol. 154 (1999) 255– 270.

54. Gotz J, Chen F, Barmettler R, Nitsch RM: Tau filament formation in transgenic mice expressing P301L tau. J Biol Chem 2001, 276:529–534
55. Lewis, J., McGowan, E., Rockwood, J., Melrose, H., Nacaraju, P., Van Slegtenhorst, M. et al. (2000) Neurofibrillary tangles, amyotrophic and progressive motor disturbance in mice expressing mutant (P301L) tau protein. Nature Genetics 25:402-406.
56. Lewis, J., Dickson, D.W., Lin, W-L., Chisholm, L., Corral, A., Jones, G. et al. (2001) Enhanced neurofibrillary degeneration in transgenic mice expressing mutant tau and APP. Science. 93:1487-1491.
57. Allen B, Ingram E, Takao M, Smith MJ, Jakes R, Virdee K. et al. Abundant tau filaments and non-apoptotic neurodegeneration in transgenic mice expressing human P301S tau protein.J Neurosci. 2002 Nov 1; 22(21):9340-51.
58. Tatebayashi Y, Miyasaka T, Chui DH, Akagi T, Mishima K, Iwasaki K, Fujiwara M, Tanemura K, Murayama M, Ishiguro K, Planel E, Sato S, Hashikawa T, Takashima A. Tau filament formation and associative memory deficit in aged mice expressing mutant (R406W) human tau. Proc Natl Acad Sci U S A. 2002 Oct 15;99(21):13896-901.
59. Tanemura K, Akagi T, Murayama M, Kikuchi N, Murayama O, Hashikawa T, Yoshiike Y, Park JM, Matsuda K, Nakao S, Sun X, Sato S, Yamaguchi H, Takashima A. Formation of filamentous tau aggregations in transgenic mice expressing V337M human tau. Neurobiol Dis. 2001 Dec;8(6):1036-45
60. Higuchi M, Zhang B, Forman MS, Yoshiyama Y, Trojanowski JQ, Lee VM. Axonal degeneration induced by targeted expression of mutant human tau in oligodendrocytes of transgenic mice that model glial tauopathies. J Neurosci. 2005 Oct 12; 25(41):9434-43.
61. Forman MS, Lal D, Zhang B, Dabir DV, Swanson E, Lee VM, Trojanowski JQ. Transgenic mouse model of tau pathology in astrocytes leading to nervous system degeneration. J Neurosci. 2005 Apr 6; 25(14):3539-50.
62. Montine KS, Quinn JF, Zhang J, Fessel JP, Roberts LJ 2nd, Morrow JD, Montine TJ. Isoprostanes and related products of lipid peroxidation in neurodegenerative diseases. Chem Phys Lipids. 2004 Mar; 128(1-2):117-24. Review.

63. Cherubini A, Ruggiero C, Polidori MC, Mecocci P. Potential markers of oxidative stress in stroke. Free Radic Biol Med. 2005 Oct 1; 39(7):841-52. Review.
64. Uttara B, Singh AV, Zamboni P, Mahajan RT. Oxidative stress and neurodegenerative diseases: a review of upstream and downstream antioxidant therapeutic options. Curr Neuropharmacol. 2009 Mar; 7(1):65-74.
65. Nunomura A, Perry G, Aliev G, Hirai K, Takeda A, Balraj EK, Jones PK, Ghanbari H, Wataya T, Shimohama S, Chiba S, Atwood CS, Petersen RB, Smith MA. Oxidative damage is the earliest event in Alzheimer disease J Neuropathol Exp Neurol. 2001 Aug; 60(8):759-67.
66. Gómez-Ramos A, Díaz-Nido J, Smith MA, Perry G, Avila J. Effect of the lipid peroxidation product acrolein on tau phosphorylation in neural cells. J Neurosci Res. 2003 Mar 15; 71(6):863-70.
67. Takeda A, Smith MA, Avilá J, Nunomura A, Siedlak SL, Zhu X, Perry G, Sayre LM. In Alzheimer's disease, heme oxygenase is coincident with Alz50, an epitope of tau induced by 4-hydroxy-2-nonenal modification. J Neurochem. 2000 Sep; 75(3):1234-41.
68. Takeda M, Shinosaki K, Nishikawa T, Tanaka T, Kudo T, Nakamura Y, Kashiwagi Y. Understanding of molecular pathogenesis of Alzheimer's disease: implications for drug development. Nihon Yakurigaku Zasshi. 2000 Feb; 115(2):79-88.
69. Christen Y. Oxidative stress and Alzheimer disease. Am J Clin Nutr. 2000 Feb; 71(2):621S-629S. Review.
70. Mariani SM. Phytoestrogens and antioxidants--bits of experimental evidence. Med Gen Med. 2005 Jan 24;7(1):25
71. Ruegsegger GN, Toedebusch RG, Braselton JF, Roberts CK, Booth FW. Reduced metabolic disease risk profile by voluntary wheel running accompanying juvenile Western diet in rats bred for high and low voluntary exercise. Physiol Behav. 2015 Sep 11; 152(Pt A):47-55.
72. Jackman MR, MacLean PS, Bessesen DH. Energy expenditure in obesity-prone and obesity-resistant rats before and after the introduction of a high-fat diet. Am J Physiol Regul Integr Comp Physiol. 2010 Oct; 299(4): R1097-105.
73. Wolozin B, Brown J 3rd, Theisler C, Silberman S. The cellular biochemistry of cholesterol and statins: insights into the pathophysiology and therapy of Alzheimer's disease. CNS Drug Rev. 2004 summer; 10(2):127-46. Review.

74. Freund-Levi Y, Eriksdotter-Jönhagen M, Cederholm T, Basun H, Faxén-Irving G, Garlind A, Vedin I, Vessby B, Wahlund LO, Palmblad J. Omega-3 fatty acid treatment in 174 patients with mild to moderate Alzheimer disease: Omeg AD study: a randomized double-blind trial. Arch Neurol. 2006 Oct; 63(10):1402-8.
75. Hashimoto M, Hossain S, Agdul H, Shido O. Docosahexaenoic acid-induced amelioration on impairment of memory learning in amyloid beta-infused rats relates to the decreases of amyloid beta and cholesterol levels in detergent-insoluble membrane fractions. Biochim Biophys Acta. 2005 Dec 30; 1738(1-3):91-8.
76. Bourre JM, Paquotte P. Seafood (wild and farmed) for the elderly: contribution to the dietary intakes of iodine, selenium, DHA and vitamins B12 and D. J Nutr Health Aging. 2008 Mar; 12(3):186-92.
77. Bourre JM. Effects of nutrients (in food) on the structure and function of the nervous system: update on dietary requirements for brain. Part 1: micronutrients. J Nutr Health Aging. 2006 Sep-Oct; 10(5):377-85. Review.
78. Bourre JM. Effects of nutrients (in food) on the structure and function of the nervous system: update on dietary requirements for brain. Part 2: macronutrients. J Nutr Health Aging. 2006 Sep-Oct; 10(5):386-99. Review.
79. Mariani E, Polidori MC, Cherubini A, Mecocci P. Oxidative stress in brain aging, neurodegenerative and vascular diseases: an overview. J Chromatogr B Analyt Technol Biomed Life Sci. 2005 Nov 15; 827(1):65-75.
80. Lovell MA, Markesbery WR. Oxidative DNA damage in mild cognitive impairment and late-stage Alzheimer's disease. Nucleic Acids Res. 2007; 35(22):7497-504.
81. Kalmijn S, Feskens EJ, Launer LJ, Kromhout D. Polyunsaturated fatty acids, antioxidants, and cognitive function in very old men. Am J Epidemiol. 1997 Jan 1; 145(1):33-41.
82. Luchsinger JA, Tang MX, Shea S, Mayeux R. Caloric intake and the risk of Alzheimer disease. Arch Neurol. 2002 Aug; 59(8):1258-63.
83. Greenwood CE, Winocur G. High-fat diets, insulin resistance and declining cognitive function. Neurobiol Aging. 2005 Dec; 26. Review.
84. Chitturi S, Farrell GC. Etiopathogenesis of nonalcoholic steatohepatitis. Semin Liver Dis 2001; 21:27–41

85. Brewer GJ. Epigenetic oxidative redox shift (EORS) theory of aging unifies the free radical and insulin signaling theories. Exp Gerontol 2010; 45:173–9
86. Pessayre D. Role of mitochondria in non-alcoholic fatty liver disease. J Gastroenterol Hepatol 2007;22 (Suppl 1): S20–7
87. Yehuda S, Rabinovitz S, Carasso RL, Mostofsky DI. Fatty acids and brain peptides. Peptides. 1998; 19(2):407-19. Review.
88. Marszalek JR, Lodish HF. Docosahexaenoic acid, fatty acid-interacting proteins, and neuronal function: breastmilk and fish are good for you. Annu Rev Cell Dev Biol. 2005; 21:633-57. Review.
89. Conquer JA, Tierney MC, Zecevic J, Bettger WJ, Fisher RH. Fatty acid analysis of blood plasma of patients with Alzheimer's disease, other types of dementia, and cognitive impairment. Lipids. 2000 Dec; 35(12):1305-12.
90. Ikemoto A, Ohishi M, Sato Y, Hata N, Misawa Y, Fujii Y, Okuyama H. Reversibility of n-3 fatty acid deficiency-induced alterations of learning behavior in the rat: level of n-6 fatty acids as another critical factor. J Lipid Res. 2001 Oct; 42(10):1655-63.
91. Björkhem I, Lütjohann D, Diczfalusy U, Ståhle L, Ahlborg G, Wahren J. Cholesterol homeostasis in human brain: turnover of 24S-hydroxycholesterol and evidence for a cerebral origin of most of this oxysterol in the circulation. J Lipid Res. 1998 Aug; 39(8):1594-600.
92. Govoni S, Lanni C, Racchi M. Advances in understanding the pathogenetic mechanisms of Alzheimer's disease. Funct Neurol. 2001; 16 (4 Suppl):17-30. Review.
93. Yan C, Huang D, Zhang Y. The involvement of ROS overproduction and mitochondrial dysfunction in PBDE-47-induced apoptosis on Jurkat cells. Exp Toxicol Pathol. 2011 Jul; 63(5):413-7.
94. Halliwell B. Oxidative stress in cell culture: an under-appreciated problem? FEBS Lett. 2003 Apr 10; 540(1-3):3-6.
95. Hooijmans CR, Graven C, Dederen PJ, Tanila H, van Groen T, Kiliaan AJ. Amyloid beta deposition is related to decreased glucose transporter-1 levels and hippocampal atrophy in brains of aged APP/PS1 mice. Brain Res. 2007 Nov 21; 1181:93-103.
96. Oksman M, Iivonen H, Hogyes E, Amtul Z, Penke B, Leenders I, Broersen L, Lütjohann D, Hartmann T, Tanila H. Impact of different saturated fatty acid, polyunsaturated fatty acid and cholesterol

containing diets on beta-amyloid accumulation in APP/PS1 transgenic mice. Neurobiol Dis. 2006 Sep; 23(3):563-72.

97. Leiter EH, Coleman DL, Ingram DK, Reynolds MA. Influence of dietary carbohydrate on the induction of diabetes in C57BL/KsJ-db/db diabetes mice. J Nutr. 1983 Jan; 113(1):184-95.
98. Keith MO, Bell JM Digestibility of nitrogen and amino acids in selected protein sources fed to mice. J Nutr. 1988 May; 118(5):561-8.
99. Knapka JJ, Smith KP, Judge FJ. Effect of open and closed formula rations on the performance of three strains of laboratory mice. Lab Anim Sci. 1974 Jun; 24(3):480-7.

CHAPTER 10

Full papers published during the PhD period:

10a) Consistency of ventilation in IVCs and open cages: their normoxic atmosphere and its impact on haematological parameters of mice

10b) The effect of two different Individually Ventilated Cage systems on anxiety-related behavior and welfare in two strains of laboratory mouse

CHAPTER 10 (section a)

Consistency of ventilation in IVCs and open cages: their normoxic atmosphere and its impact on haematological parameters of mice

Published on: Iat Journal Animal Technology and Welfare.
Aug 2013 Vol. 12 N°2 pag. 83-86

10a. Consistency of ventilation in IVCs and open cages: their normoxic atmosphere and its impact on hematological parameters of mice

AUTHORS: Gianpaolo Milite[1] and Lucia Buccarello[2]
[1] Corresponding author: Scientific Consultant Udine, Italy
[2]Veterinary Sciences for Animal Health and Food Safety, University of Milan, Italy

10.1 ABSTRACT

Oxygen concentration in an Individually Ventilated Caging systems (IVCs) was recently found to be slightly lower than optimal for an ideal microenvironment to house laboratory mice. Given the substantial technical differences between IVCs of different designs, which may yield dissimilar intra-cage environmental conditions, it was decided to monitor the micro-environment of an Individually Ventilated Cage (IVC) system and an open cage system and compare the impact on Red Blood Cell (RBC) count and related parameters in C57Bl/6J mice housed either in ventilated or open cages.
A small decrease in the intra-cage oxygen level was detected in both cage systems when approaching the cage change procedure (performed every two weeks). No differences in the hematological parameters were detectable after 6 weeks conditioning of mice in either of the two systems.
The IVC microenvironment was shown to be free from any impact on the hematological parameters taken into consideration in this trial when compared to the "open cage" set-up.

10.2 INTRODUCTION

There are a number of parameters used to assess the welfare of animals used in research, each contributing to the description of the physical and psychological health status. From a simple evaluation of appearance, coat condition, body weight, gait, posture, feeding and drinking behavior, urination and defecation to faecal or blood cortisol, the list of welfare indicators can be very long.
The choice of the most appropriate indicator is mainly down to the potential effect caused by the "factor" under investigation and hematological parameters are certainly very good indicators of state of animal health. Red Blood Cell count, total hemoglobin (Hgb) and hematocrit (HCT) are potential indicators when studying the environmental "fresh air" availability in terms of gas composition in Individually Ventilated caging systems.
The impact on the above mentioned blood parameters might be due to a reduced quality of the air because a decreased percentage of oxygen, lower than

20.9% or an increased CO_2 concentration. If alterations of intra-cage atmosphere are accepted when an IVC is not ventilated (static), it is not acceptable to detect a constant modification of its microenvironment, in terms of oxygen reduction, during standard operations.

Removal of pollutants like ammonia (NH_3) and CO_2 from a ventilated environment, stability of desired temperature and relative humidity is achieved through an efficient ventilation, an acceptable concentration of oxygen (O_2) is also maintained, provided that at room level the same parameters are controlled and within regulatory acceptable ranges.

Intra-cage microenvironment has been widely investigated especially in Individually Ventilated Cages due to their confined environmental condition.

Consistent differences between IVC systems operating at different air changes per hour and mode of air distribution have been shown to create diversity in the microenvironment: ammonia, CO_2 and oxygen with possible impact on breeding performances[1].

Some authors failed to find a relation between different concentrations of NH_3 in the cage and respiratory tract lesions[2], whereas more recently others have described the connection between cumulative pollutants (NH_3) and nasal histological identifiable lesions[3]; nevertheless, intra-cage oxygen concentration was not reported by these investigators.

Oxygen concentration was taken into consideration when a disposable cage was tested under static conditions up to six hours, showing consistent reduction of O_2 in relation with cage occupancy and time[4].

A recently published scientific paper[5] describes the impact due to reduced oxygen concentration on mouse Red Blood Cells count, hemoglobin and hematocrit, all of which increased when mice are maintained in a ventilated caging system operated at 60 Air Changes per Hour (ACH) and the air is injected at animal level vs the open cage control group.

Individually ventilated caging systems vary considerably in terms of solutions found to move the air inside the cages and the flow rate suggested by the manufacturer. The main consequence of the two mentioned substantial differences is the efficiency of ventilation responsible for the quality of the microenvironment in the cage[6].

Owing to these differences in design and performances, it was decided to test an IVC system with technical and operating solutions very different from that tested by York et al[5], to understand if the problem identified by the authors can be generalized to IVCs or is specific of that equipment.

10.3 MATERIALS AND METHODS

10.3.1 Animals and housing

A total of 24 Male C57Bl/6J (Harlan Laboratories, Italy), Specified Pathogen Free mice, 4 weeks old at arrival, weaned and maintained in open cages were randomly distributed 4 to a cage, three cages x 2 groups (open and IVC).
In addition, four mice were distributed two to a cage (one cage x group, two mice each). Prior to distribution to the assigned caging group, all mice were maintained at the same density in open cages for one week.
Each cage was filled with 150 g of autoclaved corncob bedding. Autoclaved diet was distributed and weighed on a weekly basis.
Autoclaved filtered water was provided by bottles (270 ml capacity); bottles were singly weighed when filled and after one week during change.
All mice were weighed after the random distribution to each cage. Cages were GM500 (Tecniplast S.p.a VA, Italy) 500 cm^2 each of usable surface with wire top cage lids that were either open to the environment or connected to a positive pressure mode Air Handling Unit set at 75 Air Changes Hour (ACH) in positive pressure according to the manufacturer's specification. The Air Handling Unit is connected to the rack by flexible hoses and HEPA filtered air enters and exits the cages from the rear of the plastic cage cover.

10.3.2 Oxygen, Carbon dioxide, ammonia, humidity and temperature

Intra-cage air oxygen, CO_2 and ammonia were measured using a Dragger X-Am 7000 inserting a flexible probe alternatively through the flap used for the bottle nipple in the IVC configuration or through the bar lids in the open one, to a distance from the bedding of approximately 2.5 cm.
Temperature and Relative Humidity (RH) were monitored by means of Data Loggers USB 502 (Measurement Computing, Norton MA, USA) positioned on top of the wire bar lid of the cages and set to record the two parameters every 30 minutes. One Data Logger was also positioned on top of the rack to monitor the environment.

10.3.3 Treatments and testing

IVC mice were 11 weeks old at testing and had spent almost 6 weeks in IVC or open cages. Open cages mice were 11 weeks old either at testing and had spent all their life in open cages.

10.3.4 Hematology

All mice were euthanized by carbon dioxide at ten weeks of age and blood was drawn by cardiac puncture. The approximate volume of blood was 0.4 to 0.6 ml.

A maximum volume of 0.5 ml was placed in EDTA coated microtainer tubes (Becton & Dickinson, Franklin Lakes, NJ USA).
Analysis for Red Blood Cells count (RBC), total hemoglobin content (Hgb), hematocrit (HCT), Mean Corpuscular volume (MCV), Mean Cell Hemoglobin (MCH), Mean Cell Hemoglobin Concentration (MCHC), Red Blood Cell Distribution width (RBCw) and Platelets (PLT) were performed on an Abacus Junior Vet (Diatron Messtechnik GmbH, Austria), set for mice profile.

10.4 RESULTS

10.4.1 Air oxygen and other gases

Oxygen was maintained at a concentration of 20.9% throughout the trial in both systems with minor fluctuations, down to 20.6% two days before cage change (day 14) in both open cages and IVCs.
Ammonia concentration was not detected in either system during the first 12 days before change but increased up to 3 p.p.m in the IVC system and 5 p.p.m in the open cages during the last few days before cage cleaning.
Carbon dioxide (CO_2) on day 14 (day of cage change) was 0.067 % and 0.037% respectively in both IVCs and open cages.

10.4.2 Body Weight, Feed and Water intake

Mean body weight of mice in the two groups were comparable and respectively: in IVC 26.77±0.68; in open 27.01±0.45 group (95% C.I of difference -1.154 to 1.639; two-tailed Student's *t* test, t=0.357; DF=26; p=0,723).
The mean food intake during the last two weeks of the trial was 3.68 g (±0.21) and 3.54 g (±0.18) respectively in IVCs and open cages.
Daily water intake was 4.21 g (±0.1) and 4.43 g (±0.18) respectively in IVCs and open cages.

10.4.3 Temperature and Relative humidity

All cages with 4 mice were equipped with a Data Logger. An additional Data Logger was positioned on top of the rack to record temperature and Relative Humidity in the room. One IVC cage had a mean value of RH outside the acceptable field of variation 40 to 70% (Table 1).

	IVC GM500	Open GM500	*P* values*
total n	14	14	
Red Blood Cells (10^9/L)	9.08±0.25	9.08±0.11	*P*=0.991
Haemoglobin (g/dl)	15.22±0,29	15.22±0.16	*P*=0.982
Haematocrit (%)	40.82±0.82	40.26±0.42	*P*=0.551
Mean Cell Volume (FL)	44.71±0.24	44.5±0.20	*P*=0.505
Mean Cell Haemoglobin (pg)	16.67±0.14	16.82±0.14	*P*=0.445
Mean Cell Haemoglobin Concentration (g/dl)	37.15±0.25	37.73±0.31	*P*=0.469
RBC distribution width (%)	18.15±0.22	18.28±0.14	*P*=0.628
Platelets (K/μL)	1481.9±210.8	1434.9±173.4	*P=0.864*

* t-Student test, two-tailed probability

Table 1. Red Blood Cell (RBC) count and related RBC parameters from groups housed (4 and 2/ group)

10.4.4 Hematology

A preliminary statistical evaluation for differences between the means of RBC count and related parameters in mice housed at a density of 2 and 4 to a cage in their respective groups (IVC and open) was performed. Since no statistical significant difference between the means was detected it was decided to pool the results (14 mice from IVC vs 14 mice from open cages). Table 2, shows that no differences were detected between the mean values of the hematological parameters tested for the two housing systems.

	Temperature	**Relative humidity**
	Mean (SD)	Mean (SD)
Room	21.0 (0.1)	64.4 (2.9)
Cage 1 IVC	22.9 (0.7)	68.3 (3.3)
Cage 2 Open	22.9 (0.7)	64.7 (2.9)
Cage 3 IVC	23.6 (0.6)	70.5 (4.3)
Cage 4 Open	22.7 (0.7)	65.4 (2.9)
Cage 5 IVC	22.9 (0.6)	75.4 (4.4)
Cage 6 Open	21.5 (0.4)	67.0 (3.3)

Table 2. Intra-cage and Room Temperature and Rel. Humidity were sampled by means of data loggers during the last 4 weeks of the trial every 30 minutes

10.5 DISCUSSION

The trial was carried out in the area of Milano (Italy) located at a mean altitude of 122 m above sea level. It is important to note that IVCs pressurized environment is not capable of modifying the normobaric condition (760 mm Hg). The conditioning period of approximately 6 weeks is sufficient to determine the complete turn-over of RBC in mice[7, 8, 9] which allows possible modifications due to altered environmental conditions to be expressed. In our trial the differences were found to be limited to an expected slightly higher relative humidity and temperature in IVCs vs Open cages and the room. Both RH and temperature can alter the reading of O_2 concentration in air, nevertheless recording instruments are able to maintain a linear reading in a range of temperature that includes values close to 0 °C and up to 50°C.
On the other hand, as the humidity in air increases, water vapor molecules displace O_2 molecules causing the output of the sensor to decrease. Of course the effect is larger at higher temperatures because there is more water vapor in the air.
Relative humidity in the test room was unfortunately constantly close to the upper acceptable limit stated by international guidelines/regulation (field of variation 45 to 65%) and was consequently unavoidable to find mean RH above 65% in the cages.
During the last two days before the cage change (procedural interval was 14 days), RH in some IVCs was definitely different and higher than in room and open cages. This might have played a minor role in the minor fluctuations of O_2 concentration detected in that very short phase.
However, no significant differences in mean Red Blood Cell (RBC) count and related RBC parameters, body weight, feed and water consumption were seen between mice from the two systems (ventilated and open) confirming that the concentration of O_2 in the cages of both groups was comparable and optimal for the physiological process of hematopoiesis. Differences in the design and performance of IVCs, such as the number of Air Changes per Hour (75) and air delivery point is probably the key point for the interpretation of the differences between our results and those described in York et al.[5] as an efficient turn-over of air in the cage makes its microenvironment similar to the outside macro environment, minimizing differences in the atmosphere and any impact on mice physiology.

10.6 REFERENCES

1. Grignaschi G, Corsi L, Zennaro E and Martino P.A. (2010). Breeding Performances as Welfare Indicator: A Comparative Study on C57Bl/6J Mice in Three Different Individually Ventilated Caging Systems. *Lab Animal Europ*e. Vol.10. 6, 40-41.
2. Reeb-Whitaker C K, Paigen B, Beamer W.G, Bronson R.T, Churchill G.A, Schweitzer B. & D.D. Myers. (2001). The impact of reduced frequency of cage changes on the health of mice housed in ventilated cages. *Laboratory Animals* 35, 58-73.
3. Vogelweid C. M, Zapien K.A, Honigford M.J, Li L, Li H, ad Marshall H. (2011) Effects of a 28-Day Cage-Change Interval on Intracage Ammonia Levels, Nasal histology, and Perceived Welfare of CD1 Mice. *JAALAS*. Vol.50. 6, 868-878.
4. Nagamine C.M, Long C.T, McKeon G.P and Felt S. (2012) Carbon Dioxide and Oxygen Levels in Disposable Individually Ventilated Cages after Removal from Mechanical Ventilation. *JAALAS*. Vol.51. 2, 155-161.
5. York J.M, McDaniel A.W, Blevins N.A, Guillet R.R, Allison S.O, Cengel K.A, Freund G.G. (2012) Individually ventilated cages cause chronic low-grade hypoxia impacting mice hematologically and behaviorally. *Brain, Behaviour, and Immunity*. 26:951-958.
6. Rosenbaum M.D, VandeWoude S, Volckens J, and Johnson T.E. (2010). Disparities in Ammonia, Temperature, Humidity, and Airborne Particulate Matter between the Micro and Macroenvironments of Mice in individually Ventilated Caging. JAALAS. Vol.49, 2: 177-183.
7. Dod, Bierman K.S, H.R., and Shimkin M.B. (1951). The disappearance of sulfhemoglobin in the blood as measure of erythrocyte in normal rabbits and mice and in tumor-bearing mice. *J. Nat.Cancer Inst.* 2, 1093.
8. Burwell, Buckley E.L, B.A., and Finch, C.A. (1953). Erytrocyte life span in small animals; comparison of two methods employing radio-iron. *Am. J.Physiol.* 172: 718.
9. Van Putten L.M, and Croon F. The Life Span of Red Cells in the Rat and the Mouse as Determined by Labeling with DFP^{32} in Vivo.*Blood* 13*,* 789–794.

CHAPTER 10 (section b)

The effect of two different Individually Ventilated Cage systems on anxiety-related behavior and welfare in two strains of laboratory mouse

Published on: Physiology & Behavior 124 (2014) 92–99

10. The effect of two different Individually Ventilated Cage systems on anxiety-related behavior and welfare in two strains oflaboratory mouse

AUTHORS: O. Burman[a], L. Buccarello[b], V. Redaelli[c], L. Cervo[d]

[a] School of Life Sciences, University of Lincoln, Brayford, Lincoln, UK
[b] Veterinary Sciences for Animal Health and Food Safety, University of Milan, Italy
[c] Veterinary Science Department, University of Milan, Italy
[d] IRCCS — Istituto di Ricerche Farmacologiche "Mario Negri", Experimental Psychopharmacology, Milano, Italy

10.1 ABSTRACT

The environment in which a laboratory animal is housed can significantly influence its behavior and welfare, acting as a potential confounding factor for those studies in which it is utilized. This study investigated the impact of two Individually Ventilated Cage (IVC) housing systems on anxiety-related behavior and welfare indicators in two common strains of laboratory mice. Subjects were juvenile female C57BL/6J and BALB/c mice (N = 128) housed in groups of four in two different IVC systems for 7 weeks. System One had air delivery at the cage 'cover' level at 75 ACH (Air Changes/Hour) and System Two had air delivery at the 'animal' level at 50 ACH.
Mice were assessed twice a week (e.g. bodyweight) or at the end of the study (e.g. anxiety tests). Our results showed significant differences in anxiety-related behavior between strains and housing systems. Mice in System Two, regardless of strain, defecated more in the Elevated plus Maze (EPM), spent less time in the open arms of the EPM, and less time in the central zone of the Open Field (OF). Strain differences in anxiety-like behavior were seen in the increased defecation by BALB/c mice in the OF and EPM and less time spent in the open arms of the EPM compared to C57BL/6J mice. These results suggest that different IVC housing systems can influence mouse behavior in different ways, with mice of both strains studied exhibiting more anxiety-related behavior when housed in System Two (air entry at the 'animal' level at 50 ACH), which could impact upon experimental data.

Keywords: IVC systems, Rodent housing, Anxiety-related behavior

10.2 INTRODUCTION

The housing environment of laboratory animals has been demonstrated to have a significant influence on the behavior, physiology, pathology and brain development of the animals housed within [1–5], thereby potentially impacting upon the comparability and reproducibility of the data generated [6,7].
It is therefore important to identify what impact different aspects of the housing environment (e.g. stocking density, internal cage complexity) can have in order to be able to maximize both the welfare of the animals used in scientific studies (in accordance to European and International legislation) and ensure scientific rigor. Such an approach also allows modulating environmental factors, once identified, to be taken into consideration during experimental design and subsequent statistical analysis [8]. One important aspect of the housing environment is the design of the cage itself, and the manner in which it is managed. Traditionally, 'open' (conventional) cages have been used that are ventilated by the room ventilation system in which they are located. Open cages risk exposure of the animals to microorganisms present in the room and an increased exposure to potential allergens for human workers within the same environment.
For this reason, and to maintain adequate ventilation, low relative humidity and reduced concentrations of ammonia and CO_2 [9, 10] in the cages, Individually Ventilated Cage (IVC) systems have been developed that aim to ameliorate these problems. It has been suggested that providing a more stable and protected environment is beneficial to the animals and the personnel working in the animal rooms [11]. Consequently, the use of IVC systems has proliferated. However, the design of these systems – although sharing similar features – can vary markedly in a number of ways (e.g. ventilation rates, internal air pressure, and location of air delivery), and so it cannot be assumed that different IVC systems will influence laboratory animals in the same way.
Yet, although there is so much variation between different IVC systems, little is known as to what impact these design differences can have on the animals and the data that is generated from them.
Forced ventilation, noise and vibrations could potentially constitute chronic stressors for animals housed within IVC systems – and are often used to induce major changes in behavior and neurobiology [12–16] – and these are among the factors that typically vary between IVC systems. Previous studies have demonstrated that, when given the choice, mice avoided high ventilation rates and preferred air delivery in the cover of the cage rather than at the level of the animal [10], although see [17], indicating potential aversion for different factors within the IVC environment.

However, when assessing animal welfare –when the aim is to limit an animal's exposure to negative states such as anxiety – we need to consider not only the animal's choice and preference, but also its general behavioral and physiological response to the experience of a particular environment [18–20], what is known as an 'indicator' approach.

This is because, whilst it is a valuable technique, preference/choice can be influenced by many factors, including: previous experience [21]; the balance between short and long-term preferences [22]; the influence of stress and affective state [23]; and animals making errors [24]. An indicator approach has previously been used to compare the impact of different IVC systems in comparison to conventional cages on anxiety-related behavior in mice [6,25], with the authors finding that mice housed in IVCs exhibited reduced activity and increased anxiety related behavior compared to those housed in conventional cages. However, Kallnik et al. [6] carried out their study on singly housed mice. Given that recommendations (e.g. Directive 2010/63/EU; Guide for the care and use of Laboratory Animals, U.S. National Research Council (Eighth Edition)) are for the group housing of laboratory mice, it is important to determine if a similar impact is found when mice are housed in groups — particularly given that there can be a degree of resilience against stress provided by the presence of conspecifics [26].

It is also important– given the great variation in design features between different IVC systems – to see whether an indicator approach can identify differences between types of IVC housing system, and few studies have investigated this issue. Champy et al. [27] studied the influence of three different IVC systems (M.I.C.E.® (Animal Care System), SealSafe® Plus (Tecniplast) and Innocage® (Innovive Inc.)) on mouse phenotypes, and found that there was little difference between these particular IVC systems on any of the parameters that they recorded, including anxiety-related behavior. An important consideration when investigating the impact of different IVC systems on laboratory rodent behavior is the potential influence of strain. Kallnik et al. [6] found that IVC housing (IVC Classic) influenced mouse behavior generally (i.e. having the same effect on more than one strain), reducing activity and enhancing anxiety related behavior, as well as acting in a strain-specific manner (i.e. having differential effects on strains), with increased acoustic startle response observed in C3HeB/FeJ, but not C57BL/6J, mice.

In contrast, Mineur and Crusio [25] found only strain-specific effects. For this reason, we included two different mouse strains within our study in order to reveal, to at least some extent, any differential effect of housing conditions on the behavior of different strains of laboratory mouse.

We used C57BL/6J and BALB/c as strains that are typically used within laboratory settings [28] and show contrasting levels of anxiety related behavior [29].
The aim of this study was therefore to investigate the impact of two different IVC housing systems on the anxiety-related behavior and welfare of two strains of laboratory mouse using a variety of behavioral and physiological indicators as recommended when defining and implementing protocols for the welfare assessment of laboratory animals [30].

10.3 MATERIAL AND METHODS

10.3.1 Subjects and housing

The subjects were 128 juveniles (6–7 weeks of age) female laboratory naïve mice of two commonly used, but behaviorally contrasting [31, 32], strains (C57BL/6J and BALB/c) obtained from a single external supplier (Charles River, Calco, Italy). Mice were individually identified (ear tags) as part of normal facility procedure, allowing us to record individual (e.g. injury/wounds) as well as group (e.g. position within the cage) measures. They were housed (random allocation) in groups of four individuals (same strain) in two types of IVC system. The IVCs differed in specific ways (see 'Housing systems'), but were all provisioned with the same bedding material (hard wood shavings) and ad libitum food (Global Diet 2018S, Harlan Italy, S. Pietro al Natisone, Italy) and water. The mice were kept in the same room within a Specific Pathogen-Free animal facility with a regular 12:12 h light/dark cycle (lights on 07:00 a.m.), at a constant room temperature of 22 ± 2 °C, and relative humidity approximately 55 ± 10%.
All cages were changed every 14 days after the first week, and inspected daily. At the end of the study all mice were euthanized by exposure to CO2 according to institutional protocol.
Procedures involving animals and their care were conducted in conformity with the institutional guidelines at the Mario Negri Institute in compliance with national (Decreto Legge nr 116/92, Gazzetta Ufficiale, supplement 40, February 18, 1992; Circolare nr 8, Gazzetta Ufficiale, July 14, 1994) and international laws and policies (EEC Council Directive86/609, OJL 358, 1, Dec. 12, 1987; Guide for the Care and Use of Laboratory Animals, U.S. National Research Council (Eighth Edition) 2011).

10.3.2 Housing systems

In this design we compared two IVC systems (SealSafe® Plus (Techniplast) and Allentown) that differed in their air supply delivery systems: (System One) air delivery at the cage 'cover' level; (System Two) air delivery at the 'animal' level. The air supply ventilation rate also varied as both systems were operated

according to the manufacturer's specification, with 75 ACH for System One (cover level) and 50 ACH for System Two (animal-level).
The two housing systems also differed slightly in size (System One: floor space 501 cm^2, height 17 cm, height without cover 13.5 cm, height of air delivery from the cage floor 16.5 cm; System Two: floor space 530 cm^2, height 17.8 cm, height without cover 13.5 cm, height of air delivery from the cage floor 7.2 cm) and factors including the position of the food hopper, with the food hopper for System One at the back of the cage and the food hopper for System Two at the front. This degree of variation between systems meant that, although we could not identify which specific factor (i.e. air supply delivery or air supply rate or both) resulted in any observed differences in mouse anxiety-related behavior and welfare, this 'systems approach' would allow us to determine if there were any overall differences between the two housing systems, making the results directly transferable and highly relevant to researchers.
If any system differences were identified, then these could be investigated in more detail in further studies. We observed eight cages (n = 8) for each of the housing systems (N = 16), but as two mouse strains were being studied this gave a total of 128 mice (N = 32 cages in total).

10.3.3 Experimental protocol

Cages from the two systems were balanced between racks (e.g. the same number from each system on each rack) and all cages were placed in the middle row of the racks in order to take into account any potential influence of rack location and position-within-rack on mouse behavior. Measurements were collected over a seven-week period, with the first week of the study allowing the mice to acclimatize prior to the start of the six-week experimental phase, although some measures were collected for all 7 weeks. The study was split across 2 weeks (balanced for strain/system), thus reducing the number of animals to be tested at the end of the study.
Behavioral observations took place between 09.00 and 12.00 h. For those measures that were repeatable (e.g. bodyweight), data were collected twice a week, however, open field and elevated plus-maze tests only took place at the end of the study. This allowed us to identify both short and longer-term responses to the housing systems, and this was also reflected in the choice of behavior and anxiety-related indicators utilized.

7.4 Measures of general behavior and anxiety-related behavior

Whilst we selected measures that we believed would reveal underlying differences in behavior and anxiety (both short and longer-term), we particularly focused on those measures that could be simply, quickly and reliably recorded by staff (e.g. vets, technicians) to maximize the applicability of our results.

Our measures therefore focused either on indirect recording of behavior (e.g. injury scores as a reflection of aggression), 'challenge' tests that took place outside of the home cage (e.g. tests of anxiety-related behavior) or unambiguous behavioral observations (e.g. location of mice within the cage).

10.4.1 Indirect behavioral and physical measures

These measures included: injury/wound scores [present/absent, in three zones: head zone; middle zone; and tail zone]; barbering (body hair removal) score [present/absent, in three zones: head zone; middle zone; and tail zone]; whisker-trimming (whisker area only) score [present/absent]; bedding pushing (i.e. is the bedding covering the air delivery pipe in System Two or equivalent height in System One) score (score 0 (no bedding covering the air delivery pipe or equivalent eight); 1 (bedding partially covering air delivery pipe or equivalent height); 2 (bedding completely covering air delivery pipe or equivalent eight); bodyweight (g); water utilization (ml); food utilization (g).

These observations were made twice a week (Monday and Friday) for every individual in each cage (e.g. injury/wound score) or each cage (e.g. water utilization). Bodyweight was also recorded at the end of the study prior to euthanasia. Observations were alternated between cages from the two different housing systems.

10.4.2 Within-cage behavior

Twice a week (0900–1200), the number of mice in the front half of the cage was recorded for every cage in order to give a quick and unambiguous indication of animal location (i.e. possible values ranged from 0 to 4 animals), with a mouse judged as being in one half of the cage when the majority of the animal's body was in a particular half. In the unlikely event of an animal being 50% in each half of the cage, it was counted as being in whichever side its head was positioned. Observations were alternated between cages from the two different housing systems.

10.4.3 Tests of anxiety-related behavior

Testing (Open Field (OF), Elevated Plus Maze (EPM)) took place at the same time (approx. 1000–1300) in two different rooms from where the animals were housed, under dim illumination provided by a 60 W lamp placed 1 m above the apparatus and pointed towards the ceiling.

For both tests, mice were counted as being in a particular zone/location when all four of its legs were positioned within the zone [33], and the apparatus was wiped with 70% ethanol and dried prior to each test. The order in which animals were tested was alternated between cage systems.

Two mice from each cage were tested in the OF, and the other two tested in the EPM. An average from the pairs of mice was calculated to provide a cage average for both tests. The OF was a grey Perspex box (40 × 40 × 40 cm) with the floor divided into 25 (8 × 8 cm) squares. Mice were placed in the same corner as a 'starting point' and their behavior video-recorded for 5 min. The number of internal (the nine central squares) and external (the sixteen peripheral squares) squares crossed, the time spent in the central area of the open field (the nine central squares), the number of rears, duration of self-grooming, and the number of faecal boli were scored from video by experienced researchers 'blind' to the housing system as measures of general activity and anxiety-related behavior.
The EPM was made of black Perspex with two open arms (30 × 5 cm) and two closed arms (30 × 5 cm) extending from a central platform (5 × 5 cm) raised 40 cm above the floor. The closed arms had 25 cm walls and the open arms had 0.5 cm raised lips along the edges. At the beginning of each test mice were placed on the central platform facing an open arm and their behavior video-recorded for 5 min. The number of entries and the time spent in the open and closed arms, the number of rears, the duration of self-grooming, the number of faecal boli excreted were scored from video by experienced researchers 'blind' to the housing system as measures of anxiety-related behavior.

10.4.4 Faecal corticosterone

Faecal boli (ten per cage, to get at least the 0.05 g faecal matter required for assay) were collected immediately after the tests of anxiety related behavior (i.e. at the end of the study). The boli were stored (labelled Eppendorf, frozen -20 °C) before subsequent analysis by enzyme immunoassay (EIA) to determine the levels of faecal corticosterone metabolites (EIA Kit: ADI-Nr 901-097 Enzo Life Sciences) in accordance with the manufacturer's instructions.

10.5 Data analysis

This was a between-subjects design, such that mice were only exposed to one of the two treatment groups/housing systems. Because individual mice within a cage were non-independent, we used 'cage' as our experimental unit, with data collected for all four mice within each cage and their data combined to give a cage average.
Consequently, our sample size was n = 8 cages per system/strain (N = 32 cages). Data conformed to parametric statistical requirements (e.g. normality of data). For those measures collected on more than one occasion, we used repeated measures General Linear Model (GLM) with Housing System (System One, System Two) and Strain (C57BL/6J and BALB/c) as between-subjects' factors and Time as a within-subjects factor.

For those measures (e.g. tests of anxiety-related behavior) collected at only one-time point, we used a two-way ANOVA (Housing System/Strain). The statistical package used was SPSS (version 19). Only statistically significant results are presented in full. If significant interactions were found, then related main factor results are not presented.

10.6 RESULTS

10.6.1 INDIRECT BEHAVIOR AND PHYSICAL MEASURES

10.6.1.2 Bodyweight

There was no significant difference between housing systems ($F_{1, 28} = 0.411$, $P = 0.527$). There was a statistically significant Strain ∗ Time interaction ($F_{14, 392} = 9.8$, $P < 0.001$) which revealed that for days 0, 4 and 7 the C57BL/6J mice were initially heavier than the BALB/c mice, but that this changed over time, with the BALB/c mice becoming heavier than the C57BL/6J mice for days 18, 21 and25 during the mid-point of the study, but no difference between strains by the end of the study. The growth rate of both mouse strains was comparable to figures provided by the supplier (Charles River) (data not shown).

10.6.1.3 Food utilization

It should be noted that 'food utilization' was calculated as change in total food weight (g) and therefore incorporates food removed/lost from the hopper but not necessarily ingested. There was a Time ∗ System interaction ($F_{6, 168} = 4.7$, $P < 0.001$) showing that in week 1, mice, regardless of strain, utilized more food when housed in System Two compared to System One (see Fig. 1). There was also a significant Time ∗ Strain interaction ($F_{6, 168} = 8.9$, $P < 0.001$) revealing that for weeks 1 and 3–7 C57BL/6J mice utilized more food than the BALB/c mice.

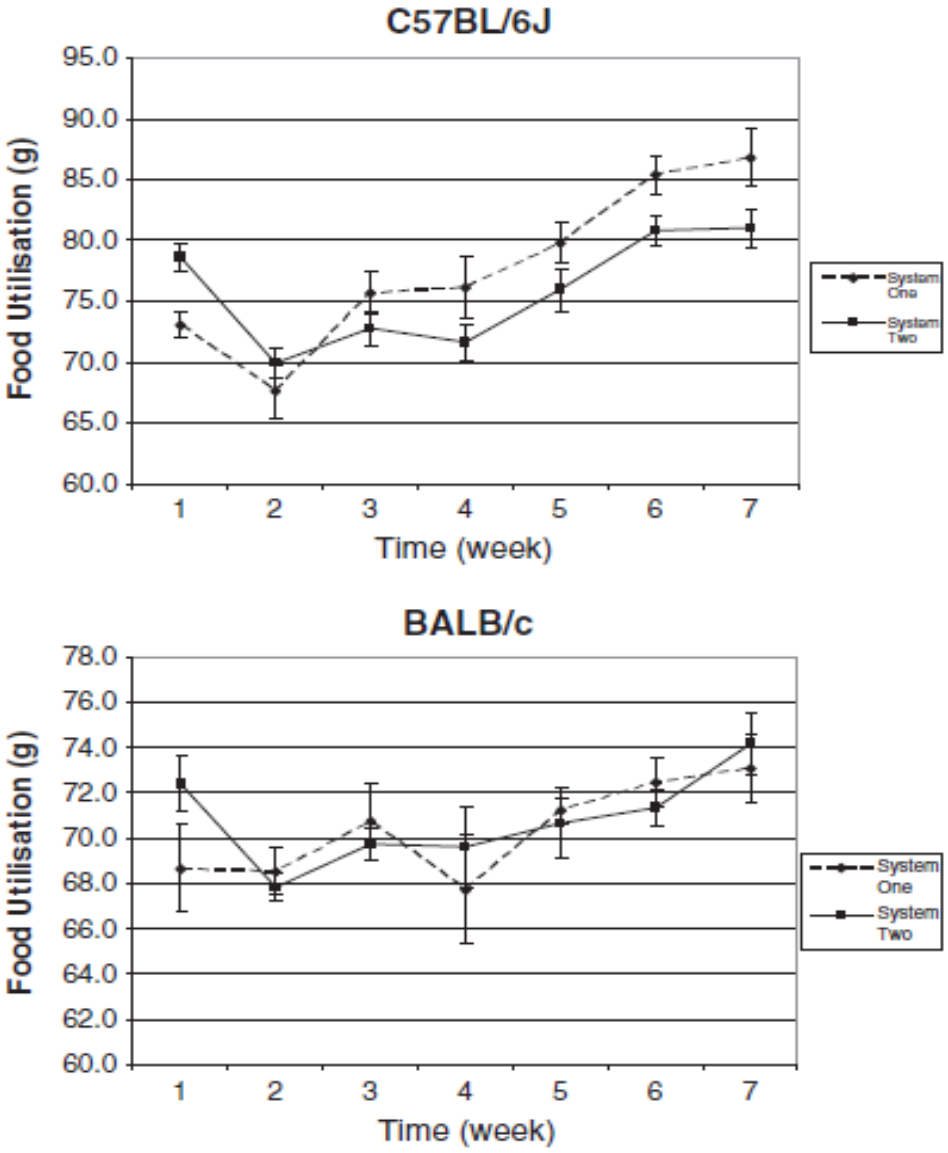

Figure 1. Food utilization (g) over time (weeks) for System One and System Two, for each mouse strain separately. Data are means ± standard error.

10.6.1.4 Water utilization

It should be noted that 'water utilization' was calculated as the change in total water volume (ml) and therefore incorporates water removed/lost (e.g. via evaporation) from the water bottle but not necessarily ingested.

There was a System effect ($F_{1, 28}$ = 10.9, P = 0.03), indicating that, regardless of strain and time, mice utilized more water in System Two compared to System One (see Fig. 2). There was also a Strain effect ($F_{1, 28}$= 143.1, P <0.001), with C57BL/6J mice utilizing more water than the BALB/c mice.

Finally, there was an effect of Time ($F_{1, 28}$ = 36.7, P b 0.001), showing that the mice (regardless of strain and housing type) utilized water significantly more in week 1, then this dropped to a lower level before gradually increasing over time.

There were no significant interaction effects (System ∗ Strain: $F_{1, 28}$= 0.03, P= 0.865; System ∗ Time: $F_{6, 168}$ = 0.753, P = 0.608; Strain ∗ Time: $F_{6, 168}$ = 0.785, P= 0.583; System ∗ Strain ∗ Time: $F_{6, 168}$ = 1.49, P= 0.184). In order to identify any potential differences between housing systems in their background water evaporation rate (e.g. due to differences in ACH), we compared water loss in four cages of both housing systems over a period of 1 week in the absence of mice. We found no difference in water loss ($F_{1, 6}$ = 0.844, P = 0.394) between the housing systems.

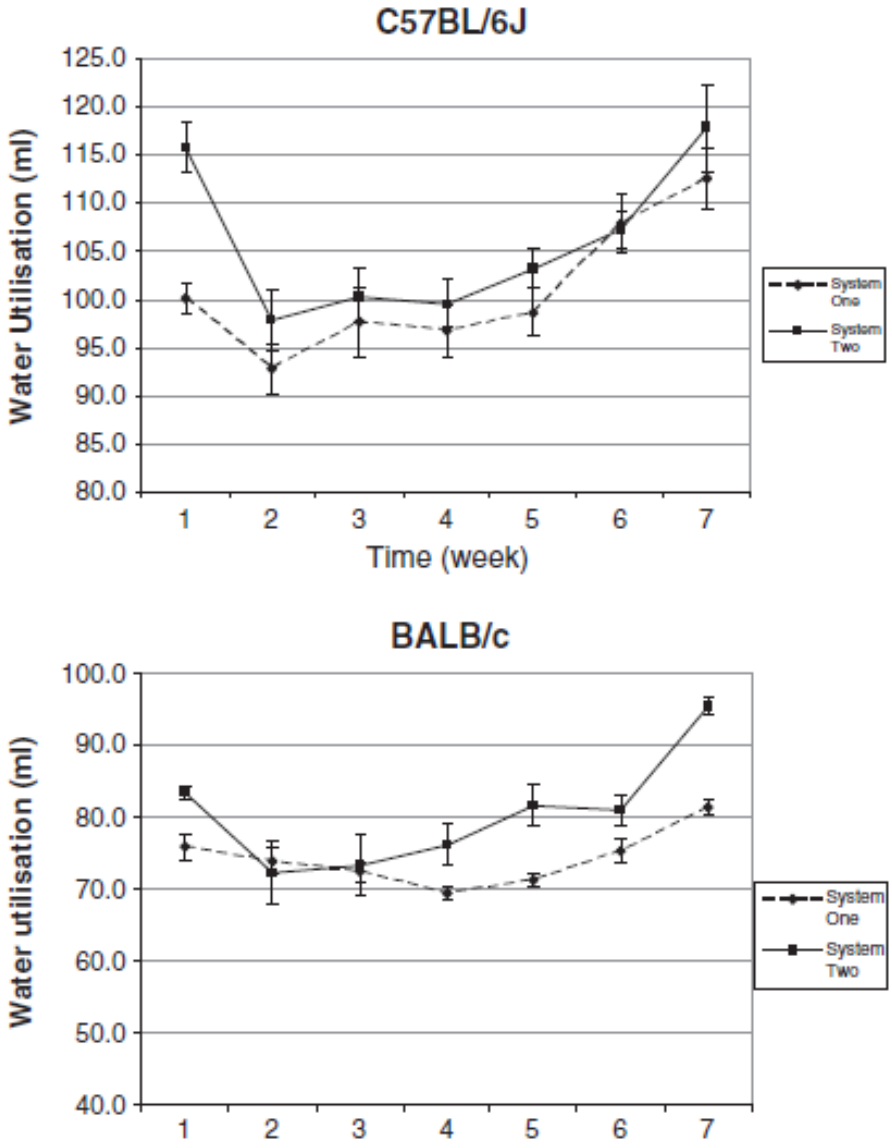

Figure 2. Water utilization (ml) over time (weeks) for System One and System Two, for each mouse strain separately. Data are means ± standard error.

10.6.1.4 Injury/wound scores

No injuries/wounds were recorded for any individual mouse of either strain/housing system.

10.6.1.5 Bedding pushing score

There was a System effect ($F_{1, 28} = 5.3$, $P = 0.029$), with mice, regardless of strain or time, having higher bedding pushing scores when housed in System Two compared to System One. There was a Time effect ($F_{13, 364} = 4.2$, $P < 0.001$), with a general increase in bedding pushing score over time. There was also a Strain effect ($F_{1, 28} = 20.3$, P b 0.001), with BALB/c mice having higher bedding pushing scores than C57BL/6J mice (see Fig. 3). There were no significant interactions (System ∗ Strain: $F_{1, 28} = 0.012$, $P = 0.913$; System ∗ Time: $F_{13, 364} = 1.298$, $P = 0.211$; Strain ∗ Time: $F_{13, 364} = 1.29$, $P = 0.216$; System ∗ Strain ∗ Time: $F_{6, 168} = 0.439$, $P = 0.955$).

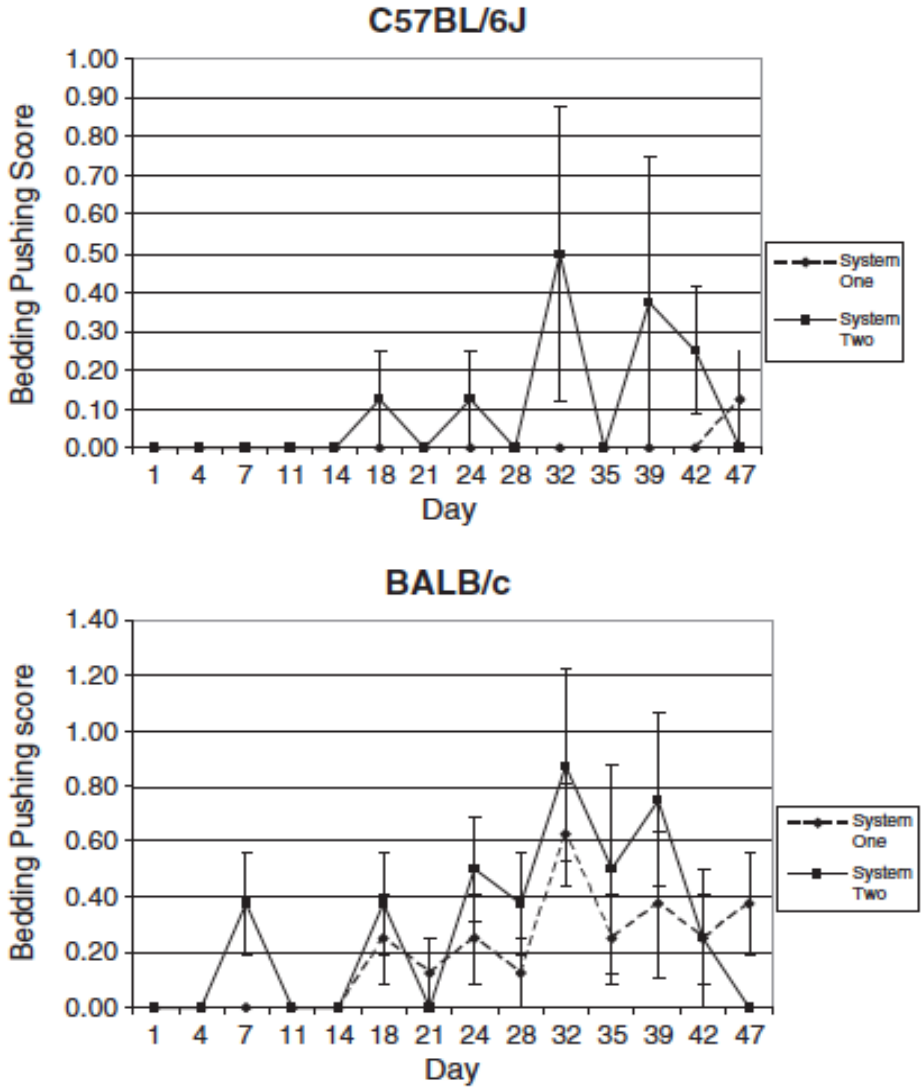

Figure 3. Bedding pushing scores over time (weeks) for System One and System Two, for each mouse strain separately. Data are means ± standard error.

10.6.1.6 Barbering

Because barbering, once observed in an individual mouse, continued for the remainder of the study, data were only analyzed for the final week of the experiment. There was no System effect ($F_{1, 28}$ = 1.201, P = 0.282). There was a Strain effect ($F_{1, 28}$ = 4.8, P = 0.037), with C57BL/6J mice showing higher scores for barbering compared to BALB/c mice.

10.6.1.7 Whisker trimming

As for barbering, whisker trimming was only analyzed for the final week of the experiment. We found no statistically significant differences either between Systems ($F_{1, 28}$ = 1.697, P = 0.203) or Strain ($F_{1, 28}$ = 0.424, P = 0.52).

10.6.2 WITHIN-CAGE BEHAVIOR

10.6.2.1 Position of mice in the cage

There was a Strain * System interaction ($F_{1, 28}$ = 8.6, P = 0.007), with both BALB/c and C57BL/6J mice having greater numbers of individuals in the front half of the cage when housed in System Two compared to the System One. There was a Time * System interaction ($F_{13, 364}$ = 2.3, P= 0.006), with all days except days 39 and 42 showing significantly more individuals in the front half of the cage for those mice housed in System Two compared to System One.

10.6.2.2 Open field

There was a strain effect ($F_{1, 28}$ = 60.2, P <0.001), with BALB/c mice producing more droppings than C57BL/6J mice. For 'internal' crossing frequency (INT to INT and EXT to INT) there was a Strain * System effect ($F_{1, 28}$ = 7.7, P = 0.01), with C57BL/6Jmice showing higher levels of internal crossing when housed in System One compared to System Two, and BALB/c mice showing no difference between housing systems.

For 'external' crossing frequency (EXT to EXT and INT to EXT) there was a Strain effect ($F_{1, 28}$ = 76, P <0.001), with C57BL/6J mice crossing more than BALB/c mice. Regardless of strain, mice housed in System One spent more time in the internal/central zone than those housed in System Two ($F_{1, 28}$ = 6.2, P = 0.019). C57BL/6J mice also spent more time in the internal/central zone than BALB/c mice ($F_{1, 28}$ = 4.9, P = 0.035) (see Fig. 4). C57BL/6Jmice were observed to rear more often than BALB/c mice ($F_{1, 28}$ = 39.6,P <0.001) and for longer ($F_{1, 28}$ = 12.4, P = 0.001). There was a System effect on grooming duration ($F_{1, 28}$ = 8.2, P = 0.008) with mice housed in the System Two spending more time grooming than those housed in the System One. Although there were no strain differences in the frequency of grooming, C57BL/6J mice spent more time grooming than the BALB/c mice ($F_{1, 28}$ = 10.3, P = 0.003).

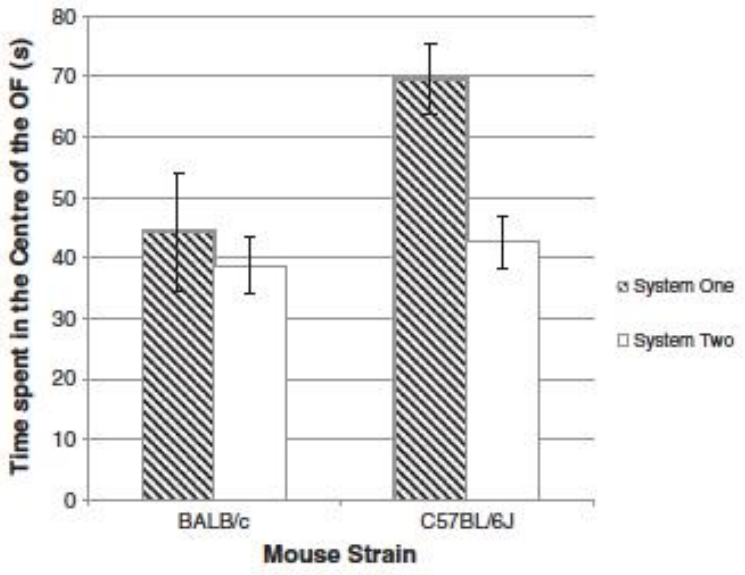

Figure 4. Time spent (s) in the central/internal zone of the OF for System One and System Two, for each mouse strain separately. Data are means ± standard error.

10.6.2.3 Elevated plus maze

There was a System effect ($F_{1, 28}$ = 12.2, P = 0.002), with mice housed in System Two producing more droppings in the EPM than those housed in System One. There was also a strain effect ($F_{1, 28}$ = 19.6, P <0.001), with BALB/c mice producing more droppings that C57BL/6J mice. We found that mice housed in the System One spent more time in the open arm of the EPM than those housed in System Two (F1, 28 = 18.5, P <0.001) (see Fig. 5).

There was also as strain effect, with C57BL/6J mice spending more time in the open ($F_{1, 28}$ = 17.2, P <0.001) and closed arms ($F_{1, 28}$ = 10.4, P = 0.003) than BALB/c mice, as well as moving more often into the open ($F_{1, 28}$ = 44, P <0.001) and closed ($F_{1, 28}$ = 29.4, P <0.001) arms. There was a Systems effect on time spent in the center of the EPM ($F_{1, 28}$ = 13.6, P = 0.001), with mice housed in System Two spending more time in the center than those housed in System One. There was also a strain effect, with BALB/c mice spending more time in the center of the EPM compared to C57BL/6J mice ($F_{1, 28}$ = 34, P <0.001).

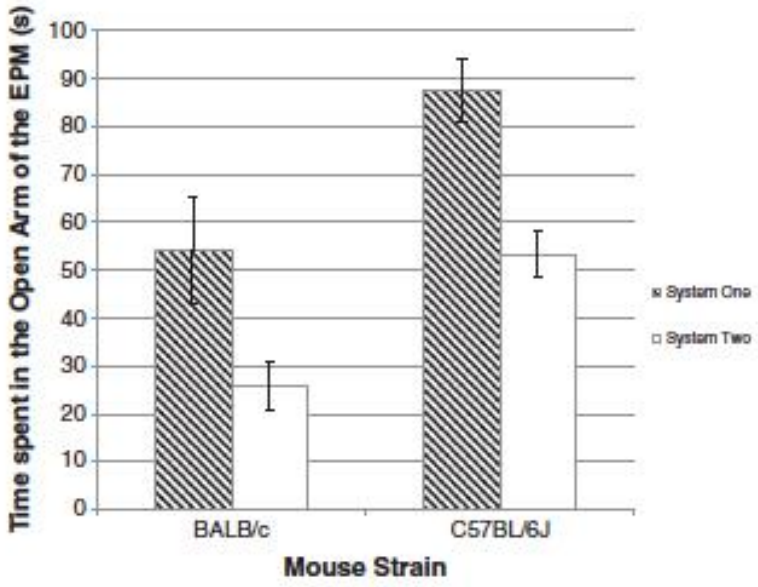

Figure 5. Time spent (s) in the open arm of the EPM for System One and System Two, for each mouse strain separately. Data are means ± standard error.

10.7 Faecal corticosterone

We found no significant differences in the level of faecal corticosterone metabolites between the housing systems ($F_{1, 43} = 0.034$, $P = 0.854$), strains ($F_{1, 43} = 0.538$, $P = 0.467$), or any interaction ($F_{1, 43} = 0.009$, $P = 0.926$) (see Fig. 6).

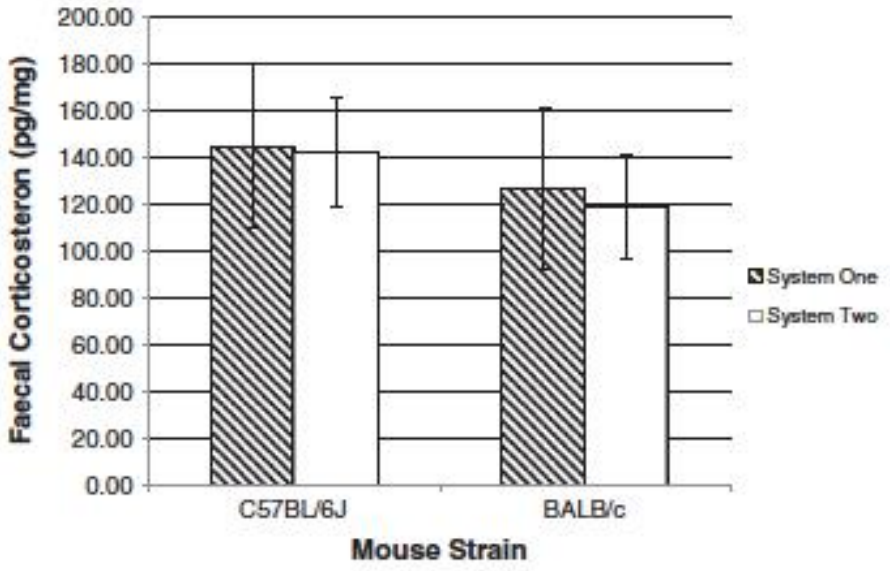

Figure 6. Faecal corticosterone metabolite levels (pg/mg) for System One and System Two for each mouse strain separately. Data are means ± standard error.

10.8 DISCUSSION

From the results it appeared that IVC housing System Two (with air delivery at the 'animal' level at 50 ACH) was more anxiety-inducing than IVC housing System One, with air delivery at the 'cover' level (and at 75 ACH), for mice of both strains (BALB/c, C57BL/6J). This was based upon observed differences in anxiety-related behavior shown by both strains of mouse housed in System Two compared to those housed in System One.

In particular, the increase in defecation in the EPM, the decreased time spent in the open arm of the EPM, and the increased time spent in the starting position in the EPM for mice housed in System Two. Similar results were found in the OF test, with mice housed in System Two spending less time in the central/internal zone of the arena, suggesting reduced confidence compared to those mice housed in System One. These findings reflect those of Kallnik et al. [6] and Mineur and Crusio [25] who observed reduced activity and enhanced anxiety related behavior in mice housed in IVC systems compared to 'conventional' housing, and extends this finding to group housed mice when housed in two different types of IVC housing system. Thus, not only does it appear that some IVC housing systems can increase anxiety, as determined by anxiety-related behavior, compared to conventional systems [6,25], but there also appear to be significant differences between IVC systems in their influence on mouse behavior and anxiety; including when group-housed.

In contrast to our findings, however, Champy et al. [27] found little effect of the three different IVC systems that they compared on any of the parameters that they recorded — including anxiety-related behavior in the open field test. The three IVC systems that they compared were IVCM.I.C.E. ® (Animal Care System), IVC SealSafe® Plus (Tecniplast), and Innocage® (Innovive Inc.).

These particular IVC systems differ in a great number of features, including shape of cage, and construction material, as well as aspects of ventilation (e.g. air flow rate and pressure). It is therefore perhaps surprising that they did not appear to observe any difference in anxiety-related behavior between the systems. However, one possibility is that because their mice were anxiety tested after 2 weeks of acclimatization, this may not have been sufficient time to induce differential levels of emotionality as compared to the 7 weeks prior to the testing of anxiety-related behavior in our study.

Although changes to the housing environment can result in immediate behavioral changes, influences on affective state may take longer to establish. For example, changes in anxiety-like behavior in mice were observed after 6 weeks of environmental enrichment [34].

When assessing animal preference in IVC systems, Baumans et al. [10] found that mice avoided high ventilation rates and preferred air supply access in the cover of the cage rather than at the level of the animal, demonstrating that mice actively choose between IVC housing systems that vary in particular features. Our results indicate that IVC systems that vary in these same features also appear to influence anxiety-related behavior (in the absence of choice). Taken together, the findings from these two approaches suggest a reduction in welfare in mice housed in animal level ventilation systems.

Interestingly, if, as determined by Baumans et al. [10], mice prefer air entry from the 'cover' level and low ventilation rates, then our data suggest that air entry level may be a significant feature in mouse choice, given that our mice exhibited least anxiety-related behavior when housed in cages with air entry at the cover level (preferred) despite also having higher ventilation rates (avoided).

This appears to reflect the findings of Krohn and Hansen [17] who found that it was the presence of draughts that influenced mouse choice rather than the number of air changes per se. Clearly, further research is needed to disentangle these features. Grooming within the OF can be considered a sign of anxiety-related behavior (e.g. as a displacement activity) and this was higher in the mice housed in System Two. However, although the strain effects observed in the OF typically followed the general pattern of Balb/c mice exhibiting more anxiety-related behavior than C57BL/6jmice (see later), grooming behavior was an exception to this, with C57BL/6j mice grooming for longer than Balb/c mice. The interpretation of grooming behavior can vary, because it increases in the contrasting contexts of both stress and comfort, as well as between strains [35]. Consequently, data relating to position within the OF (and EPM) may be more reliable indicators of putative anxiety level.

Strain differences mainly reflected the increased anxiety-like behavior of BALB/c compared to C57BL/6J mice, with BALB/c mice showing increased defecation in both OF and EPM, less time in the open arms of the EPM and less time in the internal/central zone of the OF. We also observed that BALB/c mice were reluctant to leave the starting point of the EPM. These results reflect the general finding in the research literature that BALB/c mice show more anxiety-like behavior thanC57BL/6J mice [29, 36].

We did, however, observe higher levels of barbering in the C57BL/6J mice, which reflects epidemiological research revealing that C57BL/6J mice were likely to exhibit barbering behavior [37] — suggesting a potential dissociation between barbering behavior and putative anxiety level.

The confirmation in our own study of the predicted differences in strain-related emotionality thus strengthens our results concerning the observed anxiety-related differences between the housing systems.

Although the majority of results followed a pattern of independent effects of both strain and housing system, we did also observe some interactions between these factors (e.g. internal crossing in the OF. Thus, along with Kallnik et al. [6], but in contrast to Mineur and Crusio [25], we found both general and strain-specific effects of IVC housing system on mouse anxiety-like behavior. In addition, it is perhaps worth emphasizing the importance of selecting the appropriate strain when investigating the impact of the housing environment.

In order to show a behavioral change in response to a particular housing environment, animals need to be at a level that allows for potential change. For example, BALB/c mice may not have shown the same reduction in frequency of 'internal crossing' in the OF as C57BL/6J mice when housed in System Two, because they were already at a low level of activity and could therefore not go any lower. Mouse position within a cage can be influenced by a variety of factors Including activity levels, food hopper position, and the level of light/disturbance and/or refuge location [38].

Behavior within the cages appeared to back up the findings from the tests of anxiety-related behavior, that System Two resulted in increased anxiety-like behavior, because mice housed in System Two were more frequently found in The front half of the cage — away from the position of air entry. This could suggest that the mice in System Two were avoiding the area of the cage where air entered – despite this resulting in them having to spend more time in the front of the cage – an observation that would reflect mouse avoidance of aversive stimuli/environments [39]. However, position in the cage could also have been influenced by differences in cage design between the two housing systems (e.g. location of food hopper) and so has to be interpreted with caution.

In System One the food hopper was located at the back of the cage, whilst for System Two the food hopper was at the front of the cage — the opposite end to the air delivery. This could explain the observed increase in time spent at the front of the cage in System Two — although our observations were in the light period when mice would typically be inactive rather than feeding. Mice were also found to have higher 'bedding pushing' scores in System Two, a finding that may have reflected attempts to cover the point of air entry — a potential response to what may be considered an aversive stimulus as seen in the 'defensive burying' paradigm [40].

Mice in IVC systems have previously been observed to build higher walled nests that may act to protect them against draughts [10]. Evidence that this behavior might be related to an anxiety-like state is suggested by the fact that we also observed a strain effect on 'bedding pushing', with BALB/c mice doing more bedding pushing than C57BL/6J mice in both IVC systems, potentially reflecting commonly found differences in anxiety-like behavior between these two strains [29].

There was also a potentially interesting result in that mice housed in System Two utilized more water (as measured by water loss) than those housed in System One. This result could be explained by differences in ventilation rate between the two housing systems (System One: 75ACH; System Two: 50 ACH).
However, as we found no differences in evaporation rate between the two Systems when they did not contain mice, this result suggests that the difference in water loss was due to the activity of the mice — although consumption may not be the only factor involved. Other authors have interpreted similar increases in apparent drinking behavior as indicating prolonged stress, i.e. polydipsia [41, 42], which would reflect the higher levels of anxiety-related behavior that we observed for mice housed in System Two. We observed an unexpected difference between housing systems in food utilization in the first week of the study. The overall high level of food utilization during the first week (compared to week 2) after arrivals typical for the period of initial acclimatization to the laboratory environment following the stress of transport [43].
However, it is not immediately clear why there might have been a difference during this period between the two systems — one possibility being that the previously discussed differences in food hopper location/food acquisition may have required more familiarization due to initial novelty for those animals in System One (that fed less).
Perhaps surprisingly, we did not observe a difference in the level of faecal corticosterone metabolites for those mice housed in System Two compared to System One. Other studies have demonstrated significant changes in faecal corticosterone metabolite levels as a consequence of changes to the housing environment (e.g. from14 to 70 days after environmental enrichment: [44]; following removal of individuals: [18]; following single housing: [45]). However, Gurfein et al. [44] also assessed the impact of environmental enrichment on anxiety behavior in the EPM, but found no significant effects — thereby demonstrating that expected correlations between different measures of stress and welfare may not always be revealed [46].
In conclusion, it appears that for the two strains of laboratory mice observed in this study, being housed in System Two (air entry at the 'animal' level at 50 ACH) resulted in more behavioral indicators of anxiety than being housed in System One (air entry at the 'cover 'level at 75 ACH). This provides further evidence that changes in the housing environment – even between two different types of IVC housing system– have the potential to impact upon anxiety-like behavior in mice and, as a consequence, the robustness and comparability of experimental data. This reflects the importance of taking such potential influences into consideration during experimental design and when interpreting and comparing results.

Specifically, it demonstrates that the term 'IVC' cannot be generalized across different IVC systems, but that variation between these systems may well have differential influences upon mouse behavior and research data.

10.9 ACKNOWLEDGEMENTS

This study was sponsored by the Istituto di Ricerche Farmacologiche "Mario Negri" — IRCCS, Via La Masa, 19, 20156 Milan, Italy. The authors had no financial interests in the outcome.

10.10 REFERENCES

1. Hurst JL, Barnard CJ, Nevison CM, West CD. Housing and welfare in laboratory rats: welfare implications of isolation and social contact among caged males. Anim Welf1997; 6:329–47.
2. Crabbe JC, Wahlsten D, Dudek BC. Genetics of mouse behavior: interactionswith laboratoryenvironment. Science 1999; 284:1670–2.
3. Wurbel H. Ideal homes? Housing effects on rodent brain and behaviour. TrendsNeurosci 2001; 24:207–11.
4. Van Loo PLP, Kruitwagen CLJJ, Van Zutphen LFM, Koolhaas JM, Baumans V. Modulationof aggression in male mice: influence of cage cleaning regime and scent marks. Anim Welf 2000; 9:281–95.
5. Schrijver NCA, Bahr NI, Weiss IC, Wurbel H. Dissociable effects of isolation rearingand environmental enrichment on exploration, spatial learning and HPA activity inadult rats. Pharmacol Biochem Behav 2002; 73:209–24.
6. Kallnik M, Elvert R, Ehrhardt N, Kissling D, Mahabir E, Welzl G, et al. Impact of IVChousing on emotionality and fear learning in male C3HeB/FeJ and C57BL/6J mice. Mamm Genome 2007; 18:173–86.
7. Sherwin CM. The influences of standard laboratory cages on rodents and the validityof research data. Anim Welf 2004; 13: S9–S15.
8. Richter SH, Garner JP, Wurbel H. Environmental standardization: cure or cause ofpoor reproducibility in animal experiments? Nat Methods 2009; 6:257–61.
9. Keller GL, Mattingly SF, Knapke Jr FB. A forced-air individually ventilated caging systemfor rodents. Lab Anim Sci 1983; 33:580–2.
10. Baumans V, Schlingmann F, Vonck M, van Lith HA. Individually ventilated cages: beneficial for mice and men? Contemp Top Lab Anim Sci 2002; 41:13–9.

11. Clough G, Wallace J, Gamble MR, Merryweather ER, Bailey E. A positive, individuallyventilated caging system: a local barrier system to protect both animals and personnel. Lab Anim 1995; 29:139–51.
12. Willner P, Muscat R, Papp M. Chronic mild stress-induced anhedonia: a realistic animalmodel of depression. Neurosci Biobehav Rev 1992; 16:525–34.
13. Willner P. Validity, reliability and utility of the chronic mild stress model of depression: a 10-year review and evaluation. Psychopharmacology (Berl) 1997; 134:319–29.
14. D'Aquila PS, Brain P, Willner P. Effects of chronic mild stress on performance in behaviouraltests relevant to anxiety and depression. Physiol Behav 1994; 56:861–7.
15. Mineur YS, Prasol DJ, Belzung C, Crusio WE. Agonistic behavior and unpredictablechronic mild stress in mice. Behav Genet 2003; 33:513–9.
16. Mineur YS, Belzung C, Crusio WE. Functional implications of decreases in neurogenesisfollowing chronic mild stress in mice. Neuroscience 2007; 150:251–9.
17. Krohn TC, Hansen AK. Mice prefer draught-free housing. Lab Anim 2010; 44:370–2.
18. Burman O, Owen D, Abouismail U, MendlM. Removing individual rats affects indicatorsof welfare in the remaining group members. Physiol Behav 2008; 93:89–96.
19. Abou-Ismail UA, Burman OHP, Nicol CJ, Mendl M. Can sleep behaviour be used as an indicatorof stress in group-housed rats (Rattus norvegicus)? AnimWelf 2007; 16:185–8.
20. Abou-Ismail UA, Burman OHP, Nicol CJ, Mendl M. Let sleeping rats lie: does thetiming of husbandry procedures affect laboratory rat behaviour, physiology andwelfare? Appl Anim Behav Sci 2008; 111:329–41.
21. Burman OHP, Mendl M. The influence of preexperimental experience on social discriminationin rats (Rattus norvegicus). J Comp Psychol 2003; 117:344–9.
22. Dawkins MS. From an animal's point of view — motivation, fitness, and animalwelfare. Behav Brain Sci 1990:13:1–13.
23. Mendl M. Performing under pressure: stress and cognitive function. Appl AnimBehav Sci 1999; 65:221–44.
24. Wilkie DM, Willson RJ, Carr JA. Errors made by animals in memory paradigms arenot always due to failure of memory. Neurosci Biobehav Rev 1999; 23:451–5.

25. Mineur YS, Crusio WE. Behavioral effects of ventilated micro-environment housingin three inbred mouse strains. Physiol Behav 2009; 97:334–40.
26. Rault J. Friends with benefits: social support and its relevance for farm animal welfare. Appl Anim Behav Sci 2012; 136:1–14.
27. Champy M, Goncalves Da Cruz I, Bedu E, Combe R, Petit-Demouliere B, Muller S, et al. Impact of various IVC housing systems on mouse phenotyping studies;2011.
28. Nicholson A, Malcolm RD, Russ PL, Cough K, Touma C, Palme R, et al. The response ofC57BL/6J and BALB/cJ mice to increased housing density. J Am Assoc Lab Anim Sci2009; 48:740–53.
29. Tang X, Orchard SM, Sanford LD. Home cage activity and behavioral performance ininbred and hybrid mice. Behav Brain Res 2002; 136:555–69.
30. Hawkins P, Morton DB, Burman O, Dennison N, Honess P, JenningsM, et al. UK Joint Working Group on Refinement BVAAWF/FRAME/RSPCA/UFAW.A guide to definingand implementing protocols for the welfare assessment of laboratory animals: eleventh report of the BVAAWF/FRAME/RSPCA/UFAW joint working group on refinement Lab Anim 2011; 45:1–13.
31. Mineur YS, Belzung C, Crusio WE. Effects of unpredictable chronic mild Stress on anxiety and depression-like behavior in mice. Behav Brain Res2006; 175:43–50.
32. O'Leary TP, Gunn RK, Brown RE. What are we measuring when we test strain differencesin anxiety in mice? Behav Genet 2013; 43:34–50.
33. Lister RG. The use of a plus-maze to measure anxiety in the mouse. Psychopharmacology (Berl) 1987; 92:180–5.
34. Benaroya-Milshtein N, Hollander N, Apter A, Kukulansky T, Raz N, Wilf A, et al. Environmentalenrichment in mice decreases anxiety, attenuates stress responsesand enhances natural killer cell activity. Eur J Neurosci 2004; 20:1341–7.
35. Kalueff AV, Tuohimaa P. Contrasting grooming phenotypes in C57Bl/6 and 129S1/SvImJ mice. Brain Res 2004; 1028:75–82.
36. Belzung C, Griebel G. Measuring normal and pathological anxiety-like behaviour inmice: a review. Behav Brain Res 2001; 125:141–9.
37. Garner JP, Weisker SM, Dufour B, Mench JA. Barbering (fur and whisker trimming) by laboratory mice as a model of human trichotillomania and obsessive–compulsivespectrum disorders. Comp Med 2004; 54:216–24.

38. Goulding EH, Schenk AK, Juneja P, MacKay AW, Wade JM, Tecott LH. A robust automatedsystem elucidates mouse home cage behavioral structure. Proc Natl Acad SciU S A 2008; 105:20575–82.
39. Cunningham CL, Gremel CM, Groblewski PA. Drug-induced conditioned place preferenceand aversion in mice. Nat Protoc 2006; 1:1662–70.
40. Treit D, Pinel JP, Fibiger HC. Conditioned defensive burying: a new paradigm for thestudy of anxiolytic agents. Pharmacol Biochem Behav 1981; 15:619–26.
41. Schoenecker B, Heller KE, Freimanis T. Development of stereotypies and polydipsia inwild caught bank voles (Clethrionomys glareolus) and their laboratory-bred offspring. Is polydipsia a symptomof diabetesmellitus? Appl Anim Behav Sci 2000; 68:349–57.
42. Moons CP, VanWiele P, Odberg FO. To enrich or not to enrich: providing shelter doesnot complicate handling of laboratorymice. Contemp Top Lab Anim Sci 2004; 43:18–21.
43. Tuli JS, Smith JA, Morton DB. Stress measurements in mice after transportation. LabAnim 1995; 29:132–8.
44. Gurfein BT, Stamm AW, Bacchetti P, Dallman MF, Nadkarni NA, Milush JM, et al. Thecalm mouse: an animal model of stress reduction. Mol Med 2012; 18:606–17.
45. Hunt C, Hambly C. Faecal corticosterone concentrations indicate that separatelyhoused male mice are not more stressed than group housed males. Physiol Behav2006; 87:519–26.
46. Mason G, Mendl M. Why is there no simple way of measuring animal welfare? Anim Welf 1993; 2:301.

PRESENTED AT FELASA 2013 **P-071**

The effect of two different Individually Ventilated Cage systems on anxiety-related behaviour and welfare in two strains of laboratory mouse

O Burman[1], L Buccarello[3], V Redaelli[3] & L Cervo[2]

[1]School of Life Sciences, University of Lincoln, Brayford, Lincoln.

[2]Istituto di Ricerche Farmacologiche "Mario Negri" -IRCCS, Experimental Psychopharmacology, Milano, Italy

[3]Veterinary Science Department, University of Milano

1. Introduction

The environment in which a laboratory animal is housed can influence its behaviour and anxiety, acting as a potential confounding factor for those studies in which it is utilised as well as affecting its welfare (e.g. Sherwin 2004). This study investigated the impact of two Individually Ventilated Cage (IVC) housing systems on anxiety-related behaviour and welfare of two common strains of laboratory mice.

2. Methods

Subjects were juvenile female C57BL/6J & BALB/c mice (N=128) housed in groups of four in two different IVC systems for seven weeks. System One had air delivery at the cage 'cover' level at 75 ACH (Air Changes/Hour) and System Two had air delivery at the 'animal' level at 50 ACH (see Figure One). Mice were assessed twice a week for some measures (e.g. bodyweight) or at the end of the study (e.g. anxiety tests).

Figure One: *IVC Housing Systems*

3. Results

Mice in System Two, regardless of strain, defecated more in the Elevated Plus Maze (EPM) ($F_{1,28}$=12.2, P=0.002), spent less time in the open arms of the EPM ($F_{1,28}$=18.5, P<0.001) (see Figure Two), and less time in the centre of the Open Field (OF) ($F_{1,28}$=6.2, P=0.019) (See Figure Three). Strain differences in anxiety-like behaviour were seen in the increased defecation by BALB/c mice in the OF ($F_{1,28}$=60.2, P<0.001) and EPM ($F_{1,28}$=19.6, P<0.001), and less time spent in the open arms of the EPM compared to C57BL/6J mice ($F_{1,28}$=17.2, P<0.001) (See Figure Two).

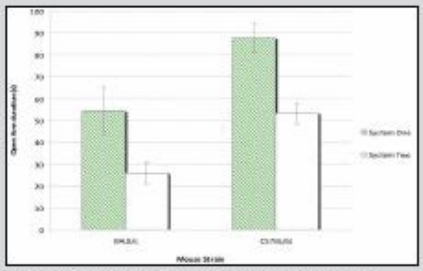

Figure Two: *Time spent in the open arm of the EPM*

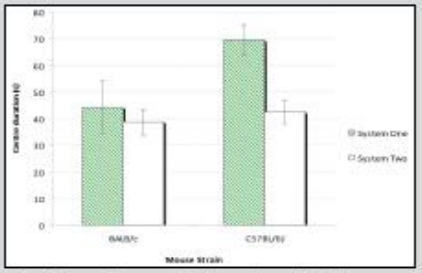

Figure Three: *Time spent in the centre of the OF*

4. Discussion

We found significant differences in anxiety-related behaviour between strains and housing systems. These results suggest that, in addition to influencing mouse choice (e.g. Baumans et al. 2002; Krohn & Hansen 2010), different IVC housing systems can influence mouse behaviour - with mice of both strains studied exhibiting more anxiety-related behaviour when housed in System Two (air entry at the 'Animal' level at 50 ACH). These results have implications for experimental design, and demonstrate that the term 'IVC' cannot be generalised across IVC housing systems, because variation between these systems may well have differential influences on mouse behaviour.

5. References

Baumans et al. 2002. Individually ventilated cages: Beneficial for mice and men? Contemp Top Lab Anim Sci, 41:13-9.

Krohn, T.C. & Hansen, A.K. 2010. Mice prefer draught-free housing. Lab Anim, 44: 370-372.

Sherwin, C.M. 2004. The influences of standard laboratory cages on rodents and the validity of research data. Anim Welf, 13: S9-S15.

CHAPTER 11

Acknowledgements

12. ACKNOWLEDGEMENTS

I wish to thank all those who have contributed to realizing this achievement. First of all, thank Prof. Cinzia Domeneghini for allowing me to carry out this research project and the availability shown me during my PhD period. I thank Prof. Alessia Digiancamillo for helping me during my PhD period and have contributed to my training. A special thanks to Dr. Giuliano Grignaschi, co-mentor of this project, with whom i shared pleasantly not only my PhD period, but also previous projects at the Institute of Pharmacological Research Mario Negri. The meeting him on my journey has enriched me both professionally and personally. The other two team members who i want to thank are Dr. Gerardo Marsella, veterinary of Mario Negri Institute and good traveling companion and Francesca Perego, not only a wonderful traveling companion, also a dear friend became part not only of my life but also of my family. And finally I want to thank my family, my mother, my father, my sister and my dog for supporting me, for their love and for being the best part of me. So i want to dedicate this achievement to my beloved mother, giving her the words of a woman who had the strength and courage as sources of life.

"Do not fear the difficult moments:

the best comes from there."

(Rita Levi Montalcini)